Università Politecnica delle Marche

PhD in Life and Environmental Sciences

Marine Biology and Ecology

XXXVI cycle

Response of phytoplankton communities to a changing Adriatic Sea: the over 30-year story of an eLTER marine area

Supervisor

Prof. Cecilia Maria Totti

PhD candidate

Francesca Neri

Co-supervisor

Prof. Stefano Accoroni

Supervisor:

Prof. Cecilia Totti, PhD

Laboratory of Marine Botany

Department of Life and Environmental Sciences

Università Politecnica delle Marche

Ancona, Italy

Co-Supervisor:

Prof. Stefano Accoroni, PhD

Laboratory of Marine Botany

Department of Life and Environmental Sciences

Università Politecnica delle Marche

Ancona, Italy

Abstract (English)

The Northern Adriatic Sea (NAS), one of the most productive areas of the Mediterranean Sea, is undergoing changes as a result of meteoclimatic alterations and climate change-related phenomena. Phytoplankton communities have the capability of responding to changes in both biotic and abiotic parameters, oceanographic conditions and climate processes, due to the fast turnover and the high sensitiveness to environmental conditions. In this scenario, we are facing many changes in the phytoplankton community structure, dynamics and seasonal cycles, with potential consequences on the entire marine ecosystem and economic sea-related activities.

The overall aim of the thesis was to elucidate the relationships between phytoplankton and both biochemical and oceanographic conditions of the NAS, alongside the effects of extreme climate events and ocean warming.

In the first chapter, a 30-year dataset related to a Long-Term Ecological Research marine site (the Senigallia-Susak Transect) was analysed, unveiling important differences in terms of phytoplankton dynamics and functioning (species interactions) between a coastal and an offshore station, mainly related to the surface circulation and thus to the different trend of physico-chemical parameters. In the offshore station, the main component of phytoplankton community was represented by phytoflagellates. The seasonal cycle markedly differed from that in the coastal station, with a maximum in summer, mainly due to the allochthonous input of nutrients carried by low salinity waters expanding eastward, during stratification.

In the second chapter, the investigation of the effects of extreme events (marine heatwaves) and ocean warming on phytoplankton biomass (chlorophyll-a) across the NAS, considering its different characteristics (i.e., circulation, depth and trophic conditions), highlighted negative correlations between increasing of Sea Surface Temperature and chl-a trends. Different correlations between chl-a and marine heatwaves in the different seasons and sub-areas of the NAS suggested that marine heatwaves are affecting phytoplankton biomass in different ways depending on the background conditions and the involved processes.

In the third chapter, phytoplankton taxonomic composition of the eLTER Senigallia coastal station (in the NAS) obtained from microscopy and metabarcoding (using V4 and V9 regions of the 18S as markers, and PR2 and SILVA as databases) was compared, highlighting that the two methods should be combined to gain more detailed information on the community and to counteract the respective drawbacks. Indeed, only a small percentage of taxa was identified by all the approaches and, while metabarcoding revealed a previously unknown diversity, microscopy detected genera and species not revealed by metabarcoding, particularly among coccolithophores.

Abstract (Italian)

Il Nord Adriatico (NA), una delle aree più produttive del Mar Mediterraneo, sta subendo intensi cambiamenti, a causa delle alterazioni meteoclimatiche e dei fenomeni correlati al cambiamento climatico. Il fitoplancton ha la capacità di rivelare cambiamenti nei parametri biologici e chimico-fisici, nelle condizioni oceanografiche e nei processi climatici, grazie al rapido turnover e alla sensibilità alle condizioni ambientali. In questo contesto, le comunità fitoplanctoniche stanno subendo numerosi cambiamenti nella struttura, nella dinamica e nei cicli stagionali, con potenziali conseguenze sull'intero ecosistema marino e sulle attività economiche legate al mare.

L'obiettivo generale della tesi è stato quello di analizzare le relazioni tra il fitoplancton e le condizioni biochimiche e oceanografiche del NA, insieme agli effetti degli eventi climatici estremi e al riscaldamento degli oceani.

Nel primo capitolo, è stato analizzato un dataset di 30 anni relativo a un sito marino LTER (il Transetto Senigallia-Susak), rivelando importanti differenze in termini di dinamiche e funzionamento della comunità (interazioni tra specie) tra una stazione costiera e una al largo, principalmente legate alla circolazione superficiale e quindi al differente andamento dei parametri fisico-chimici. Nella stazione al largo le fitoflagellate dominavano la comunità fitoplanctonica. Il ciclo stagionale differiva da quello nella stazione costiera, con il massimo estivo principalmente legato all'ingresso alloctono di nutrienti dovuti all'apporto di acqua dolce proveniente dal Po, che si espande verso est in condizioni di stratificazione.

Nel secondo capitolo, l'analisi degli effetti di eventi estremi (onde di calore) e del riscaldamento delle acque sulla biomassa del fitoplancton nel NA, considerando le sue diverse caratteristiche (i.e., circolazione, profondità e condizioni trofiche), ha evidenziato correlazioni negative tra l'aumento della temperatura superficiale del mare e i trend della clorofilla-a. Le diverse correlazioni tra la clorofilla-a e le onde di calore nelle diverse stagioni e sub-aree del NAS suggeriscono che le onde di calore stiano influenzando la biomassa del fitoplancton in modi diversi, a seconda delle condizioni e dei processi tipici delle diverse sub-aree.

Nel terzo capitolo, è stata confrontata la composizione tassonomica del fitoplancton della stazione LTER costiera del transetto di Senigallia analizzata tramite microscopia e metabarcoding (utilizzando le regioni V4 e V9 del 18S, e i database PR2 e SILVA), mostrando come entrambi i metodi dovrebbero essere combinati per ottenere informazioni più dettagliate sulla comunità e per contrastare gli svantaggi di ciascun metodo. Infatti, è stato evidenziato che solo pochi taxa venivano individuati da tutti gli approcci e, mentre il metabarcoding ha rivelato una diversità finora sconosciuta, la microscopia ha identificato generi e specie non rivelati dal metabarcoding, in particolare tra i coccolitofori.

Contents

Introduction

Marine phytoplankton

The term "phytoplankton" include extremely diverse organisms, from prokaryotes (cyanobacteria) to eukaryotes, which live in the water column and are characterized by different sizes (<2 µm for picophytoplankton, 2–20 µm for nanophytoplankton and 20–200 µm for microphytoplankton), different reproduction types, metabolism (autotrophic, heterotrophic and mixotrophic), and morphologies.

Many microalgal groups are represented in the marine phytoplankton. The most frequent phytoplankton groups in the ocean belong to diatoms (Stramenopili), dinoflagellates (Alveolata), and coccolithophores (Haptista) (Adl et al., 2012; Falkowski et al., 2004). Other groups are represented by a variety of small flagellate taxa, such as cryptophytes, chrysophytes, haptophytes (except coccolithophores), dictyochophytes, raphidophytes, chlorophytes and euglenophytes, generally included in the informal group of phytoflagellates.

Marine phytoplankton plays essential roles in the marine ecosystems: it is a fundamental primary producer, producing more than 50% of world's oxygen, it contributes to higher trophic level/food production, it is part of the microbial loop (interacting with bacteria and virus) and participates to biogeochemical cycles, drawdown of CO_2 from the air, climate regulation (Araujo et al., 2022; Blanchard et al., 2012; Falkowski, 2012; Hays et al., 2005; Käse and Geuer, 2018; Naselli-Flores and Padisák, 2023; Vallina and Simó, 2007).

Phytoplankton is characterized by a fast turnover, and it is directly related to environmental conditions (e.g. nutrient availability, penetration of light, pH, temperature and salinity) and indirectly related to climatic and oceanographic processes which can affect those parameters (e.g. upwelling, water column mixing/stratification, rain regime, riverine inputs). Therefore, changes in the phytoplankton dynamics, diversity, abundances and biomasses have the potential to reveal changes in both biotic and abiotic parameters, oceanographic conditions and climate changes. For these reasons, many metrics and indices related to phytoplankton (e.g. shifts in productivity, life forms, composition in terms of non-indigenous or toxic species, diversity indices, changes in the spatial and temporal

diversity) have been proposed and used for marine management policies, also in the context of Marine Strategy Framework Directive for the assessment of Good Environmental Status for pelagic habitats (2008/56/EC; Francé et al., 2021; McQuatters-Gollop et al., 2022, 2019; Rombouts et al., 2019; Tweddle et al., 2018; Varkitzi et al., 2018; Wasmund et al., 2017).

Phytoplankton response to and climate changes

Climate change can affect phytoplankton diversity, dynamics, phenology, abundances, and biomass in several ways, affecting those parameters that influence their production and growth. These effects can vary among different phytoplankton groups and taxa, depending on their optimal conditions for growth. For example, ocean acidification can have negative effects on the calcification of coccolithophores, which are characterized by small calcium carbonate scales (coccoliths) (D'Amario et al., 2020; Meyer and Riebesell, 2015; Wu et al., 2023), but also on the silicification of diatoms (Petrou et al., 2019; Taucher et al., 2022).

One of the most studied climate change related phenomena, is the ocean warming, as the increase of temperature can affect phytoplankton communities at different levels, from metabolism, phenology and biomass to bloom dynamics, species interactions and composition (Ajani et al., 2020; Bopp et al., 2005; López-Urrutia et al., 2006; Mesquita et al., 2020; Sommer and Lengfellner, 2008; Soulié et al., 2022; Trombetta et al., 2019). Indeed, the increase of temperature is associated to other phenomena, as increasing of vertical density gradients, longer periods of stratification and, consequently, changes in the vertical mixing of the water column (Edwards et al., 2022; Fu et al., 2016; Kwiatkowski et al., 2020; Li et al., 2020; Sallée et al., 2021). These changes in the mixing related to ocean warming and stratification, wind intensities and air-sea heat fluxes can lead to changes in the phytoplankton productivity and biomass affecting the nutrient exchange and availability.

Due to climate change, extreme climate events like intense precipitation events, long drought periods and marine heatwaves are expected to become more frequent and intense (Seneviratne et al., 2021),

with a diverse range of effects toward the phytoplankton community. Indeed, while periods of droughts can reduce biomass and productivity due to reduced nutrient availability (Masotti et al., 2018; Wetz et al., 2011), extreme rainfall coupled with increase in river runoff could modify size structure of the community (towards higher sized taxa in nutrient-rich environments) and promote or inhibit phytoplankton growth, depending on light availability and on the amount of organic and inorganic nutrients (Andersson et al., 2013; Masotti et al., 2018; Paczkowska et al., 2020).

Climate change related processes alter simultaneously several environmental factors and manifest differently around the globe; thus, the same phenomenon can lead to different effects in different areas. It is therefore crucial to study the effects of climate change on the phytoplankton communities at local scales, as changes in the phytoplankton blooms, production and composition could lead to economic loss related to fishery, aquaculture, and tourism (Hays et al., 2005).

Methods for the study of phytoplankton

Monitoring of phytoplankton communities can be performed using different methods, such as microscopy, measurement of pigment composition and concentration, satellites, molecular analyses and flow cytometry, each with its own advantages and disadvantages. Microscopy, metabarcoding and satellite data, which are among the most used methods, are described below.

Microscopy analyses

Traditionally, the monitoring of phytoplankton has been based on morphological diagnostic characteristics of the different taxa through the use of inverted microscope (Edler and Elbrachter, 2010). This method is based on the sedimentation of a subsample (volume ranging from 1 to 100 ml) in a cylinder/chamber system and on the counting of a portion of settling chamber (1–2 transects, 20–60 random fields). In this way, estimates of abundance, biomass (based on biovolume measurement) and species composition can be obtained from the same sample. However, this approach is time consuming, requires highly expert taxonomists which could influence itself the identification and can

miss or mismatch less abundant/smaller species. Furthermore, precise determination of species can be affected by (i) the fact that several taxonomical details are visible only under electron microscopy, (ii) the presence of species that do not show diagnostic morphology (i.e., cryptic species (Struck et al., 2017)), and (iii) the variation of morphological diagnostic characters under different environmental conditions (Bernardi Aubry et al., 2017; Roselli and Basset, 2015; Segura et al., 2013). Moreover, the different volume settled for the analysis, for example between coastal and offshore areas, can influence the probability to find rarer species (Neri et al., 2023).

Metabarcoding

Several molecular analyses can be performed for the study of phytoplankton, like the Sanger sequencing of specific "barcode" areas, quantitative polymerase chain reaction (qPCR), Fluorescent Hybridization Assays (FISH) and Sandwich Hybridization Assays (SHA) (Doll et al., 2014; Groben and Medlin, 2005; Medlin and Kooistra, 2010; Meek and Van Dolah, 2016).

Metabarcoding is among the most used molecular approaches for the study of the phytoplankton community, in terms of diversity and relative abundances. This method is based on the amplification of a target genetic marker through general or universal polymerase chain reaction (PCR) primers, followed by high-throughput sequencing and several bioinformatic procedures, including steps in which sequences are checked, trimmed and compared to a reference database to identify the taxa in the sample (Bokulich et al., 2018; Bolyen et al., 2019; Goodwin et al., 2017; Taberlet et al., 2012). Therefore, metabarcoding allows to detect high diversity, including smaller and cryptic taxa not detectable through microscopy, in a less time-consuming way, without the potential influence of the operator and thus with higher reproducibility and comparability.

However, key differences in the obtained biodiversity can arise based on the markers, which can have different resolution and could be not enough variable in different taxa (Gran-Stadniczeñko et al., 2019; Mordret et al., 2018; Piganeau et al., 2011), the primers, which can fail to/preferentially amplify some taxa (Kelly et al., 2019; Kezlya et al., 2023; Pawlowski et al., 2011; Stoeck et al., 2010), and

above all on the reference databases, as their incompleteness could affect or prevent the taxonomy assignment of some taxa. Moreover, errors or biases in diversity could occur in several steps, from PCR and sequencing to subsequent bioinformatic pipeline (Behnke et al., 2011; Ershova et al., 2023; Preston et al., 2022; Santoferrara, 2019; Tzafesta et al., 2022; Vasselon et al., 2017).

Despite metabarcoding is highly used for the study of phytoplankton communities, many questions are still opened, like which is the best way to compare metabarcoding and microscopy data (as the first does not provide real values of abundances) and at which taxonomic level the best match between methods can be found (Andersson et al., 2023; Xiao et al., 2014). In this way, a high expertise in phytoplankton community and taxonomy is recommended to highlight biases and bad synonymies and to interpret the list of taxa. In this perspective, Long-Term Ecological Research sites represent a precious tool by providing verified and high-quality datasets.

Satellite data

Satellite observations are based on the detection of the spectral variations of the water-leaving radiance, which is mainly influenced by the phytoplankton photosynthetic pigments (particularly in the open oceans), and on algorithms linking these radiances to in-water properties (Groom et al., 2019). Despite limitations like cloud cover, atmospheric effects, and challenges in specific areas (e.g., turbid coastal waters) (Cherif et al., 2021; Joint and Groom, 2000; Wang and Moisan, 2021), satellite data provides a wealth of information on phytoplankton communities. This includes data on (i) phytoplankton biomass and productivity (through estimates of chlorophyll-a concentration), (ii) composition in terms of Phytoplankton Functional Types (PFT), (i.e. groups of phytoplankton species with similar ecological characteristics and physiological traits (Reynolds 2002)), and (iii) Phytoplankton Size Classes (PSCs) (e.g. Blondeau-Patissier et al., 2014; Di Cicco et al., 2017; Moisan et al., 2017; Sun et al., 2018).

Therefore, remote sensing represents a powerful tool for the study of phytoplankton communities at the surface layer, offering long-term data, at regional and global scales, with higher temporal and

spatial resolutions, than those obtained through discrete samplings allowing to track changes in the seasonal patterns, blooms, and long-term trends.

The Northern Adriatic Sea

The Northern Adriatic Sea (NAS) represents the northeastern and most productive basin of the Mediterranean. The lower limit of the NAS, in origin defined as the Ancona–Zadar transect (Buljan and Zore-Armanda, 1976), is now regarded as the 100 m isobath, corresponding to the Giulianova-Sibenik transect (Artegiani et al., 1997a), while in the context of the Italian legislations related to the Marine Strategy Framework Directive, the NAS limit is placed further north.

The NAS is characterized by a shallow depth and by a dominant cyclonic circulation: the Western Adriatic Current (WAC) flows southwards along the western coast bringing fresher, nutrient-rich riverine waters from the northern areas, while the Eastern Adriatic Current (EAC) flows northwards along the eastern coast, bringing warmer and more oligotrophic waters from the southern sub-basin (Artegiani et al., 1997b; Poulain and Cushman-Roisin, 2001). Furthermore, the NAS is highly affected by riverine inputs, mainly the Po River, with a historical mean discharge rate of ~1500-1700 m^3s^{-1}, although these values are decreasing due to climate change (Campanelli et al., 2011; Montanari, 2012; Montanari et al., 2023; Raicich, 1996). The influence of the Po River inputs on the NAS vary in the different seasons, as in winter and autumn the largest amount of water flows southwards through the WAC, while in spring and summer expands south-eastwards bringing riverine water in the offshore central areas of the basin, favoured by stratification processes and small-scale features, like gyres (Artegiani et al., 1997a, 1997b; Neri et al., 2022; Vilicic et al., 2013). Another aspect influencing the characteristics of the NAS is represented by the wind regime, mainly Sirocco (SE), Bora (NE) and Mistral (NW) (Poulain and Raicich, 2001; Russo and Artegiani, 1996). Among these, the Bora wind, frequent in fall and winter, is responsible for the heat loss and cooling of the northernmost water column and plays a significant role in the formation of Northern Adriatic Dense Water (NAdDW) (Bergamasco et al., 1999; Boldrin et al., 2009; Vilibić and Supić, 2005)

The NAS shows high spatial variability in terms of physico-chemical parameters, with a seasonal longitudinal and latitudinal gradient. In winter and autumn, temperature and salinity show lower values along the north-western coasts, and higher values along the eastern coasts, while in spring and summer higher values of temperature and salinity are observed in the entire NAS (Giani et al., 2012; Grilli et al., 2020; Solidoro et al., 2009). Similarly, nutrients show high spatial gradient, with higher values of nitrate, phosphate and silicates in the northern and western areas of the NAS, particularly in winter and autumn, and lowest values in summer (Grilli et al., 2020).

The NAS has been experiencing interannual and multidecadal climate fluctuations, such as the North Atlantic Oscillation, which modify circulation patterns and impact biological communities (Conversi et al., 2010; Pisano et al., 2020; Zanchettin et al., 2006). Additionally, the combined effects of riverine inputs, circulation dynamics, shallow depths, and wind patterns contribute to the hydrological and physico-chemical alterations of the NAS, rendering it highly susceptible to climate change. Numerous changes have been identified (e.g. Cozzi et al., 2020; Gordo et al., 2011; Grilli et al., 2020; Tojčić et al., 2023), including projections towards oligotrophication, ocean warming, and acidification (Mentaschi et al., 2024; Shaltout and Omstedt, 2014). These projected tendencies underscore the significant challenges posed by climate change in this marine basin, the urgent need for comprehensive monitoring of this ecologically and economically significant marine area.

Phytoplankton in the Northern Adriatic Sea

Due to the high spatial variability, the phytoplankton cycle varies among the different areas of the NAS, due to the high spatial variability. The northwestern coast is characterized by an intense diatom winter bloom, which is responsible for the highest values of abundance and biomass of the year and is mainly related to *Skeletonema marinoi*, followed by the classic spring and autumn blooms (e.g. Bernardi Aubry et al., 2004; Totti et al., 2019, 2005). Instead, spring and autumn blooms are typical of the eastern part of the NAS (e.g. Cabrini et al., 2012; Cerino et al., 2019; Marić et al., 2012).

Offshore, the highest values are observed in the summer season, due to the spreading of riverine waters in stratified conditions (Neri et al., 2022).

However, in the NAS, the seasonality and the interannual trends of phytoplankton communities have always been influenced by the changes in the environmental conditions. From the 1970s to the mid-1980s, an increase in terms of productivity was related to eutrophication-related phenomena (Boni et al., 1983; Degobbis et al., 2000; Honsell et al., 1992), with frequent summer dinoflagellate blooms, while between the late 80s and early 2000s the NAS experienced the appearance of large mucilage aggregates. This phenomenon was probably triggered by a synergic combination of events, such as extracellular release by blooming phytoplankton, unbalanced nutrient ratio, related also to the legislative polyphosphate reduction in the detergents, and reduced circulation (Degobbis et al., 2005, 1999; Giani et al., 2005; Russo et al., 2005; Totti et al., 2005; Turk et al., 2010). The years 2000–2007 were characterized by a marked decrease in the nutrient discharge in the NAS as a consequence of prolonged droughts, which led to a strong decrease of the Po River flow, as well as of minor rivers, with negative effects for many phytoplankton taxa, general decreasing trend of chlorophyll-a and changes in the seasonality of the blooms (Bernardi Aubry et al., 2012; Cabrini et al., 2012; Cozzi et al., 2020; Djakovac et al., 2012; Giani et al., 2012; Marić et al., 2012; Mozetič et al., 2010; Zanchettin et al., 2008).

In the recent decade, other tendencies and changes in the phytoplankton communities have been reported in many studies and related to changes in the nutrient availability and climatic variability (Cerino et al., 2019; Cozzi et al., 2020; Totti et al., 2019). For example, Cerino et al. (2019) observed a decrease in the typical winter bloom which was mainly related to a decrease of *Skeletonema* abundances, possibly due to nutrient reductions, increase of temperature and teleconnections (e.g. North Atlantic Oscillation) (Borkman and Smayda, 2009; Cabrini et al., 2012).

In a climate change context, these tendencies are expected to continuously change with potential consequences on the entire marine ecosystem and economic sea-related activities, making the

interannual trends and their relationships with environmental and oceanographic conditions crucial to be studied.

Long-Term Ecological Research sites allow to highlight the inter-annual variability of both physico-chemical parameters and phytoplankton data and to disentangle the natural variability from climate change induced alterations. Four Long-Term Ecological Research (LTER) marine sites are located in the NAS, where physico-chemical parameters and phytoplankton data have been collected since a long period of time (e.g., since 1988 in the Senigallia-Susak Transect): Gulf of Venice, Gulf of Trieste, Po River delta, and Senigallia-Susak Transect.

Aims of the thesis

The overall aims of the thesis were focused on unveiling the relationships between phytoplankton and both biochemical and oceanographic conditions of the NAS, alongside the effects of extreme climate events and ocean warming. In particular the aims were: (i) to analyse the phytoplankton community and dynamics in a 30-years dataset related to a Long-Term Ecological Research marine site (the Senigallia-Susak Transect) and their relationships with oceanographic conditions, (ii) to depict the effects of extreme events (marine heatwaves) and ocean warming on the phytoplankton biomass and (iii) to highlight the strength and weakness of metabarcoding and microscopy approaches for the study of phytoplankton diversity based on eLTER station dataset.

The first objective is addressed in the second chapter, where a 30-years data set referred to an eLTER offshore station located along the Senigallia-Susak Transect, beyond the border of the Western Adriatic Current (thus not directly affected by riverine inputs) was analysed for the first time. The aims were to highlight the intra-annual and interannual variability of physico-chemical parameters and phytoplankton, the phytoplankton community composition and the relationships between phytoplankton and environmental parameters. Then, the phytoplankton community structure of a coastal and offshore stations along the LTER site was compared to depict the main forcings affecting the phytoplankton dynamics and functioning in terms of species interactions, using several statistical

descriptors to also test their suitability in highlighting the main features and dynamics of the phytoplankton community of two stations.

The third chapter focused on the effects on extreme events (marine heatwaves) and ocean warming on the phytoplankton biomass, by analysing the relationships between the trends of temperature and marine heatwaves with those of chlorophyll-a (considered as a proxy of phytoplankton biomass) in the NAS, taking into account the seasonal variability and the peculiarities of the different areas of the basin (i.e., different circulation, depth and trophic conditions).

In the fourth chapter, the information on the diversity obtained through microscopy counting and metabarcoding, using different markers (V4 and V9) and databases (PR2 and SILVA), was compared to highlight the potential strengths and weaknesses of the different methods and the completeness of the reference databases for the study of the phytoplankton community.

References

2008/56/EC. Directive 2008/56/EC of the European Parliament and of the Council of 17 June 2008 establishing a framework for community action in the field of marine environmental policy (Marine Strategy Framework Directive) (Text with EEA relevance).

Adl, S.M., Simpson, A.G.B., Lane, C.E., Lukeš, J., Bass, D., Bowser, S.S., Brown, M.W., Burki, F., Dunthorn, M., Hampl, V., Heiss, A., Hoppenrath, M., Lara, E., le Gall, L., Lynn, D.H., McManus, H., Mitchell, E.A.D., Mozley-Stanridge, S.E., Parfrey, L.W., Pawlowski, J., Rueckert, S., Shadwick, L., Schoch, C.L., Smirnov, A., Spiegel, F.W., 2012. The revised classification of eukaryotes. J. Eukaryot. Microbiol. 59, 429–514. https://doi.org/10.1111/j.1550-7408.2012.00644.x

Ajani, P.A., Davies, C.H., Eriksen, R.S., Richardson, A.J., 2020. Global warming impacts micro-phytoplankton at a long-term Pacific Ocean coastal station. Front. Mar. Sci. 7, 576011. https://doi.org/10.3389/fmars.2020.576011

Andersson, A., Jurgensone, I., Rowe, O.F., Simonelli, P., Bignert, A., Lundberg, E., Karlsson, J., 2013. Can humic water discharge counteract eutrophication in coastal waters? PLoS One 8, e61293. https://doi.org/10.1371/journal.pone.0061293

Andersson, A., Zhao, L., Brugel, S., Figueroa, D., Huseby, S., 2023. Metabarcoding vs Microscopy: comparison of methods to monitor phytoplankton communities. Water, 3, 2671-2680. https://doi.org/10.1021/acsestwater.3c00176

Araujo, G.S., Pacheco, D., Cotas, J., da Silva, J.W.A., Saboya, J., Moreira, R.T., Pereira, L., 2022. Plankton: environmental and economic importance for a sustainable future. In: Pereira, L., Gonçalves, A.M. (Eds.), *Plankton Communities.* IntechOpen, Rijeka. https://doi.org/10.5772/intechopen.100433

Artegiani, A., Bregant, D., Paschini, E., Pinardi, N., Raicich, F., Russo, A., 1997a. The Adriatic Sea general circulation. Part I: air-sea interactions and water mass structure. J. Phys. Oceanogr. 27, 1492–1514. https://doi.org/10.1175/1520-0485(1997)027<1492:TASGCP>2.0.CO;2

Artegiani, A., Bregant, D., Paschini, E., Pinardi, N., Raicich, F., Russo, A., 1997b. The Adriatic Sea general circulation. Part II: baroclinic circulation structure. J. Phys. Oceanogr. 27, 1515–1532. https://doi.org/10.1175/1520-0485(1997)027<1515:TASGCP>2.0.CO;2

Behnke, A., Engel, M., Christen, R., Nebel, M., Klein, R.R., Stoeck, T., 2011. Depicting more accurate pictures of protistan community complexity using pyrosequencing of hypervariable SSU rRNA gene regions. Environ. Microbiol. 13, 340–349. https://doi.org/10.1111/j.1462-2920.2010.02332.x

Bergamasco, A., Oguz, T., Malanotte-Rizzoli, P., 1999. Modelling dense water mass formation and winter circulation in the northern and central Adriatic Sea. J. Mar. Syst. 20, 279–300. https://doi.org/https://doi.org/10.1016/S0924-7963(98)00087-6

Bernardi Aubry, F., Berton, A., Bastianini, M., Socal, G., Acri, F., 2004. Phytoplankton succession in a coastal area of the NW Adriatic, over a 10-year sampling period (1990-1999). Cont. Shelf Res. 24, 97–115. https://doi.org/10.1016/j.csr.2003.09.007

Bernardi Aubry, F., Cossarini, G., Acri, F., Bastianini, M., Bianchi, F., Camatti, E., De Lazzari, A., Pugnetti, A., Solidoro, C., Socal, G., 2012. Plankton communities in the northern Adriatic Sea: Patterns and changes over the last 30 years. Estuar. Coast. Shelf Sci. 115, 125–137. https://doi.org/https://doi.org/10.1016/j.ecss.2012.03.011

Bernardi Aubry, F., Pugnetti, A., Roselli, L., Stanca, E., Acri, F., Finotto, S., Basset, A., 2017. Phytoplankton morphological traits in a nutrient-enriched, turbulent Mediterranean microtidal lagoon. J. Plankton Res. 39, 564–576. https://doi.org/10.1093/plankt/fbx008

Blanchard, J.L., Jennings, S., Holmes, R., Harle, J., Merino, G., Allen, J.I., Holt, J., Dulvy, N.K., Barange, M., 2012. Potential consequences of climate change for primary production and fish production in large marine ecosystems. Philos. Trans. R. Soc. B Biol. Sci. 367, 2979–2989. https://doi.org/10.1098/rstb.2012.0231

Blondeau-Patissier, D., Gower, J.F.R., Dekker, A.G., Phinn, S.R., Brando, V.E., 2014. A review of ocean color remote sensing methods and statistical techniques for the detection, mapping and analysis of phytoplankton blooms in coastal and open oceans. Prog. Oceanogr. 123, 123–144. https://doi.org/10.1016/j.pocean.2013.12.008

Bokulich, N.A., Kaehler, B.D., Rideout, J.R., Dillon, M., Bolyen, E., Knight, R., Huttley, G.A., Gregory Caporaso, J., 2018. Optimizing taxonomic classification of marker-gene amplicon sequences with QIIME 2's q2-feature-classifier plugin. Microbiome 6, 90. https://doi.org/10.1186/s40168-018-0470-z

Boldrin, A., Carniel, S., Giani, M., Marini, M., Bernardi Aubry, F., Campanelli, A., Grilli, F., Russo, A., 2009. Effects of bora wind on physical and biogeochemical properties of stratified waters in the northern Adriatic. J. Geophys. Res. 114, C08S92. https://doi.org/10.1029/2008jc004837

Bolyen, E., Rideout, J.R., Dillon, M.R., Bokulich, N.A., Abnet, C.C., Al-Ghalith, G.A., Alexander, H., Alm, E.J., Arumugam, M., Asnicar, F., Bai, Y., Bisanz, J.E., Bittinger, K., Brejnrod, A., Brislawn, C.J., Brown, C.T., Callahan, B.J., Caraballo-Rodríguez, A.M., Chase, J., Cope, E.K., Da Silva, R., Diener, C., Dorrestein, P.C., Douglas, G.M., Durall, D.M., Duvallet, C., Edwardson, C.F., Ernst, M., Estaki, M., Fouquier, J., Gauglitz, J.M., Gibbons, S.M., Gibson, D.L., Gonzalez, A., Gorlick, K., Guo, J., Hillmann, B., Holmes, S., Holste, H., Huttenhower, C., Huttley, G.A., Janssen, S., Jarmusch, A.K., Jiang, L., Kaehler, B.D., Kang, K. Bin, Keefe, C.R., Keim, P., Kelley, S.T., Knights, D., Koester, I., Kosciolek, T., Kreps, J., Langille, M.G.I., Lee, J., Ley, R.,

Liu, Y.X., Loftfield, E., Lozupone, C., Maher, M., Marotz, C., Martin, B.D., McDonald, D., McIver, L.J., Melnik, A. V., Metcalf, J.L., Morgan, S.C., Morton, J.T., Naimey, A.T., Navas-Molina, J.A., Nothias, L.F., Orchanian, S.B., Pearson, T., Peoples, S.L., Petras, D., Preuss, M.L., Pruesse, E., Rasmussen, L.B., Rivers, A., Robeson, M.S., Rosenthal, P., Segata, N., Shaffer, M., Shiffer, A., Sinha, R., Song, S.J., Spear, J.R., Swafford, A.D., Thompson, L.R., Torres, P.J., Trinh, P., Tripathi, A., Turnbaugh, P.J., Ul-Hasan, S., van der Hooft, J.J.J., Vargas, F., Vázquez-Baeza, Y., Vogtmann, E., von Hippel, M., Walters, W., Wan, Y., Wang, M., Warren, J., Weber, K.C., Williamson, C.H.D., Willis, A.D., Xu, Z.Z., Zaneveld, J.R., Zhang, Y., Zhu, Q., Knight, R., Caporaso, J.G., 2019. Reproducible, interactive, scalable and extensible microbiome data science using QIIME 2. Nat. Biotechnol. 37, 852–857. https://doi.org/10.1038/s41587-019-0209-9

Boni, L., Pompei, M., Reti, M., 1983. The occurrence of *Gonyaulax tamarensis* Lebour bloom in the adriatic sea along the coast of Emilia-Romagna. G. Bot. Ital. 117, 115–120. https://doi.org/10.1080/11263508309427964

Bopp, L., Aumont, O., Cadule, P., Alvain, S., Gehlen, M., 2005. Response of diatoms distribution to global warming and potential implications: A global model study. Geophys. Res. Lett. 32, L19606. https://doi.org/10.1029/2005GL023653

Borkman, D.G., Smayda, T., 2009. Multidecadal (1959–1997) changes in *Skeletonema* abundance and seasonal bloom patterns in Narragansett Bay, Rhode Island, USA. J. Sea Res. 61, 84–94. https://doi.org/10.1016/j.seares.2008.10.004

Buljan, M., Zore-Armanda, M., 1976. Oceanographical properties of the Adriatic Sea. Oceanogr. Mar. Biol. Ann. Rev., 14, 11–98.

Cabrini, M., Fornasaro, D., Cossarini, G., Lipizer, M., Virgilio, D., 2012. Phytoplankton temporal changes in a coastal northern Adriatic site during the last 25 years. Estuar. Coast. Shelf Sci. 115, 113–124. https://doi.org/10.1016/j.ecss.2012.07.007

Campanelli, A., Grilli, F., Paschini, E., Marini, M., 2011. The influence of an exceptional Po River flood on the physical and chemical oceanographic properties of the Adriatic Sea. Dyn. Atmos. Ocean. 52, 284–297. https://doi.org/10.1016/j.dynatmoce.2011.05.004

Cerino, F., Fornasaro, D., Kralj, M., Giani, M., Cabrini, M., 2019. Phytoplankton temporal dynamics in the coastal waters of the north-eastern Adriatic Sea (Mediterranean Sea) from 2010 to 2017. Nat. Conserv. 34, 343–372. https://doi.org/10.3897/natureconservation.34.30720

Cherif, E.K., Mozetič, P., Francé, J., Flander-Putrle, V., Faganeli-Pucer, J., Vodopivec, M., 2021. Comparison of in-situ chlorophyll-a time series and sentinel-3 ocean and land color instrument data in slovenian national waters (Gulf of Trieste, Adriatic Sea). Water 13, 1903. https://doi.org/10.3390/w13141903

Conversi, A., Fonda Umani, S., Peluso, T., Molinero, J.C., Santojanni, A., Edwards, M., 2010. The Mediterranean Sea regime shift at the end of the 1980s, and intriguing parallelisms with other European basins. PLoS One 5, e10633. https://doi.org/10.1371/journal.pone.0010633

Cozzi, S., Cabrini, M., Kralj, M., De Vittor, C., Celio, M., Giani, M., 2020. Climatic and anthropogenic impacts on environmental conditions and phytoplankton community in the Gulf of Trieste (Northern Adriatic Sea). Water 12, 2652. https://doi.org/10.3390/w12092652

D'Amario, B., Pérez, C., Grelaud, M., Pitta, P., Krasakopoulou, E., Ziveri, P., 2020. Coccolithophore community response to ocean acidification and warming in the Eastern Mediterranean Sea: results from a mesocosm experiment. Sci. Rep. 10, 12637. https://doi.org/10.1038/s41598-020-69519-5

Degobbis, D., Malej, A., Fonda Umani, S., 1999. The mucilage phenomenon in the northern Adriatic Sea. A critical review of the present scientific hypotheses. Ann. Ist. Super. Sanità 35, 373–81.

Degobbis, D., Precali, R., Ivancic, I., Smodlaka, N., Fuks, D., Kveder, S., 2000. Long-term changes in the northern Atlantic ecosystem related to anthropogenic eutrophication. Int. J. Environ. Poll. 13, 495-533 https://doi.org/10.1504/IJEP.2000.002332

Degobbis, D., Precali, R., Ferrari, C.R., Djakovac, T., Rinaldi, A., Ivančić, I., Gismondi, M., Smodlaka, N., 2005. Changes in nutrient concentrations and ratios during mucilage events in the period 1999–2002. Sci. Total Environ. 353, 103–114. https://doi.org/10.1016/j.scitotenv.2005.09.010

Di Cicco, A., Sammartino, M., Marullo, S., Santoleri, R., 2017. Regional empirical algorithms for an improved identification of Phytoplankton Functional Types and Size Classes in the Mediterranean Sea using satellite data. Front. Mar. Sci. 4, 126. https://doi.org/10.3389/fmars.2017.00126

Djakovac, T., Degobbis, D., Supić, N., Precali, R., 2012. Marked reduction of eutrophication pressure in the northeastern Adriatic in the period 2000-2009. Estuar. Coast. Shelf Sci. 115, 25–32. https://doi.org/10.1016/j.ecss.2012.03.029

Doll, C., Main, C.R., Bianco, C., Coyne, K.J., Greenfield, D.I., 2014. Comparison of sandwich hybridization assay and quantitative PCR for the quantification of live and preserved cultures of *Heterosigma akashiwo* (Raphidophyceae). Limnol. Oceanogr. Methods 12, 232–245. https://doi.org/10.4319/lom.2014.12.232

Edler, L., Elbrachter, M., 2010. The Utermöhl method for quantitative phytoplankton analysis. In: Karlson, B., Cusack, C., Bresnan, E. (Eds.), *Microscopic and Molecular Methods for Quantitative Phytoplankton Analysis*. IOC UNESCO, Manuals and Guides, 55, pp. 13–20.

Edwards, M., Beaugrand, G., Kléparski, L., Hélaouët, P., Reid, P.C., 2022. Climate variability and multi-decadal diatom abundance in the Northeast Atlantic. Commun. Earth Environ. 3, 162. https://doi.org/10.1038/s43247-022-00492-9

Ershova, E.A., Wangensteen, O.S., Falkenhaug, T., 2023. Mock samples resolve biases in diversity estimates and quantitative interpretation of zooplankton metabarcoding data. Mar. Biodivers. 53, 66. https://doi.org/10.1007/s12526-023-01372-x

Falkowski, P., 2012. Ocean Science: The power of plankton. Nature 483, S17–S20. https://doi.org/10.1038/483S17a

Falkowski, P.G., Katz, M.E., Knoll, A.H., Quigg, A., Raven, J.A., Schofield, O., Taylor, F.J.R., 2004. The evolution of modern eukaryotic phytoplankton. Science 305, 354–360. https://doi.org/10.1126/science.1095964

Francé, J., Varkitzi, I., Stanca, E., Cozzoli, F., Skejić, S., Ungaro, N., Vascotto, I., Mozetič, P., Ninčević Gladan, Ž., Assimakopoulou, G., Pavlidou, A., Zervoudaki, S., Pagou, K., Basset, A., 2021. Large-scale testing of phytoplankton diversity indices for environmental assessment in Mediterranean sub-regions (Adriatic, Ionian and Aegean Seas). Ecol. Indic. 126, 107630. https://doi.org/10.1016/j.ecolind.2021.107630

Fu, W., Randerson, J.T., Moore, J.K., 2016. Climate change impacts on net primary production (NPP) and export production (EP) regulated by increasing stratification and phytoplankton community structure in the CMIP5 models. Biogeosciences 13, 5151–5170. https://doi.org/10.5194/bg-13-5151-2016

Giani, M., Rinaldi, A., Degobbis, D., 2005. Mucilages in the Adriatic and Tyrrhenian Sea: An introduction. Sci. Total Environ. 353, 3–9. https://doi.org/10.1016/j.scitotenv.2005.09.006

Giani, M., Djakovac, T., Degobbis, D., Cozzi, S., Solidoro, C., Fonda Umani, S., 2012. Recent changes in the marine ecosystems of the northern Adriatic Sea. Estuar. Coast. Shelf Sci. 115, 1–13. https://doi.org/10.1016/j.ecss.2012.08.023

Goodwin, K.D., Thompson, L.R., Duarte, B., Kahlke, T., Thompson, A.R., Marques, J.C., Caçador, I., 2017. DNA Sequencing as a tool to monitor marine ecological status. Front. Mar. Sci. 4, 107. https://doi.org/10.3389/fmars.2017.00107

Gordo, O., Barriocanal, C., Robson, D. (2011). Ecological impacts of the North Atlantic Oscillation (NAO) in Mediterranean ecosystems. In: Vicente-Serrano, S., Trigo, R. (Eds), *Hydrological, socioeconomic and ecological impacts of the North Atlantic Oscillation in the Mediterranean region*. *Advances in Global Change Research*, vol 46. Springer, Dordrecht. https://doi.org/10.1007/978-94-007-1372-7_11

Gran-Stadniczeñko, S., Egge, E., Hostyeva, V., Logares, R., Eikrem, W., Edvardsen, B., 2019. Protist diversity and seasonal dynamics in Skagerrak plankton communities as revealed by metabarcoding and microscopy. J. Eukaryot. Microbiol. 66, 494–513. https://doi.org/10.1111/jeu.12700

Grilli, F., Accoroni, S., Acri, F., Bernardi Aubry, F., Bergami, C., Cabrini, M., Campanelli, A., Giani, M., Guicciardi, S., Marini, M., Neri, F., Penna, A., Penna, P., Pugnetti, A., Ravaioli, M., Riminucci, F., Ricci, F., Totti, C., Viaroli, P., Cozzi, S., 2020. Seasonal and interannual trends of oceanographic parameters over 40 years in the Northern Adriatic Sea in relation to nutrient loadings using the EMODnet chemistry data portal. Water 12, 2280. https://doi.org/10.3390/w12082280

Groben, R., Medlin, L., 2005. *In situ* hybridization of phytoplankton using fluorescently labeled rRNA probes Method. Enzymol. 395, 299–310. https://doi.org/10.1016/S0076-6879(05)95018-0

Groom, S., Sathyendranath, S., Ban, Y., Bernard, S., Brewin, R., Brotas, V., Brockmann, C., Chauhan, P., Choi, J., Chuprin, A., Ciavatta, S., Cipollini, P., Donlon, C., Franz, B., He, X., Hirata, T., Jackson, T., Kampel, M., Krasemann, H., Lavender, S., Pardo-Martinez, S., Mélin, F., Platt, T., Santoleri, R., Skakala, J., Schaeffer, B., Smith, M., Steinmetz, F., Valente, A., Wang, M., 2019. Satellite ocean colour: current status and future perspective. Front. Mar. Sci. 6, 485. https://doi.org/10.3389/fmars.2019.00485

Hays, G.C., Richardson, A.J., Robinson, C., 2005. Climate change and marine plankton. Trends Ecol. Evol. 20, 337–344. https://doi.org/10.1016/j.tree.2005.03.004

Honsell, G., Boni, L., Cabrini, M., Pompei, M., 1992. Toxic or potentially toxic dinoflagellates from the Northern Adriatic Sea. In: R.A. Vollenweider, R. Marchetti, R. Viviani (Eds.), *Marine coastal eutrophication*, Elsevier, Amsterdam, pp. 107-114. https://doi.org/10.1016/B978-0-444-89990-3.50015-8

Joint, I., Groom, S.B., 2000. Estimation of phytoplankton production from space: current status and future potential of satellite remote sensing. J. Exp. Mar. Bio. Ecol. 250, 233–255. https://doi.org/10.1016/S0022-0981(00)00199-4

Käse, L., Geuer, J.K. (2018). Phytoplankton responses to marine climate change – An introduction. In: Jungblut, S., Liebich, V., Bode, M. (Eds), *YOUMARES 8 – Oceans Across Boundaries: Learning from each other*. Springer, Cham. https://doi.org/10.1007/978-3-319-93284-2_5

Kelly, R.P., Shelton, A.O., Gallego, R., 2019. Understanding PCR processes to draw meaningful conclusions from environmental DNA studies. Sci. Rep. 9, 12133. https://doi.org/10.1038/s41598-019-48546-x

Kezlya, E., Tseplik, N., Kulikovskiy, M., 2023. Genetic markers for metabarcoding of freshwater microalgae: review. Biology 12, 1038. https://doi.org/10.3390/biology12071038

Kwiatkowski, L., Torres, O., Bopp, L., Aumont, O., Chamberlain, M., Christian, J.R., Dunne, J.P., Gehlen, M., Ilyina, T., John, J.G., Lenton, A., Li, H., Lovenduski, N.S., Orr, J.C., Palmieri, J., Santana-Falcón, Y., Schwinger, J., Séférian, R., Stock, C.A., Tagliabue, A., Takano, Y., Tjiputra, J., Toyama, K., Tsujino, H., Watanabe, M., Yamamoto, A., Yool, A., Ziehn, T., 2020. Twenty-first century ocean warming, acidification, deoxygenation, and upper-ocean nutrient and primary production decline from CMIP6 model projections. Biogeosciences 17, 3439–3470. https://doi.org/10.5194/bg-17-3439-2020

Li, G., Cheng, L., Zhu, J., Trenberth, K.E., Mann, M.E., Abraham, J.P., 2020. Increasing ocean stratification over the past half-century. Nat. Clim. Chang. 10, 1116–1123. https://doi.org/10.1038/s41558-020-00918-2

López-Urrutia, Á., Martin, E.S., Harris, R.P., Irigoien, X., 2006. Scaling the metabolic balance of the oceans. Proc. Natl. Acad. Sci. 103, 8739–8744. https://doi.org/10.1073/pnas.0601137103

Marić, D., Kraus, R., Godrijan, J., Supić, N., Djakovac, T., Precali, R., 2012. Phytoplankton response to climatic and anthropogenic influences in the north-eastern Adriatic during the last four decades. Estuar. Coast. Shelf Sci. 115, 98–112. https://doi.org/10.1016/j.ecss.2012.02.003

Masotti, I., Aparicio-Rizzo, P., Yevenes, M.A., Garreaud, R., Belmar, L., Farías, L., 2018. The influence of river discharge on nutrient export and phytoplankton biomass off the central Chile Coast (33°–37°S): seasonal cycle and interannual variability. Front. Mar. Sci. 5, 423. https://doi.org/10.3389/fmars.2018.00423

McQuatters-Gollop, A., Atkinson, A., Aubert, A., Bedford, J., Best, M., Bresnan, E., Cook, K., Devlin, M., Gowen, R., Johns, D.G., Machairopoulou, M., McKinney, A., Mellor, A., Ostle, C., Scherer, C., Tett, P., 2019. Plankton lifeforms as a biodiversity indicator for regional-scale assessment of pelagic habitats for policy. Ecol. Indic. 101, 913–925. https://doi.org/10.1016/j.ecolind.2019.02.010

McQuatters-Gollop, A., Guérin, L., Arroyo, N.L., Aubert, A., Artigas, L.F., Bedford, J., Corcoran, E., Dierschke, V., Elliott, S.A.M., Geelhoed, S.C.V., Gilles, A., González-Irusta, J.M., Haelters, J., Johansen, M., Le Loc'h, F., Lynam, C.P., Niquil, N., Meakins, B., Mitchell, I., Padegimas, B., Pesch, R., Preciado, I., Rombouts, I., Safi, G., Schmitt, P., Schückel, U., Serrano, A., Stebbing, P., De la Torriente, A., Vina-Herbon, C., 2022. Assessing the state of marine biodiversity in the Northeast Atlantic. Ecol. Indic. 141, 109148. https://doi.org/10.1016/j.ecolind.2022.109148

Medlin, L.K., Kooistra, W.H.C.F., 2010. Methods to estimate the diversity in the marine photosynthetic protist community with illustrations from case studies: a review. Diversity 2, 973–1014. https://doi.org/10.3390/d2070973

Meek, M.E., Van Dolah, F.M., 2016. Phytoplankton IF-FISH: Species-specific labeling of cellular proteins by immunofluorescence (IF) with simultaneous species identification by fluorescence immunohybridization (FISH). J. Microbiol. Methods 124, 21–27. https://doi.org/https://doi.org/10.1016/j.mimet.2016.02.017

Mentaschi, L., Lovato, T., Butenschön, M., Alessandri, J., Aragão, L., Verri, G., Guerra, R., Coppini, G., Pinardi, N., 2024. Projected climate oligotrophication of the Adriatic marine ecosystems. Front. Clim. 6, 1338374. https://doi.org/10.3389/fclim.2024.1338374

Mesquita, M.C.B., Prestes, A.C.C., Gomes, A.M.A., Marinho, M.M., 2020. Direct Effects of Temperature on Growth of Different Tropical Phytoplankton Species. Microb. Ecol. 79, 1–11. https://doi.org/10.1007/s00248-019-01384-w

Meyer, J., Riebesell, U., 2015. Reviews and Syntheses: responses of coccolithophores to ocean acidification: a meta-analysis. Biogeosciences 12, 1671–1682. https://doi.org/10.5194/bg-12-1671-2015

Moisan, T.A., Rufty, K.M., Moisan, J.R., Linkswiler, M.A., 2017. Satellite observations of Phytoplankton Functional Type spatial distributions, phenology, diversity, and ecotones. Front. Mar. Sci. 4, 189. https://doi.org/10.3389/fmars.2017.00189

Montanari, A., 2012. Hydrology of the Po River: looking for changing patterns in river discharge. Hydrol. Earth Syst. Sci. 16, 3739–3747. https://doi.org/10.5194/hess-16-3739-2012

Montanari, A., Nguyen, H., Rubinetti, S., Ceola, S., Galelli, S., Rubino, A., Zanchettin, D., 2023. Why the 2022 Po River drought is the worst in the past two centuries. Sci. Adv. 9, eadg8304. https://doi.org/10.1126/sciadv.adg8304

Mordret, S., Piredda, R., Vaulot, D., Montresor, M., Kooistra, W.H.C.F., Sarno, D., 2018. dinoref: A curated dinoflagellate (Dinophyceae) reference database for the 18S rRNA gene. Mol. Ecol. Resour. 18, 974–987. https://doi.org/https://doi.org/10.1111/1755-0998.12781

Mozetič, P., Solidoro, C., Cossarini, G., Socal, G., Precali, R., Francé, J., Bianchi, F., De Vittor, C., Smodlaka, N., Fonda Umani, S., 2010. Recent trends towards oligotrophication of the Northern Adriatic: evidence from chlorophyll a time series. Estuaries Coasts 33, 362–375. https://doi.org/10.1007/s12237-009-9191-7

Naselli-Flores, L., Padisák, J., 2023. Ecosystem services provided by marine and freshwater phytoplankton. Hydrobiologia 850, 2691–2706. https://doi.org/10.1007/s10750-022-04795-y

Neri, F., Romagnoli, T., Accoroni, S., Campanelli, A., Marini, M., Grilli, F., Totti, C., 2022. Phytoplankton and environmental drivers at a long-term offshore station in the northern Adriatic Sea (1988–2018). Cont. Shelf Res. 242, 104746. https://doi.org/10.1016/j.csr.2022.104746

Neri, F., Romagnoli, T., Accoroni, S., Ubaldi, M., Garzia, A., Pizzuti, A., Campanelli, A., Grilli, F., Marini, M., Totti, C., 2023. Phytoplankton communities in a coastal and offshore stations of the northern Adriatic Sea approached by network analysis and different statistical descriptors. Estuar. Coast. Shelf Sci. 282, 108224. https://doi.org/10.1016/j.ecss.2023.108224

Paczkowska, J., Brugel, S., Rowe, O., Lefébure, R., Brutemark, A., Andersson, A., 2020. Response of coastal phytoplankton to high inflows of terrestrial matter. Front. Mar. Sci. 7, 80. https://doi.org/10.3389/fmars.2020.00080

Pawlowski, J., Christen, R., Lecroq, B., Bachar, D., Shahbazkia, H.R., Amaral-Zettler, L., Guillou, L., 2011. Eukaryotic richness in the abyss: Insights from Pyrotag sequencing. PLoS One 6, e18169. https://doi.org/10.1371/journal.pone.0018169

Petrou, K., Baker, K.G., Nielsen, D.A., Hancock, A.M., Schulz, K.G., Davidson, A.T., 2019. Acidification diminishes diatom silica production in the Southern Ocean. Nat. Clim. Chang. 9, 781–786. https://doi.org/10.1038/s41558-019-0557-y

Piganeau, G., Eyre-Walker, A., Grimsley, N., Moreau, H., 2011. How and Why DNA Barcodes Underestimate the Diversity of Microbial Eukaryotes. PLoS One 6, e16342. https://doi.org/10.1371/journal.pone.0016342

Pisano, A., Marullo, S., Artale, V., Falcini, F., Yang, C., Leonelli, F.E., Santoleri, R., Nardelli, B.B., 2020. New evidence of Mediterranean climate change and variability from Sea Surface Temperature observations. Remote Sens. 12, 132. https://doi.org/10.3390/RS12010132

Poulain, P.-M., Cushman-Roisin, B., 2001. Circulation. In: Cushman-Roisin, B., Gačić, M., Poulain, P.-M., Artegiani, A. (Eds), *Physical oceanography of the Adriatic Sea: Past, present and future.* Kluwer Academic Publishers, Dordrecht, The Netherlands, pp. 67–109.

Poulain, P.-M., Raicich, F., 2001. Forcings. In: Cushman-Roisin, B., Gačić, M., Poulain, P.-M., Artegiani, A. (Eds.), *Physical oceanography of the Adriatic Sea: past, present and future.* Springer Netherlands, Dordrecht, pp. 45–65. https://doi.org/10.1007/978-94-015-9819-4_2

Preston, M., Fritzsche, M., Woodcock, P., 2022. JNCC Report Understanding and mitigating errors and biases in metabarcoding: an introduction for non-specialists. JNCC Report No. 699 JNCC, Peterborough.

Raicich, F., 1996. On the fresh balance of the Adriatic Sea. J. Mar. Syst. 9, 305–319. https://doi.org/10.1016/S0924-7963(96)00042-5

Rombouts, I., Simon, N., Aubert, A., Cariou, T., Feunteun, E., Guérin, L., Hoebeke, M., McQuatters-Gollop, A., Rigaut-Jalabert, F., Artigas, L.F., 2019. Changes in marine phytoplankton diversity: Assessment under the Marine Strategy Framework Directive. Ecol. Indic. 102, 265–277. https://doi.org/10.1016/j.ecolind.2019.02.009

Roselli, L., Basset, A., 2015. Decoding size distribution patterns in marine and transitional water phytoplankton: from community to species level. PLoS One 10, e0127193. https://doi.org/10.1371/journal.pone.0127193

Russo, A., Artegiani, A., 1996. Adriatic Sea hydrography. Sci. Mar. 60, 33–43.

Russo, A., Maccaferri, S., Djakovac, T., Precali, R., Degobbis, D., Deserti, M., Paschini, E., Lyons, D.M., 2005. Meteorological and oceanographic conditions in the northern Adriatic Sea during the period June 1999–July 2002: Influence on the mucilage phenomenon. Sci. Total Environ. 353, 24–38. https://doi.org/10.1016/j.scitotenv.2005.09.058

Sallée, J.-B., Pellichero, V., Akhoudas, C., Pauthenet, E., Vignes, L., Schmidtko, S., Garabato, A.N., Sutherland, P., Kuusela, M., 2021. Summertime increases in upper-ocean stratification and mixed-layer depth. Nature 591, 592–598. https://doi.org/10.1038/s41586-021-03303-x

Santoferrara, L.F., 2019. Current practice in plankton metabarcoding: Optimization and error management. J. Plankton Res. 41, 571–582. https://doi.org/10.1093/plankt/fbz041

Segura, A.M., Kruk, C., Calliari, D., García-Rodriguez, F., Conde, D., Widdicombe, C.E., Fort, H., 2013. Competition Drives Clumpy Species Coexistence in Estuarine Phytoplankton. Sci. Rep. 3, 1037. https://doi.org/10.1038/srep01037

Seneviratne, S.I., Zhang, X., Adnan, M., Badi, W., Dereczynski, C., Di Luca, A., Ghosh, S., Iskandar, I., Kossin, J., Lewis, S., Otto, F., Pinto, I., Satoh, M., Vicente-Serrano, S.M., Wehner, M., Zhou, B., 2021. Weather and climate extreme events in a changing climate. In: Masson-Delmotte, V., Zhai, P., Pirani, A., Connors, S.L., Péan, C., Berger, S., Caud, N., Chen, Y., Goldfarb, L., Gomis, M.I., Huang, M., Leitzell, K., Lonnoy, E., Matthews, J.B.R., Maycock, T.K., Waterfield, T., Yelekçi, O., Yu, R., B.Z. (Eds.), *Climate Change 2021 – The Physical Science Basis: Working Group I Contribution to the Sixth Assessment Report of the Intergovernmental Panel on Climate Change*. Cambridge University Press, Cambridge, United Kingdom and New York, NY, USA, pp. 1513–1766. https://doi.org/10.1017/9781009157896.013

Shaltout, M., Omstedt, A., 2014. Recent sea surface temperature trends and future scenarios for the Mediterranean Sea. Oceanologia 56, 411–443. https://doi.org/https://doi.org/10.5697/oc.56-3.411

Solidoro, C., Bastianini, M., Bandelj, V., Codermatz, R., Cossarini, G., Melaku Canu, D., Ravagnan, E., Salon, S., Trevisani, S., 2009. Current state, scales of variability, and trends of biogeochemical properties in the northern Adriatic Sea. J. Geophys. Res. Ocean. 114, C07S91. https://doi.org/10.1029/2008JC004838

Sommer, U., Lengfellner, K., 2008. Climate change and the timing, magnitude, and composition of the phytoplankton spring bloom. Glob. Chang. Biol. 14, 1199–1208. https://doi.org/https://doi.org/10.1111/j.1365-2486.2008.01571.x

Soulié, T., Vidussi, F., Mas, S., Mostajir, B., 2022. Functional stability of a coastal Mediterranean plankton community during an experimental marine heatwave. Front. Mar. Sci. 9, 831496. https://doi.org/10.3389/fmars.2022.831496

Stoeck, T., Bass, D., Nebel, M., Christen, R., Jones, M.D.M., Breiner, H.W., Richards, T.A., 2010. Multiple marker parallel tag environmental DNA sequencing reveals a highly complex eukaryotic community in marine anoxic water. Mol. Ecol. 19, 21–31. https://doi.org/10.1111/j.1365-294X.2009.04480.x

Struck, T.H., Feder, J.L., Bendiksby, M., Birkeland, S., Cerca, J., Gusarov, V.I., Kistenich, S., Larsson, K.H., Liow, L.H., Nowak, M.D., Stedje, B., Bachmann, L., Dimitrov, D., 2017. Finding evolutionary processes hidden in cryptic species. Trends Ecol. Evol. 33, 153–163. https://doi.org/10.1016/j.tree.2017.11.007

Sun, X., Shen, F., Liu, D., Bellerby, R.G.J., Liu, Y., Tang, R., 2018. In situ and satellite observations of phytoplankton size classes in the entire continental shelf sea, China. J. Geophys. Res. Ocean. 123, 3523–3544. https://doi.org/https://doi.org/10.1029/2017JC013651

Taberlet, P., Coissac, E., Pompanon, F., Brochmann, C., Willerslev, E., 2012. Towards next-generation biodiversity assessment using DNA metabarcoding. Mol. Ecol. 21, 2045–2050. https://doi.org/https://doi.org/10.1111/j.1365-294X.2012.05470.x

Taucher, J., Bach, L.T., Prowe, A.E.F., Boxhammer, T., Kvale, K., Riebesell, U., 2022. Enhanced silica export in a future ocean triggers global diatom decline. Nature 605, 696–700. https://doi.org/10.1038/s41586-022-04687-0

Tojčić, I., Denamiel, C., Vilibić, I., 2023. Kilometer-scale trends and variability of the Adriatic present climate (1987–2017). Clim. Dyn. 61, 2521–2545. https://doi.org/10.1007/s00382-023-06700-2

Totti, C., Cangini, M., Ferrari, C., Kraus, R., Pompei, M., Pugnetti, A., Romagnoli, T., Vanucci, S., Socal, G., 2005. Phytoplankton size-distribution and community structure in relation to mucilage occurrence in the northern Adriatic Sea. Sci. Total Environ. 353, 204–217. https://doi.org/10.1016/j.scitotenv.2005.09.028

Totti, C., Romagnoli, T., Accoroni, S., Coluccelli, A., Pellegrini, M., Campanelli, A., Grilli, F., Marini, M., 2019. Phytoplankton communities in the northwestern Adriatic Sea: interdecadal variability over a 30-years period (1988–2016) and relationships with meteoclimatic drivers. J. Mar. Syst. 193, 137–153. https://doi.org/10.1016/j.jmarsys.2019.01.007

Trombetta, T., Vidussi, F., Mas, S., Parin, D., Simier, M., Mostajir, B., 2019. Water temperature drives phytoplankton blooms in coastal waters. PLoS One 14, e0214933. https://doi.org/10.1371/journal.pone.0214933

Turk, V., Hagström, Å., Kovač, N., Faganeli, J., 2010. Composition and function of mucilage macroaggregates in the northern Adriatic. Aquat. Microb. Ecol. 61, 279-289 https://doi.org/10.3354/ame01447

Tweddle, J.F., Gubbins, M., Scott, B.E., 2018. Should phytoplankton be a key consideration for marine management? Mar. Policy 97, 1–9. https://doi.org/10.1016/j.marpol.2018.08.026

Tzafesta, E., Saccomanno, B., Zangaro, F., Vadrucci, M.R., Specchia, V., Pinna, M., 2022. DNA barcode gap analysis for multiple marker genes for phytoplankton species biodiversity in Mediterranean aquatic ecosystems. Biology 11, 1277. https://doi.org/10.3390/biology11091277

Vallina, S.M., Simó, R., 2007. Strong relationship between DMS and the solar radiation dose over the global surface ocean. Science 315, 506–508. https://doi.org/10.1126/science.1133680

Varkitzi, I., Francé, J., Basset, A., Cozzoli, F., Stanca, E., Zervoudaki, S., Giannakourou, A., Assimakopoulou, G., Venetsanopoulou, A., Mozetič, P., Tinta, T., Skejic, S., Vidjak, O., Cadiou, J.F., Pagou, K., 2018. Pelagic habitats in the Mediterranean Sea: a review of Good Environmental Status (GES) determination for plankton components and identification of gaps and priority needs to improve coherence for the MSFD implementation. Ecol. Indic. 95, 203–218. https://doi.org/10.1016/j.ecolind.2018.07.036

Vasselon, V., Domaizon, I., Rimet, F., Kahlert, M., Bouchez, A., 2017. Application of high-throughput sequencing (HTS) metabarcoding to diatom biomonitoring: do DNA extraction methods matter? Freshw. Sci. 36, 162–177. https://doi.org/10.1086/690649

Vilibić, I., Supić, N., 2005. Dense water generation on a shelf: the case of the Adriatic Sea. Ocean Dyn. 55, 403–415. https://doi.org/10.1007/s10236-005-0030-5

Vilicic, D., Kuzmic, M., Tomažić, I., Ljubešić, Z., Bosak, S., Precali, R., Djakovac, T., Marić, D., Godrijan, J., 2013. Northern Adriatic phytoplankton response to short Po River discharge pulses during summer stratified conditions. Mar. Ecol. 34, 451–466. https://doi.org/10.1111/maec.12046

Wang, G., Moisan, J., 2021. Remote sensing of phytoplankton pigments. In: Pereira, L., Gonçalves, A.M. (Eds.), *Plankton Communities*. IntechOpen, Rijeka. https://doi.org/10.5772/intechopen.95381

Wasmund, N., Kownacka, J., Göbel, J., Jaanus, A., Johansen, M., Jurgensone, I., Lehtinen, S., Powilleit, M., 2017. The diatom/dinoflagellate index as an indicator of ecosystem changes in the Baltic Sea 1. principle and handling instruction. Front. Mar. Sci. 4, 22. https://doi.org/10.3389/FMARS.2017.00022

Wetz, M.S., Hutchinson, E.A., Lunetta, R.S., Paerl, H.W., Christopher Taylor, J., 2011. Severe droughts reduce estuarine primary productivity with cascading effects on higher trophic levels. Limnol. Oceanogr. 56, 627–638. https://doi.org/https://doi.org/10.4319/lo.2011.56.2.0627

Wu, F., Guo, J., Duan, H., Li, T., Wang, Yanan, Wang, Yuntao, Wang, S., Feng, Y., 2023. Ocean acidification affects the response of the coastal coccolithophore *Pleurochrysis carterae* to irradiance. Biology 12, 1249. https://doi.org/10.3390/biology12091249

Xiao, X., Sogge, H., Lagesen, K., Tooming-Klunderud, A., Jakobsen, K.S., Rohrlack, T., 2014. Use of High Throughput Sequencing and light microscopy show contrasting results in a study of phytoplankton occurrence in a freshwater environment. PLoS One 9, e106510. https://doi.org/10.1371/journal.pone.0106510

Zanchettin, D., Traverso, P., Tomasino, M., 2006. Discussion on sea level fluctuations along the Adriatic coasts coupling to climate indices forced by solar activity: Insights into the future of Venice. Glob. Planet. Change 50, 226–234. https://doi.org/https://doi.org/10.1016/j.gloplacha.2006.01.001

Zanchettin, D., Traverso, P., Tomasino, M., 2008. Po River discharges: a preliminary analysis of a 200-year time series. Clim. Change 89, 411–433. https://doi.org/10.1007/s10584-008-9395-z

Chapter 1

Phytoplankton community and dynamics in an eLTER site

Chapter 1.1

Phytoplankton and environmental drivers at a long-term offshore station in the northern Adriatic Sea (1988–2018)

Neri F., Romagnoli T., Accoroni S., Campanelli A., Marini M., Grilli F., Totti C. (2022) Phytoplankton and environmental drivers at a long-term offshore station in the northern Adriatic Sea (1988-2018). *Continental Shelf Research*, 242: 104746. DOI: 10.1016/j.csr.2022.104746

Phytoplankton and environmental drivers at a long-term offshore station in the northern Adriatic Sea (1988–2018)

Francesca Neri[1], Tiziana Romagnoli[1], Stefano Accoroni[1,2*], Alessandra Campanelli[3], Mauro Marini[3], Federica Grilli[3], Cecilia Totti[1,2]

[1]Dipartimento di Scienze della Vita e dell'Ambiente, Università Politecnica delle Marche, via Brecce Bianche, 60131 Ancona, Italy

[2]Consorzio Interuniversitario per le Scienze del Mare, CoNISMa, ULR Ancona, Ancona, Italy

[3]Consiglio Nazionale delle Ricerche, CNR-IRBIM, Largo Fiera della Pesca, 2, 60125 Ancona, Italy

*Corresponding Author: s.accoroni@univpm.it

Keywords:

Phytoplankton; Interannual variability; LTER-Long-term ecosystem research; Biodiversity; Biological oceanography

1.1.1 Abstract

A long term (1988–2018) data set of phytoplankton and physico-chemical parameters was analyzed for the first time in an offshore station of the LTER Senigallia-Susak transect (northern Adriatic Sea) not directly affected by the coastal nutrient input. The mean annual cycle of phytoplankton markedly differed from that observed in the coastal areas, showing the maximum in June and the minimum in November. The main component of phytoplankton community was represented by phytoflagellates, whose trend paralleled that of total phytoplankton. On average, diatoms peaked in July, dinoflagellates in June and coccolithophores in April. The phytoplankton maximum in summer is explained mainly by the allochthonous input of DIN and PO_4 carried by the low salinity waters expanding eastward, during the stratification of water column. Resuspension processes seem to be less effective for PO_4 than for DIN. The most representative phytoplankton taxa for each season as indicated by the IndVal analysis were identified and were only in part similar to those observed in the coastal area. The interannual anomaly trend showed a significant increase of temperature, DIN and phosphates. Although no significant changes were found for the total phytoplankton, a reduction of winter dinoflagellate and coccolithophore abundances was observed.

1.1.2 Introduction

Phytoplankton community dynamics are considered as a key indicator to detect changes in the marine ecosystems as they show a rapid turnover, and they are directly related to the abiotic parameters. For these reasons, phytoplankton diversity and temporal changes are included in the Marine Strategy Framework Directive (MSFD) as an indicator for the Good Environmental Status assessment (2008/56/EC). In the light of this, long-term studies focusing on the status of biological communities and environmental conditions in pelagic habitats are strategic and precious tools, as they allow to detect changes and trends and they serve as baseline for the GES definition.

The Northern Adriatic (NA), one of the most productive areas of the Mediterranean (D'Ortenzio and Ribera d'Alcalà, 2009), is highly influenced by river floods that affect both the circulation and the

trophic state (Campanelli et al., 2011; Cozzi and Giani, 2011), by introducing a large amount of both inorganic and organic nutrients (Brush et al., 2021; Degobbis et al., 2000; Marini et al., 2008). These low-salinity and nutrient-rich waters affect the NA trophic state in different ways depending on the stability conditions of water column: during the stratification regime (spring-summer), the Po River outflow spreads horizontally at the surface layer forming a plume that affect a great part of the NA (Viličić et al., 2013), while during mixing regime (autumn-winter) the plume is less pronounced, and the freshwater input is mainly deviated southward by the Western Adriatic Current (WAC). As a result, the position of frontal system, separating the low salinity eutrophic waters from the high salinity oligotrophic ones, is highly dynamic and dependent on the above-mentioned conditions (Franco and Michelato, 1992). Another factor affecting the nutrient cycle in the NA is the general water masses' circulation that is strongly influenced by winds, with significant differences between winter, mainly Sirocco (SE) and Bora (NE) and summer mainly Mistral (NW) (Russo and Artegiani, 1996). In particular, the cold Bora wind, occurring frequently in fall and winter seasons, plays a significant role in determining the cooling and mixing of the water column and in the formation of Northern Adriatic Dense Water (NAdDW), flowing then southward (Bergamasco et al., 1999; Marini et al., 2006; Vilibić and Supić, 2005).

In the Adriatic Sea, four subregions have been recognized so far, based on their differences in terms of trophic state, phytoplankton biomass and annual trend (Fonda Umani, 1996; Franco and Michelato, 1992): (i) the NA, including a narrow coastal belt along the western coast, which is characterized by high production, (ii) the open waters characterized by low production, (iii) the eastern coastal waters with moderate production and (iv) the zones (lagoons and embayments) under strong coastal influences.

The bulk of knowledge about phytoplankton trends and community composition of the NA is concentrated in coastal areas of both western (Bernardi Aubry et al., 2004, 2006, 2012; Penna et al., 2004; Pugnetti et al., 2004, 2008; Totti et al., 1999, 2005, 2019; Zoppini et al., 1995) and eastern

(Cabrini et al., 2012; Cerino et al., 2019; Fuks et al., 2012; Mozetič et al., 1998, 2010, 2012; Viličić et al., 2009) sides, where monitoring activities are easier and more frequent than offshore, where data are collected with an irregular frequency. The phytoplankton annual cycle varies among the NA areas. Along the northwestern coast, there is an intense diatom winter bloom, which is responsible for the highest values of abundance and biomass of the year, followed by classic spring and autumn blooms (Bernardi Aubry et al., 2004; Totti et al., 2019). Instead, the eastern part of the NA is characterized by typical spring and autumn blooms (Cerino et al., 2019; Marić et al., 2012). Anyway, at interannual scale, several studies have reported changes in the phytoplankton annual maximum and shifts in the seasonality of blooms in the entire NA (Cerino et al., 2019; Marić et al., 2012; Mozetič et al., 2010; Totti et al., 2019).

The Senigallia-Susak transect (SS), located in the lower part of the NA, represents a LTER (Long-Term Ecosystem Research) site, where physico-chemical parameters and phytoplankton abundance, biomass and species composition have been recorded since 1988. In the SS, the WAC is sharper than in the northernmost part of the NA (Russo and Artegiani, 1996), and the position of the frontal system separating nutrient rich coastal waters from oligotrophic offshore waters is located near the 10 nM.

In this study, we analyzed a long-term data set referred to a station located at 15 nM, beyond the border of the WAC, with the aim to depict (i) the temporal variability of physico-chemical parameters and phytoplankton both at an intra-annual and interannual scale, (ii) the phytoplankton community composition and (iii) the relationships between phytoplankton and environmental parameters in an offshore area not directly affected by the coastal nutrients input.

1.1.3 Materials and methods

Sampling

Sampling was carried out at the SG05 station (43°54.460 N, 13°26.941 E) (bottom depth 55 m) located at 15 nM from the Italian coast (Fig. 1) on board of several oceanographic vessels (S. Lo Bianco, G. Dallaporta, Tethis, Copernaut Franca, Urania, Alliance, Minerva, Bannock, D'Ancona)

since July 1988 to December 2018 with a variable time frequency (from monthly to quarterly) and with periods of interruptions the longest of which was between 2003 and 2012 for phytoplankton sampling. A total of 11,339 samples were collected. Sampling dates for each parameter are indicated in the Table S1.

From 1988 to 1991, Conductivity-Temperature-Depth (CTD) data were acquired by a Neil Brown Instrument System (NBIS), while after 1992 with a SeaBird Electronic SBE 911plus. Dissolved oxygen was directly analyzed on board according to Winkler (1888), and samples were immediately fixed and stored in the dark and analyzed within 24 h. From 1988 to 1998 the oxygen concentrations were determined using titration and then after 1998 by potentiometric method (Furuya and Harada, 1995).

Water samples for determination of dissolved inorganic nutrients (nitrite-NO_2, nitrate-NO_3, ammonia-NH_4, orthophosphate-PO_4 and orthosilicate-$Si(OH)_4$) and for phytoplankton analysis were collected by Rosette system equipped with Niskin bottles. Filtration was done directly on board and significant sample alterations were excluded as: (i) as soon as the Niskin bottle was on board, water was sampled with a closed filtration system without any contact with air, (ii) the filtrated was closed in a 4 ml compressed polyethylene tube and rapidly frozen, (iii) unfreezing phase was as rapidly and the analysis was done directly on the tube, without further pouring. Sampled quotes for nutrients and phytoplankton were: surface (0–5 m layer), 1–2 intermediate depths, generally at the base of mixed layer and the maximum fluorescence depth (between 10 and 40 m) and 1 m above the bottom (54 m). Samples for nutrient analysis were filtered (GF/F Whatman, 0.7 μm), and stored at –22 °C in polyethylene vials until analysis. Water samples for phytoplankton analysis were collected in 250 ml dark glass bottles and preserved by adding 0.8% formaldehyde (prefiltered and neutralized with hexamethylenetetramine) (Throndsen, 1978) until analysis.

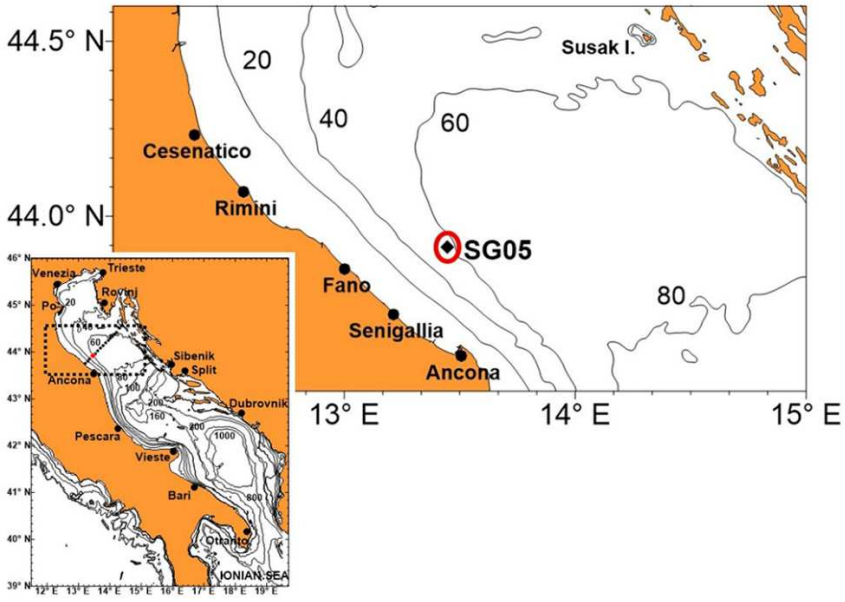

Fig. 1. Map of the study area indicating the position of sampling station. In the small box, the Senigallia-Susak transect is shown and the study station is indicated by the red colour.

Nutrient analysis

Nutrient analysis was carried out using a PerkinElmer spectrophotometer 550A model in the period 1988 to 1998, an autoanalyzer TRAACS 800 BRAN + LUEBBE in 1999–2005 and an autoanalyzer QUAATRO Technicon (Strickland and Parsons, 1972) after 2005. Dissolved Inorganic Nitrogen (DIN) is intended as the sum of NO_2, NO_3 and NH_4 concentrations.

Phytoplankton analysis

Identification and counting of phytoplankton were carried out using an inverted microscope (ZEISS Axiovert 135) equipped with phase contrast, following the Utermöhl method (Edler and Elbrachter, 2010). Counting was carried out at 400x magnification, along transects or in random visual fields, depending on cell abundance, to count a minimum of 200 cells. Moreover, a half of the Utermöhl chamber was analyzed at 200x magnification for a more precise estimation of less abundant microphytoplanktonic taxa.

Phytoplankton taxa were grouped into major groups (diatoms, dinoflagellates, coccolithophores, phytoflagellates and others), and abundances were expressed as cells l^{-1}. Biomass measurements through biovolumes did not cover all the sampling period, therefore they were not considered in this study. Dinoflagellates were considered as a taxonomical group and both autotrophic and heterotrophic species were included in counting. Phytoflagellates are an informal group that includes haptophytes (except coccolithophores), cryptophytes, chrysophytes, dictyochophytes, raphidophytes, chlorophytes and euglenophytes. Others include cyanophytes and incertae sedis.

Statistical analysis

The surface layer (0–5 m) was considered for the statistical analysis. The interannual anomalies of physico-chemical parameters were calculated by the difference between each monthly value and the mean monthly value of the entire series. Then linear regression was calculated by means of the ordinary least square method. Unfortunately, due to the interruption in the phytoplankton sampling from 2003 to 2012, we could not analyze the interannual variability of phytoplankton using the same method as for physico-chemical parameters. Therefore, we compared, in terms of phytoplankton abundances, two periods (1988–2002 and 2013–2018), by a one-way analysis of variance (ANOVA). Abundances were rank transformed prior to analysis. When significant differences for the main effect were observed ($p < 0.05$), a Tukey's pairwise comparison test was also performed.

Relationships between environmental parameters and phytoplankton group abundances were studied through Principal Component Analysis (PCA) performed on a correlation matrix of ranked monthly values of physico-chemical parameters, as active variables, and phytoplankton group abundances, as supplementary variables. Furthermore, Pearson's correlations were performed on the same rank transformed variables.

The above statistical analyses were conducted using STATISTICA 12 (StatSoft Inc., Tulsa, OK, USA) software.

To identify phytoplankton key species, the Indicator Value (IndVal) was applied, which combines the relative abundance of a species with its relative frequency of occurrence in a given period (Dufrêne and Legendre, 1997). The IndVal was here calculated on a seasonal basis, considering climatological seasons, as done in other oceanographic studies (Bernardi-Aubry et al., 2006; Grilli et al., 2005, 2020; Totti et al., 2019): winter = January, February, March; spring = April, May, June; summer = July, August, September; autumn = October, November, December.

1.1.4 Results

Physico-chemical parameters

Temporal variability in the water column

The time evolution of physico-chemical parameters in the water column from 1988 to 2018 at the SG05 station is shown in Figs. 2 and 3.

Temperature (Fig. 2A) showed a strong interannual signal. An overall increase of temperature can be visually detected, with prolonged cooler periods in the bottom layer at the beginning of the series (e.g., 1988–1994) and shorter periods of warmer temperatures more frequent in the second part of the series (e.g., 2000–2001, 2007, 2014 and 2017). Maximum values (around 26–27 °C) at the surface were reached in summer 1998, 2000 and 2012. Regarding the salinity, prolonged periods of high salinity (i.e., >38) were observed below 10 m depth (e.g., 1988–1991, 2002–2007 and 2012–2013, 2015–2018), interrupted by shorter periods of lower salinity values (e.g., 1996, 1998–1999, 2001 and 2009–2011, 2014) (Fig. 2B).

Seawater density (Fig. 2C) showed values higher than 29.2 kg m^{-3} (considered the threshold for the Adriatic dense waters, Artegiani et al., 1989) measured from 30 m down to the bottom in winter 1993, 1998, 2000, 2002, 2004, 2017 and 2018. The highest value (>29. 6 kg m^{-3} corresponding to NAdDW) was recorded at the bottom layer in 2012 in accordance with the well documented exceptional dense water formation on the Adriatic shelf (Mihanović et al., 2013).

Oxygen saturation showed values under 100% in the bottom layer of the entire series and along the water column in 1999, 2010–2011 and 2013–2014. The deeper part of the SG05 station with lower dissolved oxygen values (Fig. 2D) was characterized by higher concentration of $Si(OH)_4$ (Fig. 3D).

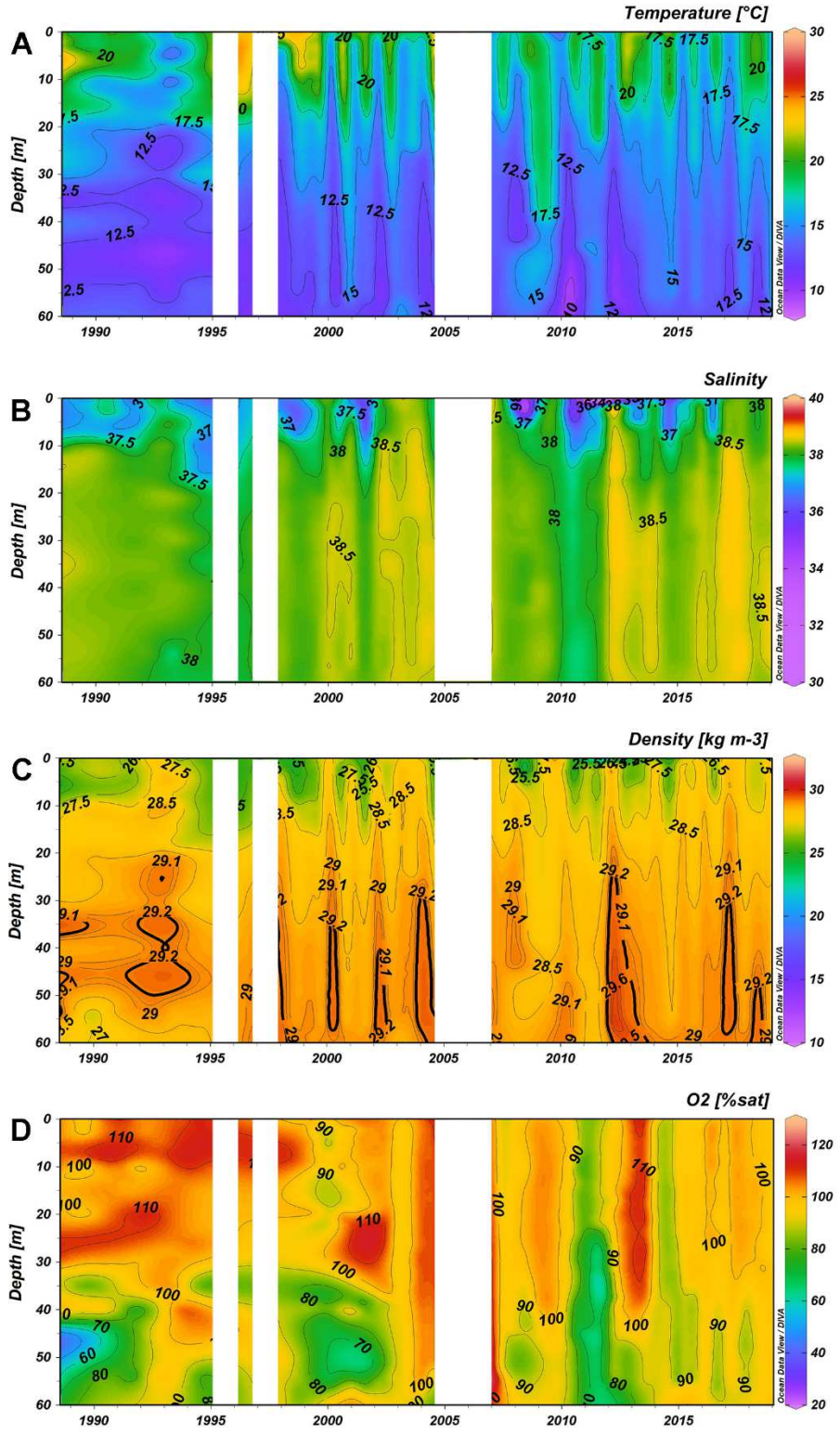

Fig. 2. Temporal and vertical variations of (A) temperature (°C), (B) salinity, (C) density (kg m^{-3}), where the 29.2 kg m^{-3} isoline is thicker marked, and (D) dissolved oxygen (% sat) at SG05 station.

Nutrient concentrations in the water column along the study period are shown in Fig. 3. High concentrations of DIN (Fig. 3A) were recorded in correspondence of lower salinity values (Fig. 2B) related to the higher Po River flow (not shown) in November 2010, May 2013, and November 2014. In winter 2012, a cold and high-salinity water mass with high DIN values was observed at 20 m depth (Fig. 3A), and this water mass extended even eastward (data not shown). Time evolution of orthophosphate (Fig. 3B) showed higher values in the last decade. High values were often observed below 40 m depth, and at 0–10 m layer in December 2007 and June 2008, corresponding to relatively low salinity values. Concentrations of silicate were higher (>3 µM) below the 30 m depth, with peaks in 2001, 2010 and 2014. Only in 1989 a higher value (6 µM) was recorded at 10 m (Fig. 3C).

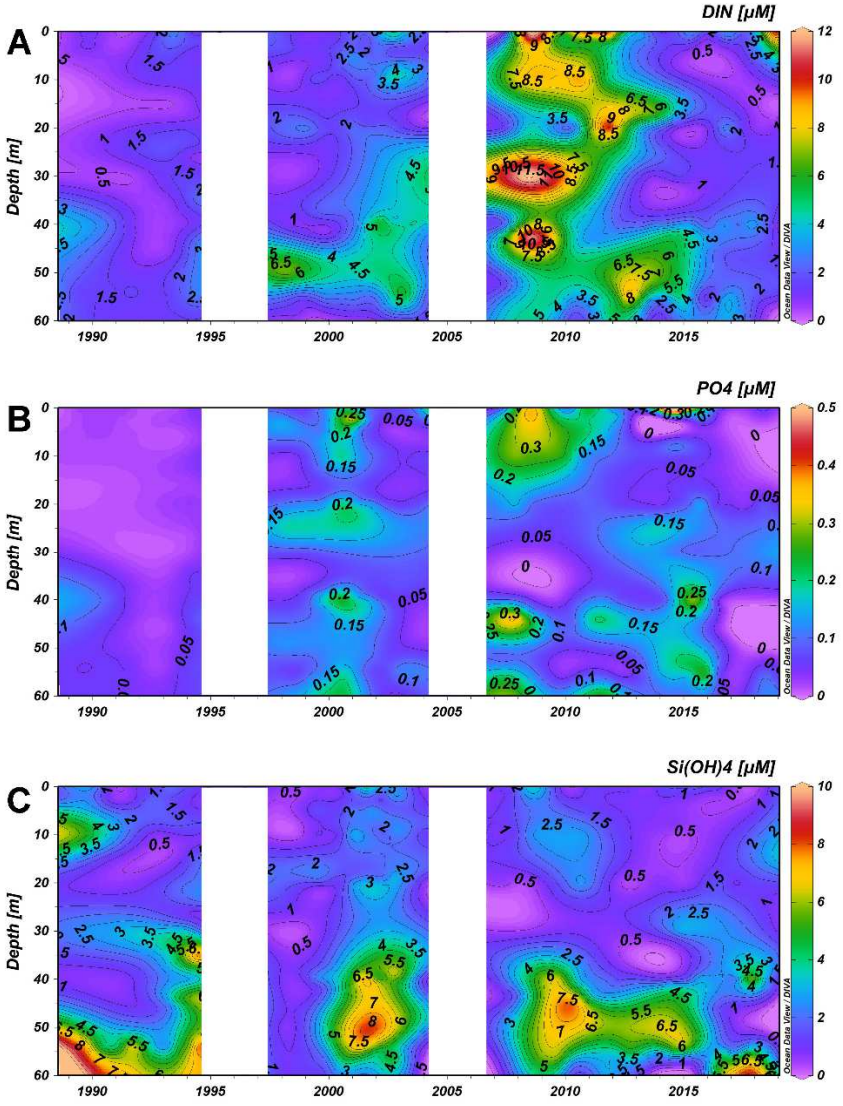

Fig. 3. Temporal and vertical variations of (A) Dissolved Inorganic Nitrogen (DIN), (B) orthophosphate (PO_4) and (C) orthosilicate ($Si(OH)_4$) concentrations (µM).

Mean annual cycle

The annual cycle of physico-chemical parameters at the surface layer is shown in Fig. 4, where mean monthly values (mean ± standard error) are shown.

Seawater temperature showed minimum mean values in February (11.7 ± 0.3 °C) and maximum mean values in August (24.8 ± 0.4 °C) (Fig. 4A).

Salinity showed the maximum in February (38.43 ± 0.06), followed by a decreasing trend, reaching the minimum in June (35.84 ± 0.53), after which an increasing trend was observed (Fig. 4B).

The mean annual trend of water density at surface showed the highest values in February (29.31 ± 0.08 kg m^{-3}), then a decrease was observed in spring and the minimum (24.38 ± 0.38 kg m^{-3}) was recorded in July (Fig. 4C).

On average, at surface dissolved oxygen showed oversaturation values (above 100%) from April to August (Fig. 4D) indicating a predominance of oxygen production than consumption.

The mean annual cycle of Dissolved Inorganic Nitrogen (DIN) showed the minimum values in September (0.95 ± 0.21 μM), and an increase in spring and autumn, with maximum in October (3.19 ± 1.54 μM, Fig. 4E). Orthophosphate showed the minimum in May (0.03 ± 0.01 μM) and maximum in June (0.13 ± 0.06 μM) followed by a decrease in summer and a new peak in September (Fig. 4F).

Silicate values ranged from 0.85 ± 0.15 μM in March and 3.23 ± 0.78 μM in January (Fig. 4G).

On a mean monthly basis, the N:P ratio showed lower values in summer with the minimum in July (23.42 ± 6.83), whilst the maximum was found in October (143.41 ± 81.23) (Fig. S1A). Regarding the Si:N ratio, the lowest values were observed in winter (minimum in February, 0.66 ± 0.20), followed by an increase in spring with the maximum in June (6.35 ± 3.11), high values in summer and a new peak in October (Fig. S1B).

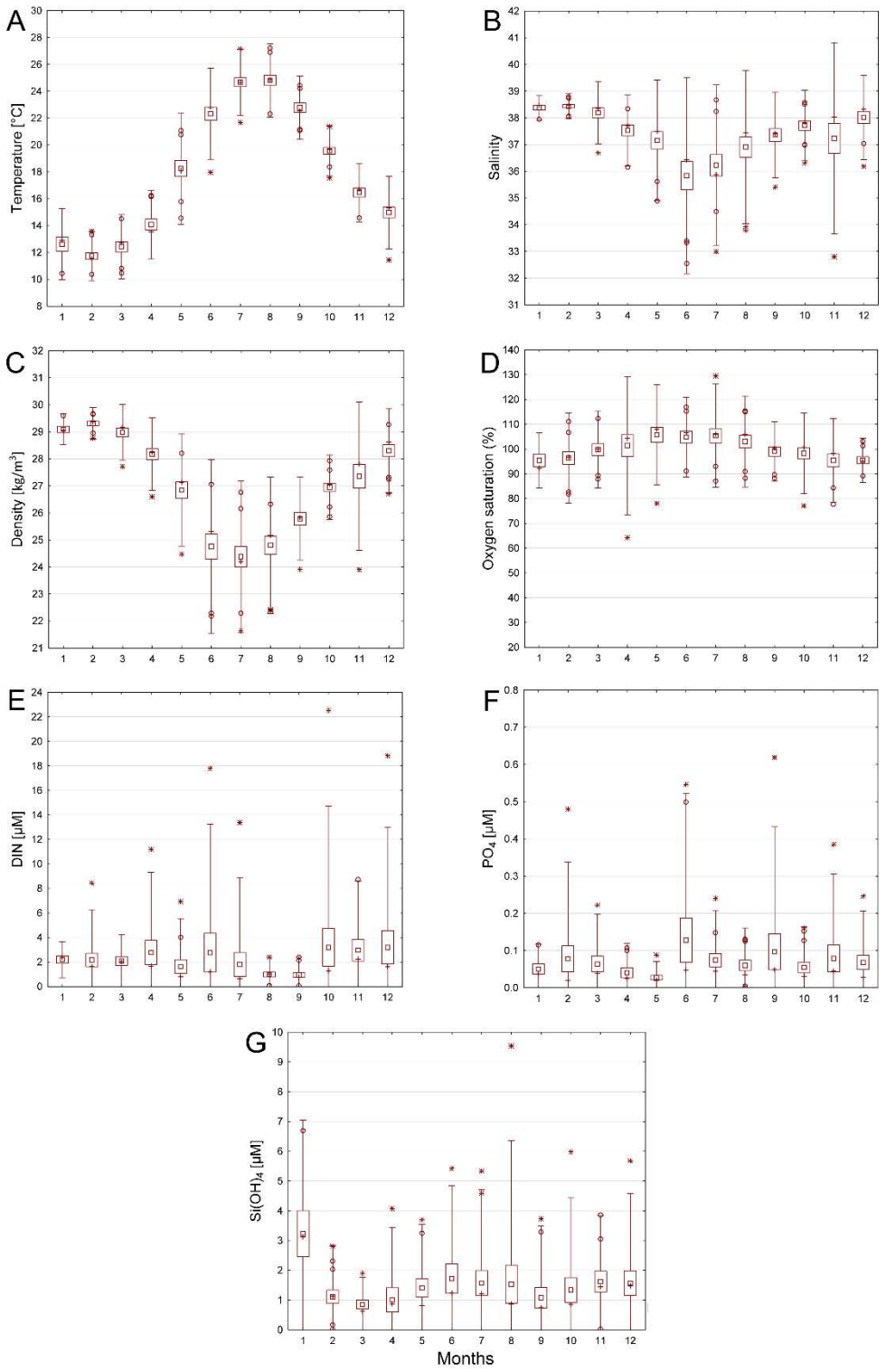

Fig. 4. Mean annual cycle of physicochemical parameters calculated on a mean monthly basis from 1988 to 2018 in SG05 station at surface: (A) water temperature (°C), (B) salinity, (C) density (kg m^{-3}), (D) oxygen saturation (%), (E) Dissolved Inorganic Nitrogen (DIN, µM), (F) orthophosphate (PO_4, µM) and (G) silicate concentrations ($Si(OH)_4$, µM). Box plots report the data distribution with the mean (+), the median (□), the interquartile range (box), the non-outlier range (vertical bars), the outliers (○) and the extremes (*).

Interannual trend

The trends of physico-chemical parameters in terms of anomalies are shown in Fig. 5. Temperature anomaly (Fig. 5A) showed a significant increase ($p < 0.05$). On the contrary, the salinity trend did not reveal any significant interannual variations (Fig. 5B).

Regarding nutrients, both DIN and PO_4 (Fig. 5C and D) showed a significantly increasing trend ($p < 0.01$), whilst silicate (Fig. 5E) did not reveal any significant interannual variations. Considering N:P and Si:N ratios (Fig. S1C and D), no significant interannual trend was observed ($p > 0.05$).

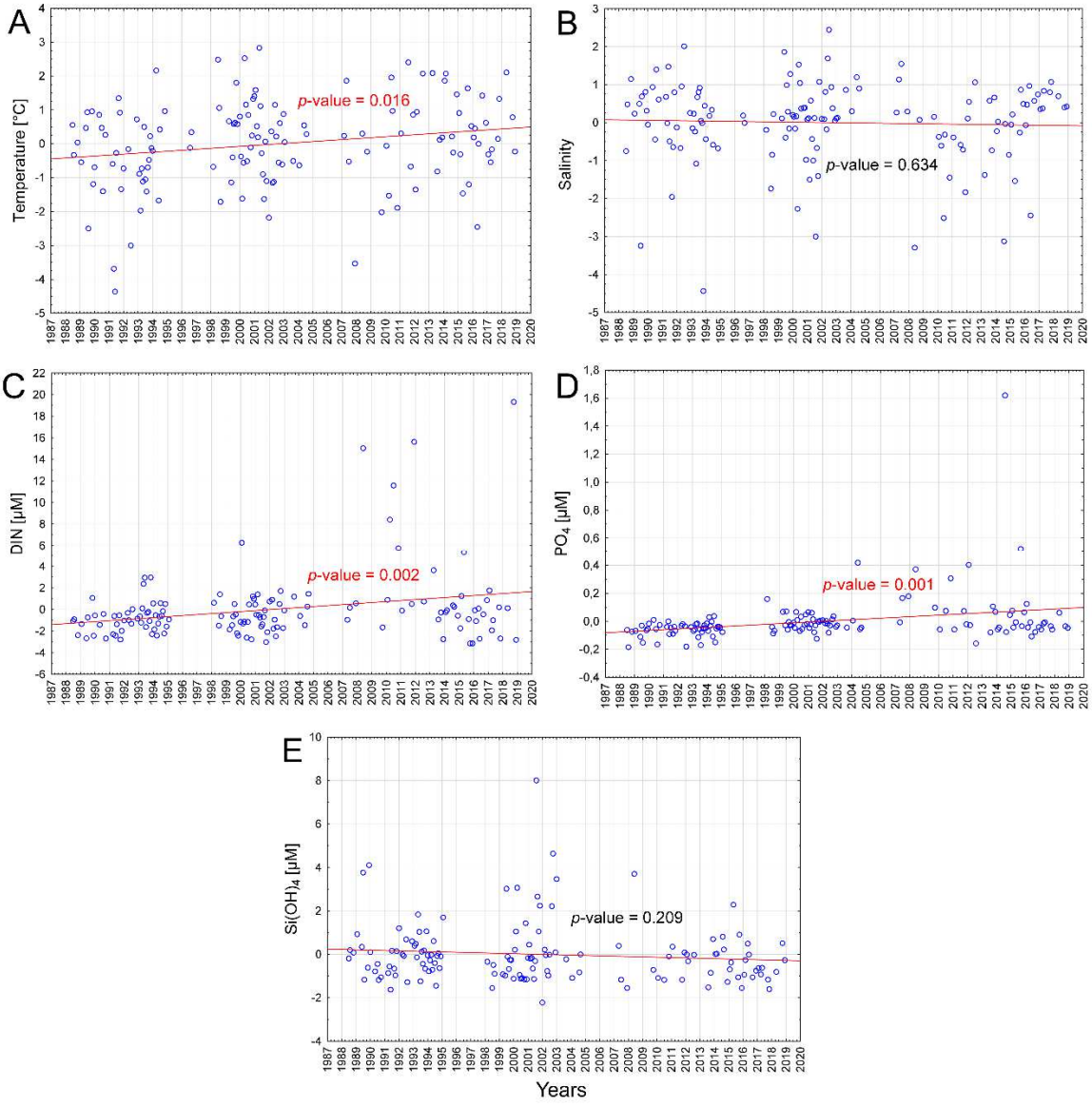

Fig. 5. Trend of anomalies of physical and chemical parameters at surface layers: (A) water temperature (°C), (B) salinity, (C) Dissolved Inorganic Nitrogen concentrations (DIN) (µM), (C) PO_4 concentration (µM) and (E) silicate concentration ($Si(OH)_4$) (µM).

Phytoplankton

Temporal variability in the water column

The vertical distribution of phytoplankton is showed in Fig. S2. Diatom abundances (Fig. S2A) showed that in the period 1988 to 1998 higher values were observed in the 0–20 m layer than in the underlying water column, while in the period 2013–2018 high abundances were concentrated in a narrower layer (i.e., 0–10 m). Subsurface maxima were found in the layer 20–30 m in June 2002 and in December 2018. Lower abundances were observed in years 2013 and 2015.

Dinoflagellates showed higher values in the upper water column than in the underlying layers, particularly in the 1988–2002 period and in 2018 (Fig. S2B). A subsurface maximum (20 m) was observed in June 2002. The lowest values were found below 35 m since 2015 (minimum in autumn 2017, 40m).

The vertical distribution of coccolithophores abundance showed that the highest values were observed in the mid water column and at bottom, from 1988 to 2000 (Fig. S2C). In the second period, very low values were found from 2013 to 2015, particularly at bottom, and from 2016 coccolithophore maxima occurred at surface.

Phytoflagellates (Fig. S2D) were always the most abundant group. Their vertical distribution showed several subsurface maxima that occurred with those of diatoms.

Mean annual cycle

The annual cycle (on a monthly basis) of phytoplankton groups calculated at the surface layer from 1988 to 2018 in SG05 station is shown in Fig. 6. Considering the total phytoplankton (Fig. 6A), the annual maximum was observed in June (1,838,830 ± 400,360 cells l^{-1}), whilst the minimum was recorded in November (533,496 ± 71,092 cells l^{-1}). Phytoflagellates were the most abundant group throughout the year representing from 44 to 78% of the total community. The minimum contribution of phytoflagellates was observed in July when diatom maximum occurred. Diatoms represented the second group with a percent contribution ranging from 13 to 45%. Dinoflagellate and coccolithophore

contribution ranged from 3 to 5% and from 1 to 5% respectively.

Observing the mean annual trend of diatoms (Fig. 6B), low values were observed in winter months, then abundances increased in spring reaching their maximum in July (526,278 ± 234,168 cells l^{-1}). At the end of summer, values decreased, and in August minimum was observed (83,125 ± 27,492 cells l^{-1}). A second peak was found in autumn (October, 228,213 ± 75,201 cells l^{-1}).

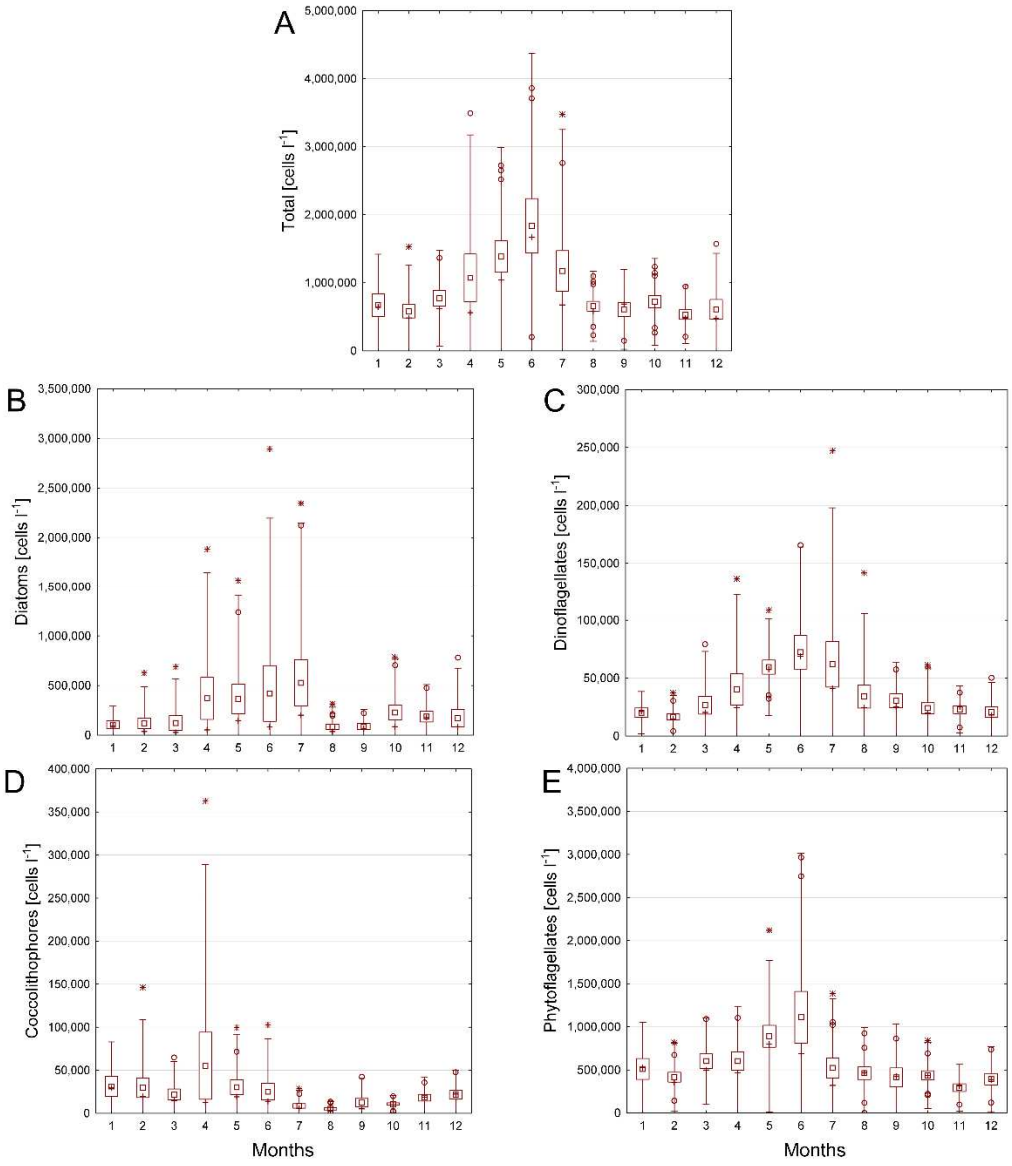

Fig. 6. Mean annual cycle of phytoplankton abundance (cells l^{-1}) calculated on a mean monthly basis from 1988 to 2018 in SG05 station at surface: (A) total phytoplankton, (B) diatoms, (C) dinoflagellates, (D) coccolithophores and (E) phytoflagellates. Box plots report the data distribution with the mean (+), the median (□), the interquartile range (box), the non-outlier range (vertical bars), the outliers (○) and the extremes (*).

Dinoflagellate abundances showed minimum values in February (16,496 ± 2670 cells l^{-1}) and an increase in spring, showing the maximum in June (72,381 ± 14,495 cells l^{-1}) (Fig. 6C).

The mean annual cycle of coccolithophores was characterize by minimum values in summer (August, 5060 ± 1201 cells l^{-1}), an increase in autumn and winter, and the maximum in April (55,192 ± 38,987 cells l^{-1}) (Fig. 6D).

Being the dominant group in the total community, phytoflagellates' trend paralleled that of total phytoplankton, with the annual peak in June (1,110,694 ± 300,909 cells l^{-1}) and the minimum in November (294,238 ± 45,046 cells l^{-1}) (Fig. 6E).

Phytoplankton community composition

In the whole study period, the number of identified taxa was 320: 153 diatoms, 112 dinoflagellates, 32 haptophytes (among which 28 coccolithophores), 3 cryptophytes, 5 chrysophytes, 5 dictyochophytes, 2 raphidophytes, 5 chlorophytes, 2 euglenophytes, 1 cyanophyte (Table S2). The IndVal analysis, calculated for the surface layer, revealed the taxa that were significant for each season in terms of both abundance and frequency of occurrence (Table 1). In winter, significantly high values were observed for *Emiliania huxleyi*, *Skeletonema marinoi*, *Dactyliosolen phuketensis*, *Pseudosolenia calcar avis* and *Chaetoceros affinis*. In spring, significant taxa were *Dactyliosolen fragilissimus*, *Chaetoceros throndsenii*, *C. simplex*, and *Cyclotella* spp. In summer, the most representative taxa were *Calycomonas vangoorii*, *Pseudoscourfieldia marina* and *Chaetoceros anastomosans*. *Nitzschia gobbii* showed a high Ind-Val although not significant. In autumn, a high number of taxa resulted significant: *Guinardia striata*, *Lioloma pacificum*, Pseudo-*nitzschia* cfr. *delicatissima*, *Chaetoceros danicus*, *C. curvisetus*, *C. costatus*, *C. socialis*, *Asterionellopsis glacialis*, *Pleurosigma* sp., *Cylindrotheca closterium*, *Navicula* spp.

Table 1. List of phytoplankton taxa characterized by the highest IndVal for each season calculated for the surface layer. Values indicated in italic are significant at $p < 0.05$, those in bold italic are significant at $p < 0.01$, those in bold italic and underlined are significant at $p < 0.001$. The shades of colour are proportional to the IndVal values, from dark green to white, in decreasing order.

	Winter	Spring	Summer	Autumn
Emiliania huxleyi	***42.54***	24.83	0.733	17.999
Skeletonema marinoi	***38.423***	3.191	0	0.327
Chaetoceros affinis	*26.577*	0	3.153	1.228
Dactyliosolen phuketensis	***26.404***	0	0	6.432
Pseudosolenia calcar avis	*26.262*	0	5.616	0.084
Syracosphaera pulchra	16.486	1.948	6.68	10.168
Dactyliosolen fragilissimus	0.486	*46.141*	21.095	3.983
Chaetoceros throndsenii	0.109	***32.254***	0.091	0.547
Cyclotella spp.	0.046	***28.971***	2.227	0.165
Prorocentrum micans	0.268	26.011	6.895	0.894
Diplopsalis group	0.315	23.196	0.339	0.049
Prorocentrum compressum	0.173	18.47	0.591	0.033
Chaetoceros cfr. *simplex*	0.069	*18.417*	0.146	0.327
Tripos furca	0.04	17.647	0.832	0.92
Thalassionema nitzschioides	3.082	16.79	0.794	3.42
Tripos muelleri	3.543	16.375	0.435	0.281
Prorocentrum cordatum	1.95	15.826	1.469	0.493
cfr. *Chrysochromulina* sp.	3.418	14.561	2.491	1.363
Pseudokephyrion spp.	1.703	14.216	0.686	5.267
cfr. *Scrippsiella* sp.	0	13.659	7.549	0
Thalassiosira spp.	3.597	13.622	0.071	0.11
Leptocylindrus minimus	0	12.803	0.923	0.646
Nitzschia longissima	0.36	11.303	1.711	1.684
Protoperidinium cfr. *steinii*	0.473	10.693	1.434	4.161
Calycomonas vangoorii	0.086	7.657	***62.851***	5.02
Proboscia alata	0.169	2.547	52.331	5.089
Cerataulina pelagica	2.135	7.275	50.861	5.035
Pseudoscourfieldia marina	0	11.864	***46.203***	0.185
Nitzschia gobbii	1.477	0.1	30.879	4.731
Hemiaulus hauckii	7.971	0.065	24.689	7.097
Guinardia flaccida	8.291	0.121	24.549	8.497
Leptocylindrus danicus	0.248	4.516	23.768	17.729
Rhizosolenia spp.	6.738	0.005	22.26	2.866
Chaetoceros anastomosans	0	0.317	*21.996*	0.223
Chaetoceros spp.	1.668	20.953	20.985	7.397
Pseudo-nitzschia cfr. *pseudodelicatissima*	0.678	12.362	20.647	10.208
Rhabdosphaera clavigera claviger	0.432	1.485	18.817	9.875
Gymnodinium spp.	1.099	4.14	17.411	3.576
Bacteriastrum spp.	1.005	1.622	12.364	4.518
Guinardia striata	3.971	0	3.882	***49.879***
Lioloma pacificum	0	0	2.426	***45.529***
Pseudo-nitzschia cfr. *delicatissima*	0.495	2.995	0.164	*38.253*
Chaetoceros danicus	2.916	0	0.036	***36.487***
Asterionellopsis glacialis	4.717	0	0	***34.209***
Cylindrotheca closterium	1.951	1.937	22.752	*31.752*
Pleurosigma spp.	8.545	0	0.165	***30.085***
Chaetoceros curvisetus	13.009	0	0.088	*27.995*
Chaetoceros lorenzianus	0.953	5.228	6.099	27.339
Navicula spp.	10.499	0.146	0.299	*26.138*
Chaetoceros socialis	1.317	0	0.239	*22.027*

Dictyocha fibula	10.262	0.076	0	21.645
Chaetoceros costatus	2.42	0	0	*21.037*
Hemiaulus sinensis	2.606	1.613	0.077	18.444
Calciosolenia brasiliensis	2.258	0.97	1.525	18.203
Pseudo-nitzschia spp.	2.605	0.57	0.725	17.913
Calciosolenia murrayi	0.012	1.061	1.404	17.077
Euglena spp.	3.231	2.6	0.86	16.967

Interannual variations

Due to the interruption in the phytoplankton sampling from 2003 to 2012, to assess if changes occurred in the phytoplankton communities along the study period, we compared the mean seasonal abundances at surface between two periods 1988–2002 and 2013–2018, through one-way ANOVA test. Results highlighted that the winter abundances of dinoflagellates and coccolithophores were significantly higher ($p < 0.01$ and $p < 0.05$, respectively) in first period than in the second one (Table 2), while no significant differences were observed for the other groups and for the total phytoplankton).

Table 2. Results of ANOVA and Tukey's tests performed on the abundances (cells l^{-1}) of diatoms, dinoflagellates, coccolithophores, flagellates and total phytoplankton in the period 1988–2002 and 2013–2018 at surface layer. Mean values ± standard error (SE) are shown. As: ns, not significant; *$p < 0.05$; **$p < 0.01$; ***$p < 0.001$.

Parameter	Season	1988-2002 Avg ± SE	2013-2018 Avg ± SE	p-level	Tukey test
Diatoms (cells l^{-1})	**Winter**	270,576 ± 52,820	112,754 ± 29,515	ns	ns
	Spring	438,586 ± 145,388	155,989 ± 96,916	ns	ns
	Summer	258,821 ± 100,686	108,899 ± 54,128	ns	ns
	Autumn	213,083 ± 51,227	106,662 ± 43,421	ns	ns
Dinoflagellates (cells l^{-1})	**Winter**	40,017 ± 3,801	27,285 ± 6,612	**	88-02 > 13-18
	Spring	57,554 ± 6,560	60,226 ± 23,258	ns	ns
	Summer	44,532 ± 9,241	30,974 ± 4,161	ns	ns
	Autumn	25,818 ± 3,479	17,767 ± 1,915	ns	ns
Coccolithophores (cells l^{-1})	**Winter**	23,228 ± 4,348	15,081 ± 4,040	**	88-02 > 13-18
	Spring	38,151 ± 14,430	26,275 ± 15,682	ns	ns
	Summer	8,501 ± 1,766	3,974 ± 1,693	ns	ns
	Autumn	15,640 ± 2,654	17,722 ± 2,843	ns	ns
Flagellates (cells l^{-1})	**Winter**	552,546 ± 42,610	594,488 ± 104,196	ns	ns
	Spring	846,407 ± 111,278	1,009,411 ± 398,669	ns	ns
	Summer	456,606 ± 59,475	622,905 ± 176,270	ns	ns
	Autumn	354,789 ± 47,219	437,893 ± 27,120	ns	ns
Total (cells l^{-1})	**Winter**	941,984 ± 79,779	750,418 ± 134,936	ns	ns
	Spring	1,486,528 ± 202,217	1,253,552 ± 528,283	ns	ns
	Summer	839,434 ± 132,973	769,163 ± 128,399	ns	ns
	Autumn	629,423 ± 79,279	580,201 ± 50,405	ns	ns

Relationships between phytoplankton and environmental parameters

The PCA analysis, performed for the surface layer, showed a 53.02% of explained variance of the first two components (Fig. 7). The first component (PC1) showed salinity opposite to temperature, highlighting the seasonal behaviour of the site. The second axis (PC2) was determined by nutrient concentrations. Diatom abundances were directly related to temperature and inversely related to salinity. On the contrary, coccolithophores were found to be directly associated to salinity and inversely related to temperature and PO_4. Flagellates and dinoflagellates were found both to be associated to temperature and oxygen saturation, being inversely related to salinity.

The analysis of correlation between environmental parameters and phytoplankton abundances highlighted a negative correlation between salinity and diatoms ($r = –0.38$, $p < 0.05$), dinoflagellates ($r = –0.47$, $p < 0.05$) and phytoflagellates ($r = –0.27$, $p < 0.05$). A positive and negative correlation was detected between temperature and dinoflagellates ($r = 0.32$, $p < 0.05$), and temperature and coccolithophores ($r = –0.37$, $p < 0.05$), respectively. Furthermore, a negative correlation between coccolithophores and PO_4 ($r = –0.23$, $p < 0.05$) was found.

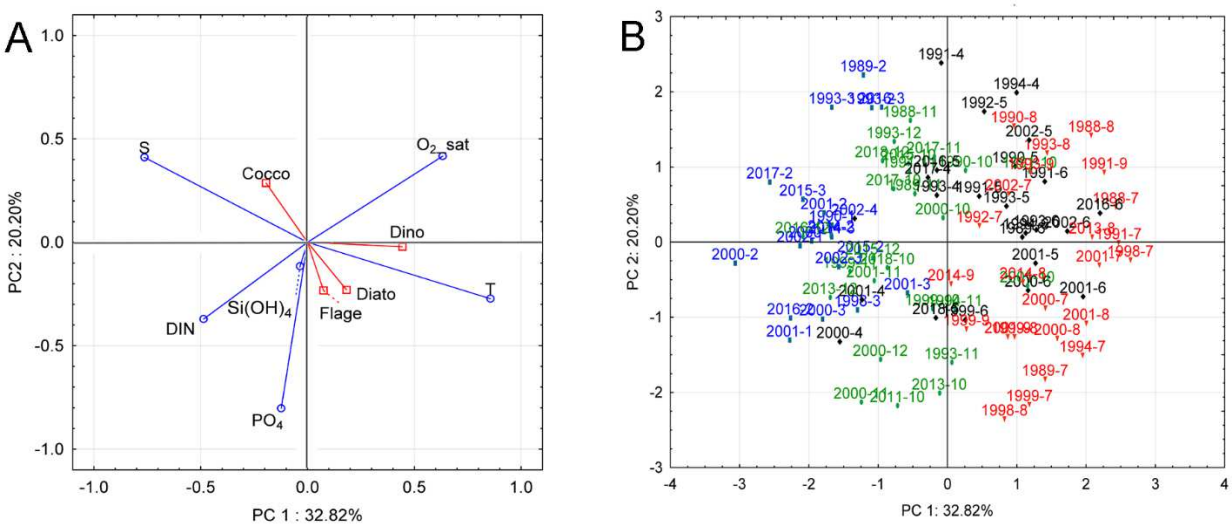

Fig. 7. Principal Component Analysis (PCA) based on correlation matrix of ranked environmental variables and main phytoplankton group abundance values, used as supplementary variables, performed for the surface layer. (A) Loading plot (T = temperature, S = salinity, DIN = Dissolved Inorganic Nitrogen, PO_4 = Orthophosphate, $Si(OH)_4$ = silicates, O_2_sat = oxygen saturation, Diato = Diatoms, Dino = Dinoflagellates, Cocco = Coccolithophores, Flage = Flagellates. (B) Score plot (colours and markers represent the seasons: blue ■ = winter, black ◆ = spring, red ▲ = summer, green ● = autumn).

1.1.5 Discussion

In this study, we highlighted for the first time the intra and interannual variability of phytoplankton, the community composition, and their relationships with the oceanographic and trophic condition, in an offshore area of the northern Adriatic basin based on a long-term dataset.

Mean annual cycle

The mean annual cycle of phytoplankton in an open-water station of the LTER Senigallia-Susak transect (NA) indicated that highest abundances occurred in early summer mainly due to phytoflagellates' and diatoms' maxima. Minimum abundances occurred in autumn and winter.

This cycle markedly differed from that recorded both in the western and eastern NA coastal waters. In the E Adriatic coast, spring and autumn peaks are commonly observed mainly related to diatom proliferation (Cerino et al., 2019; Marić et al., 2012; Mozetič et al., 2010). Instead, in the coastal

waters of the NW Adriatic Sea, the winter diatom bloom represents the most relevant plankton increase throughout the year (Totti et al., 2019), as already observed in other Mediterranean areas (Goffart et al., 2015), followed by the classic peaks in spring and autumn again due to diatoms and phytoflagellates. The observed differences between the offshore and costal sites of the Senigallia-Susak transect could be explained considering the different oceanographic conditions. In the coastal station, the strong winter bloom is related to the shallowness of water column (11 m depth) that allows phytoplankton to remain in the photic zone even in winter mixing conditions, allowing the bloom of *Skeletonema marinoi*, a small colonial diatom with a marked seasonal behaviour (Totti et al., 1999). On the contrary, in the deeper offshore station, the winter phytoplankton abundance is low, according to the classical Sverdrup model (Sverdrup, 1953). Furthermore, the offshore station is located in the waters beyond the coastal front, not directly affected by the coastal input, except than during the stratification period (see below). In the study area the nutrient source is partly autochthonous, i.e. represented by the regeneration processes occurring in the water column and by the release from bottom sediments (Baric et al., 2002), and partly allochthonous due to the spreading south-eastward of the floods of the Po River in stratified conditions as demonstrated by several recorded events of plume extension beyond the midline (Campanelli et al., 2011; Grilli et al., 2020).

As regards as DIN, the allochthonous source is highlighted by the June peak coinciding with the minimum of salinity, while the autochthonous (i.e. resuspension) due to the thermocline rupture, is highlighted by the October peak. The same peaks were observed for the silicates, suggesting the importance of both allochthonous and autochthonous (i.e. weathering of rocks and sediments) source also for this nutrient. The Si:N ratio in the study area was higher than in other areas of the NA (Cozzi et al., 2020; Giani et al., 2012). N:P values were comparable to those recorded in other NA areas (Accoroni et al., 2015; Cozzi et al., 2020; Degobbis et al., 2005; Djakovac et al., 2012; Giani et al., 2012), highlighting the P-limitation condition typical of the NA. Concentrations of orthophosphate in the study area were often below 0.2 μM as typically recorded in all the long-term data records in the Adriatic Sea (Grilli et al., 2020). The high P concentrations often recorded below 40 m depth

suggests that the main inorganic P source in the study area would be the remineralization processes at the bottom, although even an allochthonous source was revealed by low salinity values at surface. The fact that the autumn peak was observed for the DIN but not for the PO_4 would suggest that the resuspension process is less effective for P than for DIN, probably due to phosphate absorption into particles (Boldrin et al., 2009; Tengberg et al., 2003). In warm months, the water stratification was often associated to the decrease of salinity and the increase of nutrients' concentration (mainly P), indicating the spreading eastwards of the riverine waters. Such conditions in which nutrients became available in a stratified photic zone represent optimal conditions for phytoplankton to proliferate. Similar conditions in which phytoplankton was influenced by riverine plumes were observed in other studies (Diaz et al., 2008; O'Connor et al., 2016; Tang et al., 2004).

In our study, almost all phytoplankton groups showed their maximum abundances in early summer and multivariate statistical analysis highlighted an inverse relation between their abundances and salinity. These maxima were pointed out by oxygen oversaturation during the same period. Diatoms and phytoflagellates represented the dominant groups, while dinoflagellates showed abundances one order of magnitude lower than the others. This behaviour agrees with that observed in the coastal areas of the NA Sea (Cerino et al., 2019; Totti et al., 2019). On the contrary, coccolithophores' mean annual cycle showed the peak in April, while in the coastal station they occurred with high abundances even from February to April (Totti et al., 2019).

Community structure

The phytoplankton community composition in the offshore area of the Senigallia-Susak transect has been characterized for the first time in this study. Despite the low abundances, the winter community is characterized by taxa expressing a marked seasonal behaviour, such as the coccolithophore *Emiliania huxleyi*, and the diatom *Skeletonema marinoi*, which have been reported in winter even in the coastal station (Totti et al., 2019), as well as in other Mediterranean coastal areas (Cerino et al., 2019; Turkoglu, 2010; Zingone et al., 2010a). The occurrence of *E. huxleyi* together with rapid

growth/small-chained diatoms as *S. marinoi* would indicate the aptitude of that species to proliferate in mixing in turbulence regime, as already observed in other areas (Guerreiro et al., 2013). Surprisingly even some large-sized diatom species, i.e., *Pseudosolenia calcar avis*, and *Dactyliosolen phuketensis* resulted significant for winter. Spring communities were dominated by phytoflagellates and only a few indicator taxa were observed, e.g. some nanoplanktonic species belonging to *Chaetoceros* and *Cyclotella* genera and the large sized *Dactyliosolen fragilissimus*. The composition of summer communities was characterized by small nanoplanktonic species as expected in oligotrophic conditions, such as the chrysophyte *Calycomonas vangoorii*, the prasinophyte *Pseudoscourfieldia marina* and the diatom *Chaetoceros anastomosans*. In autumn, a number of taxa resulted significant, including some autumn species also typical in coastal stations, such as *Asterionellopsis glacialis* and *Chaetoceros curvisetus* (Bernardi Aubry et al., 2004; Totti et al., 2019). The presence of *Pseudo-nitzschia delicatissima* species complex as autumn taxa was surprising, as in coastal areas it is typical of late winter (Bernardi Aubry et al., 2004; Giulietti et al., 2021a; Totti et al., 2019). However, we should consider that the *Pseudo-nitzschia delicatissima* species complex actually includes several cryptic species, each expressing different seasonal behaviour also in geographically close areas (Turk Dermastia et al., 2020; Giulietti et al., 2021b).

On the whole, the community of the offshore site reflected only in part that of the coastal area and only some species were found to be key taxa of a certain season in both stations (e.g. *Skeletonema marinoi* in winter and *Chaetoceros* costatus in autumn), whilst many taxa were found to be indicative of a different season (e.g. *Guinardia striata* for the summer and autumn community in the coastal and offshore site, respectively) or significant only in the offshore site (e.g. *Chaetoceros throndsenii* in spring, *C. anastomosans* in summer, *C. danicus* in autumn).

Interannual variations

The interannual trend of the physico-chemical parameters highlighted a significant increase in the temperature values, as previously reported in the NA basin (Vilibić et al., 2019). On the contrary,

salinity did not show significant trends. A significant increase was observed even for inorganic nitrogen, as already observed by Grilli et al. (2020) through a basin-scale interannual analysis. This could be explained by the increasing inputs of anthropogenic nitrogen in the drainage basin of the Po River, which cause high nitrogen loads during those years of high river waters discharge (Cozzi et al., 2019; Cozzi and Giani, 2011; Viaroli et al., 2018) coupled with a limited N use by a P-limited phytoplankton community. Although in coastal areas of the NA, silicates showed an increasing trend (Cozzi et al., 2020; Totti et al., 2019), in the offshore station of the SS they did not show a significant trend, as already observed by Grilli et al. (2020). The temporal trend of inorganic phosphorous concentrations in the study area increased significantly, as already found by Totti et al. (2019) in the coastal station of the same transect. However, Grilli et al. (2020) did not find any significant trend for orthophosphate at a whole sub-basin scale, highlighting that the evaluation of P trend is particularly controversial. In fact, the NA is in an almost permanent P-deficient status (Brush et al., 2021), and the availability of phosphate, particularly in offshore waters not directly affected by the riverine runoff, depends mainly on the regenerative processes in the water column and on the sediment resuspension (see above). Moreover, it is becoming increasingly clear that an important source of phosphorus is its organic form (not investigated in this study), whom availability has been proved in many studies by high values of alkaline phosphatase activity in sea water (Ivančić et al., 2012, 2016; Tanković et al., 2018). In addition, Baturin (2003) suggested that phosphorus cycling is tightly connected to carbon dioxide on the atmosphere. An increase in carbon dioxide lead to warming and the rise of the phosphorus input into the sea, an accelerated rate of sinking of organic matter and phosphorus. No significant trends were found for DIN/PO_4 and $Si(OH)_4/DIN$. The latter has been suggested as able to affect the phytoplankton community, facilitating flagellate growth at the expense of diatoms (Gilpin et al., 2004; Turner et al., 1998). This could be one reason why no changes in the study periods were detected in terms of phytoflagellate and diatom abundances.

Unfortunately, in this study the interannual variations in the phytoplankton communities in the whole period was not represented, as data in the period 2003–2012 were too irregular. Comparing abundance

values of 1988–2002 period with 2013–2018 on a seasonal basis, we did not observe significant changes. However, considering groups, we observed significant lower values in winter during the second period for both dinoflagellates and coccolithophores, in agreement with that reported in the coastal area of the transect (Totti et al., 2019). The major reason of the coccolithophore decrease is the decrease of *Emiliania huxleyi* abundance in winter. The observed decreasing trend of coccolithophores is difficult to explain. Coccolithophores are a complex group with diverse life strategies and, although they have been traditionally associated to oligotrophic conditions, they also proliferate in very diverse trophic conditions (Balch, 2018; Guerreiro et al., 2013; Moita et al., 2010). Moreover, their haplodiplontic life cycle complicates a correct estimation of their occurrence. This is particularly problematic with *Emiliania huxleyi* for which the haploid life phase does not bear coccoliths (Frada et al., 2012), and a hypothetical occurrence and proliferation of that phase would surely go completely unnoticed, unless other methodological approaches are used. Regarding the observed decrease of dinoflagellates, we need to evaluate it carefully in a longer data set.

The long-time changes in the trophic state and phytoplankton communities have been highlighted in a number of Mediterranean sites (Goffart et al., 2002, 2015; Mercado et al., 2005; Ninčević Gladan et al., 2010; Totti et al., 2019; Zingone et al., 2010b), where to date longer and longer temporal series are becoming available. In the Adriatic Sea, long-term studies sometimes have highlighted tendencies apparently contrasting, depending on the studied area and/or on the considered starting and ending points to trace the traits. For example, a number of studies highlighted a tendency to oligotrophication (Cabrini et al., 2012; Djakovac et al., 2012; Mozetič et al., 2010), whereas others did not (Bernardi Aubry et al., 2012; Totti et al., 2019). In any case, all agree that the main forcing that is responsible for this variability is the rate of the Po River outflow, i.e., the rain regime. In that sense, it has recently been highlighted that an increase in the frequency of intense rains and extremely high Po River discharges have occurred during the last decade, and that could have affected the annual availability of nutrients, particularly of DIN, in the NA (Grilli et al., 2020; Totti et al., 2019).

1.1.6 Conclusions

In this study, the phytoplankton communities in their oceanographic scenario in an LTER-offshore station not directly affected by riverine inputs, were highlighted over 30 years. The mean monthly cycle of the phytoplankton was found to be highly dependent on the oceanographic conditions of the water column, as during water stratification the spreading of the fresher and nutrient-rich waters beyond the coastal front allows the phytoplankton annual peak. This study confirmed the P limiting conditions of the N Adriatic Sea, suggesting the importance of organic P sources and remineralization processes along the water column. Instead, the resuspension processes seemed less effective for P than for DIN. Species composition in the offshore station was found to reflect only in part the coastal community, as many taxa were significant only in the offshore site or related to a different season. Temperature, DIN and P showed a significant increase, highlighting long-term changes in the environmental conditions in this offshore station as highlighted in other Mediterranean sites. A decreasing of winter dinoflagellates and coccolithophores was observed, although more data and a longer time series would be necessary to better understand the phytoplankton trends.

1.1.7 Acknowledgements

This study was partly funded by EU 2014–2020 Interreg V-A Italy-Croatia CBC project ECOSS (Observing System in the Adriatic Sea: oceanographic observations for biodiversity) ID: 10042301 and was carried out in the framework LTER-ITALY (Italian Long-Term Ecological Research Network).

Authors acknowledge the crews of all the oceanographic vessels involved in the sampling cruises: S. Lo Bianco, Tecnopesca 2, G. Dallaporta, Tethis, Copernaut Franca, Urania, Alliance, Minerva, Bannock, D'Ancona. This long-term research was supported by the following projects: Italian Ministry of Merchant Navy monitoring program (1988–1990); ELNA (Eutrophic Limits of the NA Sea), Rome, European Commission (1992–1994); PRISMA (Program of Research and Experimentation in the Adriatic Sea) Italian Ministry of University and Research (1994–1998); MAT

(Processes of formation of mucilage aggregates in the Adriatic and Tyrrhenian Seas) Italian Ministry of Environment (1999–2002); SINAPSI - Seasonal, Interannual and decadal variability of the atmosPhere, oceanS and related marIne ecosystems Italian Ministry of University and Research (1997–2001); EU/FP6- SUSTDEV SESAME (Southern European Seas: Assessing and Modelling Ecosystem changes) European Commission (2006–2010); RITMARE (Ricerca ITaliana in MARE) Italian Ministry of University and Research (2012–2016); BALMAS IPA Adriatic Cross-Border Cooperation Programme - strategic project Ballast Water Management System for Adriatic Sea Protection (2014–2016). We thank the reviewers for helpful comments.

1.1.8 References

2008/56/EC. Directive of the European Parliament and of the Council of 17 June 2008 establishing a framework for community action in the field of marine environmental policy (Marine Strategy Framework Directive) (Text with EEA relevance).

Accoroni, S., Glibert, P.M., Pichierri, S., Romagnoli, T., Marini, M., Totti, C., 2015. A conceptual model of annual *Ostreopsis* cf. *ovata* blooms in the Northern Adriatic Sea based on the synergic effects of hydrodynamics, temperature, and the N:P ratio of water column nutrients. Harmful Algae, 45, 14–25. https://doi.org/10.1016/j.hal.2015.04.002

Artegiani, A., Azzolini, R., Salusti E., 1989. On the dense water in the Adriatic Sea. Oceanol. Acta, 12, 151–160.

Balch, W.M., 2018. The ecology, biogeochemistry, and optical properties of coccolithophores. Ann. Rev. Mar. Sci 10, 71–98. https://doi.org/10.1146/annurev-marine-121916-063319

Baric, A., Kuspilic, G., Matijevic, S., 2002. Nutrient (N, P, Si) fluxes between marine sediments and water column in coastal and open Adriatic. Hydrobiologia 475/476, 151–159.

Baturin, G., 2003. Phosphorus cycle in the ocean. Lithol. Miner. Resour. 38, 101–119.

Bergamasco, A., Oguz, T., Malanotte-Rizzoli, P., 1999. Modelling dense water mass formation and winter circulation in the northern and central Adriatic Sea. J. Mar. Syst. 20, 279–300. https://doi.org/10.1016/S0924-7963(98)00087-6

Bernardi Aubry, F., Berton, A., Bastianini, M., Socal, G., Acri, F., 2004. Phytoplankton succession in a coastal area of the NW Adriatic, over a 10-year sampling period (1990–1999). Cont. Shelf Res. 24, 97–115. https://doi.org/10.1016/j.csr.2003.09.007

Bernardi Aubry, F., Acri, F., Bastianini, M., Bianchi, F., Cassin, D., Pugnetti, A., Socal, G., 2006. Seasonal and interannual variations of phytoplankton in the Gulf of Venice (Northern Adriatic Sea). Chem. Ecol. 22, 71–91. https://doi.org/10.1080/02757540600687962

Bernardi Aubry, F., Cossarini, G., Acri, F., Bastianini, M., Bianchi, F., Camatti, E., De Lazzari, A., Pugnetti, A., Solidoro, C., Socal, G., De Lazzari, A., Pugnetti, A., Solidoro, C., Socal, G., 2012. Plankton communities in the northern Adriatic Sea: patterns and changes over the last 30 years. Estuar. Coast. Shelf Sci. 115, 125–137. https://doi.org/10.1016/j.ecss.2012.03.011

Boldrin, A., Carniel, S., Giani, M., Marini, M., Bernardi Aubry, F., Campanelli, A., Grilli, F., Russo, A., 2009. Effects of bora wind on physical and biogeochemical properties of stratified waters in the northern Adriatic. J. Geophys. Res. 114, 1–19. https://doi.org/10.1029/2008jc004837

Brush, M.J., Giani, M., Totti, C., Testa, J.M., Faganeli, J., Ogrinc, N., Kemp, W.M., Fonda Umani, S., 2021. Eutrophication, Harmful Algae, Oxygen Depletion, and Acidification. In: Malone, T.C., Malej, A., Faganeli, J. (Eds.), *Coastal Ecosystems in Transition: A Comparative Analysis of the Northern Adriatic and Chesapeake Bay*. *Geophysical Monograph 256*. John Wiley & Sons, Inc., pp. 75–104. https://doi.org/10.1002/9781119543626.ch5

Cabrini, M., Fornasaro, D., Cossarini, G., Lipizer, M., Virgilio, D., 2012. Phytoplankton temporal changes in a coastal northern Adriatic site during the last 25 years. Estuar. Coast. Shelf Sci. 115, 113–124. https://doi.org/10.1016/j.ecss.2012.07.007

Campanelli, A., Grilli, F., Paschini, E., Marini, M., 2011. The influence of an exceptional Po River flood on the physical and chemical oceanographic properties of the Adriatic Sea. Dynam. Atmos. Oceans 52, 284–297. https://doi.org/10.1016/j.dynatmoce.2011.05.004

Cerino, F., Fornasaro, D., Kralj, M., Giani, M., Cabrini, M., 2019. Phytoplankton temporal dynamics in the coastal waters of the north-eastern Adriatic Sea (Mediterranean Sea) from 2010 to 2017. Nat. Conserv. 372, 343–372. https://doi.org/10.3897/natureconservation.34.30720

Cozzi, S., Giani, M., 2011. River water and nutrient discharges in the Northern Adriatic Sea: Current importance and long-term changes. Cont. Shelf Res. 31, 1881–1893. https://doi.org/10.1016/j.csr.2011.08.010

Cozzi, S., Ibáñez, C., Lazar, L., Raimbault, P., Giani, M., 2018. Flow regime and nutrient-loading trends from the largest South European watersheds: implications for the productivity of Mediterranean and Black Sea's coastal areas. Water 11, 1–27. https://doi.org/10.3390/w11010001

Cozzi, S., Cabrini, M., Kralj, M., De Vittor, C., Celio, M., Giani, M., 2020. Climatic and anthropogenic impacts on environmental conditions and phytoplankton community in the Gulf of Trieste (Northern Adriatic Sea). Water, 12, 2652. https://doi.org/10.3390/w12092652

Degobbis, D., Precali, R., Ivancic, I., Smodlaka, N., Fuks, D., Kveder, S., 2000. Long-term changes in the northern Adriatic ecosystem related to anthropogenic eutrophication. Int. J. Environ. Pollut. 13, 495–533. https://doi.org/10.1504/IJEP.2000.002332

Degobbis, D., Precali, R., Ferrari, C. R., Djakovac, T., Rinaldi, A., Ivančić, I., Gismondi, M., & Smodlaka, N., 2005. Changes in nutrient concentrations and ratios during mucilage events in the period 1999-2002. Sci. Total Environ., 353, 103–114. https://doi.org/10.1016/j.scitotenv.2005.09.010

Diaz, F., Naudin, J.J., Courties, C., Rimmelin, P., Oriol, L., 2008. Biogeochemical and ecological functioning of the low-salinity water lenses in the region of the Rhone River freshwater influence, NW Mediterranean Sea. Cont. Shelf Res., Volume 28, 1511–1526. https://doi.org/10.1016/j.csr.2007.08.009

Djakovac, T., Degobbis, D., Supic, N., Precali, R., 2012. Marked reduction of eutrophication pressure in the northeastern Adriatic in the period 2000-2009. Estuar. Coast. Shelf Sci. 115, 25–32. https://doi.org/10.1016/j.ecss.2012.03.029

D'Ortenzio, F., Ribera d'Alcalà, M., 2009. On the trophic regimes of the Mediterranean Sea: a satellite analysis. Biogeosciences 5, 139–148. https://doi.org/10.5194/bgd-5-2959-2008

Dufrêne, M., Legendre, P., 1997. Species assemblages and indicator species: the need for a flexible asymmetrical approach. Ecol. Monogr. 67, 345–366. https://doi.org/10.2307/2963459

Edler, L., Elbrachter, M., 2010. The Utermöhl method for quantitative phytoplankton analysis. In: Karlson, B., Cusack, C., Bresnan, E. (Eds.), *Microscopic and Molecular Methods for Quantitative Phytoplankton Analysis*. IOC UNESCO, Manuals and Guides, 55, pp. 13–20.

Fonda Umani, S., 1996. Pelagic production and biomass in the Adriatic Sea. Sci. Mar. 60, 65–77.

Frada, M.J., Bidle, K.D., Probert, I., de Vargas, C., 2012. *In situ* survey of life cycle phases of the coccolithophore *Emiliania huxleyi* (Haptophyta). Environ. Microbiol. 14, 1558–1569. https://doi.org/10.1111/j.1462-2920.2012.02745.x

Franco, P., Michelato, A., 1992. Northern Adriatic Sea: oceanography of the basin proper and of the western coastal zone. Sci. Total Environ. Suppl. 199, 35–62.

Fuks, D., Ivančić, I., Najdek, M., Lučić, D., Njire, J., Godrijan, J., Marić, D., Šilović, T., Paliaga, P., Blažina, M., Precali, R., Orlić, S., 2012. Changes in the planktonic community structure related to trophic conditions: the case study of the northern Adriatic Sea. J. Mar. Syst 96–97, 95–102. https://doi.org/10.1016/j.jmarsys.2012.02.006

Furuya, K., Harada, K., 1995. An automated precise Winkler titration for determining dissolved oxygen on board ship. J. Oceanogr. 51, 375–383. https://doi.org/10.1007/BF02285173

Gilpin, L.C., Davidson, K., Roberts, E., 2004. The influence of changes in nitrogen: silicon ratios on diatom growth dynamics. J. Sea Res. 51, 21–35. https://doi.org/10.1016/j.seares.2003.05.005

Giulietti, S., Romagnoli, T., Campanelli, A., Totti, C., Accoroni, S., 2021a. Ecology and seasonality of *Pseudo-nitzschia* species (Bacillariophyceae) in the northwestern Adriatic Sea over a 30-year period (1988-2020). Mediterr. Mar. Sci. 22, 505–520. https://doi.org/10.12681/mms.26021

Giulietti, S., Romagnoli, T., Siracusa, M., Bacchiocchi, S., Totti, C., Accoroni, S., 2021b. Integrative taxonomy of the *Pseudo-nitzschia* (Bacillariophyceae) populations in the NW Adriatic Sea, with a focus on a novel cryptic species in the *P. delicatissima* species complex. Phycologia 60, 247–264. https://doi.org/10.1080/00318884.2021.1899733

Goffart, A., Hecq, J.-H., Legendre, L., 2002. Changes in the development of the winter-spring phytoplankton bloom in the Bay of Calvi (NW Mediterranean) over the last two decades: a response to changing climate? Mar. Ecol. Prog. Ser. 236, 45–60.

Goffart, A., Hecq, J.H., Legendre, L., 2015. Drivers of the winter-spring phytoplankton bloom in a pristine NW Mediterranean site, the Bay of Calvi (Corsica): a long-term study (1979-2011). Prog. Oceanogr. 137, 121–139. https://doi.org/10.1016/j.pocean.2015.05.027

Giani, M., Djakovac, T., Degobbis, D., Cozzi, S., Solidoro, C., Fonda Umani, S., 2012. Recent changes in the marine ecosystems of the northern Adriatic Sea. Estuar. Coast. Shelf Sci., 115, 1–13. https://doi.org/10.1016/j.ecss.2012.08.023

Grilli, F., Paschini, E., Precali, R., Russo, A., Supić, N., 2005. Circulation and horizontal fluxes in the northern Adriatic Sea in the period June 1999–July 2002. Part I: geostrophic circulation and current measurement. Sci. Total Environ. 353, 57–67.

Grilli, F., Accoroni, S., Acri, F., Bernardi Aubry, F., Bergami, C., Cabrini, M., Campanelli, A., Giani, M., Guicciardi, S., Marini, M., Neri, F., Penna, A., Penna, P., Pugnetti, A., Ravaioli, M., Riminucci, F., Ricci, F., Totti, C., Viaroli, P., Cozzi, S., 2020. Seasonal and interannual trends of oceanographic parameters over 40 years in the Northern Adriatic Sea in relation to nutrient loadings using the EMODnet chemistry data portal. Water 12, 2280. https://doi.org/10.3390/w12082280

Guerreiro, C., Oliveira, A., De Stigter, H., Cachão, M., Sá, C., Borges, C., Cros, L., Santos, A., Fortuño, J.M., Rodrigues, A., 2013. Late winter coccolithophore bloom off central Portugal in

response to river discharge and upwelling. Cont. Shelf Res. 59, 65–83. https://doi.org/10.1016/j.csr.2013.04.016

Ivančić, I., Godrijan, J., Pfannkuchen, M., Marić, D., Gašparović, B., Djakovac, T., Najdek, M., 2012. Survival mechanisms of phytoplankton in conditions of stratification-induced deprivation of orthophosphate: Northern Adriatic case study. Limnol. Oceanogr. 57, 1721–1731. https://doi.org/10.4319/lo.2012.57.6.1721

Ivančić, I., Pfannkuchen, M., Godrijan, J., Djakovac, T., Marić Pfannkuchen, D., Korlević, M., Gašparović, B., Najdek, M., 2016. Alkaline phosphatase activity related to phosphorus stress of microphytoplankton in different trophic conditions. Prog. Oceanogr. 146, 175–186. https://doi.org/10.1016/j.pocean.2016.07.003

Marić, D., Kraus, R., Godrijan, J., Supić, N., Djakovac, T., Precali, R., 2012. Phytoplankton response to climatic and anthropogenic influences in the north-eastern Adriatic during the last four decades. Estuar. Coast. Shelf Sci. 115, 98–112. https://doi.org/10.1016/j.ecss.2012.02.003

Marini, M., Russo, A., Paschini, E., Grilli, F., Campanelli, A., 2006. Short-term physical and chemical variations in the bottom water of middle Adriatic depressions. Clim. Res. 31, 227–237. https://doi.org/10.3354/cr031227

Marini, M., Jones, B.H., Campanelli, A., Grilli, F., Lee, C.M., 2008. Seasonal variability and Po River plume influence on biochemical properties along western Adriatic coast. J. Geophys. Res.: Oceans 113, 1–18. https://doi.org/10.1029/2007JC004370

Mercado, J.M., Ramírez, T., Cortés, D., Sebastián, M., Vargas-Yáñez, M., 2005. Seasonal and inter-annual variability of the phytoplankton communities in an upwelling area of the Alborán Sea (SW Mediterranean Sea). Sci. Mar. 69, 451–465. https://doi.org/10.3989/scimar.2005.69n4451

Mihanović, H., Vilibić, I., Carniel, S., Tudor, M., Russo, A., Bergamasco, A., Bubić, N., Ljubešić, Z., Viličić, D., Boldrin, A., Malačič, V., Celio, M., Comici, C., Raicich, F., 2013. Exceptional dense water formation on the Adriatic shelf in the winter of 2012. Ocean Sci. 9, 561–572. https://doi.org/10.5194/os-9-561-2013

Moita, M.T., Silva, A., Palma, S., Vilarinho, M.G., 2010. The coccolithophore summer-autumn assemblage in the upwelling waters of Portugal: patterns of mesoscale distribution (1985-2005). Estuar. Coast. Shelf Sci. 87, 411–419. https://doi.org/10.1016/j.ecss.2010.01.025

Mozetič, P., Fonda Umani, S., Cataletto, B., Malej, A., 1998. Seasonal and inter-annual plankton variability in the Gulf of Trieste (northern Adriatic). ICES J. Mar. Sci. 55, 711–722. https://doi.org/10.1006/jmsc.1998.0396

Mozetič, P., Solidoro, C., Cossarini, G., Socal, G., Fonda Umani, S., 2010. Recent trends towards oligotrophication of the northern Adriatic: evidence from chlorophyll a time series. Estuaries and Coasts 33, 362–375. https://doi.org/10.1007/s12237-009-9191-7

Mozetič, P., Francé, J., Kogovsek, T., Talaber, I., Malej, A., 2012. Plankton trends and community changes in a coastal sea (northern Adriatic): bottom-up vs. top-down control in relation to environmental drivers. Estuar. Coast. Shelf Sci. 115, 138–148. https://doi.org/10.1016/j.ecss.2012.02.009

Ninčević Gladan, Ž., Marasović, I., Grbec, B., Skejić, S., Bužančić, M., Kušpilić, G., Matijević, S., Matić, F., 2010. Inter-decadal variability in phytoplankton community in the middle Adriatic (Kaštela Bay) in relation to the North Atlantic Oscillation. Estuaries and Coasts 33, 376–383. https://doi.org/10.1007/s12237-009-9223-3

O'Connor, B.S., Muller-Karger, F.E., Nero, R.W., Hu, C., Peebles, E.B., 2016. The role of Mississippi River discharge in offshore phytoplankton blooming in the northeastern Gulf of Mexico during

August 2010. Remote Sens. of Environ. 173, 133–144. http://dx.doi.org/10.1016/j.rse.2015.11.004

Penna, N., Capellacci, S., Ricci, F., 2004. The influence of the Po River discharge on phytoplankton bloom dynamics along the coastline of Pesaro (Italy) in the Adriatic Sea. Mar. Pollut. Bull. 48, 321–326. https://doi.org/10.1016/j.marpolbul.2003.08.007

Pugnetti, A., Acri, F., Alberighi, L., Barletta, D., Bastianini, M., Bernardi Aubry, F., Berton, A., Bianchi, F., Socal, G., Totti, C., 2004. Phytoplankton photosynthetic activity and growth rates in the NW Adriatic Sea. Chem. Ecol. 20, 399–409. https://doi.org/10.1080/02757540412331294902

Pugnetti, A., Bazzoni, A.M., Beran, A., Bernardi Aubry, F., Camatti, E., Celussi, M., Coppola, J., Crevatin, E., Negro, P. Del, Paoli, A., 2008. Changes in biomass structure and trophic status of the plankton communities in a highly dynamic ecosystem (Gulf of Venice, Northern Adriatic Sea). Mar. Ecol. 29, 367–374. https://doi.org/10.1111/j.1439-0485.2008.00237.x

Russo, A., Artegiani, A., 1996. Adriatic Sea hydrography. Sci. Mar. 60, 33–43.

Strickland, J.D.H., Parsons, T.R., 1972. *A practical handbook of seawater analysis*. *Bulletin 167, 2nd ed*. Supply and Services Canada, Ottawa; Canada. https://doi.org/10.1002/iroh.19700550118

Sverdrup, H.U., 1953. On conditions for the vernal blooming of phytoplankton. ICES J. Mar. Sci. 18, 287–295. https://doi.org/10.1093/icesjms/18.3.287

Tang, D., Kawamura, H., Van Dien, T., Lee, M., 2004. Offshore phytoplankton biomass increase and its oceanographic causes in the South China Sea. Inter-Res. Sci. Publ. 268, 31–41. https://www.int-res.com/abstracts/meps/v268/p31-41/

Tanković, M.S., Baričević, A., Ivančić, I., Kužat, N., Medić, N., Pustijanac, E., Novak, T., Gašparović, B., Pfannkuchen, D.M., Pfannkuchen, M., 2018. Insights into the life strategy of the common marine diatom *Chaetoceros peruvianus* Brightwell. PLoS ONE 13, e0203634. https://doi.org/10.1371/journal.pone.0203634

Tengberg, A., Almroth, E., Hall, P., 2003. Resuspension and its effects on organic carbon recycling and nutrient exchange in coastal sediments: in situ measurements using new experimental technology. J. Exp. Mar. Biol. Ecol. 285–286, 119–142. https://doi.org/10.1016/S0022-0981(02)00523-3

Throndsen, J., 1978. Preservation and storage. In: Sournia, A. (Eds.), *Phytoplankton Manual. Monographs on Oceanographic Methodology*. UNESCO, Paris, pp. 69–74.

Totti, C., Ghetti, A., Pariante, R., Hopkins, T.S., 1999. Biological coherence in theWestern Adriatic coastal current: phytoplankton assemblages. In: Hopkins, T.S., Artegiani, A., Cauwet, G., Degobbis, D., Malej, A. (Eds.), *Ecosystems Research Report, No.32. The Adriatic Sea.* European Commission, Brussels, Belgium, pp. 385–400.

Totti, C., Cangini, M., Ferrari, C., Kraus, R., Pompei, M., Pugnetti, A., Romagnoli, T., Vanucci, S., Socal, G., 2005. Phytoplankton size-distribution and community structure in relation to mucilage occurrence in the northern Adriatic Sea. Sci. Total Environ. 353, 204–217. https://doi.org/10.1016/j.scitotenv.2005.09.028.

Totti, C., Romagnoli, T., Accoroni, S., Coluccelli, A., Pellegrini, M., Campanelli, A., Grilli, F., Marini, M., 2019. Phytoplankton communities in the northwestern Adriatic Sea: interdecadal variability over a 30-years period (1988– 2016) and relationships with meteoclimatic drivers. J. Mar. Syst. 193, 137–153. https://doi.org/10.1016/j.jmarsys.2019.01.007.

Turk Dermastia, T., Cerino, F., Stanković, D., Francé, J., Ramšak, A., Žnidarič Tušek, M., Beran, A., Natali, V., Cabrini, M., Mozetič, P., 2020. Ecological time series and integrative taxonomy unveil

seasonality and diversity of the toxic diatom *Pseudo-nitzschia* H. Peragallo in the northern Adriatic Sea. Harmful Algae 93. https://doi.org/https://doi.org/10.1016/j.hal.2020.101773

Turkoglu, M., 2010. Winter bloom of coccolithophore *Emiliania huxleyi* and environmental conditions in the Dardanelles. Hydrol. Res. 41, 104–114. https://doi.org/10.2166/nh.2010.124

Turner, R.E., Qureshi N., Rabalais, N.N., Dortch, Q., Justić D., Shaw, R.F., Cope, J., 1998. Fluctuating silicate:nitrate ratios and coastal plankton food webs. Proc. Natl. Acad. Sci. Unit. States Am. 95, 13048–13051. https://doi.org/10.1073/pnas.95.22.13048

Viaroli, P., Soana, E., Pecora, S., Laini, A., Naldi, M., Fano, E.A., Nizzoli, D., 2018. Space and time variations of watershed N and P budgets and their relationships with reactive N and P loadings in a heavily impacted river basin (Po River, Northern Italy). Sci. Total Environ. 639, 1574–1587. https://doi.org/10.1016/j.scitotenv.2018.05.233

Vilibić, I., Supić, N., 2005. Dense water generation on a shelf: the case of the Adriatic Sea. Ocean Dyn. 55, 403–415. https://doi.org/10.1007/s10236-005-0030-5

Vilibić, I., Zemunik, P., Šepić, J., Dunić, N., Marzouk, O., Mihanović, H., Denamiel, C., Precali, R., Djakovac, T., 2019. Present climate trends and variability in thermohaline properties of the northern Adriatic shelf. Ocean Sci. 15, 1351–1362. https://doi.org/10.5194/os-15-1351-2019

Viličić, D., Djakovac, T., Burić, Z., Bosak, S., 2009. Composition and annual cycle of phytoplankton assemblages in the northeastern Adriatic Sea. Bot. Mar. 52, 291–305. https://doi.org/10.1515/BOT.2009.004

Viličić, D., Kuzmic, M., Tomažić, I., Ljubešić, Z., Bosak, S., Precali, R., Djakovac, T., Marić, D., Godrijan, J., 2013. Northern Adriatic phytoplankton response to short Po River discharge pulses during summer stratified conditions. Mar. Ecol 34, 451–466. https://doi.org/10.1111/maec.12046

Zingone, A., Dubroca, L., Iudicone, D., Margiotta, F., Corato, F., Ribera d'Alcalà, M., Saggiomo, V., Sarno, D., 2010a. Coastal phytoplankton do not rest in winter. Estuaries and Coasts 33, 342–361. https://doi.org/10.1007/s12237-009-9157-9

Zingone, A., Phlips, E.J., Harrison, P.J., 2010b. Multiscale variability of twenty-two coastal phytoplankton time series: a global scale comparison. Estuaries and Coasts 33, 224–229. https://doi.org/10.1007/s12237-009-9261-x.

Zoppini, A., Pettine, M., Totti, C., Puddu, A., Artegiani, A., Pagnotta, R., 1995. Nutrients, standing crop and primary production in western coastal waters of the Estuar. Coast. Shelf Sci. 41, 493–513.

1.1.9 Supplementary materials

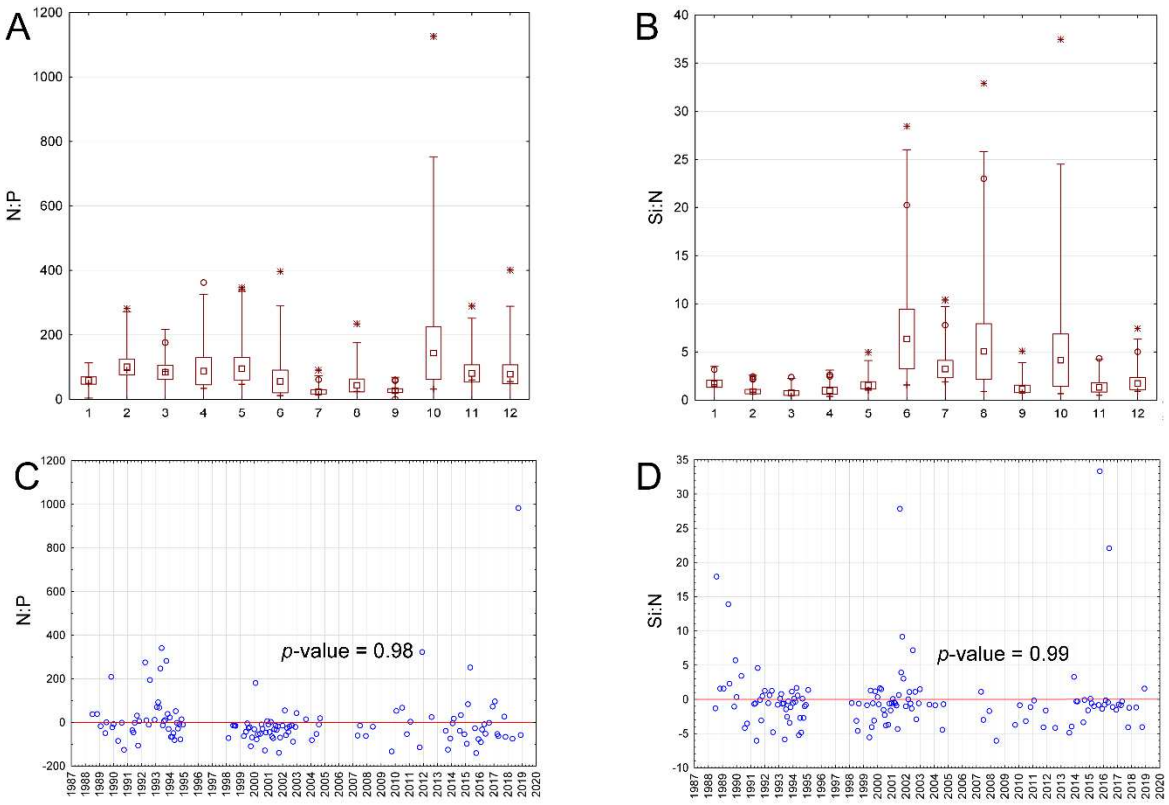

Fig. S1. Mean annual cycle (A,B) calculated on a mean monthly basis and trend of anomalies (C,D) of N:P (A,C) and Si:N (B,D) ratios from 1988 to 2018.

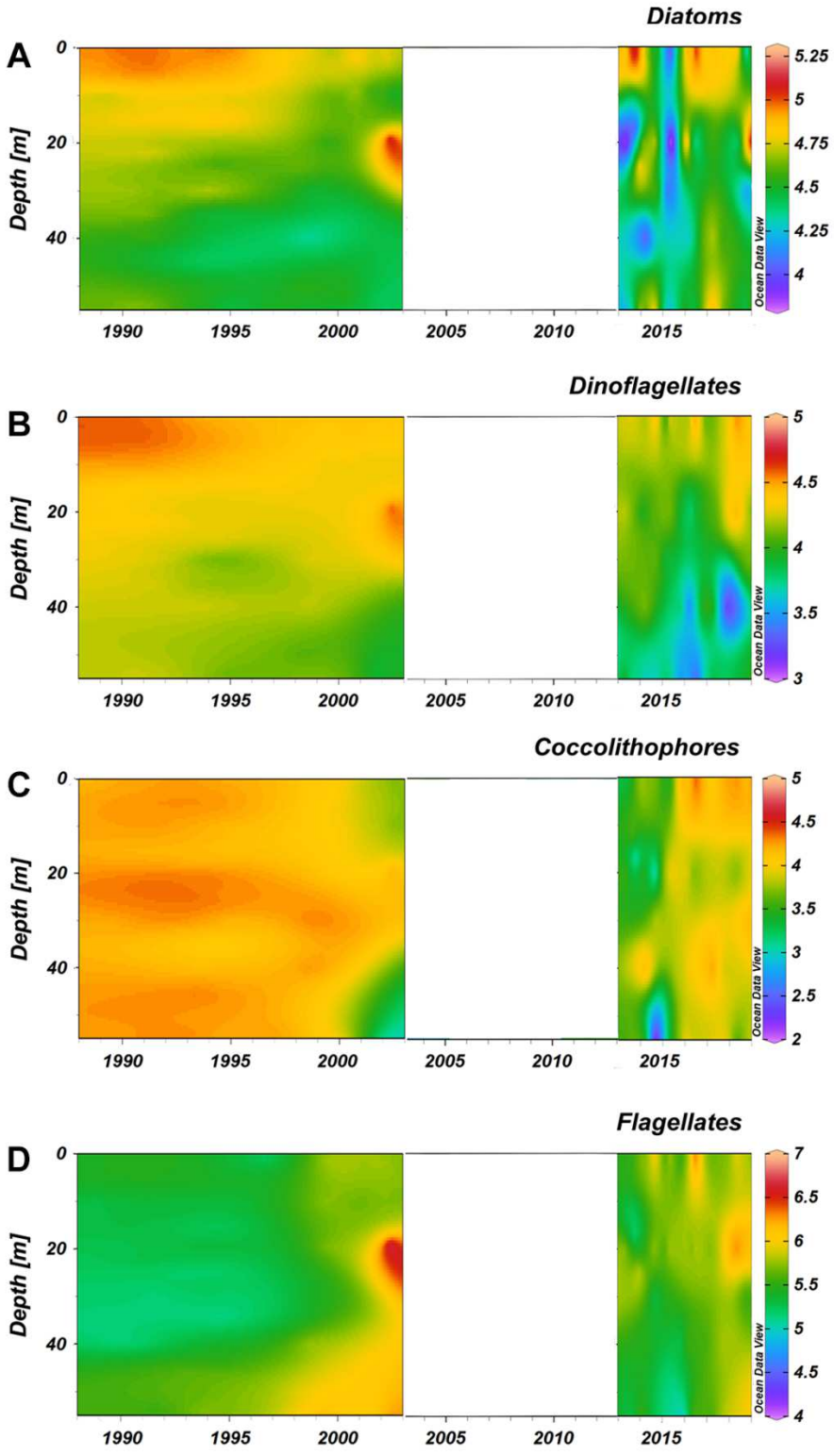

Fig. S2. Temporal and vertical variations of phytoplankton abundances (logarithm of abundances in cells l^{-1}) in the period 1988-2002 and 2013-2018: (A) diatoms, (B) dinoflagellates, (C) coccolithophores, (D) flagellates. The period 2003-2012 was not considered as the sampling frequency was too irregular.

Table S1. Sampling months and years

YEAR	MONTH	SEASON	Temperature [°C]	Salinity [psu]	Density [kg/m^3]	O_2 %	PO_4 µM	$Si(OH)_4$ µM	DIN µM	Phytoplankton [cell l^{-1}]
1988	1	Win								
1988	2	Win								
1988	3	Win								
1988	4	Spr								
1988	5	Spr								
1988	6	Spr								
1988	7	Sum	X	X	X	X	X	X	X	X
1988	8	Sum	X	X	X	X	X	X	X	X
1988	9	Sum								
1988	10	Aut								
1988	11	Aut	X	X	X	X	X	X	X	X
1988	12	Aut								
1989	1	Win								
1989	2	Win	X	X	X	X	X	X	X	X
1989	3	Win								
1989	4	Spr								
1989	5	Spr								
1989	6	Spr	X	X	X	X	X	X	X	X
1989	7	Sum	X	X	X	X	X	X	X	X
1989	8	Sum	X	X	X	X	X	X		X
1989	9	Sum								
1989	10	Aut								
1989	11	Aut	X	X	X	X	X	X	X	X
1989	12	Aut	X	X	X	X	X	X	X	
1990	1	Win	X	X	X	X	X	X	X	X
1990	2	Win								
1990	3	Win								
1990	4	Spr								
1990	5	Spr	X	X	X	X	X	X	X	X
1990	6	Spr								
1990	7	Sum	X	X	X	X	X	X		X
1990	8	Sum	X	X	X	X	X	X	X	X
1990	9	Sum								
1990	10	Aut	X	X	X	X	X	X	X	X
1990	11	Aut								
1990	12	Aut								
1991	1	Win								
1991	2	Win								
1991	3	Win								
1991	4	Spr	X	X	X	X	X	X	X	X
1991	5	Spr	X	X	X	X	X	X	X	X
1991	6	Spr	X	X	X	X	X	X	X	X
1991	7	Sum	X	X	X	X	X	X	X	X
1991	8	Sum								
1991	9	Sum	X	X	X	X	X	X	X	X
1991	10	Aut	X	X	X	X	X	X	X	X

1991	11	Aut	X	X	X	X	X	X	X	X
1991	12	Aut								
1992	1	Win								
1992	2	Win	X	X	X	X		X	X	X
1992	3	Win								
1992	4	Spr		X		X	X	X	X	X
1992	5	Spr	X	X	X	X	X	X	X	X
1992	6	Spr								
1992	7	Sum	X	X	X	X	X	X	X	X
1992	8	Sum				X	X	X	X	X
1992	9	Sum								
1992	10	Aut								
1992	11	Aut								
1992	12	Aut	X	X	X	X	X	X	X	X
1993	1	Win								
1993	2	Win	X	X	X	X	X	X	X	X
1993	3	Win	X	X	X	X	X	X	X	X
1993	4	Spr	X	X	X	X	X	X	X	X
1993	5	Spr	X	X	X	X	X	X	X	X
1993	6	Spr	X	X	X	X	X	X	X	X
1993	7	Sum	X	X	X		X	X	X	X
1993	8	Sum	X	X	X	X	X	X	X	X
1993	9	Sum	X	X	X	X	X	X	X	X
1993	10	Aut	X	X	X		X	X	X	X
1993	11	Aut	X	X	X	X	X	X	X	X
1993	12	Aut	X	X	X	X	X	X	X	X
1994	1	Win	X	X	X		X	X	X	X
1994	2	Win				X	X	X	X	X
1994	3	Win					X	X	X	X
1994	4	Spr	X	X	X	X	X	X	X	X
1994	5	Spr				X	X	X	X	X
1994	6	Spr	X	X	X	X	X	X	X	X
1994	7	Sum	X	X	X	X	X	X	X	X
1994	8	Sum					X	X	X	X
1994	9	Sum				X	X	X	X	X
1994	10	Aut				X	X	X	X	X
1994	11	Aut	X	X	X	X	X	X	X	X
1994	12	Aut				X	X	X	X	X
1995	1	Win								
1995	2	Win				X	X	X	X	X
1995	3	Win								
1995	4	Spr								
1995	5	Spr								
1995	6	Spr								
1995	7	Sum								
1995	8	Sum								
1995	9	Sum								
1995	10	Aut								
1995	11	Aut								

1995	12	Aut								
1996	1	Win								
1996	2	Win								
1996	3	Win								
1996	4	Spr								
1996	5	Spr								
1996	6	Spr								
1996	7	Sum								
1996	8	Sum	X	X	X	X				X
1996	9	Sum	X	X	X					X
1996	10	Aut								
1996	11	Aut								
1996	12	Aut								
1997	1	Win								
1997	2	Win								X
1997	3	Win								
1997	4	Spr								
1997	5	Spr								
1997	6	Spr								
1997	7	Sum								
1997	8	Sum								
1997	9	Sum								X
1997	10	Aut								X
1997	11	Aut								
1997	12	Aut								
1998	1	Win								
1998	2	Win								
1998	3	Win	X	X	X		X	X	X	X
1998	4	Spr								
1998	5	Spr								X
1998	6	Spr								X
1998	7	Sum	X	X	X		X	X	X	X
1998	8	Sum	X	X	X		X	X	X	X
1998	9	Sum	X	X	X		X	X	X	
1998	10	Aut								
1998	11	Aut								
1998	12	Aut								
1999	1	Win								
1999	2	Win								
1999	3	Win								
1999	4	Spr	X	X	X	X	X	X	X	
1999	5	Spr								
1999	6	Spr	X	X	X	X	X	X	X	X
1999	7	Sum	X	X	X	X	X	X	X	X
1999	8	Sum	X	X	X	X	X	X	X	X
1999	9	Sum	X	X	X	X	X	X	X	X
1999	10	Aut	X	X	X	X	X	X	X	X
1999	11	Aut	X	X	X	X	X	X	X	X
1999	12	Aut								

2000	1	Win	X	X	X	X	X	X	X	X
2000	2	Win	X	X	X	X	X	X	X	X
2000	3	Win	X	X	X	X	X	X	X	X
2000	4	Spr	X	X	X	X	X	X	X	X
2000	5	Spr	X	X	X	X				X
2000	6	Spr	X	X	X	X	X	X	X	X
2000	7	Sum	X	X	X	X	X	X	X	X
2000	8	Sum	X	X	X	X	X	X	X	X
2000	9	Sum								
2000	10	Aut	X	X	X	X	X	X	X	X
2000	11	Aut	X	X	X	X	X	X	X	X
2000	12	Aut	X	X	X	X	X	X	X	X
2001	1	Win	X	X	X	X	X	X	X	X
2001	2	Win	X	X	X	X	X	X	X	X
2001	3	Win	X	X	X	X	X	X	X	X
2001	4	Spr	X	X	X	X	X	X	X	X
2001	5	Spr	X	X	X	X	X	X	X	X
2001	6	Spr	X	X	X	X	X	X	X	X
2001	7	Sum	X	X	X	X	X	X	X	X
2001	8	Sum	X	X	X	X	X	X	X	X
2001	9	Sum	X	X	X	X	X	X	X	X
2001	10	Aut	X	X	X	X	X	X	X	X
2001	11	Aut	X	X	X	X	X	X	X	X
2001	12	Aut								
2002	1	Win	X	X	X	X	X	X	X	X
2002	2	Win								
2002	3	Win	X	X	X	X	X	X	X	X
2002	4	Spr	X	X	X	X	X	X	X	X
2002	5	Spr	X	X	X	X	X	X	X	X
2002	6	Spr	X	X	X	X	X	X	X	X
2002	7	Sum	X	X	X	X	X	X	X	X
2002	8	Sum								
2002	9	Sum	X	X	X	X	X	X	X	
2002	10	Aut	X	X	X	X	X	X	X	
2002	11	Aut								
2002	12	Aut	X	X	X	X	X	X	X	
2003	1	Win	X	X	X	X	X	X	X	
2003	2	Win	X	X	X	X				
2003	3	Win								
2003	4	Spr								
2003	5	Spr								
2003	6	Spr								
2003	7	Sum								
2003	8	Sum								
2003	9	Sum	X	X	X	X	X	X	X	
2003	10	Aut								
2003	11	Aut								
2003	12	Aut								
2004	1	Win								

2004	2	Win	X	X	X	X	X	X	X	
2004	3	Win								
2004	4	Spr								
2004	5	Spr								
2004	6	Spr	X	X	X	X	X		X	
2004	7	Sum								
2004	8	Sum	X	X	X	X	X	X	X	
2004	9	Sum					X	X	X	
2004	10	Aut								
2004	11	Aut								
2004	12	Aut								
2005	1	Win								
2005	2	Win								
2005	3	Win								
2005	4	Spr								
2005	5	Spr								
2005	6	Spr								
2005	7	Sum								
2005	8	Sum								
2005	9	Sum								
2005	10	Aut								
2005	11	Aut								
2005	12	Aut								
2006	1	Win								
2006	2	Win								
2006	3	Win								
2006	4	Spr								
2006	5	Spr								
2006	6	Spr								
2006	7	Sum								
2006	8	Sum								
2006	9	Sum								
2006	10	Aut								
2006	11	Aut								
2006	12	Aut								
2007	1	Win								
2007	2	Win								
2007	3	Win	X	X	X	X				
2007	4	Spr								
2007	5	Spr	X	X	X	X	X	X	X	
2007	6	Spr								
2007	7	Sum	X	X	X	X	X	X	X	
2007	8	Sum								
2007	9	Sum								
2007	10	Aut								
2007	11	Aut								
2007	12	Aut	X	X	X	X	X	X	X	
2008	1	Win								
2008	2	Win								

2008	3	Win								
2008	4	Spr								
2008	5	Spr								
2008	6	Spr	X	X	X	X	X	X	X	
2008	7	Sum								
2008	8	Sum								
2008	9	Sum								
2008	10	Aut	X	X	X	X				
2008	11	Aut								
2008	12	Aut								
2009	1	Win								
2009	2	Win								
2009	3	Win								
2009	4	Spr								
2009	5	Spr								
2009	6	Spr								
2009	7	Sum								
2009	8	Sum								
2009	9	Sum								
2009	10	Aut	X	X	X		X	X	X	
2009	11	Aut								
2009	12	Aut								
2010	1	Win								
2010	2	Win	X	X	X	X	X	X	X	
2010	3	Win								
2010	4	Spr	X	X	X	X			X	
2010	5	Spr								
2010	6	Spr	X	X	X	X				
2010	7	Sum	X	X	X	X	X	X	X	
2010	8	Sum								
2010	9	Sum								
2010	10	Aut								
2010	11	Aut	X	X	X	X	X	X	X	
2010	12	Aut								
2011	1	Win								
2011	2	Win	X	X	X	X	X	X	X	
2011	3	Win								
2011	4	Spr								
2011	5	Spr								
2011	6	Spr								
2011	7	Sum								
2011	8	Sum	X	X	X	X				
2011	9	Sum								
2011	10	Aut	X	X	X	X	X	X	X	X
2011	11	Aut								
2011	12	Aut	X	X	X		X	X	X	
2012	1	Win								
2012	2	Win	X	X	X		X	X		
2012	3	Win	X	X	X	X	X	X		

2012	4	Spr								
2012	5	Spr								
2012	6	Spr								
2012	7	Sum								
2012	8	Sum	X	X	X	X	X	X	X	
2012	9	Sum								
2012	10	Aut								
2012	11	Aut								
2012	12	Aut								
2013	1	Win								
2013	2	Win								
2013	3	Win								
2013	4	Spr	X	X	X	X			X	X
2013	5	Spr								
2013	6	Spr								
2013	7	Sum								
2013	8	Sum	X	X	X	X	X	X	X	X
2013	9	Sum								
2013	10	Aut	X	X	X	X	X	X	X	X
2013	11	Aut								
2013	12	Aut	X	X	X	X	X	X	X	X
2014	1	Win								
2014	2	Win	X	X	X	X	X	X	X	X
2014	3	Win	X	X	X	X	X	X	X	X
2014	4	Spr								
2014	5	Spr								
2014	6	Spr								
2014	7	Sum								
2014	8	Sum	X	X	X	X	X	X	X	X
2014	9	Sum	X	X	X	X	X	X	X	X
2014	10	Aut								
2014	11	Aut								
2014	12	Aut	X	X	X	X	X	X	X	
2015	1	Win								
2015	2	Win	X	X	X	X	X	X	X	X
2015	3	Win	X	X	X	X	X	X	X	X
2015	4	Spr								
2015	5	Spr	X	X	X		X	X	X	X
2015	6	Spr								
2015	7	Sum								
2015	8	Sum								
2015	9	Sum	X	X	X	X	X	X	X	
2015	10	Aut	X	X	X	X	X	X	X	X
2015	11	Aut								
2015	12	Aut	X	X	X	X	X	X	X	X
2016	1	Win								
2016	2	Win	X	X	X	X	X	X	X	X
2016	3	Win	X	X	X	X	X	X	X	X
2016	4	Spr								

2016	5	Spr	X	X	X	X	X	X	X	X
2016	6	Spr	X	X	X	X	X	X	X	X
2016	7	Sum								
2016	8	Sum								
2016	9	Sum	X	X	X	X	X	X	X	
2016	10	Aut								
2016	11	Aut								
2016	12	Aut	X	X	X	X	X	X	X	X
2017	1	Win								
2017	2	Win	X	X	X	X	X	X	X	X
2017	3	Win								
2017	4	Spr	X	X	X	X	X	X	X	X
2017	5	Spr	X	X	X	X	X	X	X	
2017	6	Spr								
2017	7	Sum								
2017	8	Sum								
2017	9	Sum								
2017	10	Aut	X	X	X	X	X	X	X	X
2017	11	Aut	X	X	X	X	X	X	X	X
2017	12	Aut								
2018	1	Win								
2018	2	Win								
2018	3	Win								
2018	4	Spr								
2018	5	Spr	X	X	X	X	X	X	X	X
2018	6	Spr								
2018	7	Sum								
2018	8	Sum								
2018	9	Sum								
2018	10	Aut	X	X	X	X	X	X	X	X
2018	11	Aut								
2018	12	Aut	X	X	X	X	X	X	X	X

Table S2. List of taxa

Diatoms

Amphiprora spp.
Amphora ovalis (Kützing) Kützing
Amphora spp.
Asterionellopsis glacialis (Castracane) Round
Asterolampra spp.
Asteromphalus cfr. *hookeri* Ehrenberg
Asteromphalus cfr. *hyalinus* Karsten
Asteromphalus cfr. *sarcophagus* Wallich
Asteromphalus spp.
Bacillaria paxillifera (O.F. Müller) Hendey
Bacteriastrum cfr. *biconicum* J. Pavillard
Bacteriastrum cfr. *delicatulum* Cleve
Bacteriastrum cfr. *elongatum* Cleve
Bacteriastrum cfr. *hyalinum* Lauder
Bacteriastrum cfr. *mediterraneum* J. Pavillard
Bacteriastrum elegans J. Pavillard
Bacteriastrum spp.
Caloneis spp.
Cerataulina pelagica (Cleve) Hendey
Cerataulus sp.
Chaetoceros affinis Lauder
Chaetoceros anastomosans Grunow in van Heurck
Chaetoceros atlanticus Cleve
Chaetoceros atlanticus var. *neapolitanus* (Schröder) Hustedt
Chaetoceros bacteriastroides Karsten
Chaetoceros brevis Schutt
Chaetoceros cfr. *constrictus* Gran
Chaetoceros cfr. *fragilis* Meunier
Chaetoceros cfr. *holsaticus* F.Schütt
Chaetoceros cfr. *vixvisibilis* Schiller
Chaetoceros cfr. *wighami* Brightwell
Chaetoceros compressus Lauder
Chaetoceros concavicornis Mangin
Chaetoceros costatus Pavillard
Chaetoceros curvisetus Cleve
Chaetoceros danicus Cleve
Chaetoceros decipiens Cleve
Chaetoceros densus (Cleve) Cleve
Chaetoceros dichaeta Ehrenberg
Chaetoceros didymus Ehremberg
Chaetoceros diversus Cleve
Chaetoceros cfr. *gracilis* Pantocsek
Chaetoceros laciniosus Schütt
Chaetoceros laevis Leuduger-Fortmorel
Chaetoceros lauderi Ralfs in Lauder
Chaetoceros lorenzianus Grunow
Chaetoceros messanensis Castracane
Chaetoceros muelleri Lemmermann
Chaetoceros peruvianus Brightwell
Chaetoceros rostratus Lauder
Chaetoceros simplex Ostenfeld
Chaetoceros socialis Lauder
Chaetoceros tenuissimus Meunier
Chaetoceros teres Cleve
Chaetoceros tetrastichon Cleve
Chaetoceros throndsenii Marino, Montresor & Zingone
Chaetoceros tortissimus Gran
Chaetoceros spp.
Undetermined Chaetocerotaceae
Cocconeis scutellum Ehrenberg
Cocconeis spp.
Coscinodiscus cfr. *apiculatus* Ehrenberg
Coscinodiscus cfr. *granii* Gough
Coscinodiscus spp.
Cyclotella spp.
Cylindrotheca closterium (Ehrenberg) Lewin & Reimann
Cymatosira spp.
Dactyliosolen blavyanus (H. Peragallo) Hasle
Dactyliosolen fragilissimus (Bergon) Hasle
Dactyliosolen mediterraneus (H.Peragallo) H.Peragallo
Dactyliosolen phuketensis (Sundström) Hasle
Detonula pumila (Castracane) Gran
Diploneis spp.
Ditylum brightwellii (West) Grunow in Van Heurck
Entomoneis cfr. *ornata* (J.W.Bailey) Reimer
Entomoneis spp.
Eucampia cornuta (Cleve) Grunow
Eucampia zodiacus f. *cylindricornis* Syvertsen
Fragilariopsis spp.
Grammatophora sp.
Guinardia flaccida (Castracane) H. Peragallo
Guinardia striata (Stolterfoth) Hasle
Guinardia spp.
Gyrosigma spp.
Haslea wawrickae (Hustedt) Simonsen
Hemiaulus hauckii Grunow in van Heurck
Hemiaulus sinensis Greville
Hemiaulus spp.
Hobaniella longicruris (Greville) P.A.Sims & D.M.Williams
Lauderia annulata Cleve
Leptocylindrus cfr. *danicus* Cleve
Leptocylindrus convexus Nanjappa and Zingone
Leptocylindrus danicus Cleve
Leptocylindrus minimus Gran
Leptocylindrus spp.
Licmophora spp.
Lioloma pacificum (Cupp) Hasle
Melosira cfr. *moniliformis* (Mull.)Agardh
Melosira cfr. *nummuloides* C.Agardh
Melosira spp.
Navicula cancellata var. *retusa* (Brébisson) Cleve
Navicula coffeiformis A.W.F.Schmidt
Navicula spp.
Nitzschia cfr. *bilobata* W.Smith
Nitzschia cfr. *incurva* Grunow
Nitzschia cfr. *lanceolata* W.Smith
Nitzschia cfr. *sigma* (Kützing) W.Smith
Nitzschia gobbii Accoroni, Romagnoli, Giulietti & Totti
Nitzschia longissima (Brébisson in Kützing) Ralfs in Pritchard
Nitzschia sigma (Kützing) W.Smith
Nitzschia spp.
Paralia sulcata (Ehremberg) Cleve
Phaeodactylum tricornutum Bohlin
Pinnularia spp.
Plagiotropis lepidoptera (Gregory) Kuntze
Plagiotropis spp.
Pleurosigma affine
Pleurosigma angulatum (Quekett) W.Smith
Pleurosigma rigidum W.Smith
Pleurosigma spp.
Proboscia alata (Brightwell) Sundström
Psammodictyon spp.

Pseudoguinardia recta von Stosch
Pseudo-nitzschia cfr. *delicatissima* (Cleve) Heiden
Pseudo-nitzschia cfr. *galaxiae* N.Lundholm & Moestrup
Pseudo-nitzschia cfr. *pseudodelicatissima* (Hasle) Hasle
Pseudo-nitzschia fraudulenta (Cleve) Hasle
Pseudo-nitzschia multistriata (Takano) Takano
Pseudo-nitzschia pungens (Grunow ex Cleve) Hasle
Pseudo-nitzschia spp.
Pseudosolenia calcar avis (Schultze) B.G.Sundström
Rhabdonema adriaticum Kutzing
Rhizosolenia castracanei
Rhizosolenia hebetata f. *semispina* Bailey
Rhizosolenia imbricata Brightwell
Rhizosolenia robusta Norman in Pritchard
Rhizosolenia setigera Brightwell
Rhizosolenia styliformis T.Brightwell
Rhizosolenia spp.
Skeletonema marinoi Sarno & Zingone
Surirella ovata Kutzing
Surirella spp.
Thalassionema bacillare (Heiden) Kolbe
Thalassionema frauenfeldii (Grunow) Hallegraeff
Thalassionema nitzschioides (Grunow) Mereschkowsky
Thalassionema spp.
Thalassiosira cfr. *angulata* (W.Gregory) Hasle
Thalassiosira rotula Meunier
Thalassiosira subtilis (Ostenfeld) Gran
Thalassiosira spp.
Trichotoxon sp.
Tropidoneis spp.
Tryblionella spp.
Und. centric diatoms
Und. pennate diatoms

Dinoflagellates
Akashiwo sanguinea (K.Hirasaka) Gert Hansen & Moestrup
Alexandrium minutum Halim
Alexandrium spp.
Amphidinium spp.
Amphidoma spp.
Azadinium caudatum (Halldal) Nézan & Chomérat
Azadinium spp.
Ceratocorys kofoidii Paulsen
Cochlodinium spp.
Corythodinium constrictum (F.Stein) F.J.R.Taylo
Corythodinium tesselatum (F.Stein) Loeblich Jr. & Loeblich III
Desmocapsa gelatinosa Pascher
Dinophysis acuminata Claparède & Lachmann
Dinophysis caudata Saville-Kent
Dinophysis cfr. *ovum* F.Schütt
Dinophysis fortii Pavillard
Dinophysis sacculus Stein
Dinophysis sphaerica F.Stein
Dinophysis tripos Gourret
Dinophysis spp.
Diplopsalis group Bergh
Ensiculifera sp.
Goniodoma polyedricum (Pouchet) Jorgensen
Gonyaulax fragilis (Schutt) Kofoid
Gonyaulax polygramma Stein
Gonyaulax scrippsae Kofoid
Gonyaulax spinifera (Claparède & Lachmann) Diesing
Gonyaulax spp.
Gymnodinium cfr. *caput* J.Schiller
Gymnodinium elongatum Hope
Gymnodinium spp.
Gyrodinium cfr. *acutum* (F.Schütt) Kofoid & Swezy
Gyrodinium lachrima (Meunier) Kofoid & Swezy
Gyrodinium spp.
Kofoidinium velleloides Pavillard
Lingulodinium polyedra (Stein) Dodge
Mesoporos perforatus (Gran) Lillick
Mesoporos spp.
Micracanthodinium setiferum (Lohmann) Deflandre
Noctiluca scintillans (Macartney) Kofoid & Swezy
Ornithocercus spp.
Oxytoxum caudatum Schiller
Oxytoxum cfr. *elongatum* Wood
Oxytoxum cfr. *ovale* Schiller
Oxytoxum crassum Schiller
Oxytoxum gracile Schiller
Oxytoxum laticeps Schiller
Oxytoxum sceptrum (F.Stein) Schröder
Oxytoxum scolopax Stein
Oxytoxum variabile Schiller
Phalacroma cfr. *porosum* Kofoid
Phalacroma rotundatum (Claparéde & Lachmann) Kofoid & Michener
Podolampas palmipes Stein
Pronoctiluca pelagica Fabre-Domergue
Pronoctiluca spinifera (Lohmann) Schiller
Pronoctiluca sp.
Prorocentrum balticum (Lohmann) Loeblich
Prorocentrum cfr. *aporum* (Schiller) J.D.Dodge
Prorocentrum cfr. *lima*
Prorocentrum cfr. *nanum* Schiller
Prorocentrum cfr. *ovum* (J.Schiller) J.D.Dodge
Prorocentrum cfr. *rotundatum* J.Schiller
Prorocentrum cfr. *vaginulum* (Stein) Dodge
Prorocentrum compressum (J.W.Bailey) Abé ex Dodge
Prorocentrum cordatum (Pavillard) J.Schiller
Prorocentrum dactylus (Stein) Dodge
Prorocentrum dentatum Stein
Prorocentrum micans Ehremberg
Prorocentrum triestinum Schiller
Prorocentrum spp.
Protoceratium reticulatum (Claparède & Lachmann) Bütschli
Protoceratium spp.
Protoperidinium bipes (Paulsen) Balech
Protoperidinium cfr. *breve* Paulsen
Protoperidinium cfr. *brochi* (Kofoid & Swezy) Balech
Protoperidinium cfr. *globulus* (F.Stein) Balech
Protoperidinium cfr. *ovum* (Schiller) Balech
Protoperidinium cfr. *pallidum* (Ostenfeld) Balech
Protoperidinium cfr. *steinii* (Jorgensen) Balech
Protoperidinium conicum (Gran) Balech
Protoperidinium crassipes (Kof.) Bal.
Protoperidinium depressum (Bailey) Balech
Protoperidinium diabolus (Cleve) Balech
Protoperidinium divergens (Ehrenberg) Balech
Protoperidinium minusculum Pavillard
Protoperidinium oceanicum (VanHoffen) Balech
Protoperidinium steinii (E.G.Jørgensen) Balech
Protoperidinium tuba (J.Schiller) Balech

Protoperidinium spp.
Pseliodinium vaubanii Sournia
Pyrocystis cfr. *obtusa* Pavillard
Pyrocystis lunula (Schutt) Schutt
Pyrophacus horologicum Stein
Scrippsiella spp.
Sinophysis ebriola (Herdman) Balech
Tripos candelabrum (Ehrenberg) F.Gómez
Tripos carriensis (Gourret) F.Gómez
Tripos cf. *strictus* (Okamura & Nishikawa) F.Gómez
Tripos extensus (Gourret) F.Gómez
Tripos furca (Ehrenberg) F.Gómez
Tripos fusus (Ehrenberg) F.Gómez
Tripos horridus (Cleve) F.Gómez
Tripos kofoidii (Jörgenen) F.Gómez
Tripos lineatus (Ehrenberg) F.Gómez
Tripos macroceros (Ehrenberg) F.Gómez
Tripos muelleri Bory
Tripos setaceus (Jørgesen) F.Gómez
Tripos symmetricus (Pavillard) F.Gómez
Tripos teres (Kofoid) F.Gómez
Tripos trichoceros (Ehrenberg) Gómez
Tripos vultur (Cleve) Hallegraeff & Huisman
Tripos spp.
Und. naked dinoflagellates
Und. thecate dinoflagellates
Dinoflagellate cysts

Haptophytes
Chrysochromulina alifera Parke & Manton
Chrysochromulina sp.
Phaeocystis sp.
Corymbellus aureus Green
Und. haptophytes
Coccolithophores
Acanthoica quattrospina Ehrenberg
Calcidiscus leptoporus (Murray & Black.) Loeb. & Tappan
Calciopappus caudatus Gaarder & Ramsfjell
Calciosolenia brasiliensis (Lohmann) J.R.Young
Calciosolenia murrayi Gran
Calyptrosphaera oblonga Lohmann
Calyptrosphaera sphaeroidea Schiller
Calyptrosphaera spp.
cfr. *Algirosphaera oryza* Schlauder
cfr. *Helicosphaera hyalina* Gaarder
Coccolithus pelagicus (Wallich) Sch.
Coccolithus pelagicus f. *hyalinus* (K.R.Gaarder & J.Markali) A.Kleijne
Coronosphaera mediterranea (Lohmann) Gaarder in Gaarder & Heimdal
Daktylethra pirus (Kamptner) Norris
Emiliania huxleyi (Lohmann) W.W.Hay & H.P.Mohler
Halopappus adriaticus Schiller
Helicosphaera carteri (Wallich) Kamptner
Helladosphaera cornifera (Sch.) Kamptner
Michaelsarsia elegans Gran
Ophiaster hydroideus (Lohmann) Lohmann
Ophiaster sp.
Rhabdosphaera clavigera Murray & Blackman
Rhabdosphaera clavigera var. *stylifera* (Lohmann) Kleijne & R.W.Jordan
Syracosphaera histrica Kamptner
Syracosphaera pulchra Lohmann
Syracosphaera spp.
Tergestiella adriatica Kamptner
Umbellosphaera tenuis (Kamptner) Paasche
Und. coccolithophores

Cryptophytes
Hillea fusiformis Schiller
Hillea marina Butcher
Leucocryptos cfr. *marina* (Braarud) Butcher
Und. cryptophytes

Chrysophytes
Calycomonas vangoorii J.W.G.Lund
Dinobryon faculiferum (Willén) Willén
Dinobryon spp.
Meringosphaera mediterranea Lohmann
Pseudokephyrion spp.
Und. chrysophytes

Dictyochophytes
Dictyocha fibula Ehrenberg
Distephanopsis staurodon (Ehrenberg) Desikachary & Prema
Octactis octonaria (Ehrenberg) Hovasse
Octactis speculum (Ehrenberg) F.H.Chang, J.M.Grieve & J.E.Sutherland
Parapedinella cfr. *reticulata* S.M. Pedersen & Thomsen in Pedersen, Beech, & Thomsen
Und. silicoflagellates

Raphidophytes
cfr. *Olisthodiscus luteus* N.Carter
Heterosigma spp.

Chlorophytes
Nephroselmis sp.
Pachysphaera spp.
Pseudoscourfieldia marina (Throndsen) Manton
Pyramimonas spp.
Tetraselmis spp.
Und. chlorophytes

Euglenophytes
Euglena spp.
Eutreptiella hirudoidea Butcher
Und. Euglenophyceae

Cyanophytes
Spirulina sp.
Und. Cyanophyceae

Chapter 1.2

Phytoplankton communities in a coastal and offshore stations of the northern Adriatic Sea approached by network analysis and different statistical descriptors

Neri F., Romagnoli T., Accoroni S., Ubaldi M., Garzia A., Pizzuti A., Campanelli A., Grilli F., Marini M., Totti C. (2023) Phytoplankton communities in a coastal and offshore stations of the northern Adriatic Sea approached by network analysis and different statistical descriptors. *Estuarine, Coastal and Shelf Science*, 282: 108224. https://doi.org/10.1016/j.ecss.2023.108224

Phytoplankton communities in coastal and offshore stations of the northern Adriatic Sea approached by network analysis and different statistical descriptors

Francesca Neri[1], Tiziana Romagnoli[1], Stefano Accoroni[1,2], Marika Ubaldi[1], Angela Garzia[1], Andrea Pizzuti[3], Alessandra Campanelli[4], Federica Grilli[4], Mauro Marini[2,4], Cecilia Totti[1,5]

[1]Dipartimento di Scienze della Vita e dell'Ambiente, Università Politecnica delle Marche, via Brecce Bianche, 60131 Ancona, Italy

[2]Fano Marine Center, The Inter-Institute Center for Research on Marine Biodiversity, Resources and Biotechnologies (FMC), viale Adriatico 1/N, 61032 Fano, Italy

[3]Dipartimento di Ingegneria dell'informazione, Università Politecnica delle Marche, via Brecce Bianche, 60131 Ancona, Italy

[4]Consiglio Nazionale delle Ricerche, CNR-IRBIM, largo Fiera della Pesca, 2, 60125 Ancona, Italy

[5]Consorzio Interuniversitario per le Scienze del Mare, CoNISMa, ULR Ancona, Ancona, Italy

*Corresponding Author: f.neri@pm.univpm.it

Keywords:

Phytoplankton; Long-term series; Graph-network analysis; Community ecology; Marine strategy framework directive

1.2.1 Abstract

The Northern Adriatic Sea is one of the most productive areas of the Mediterranean Sea. Long-term series of phytoplankton are crucial to detect changes in the marine ecosystems, due to its high sensitiveness to environmental conditions.

In this study, we compared two long-term phytoplankton time series (1988–2019) related to a coastal and an offshore station located along the LTER Senigallia-Susak transect (Northern Adriatic Sea), using several statistical descriptors: diversity indices, multivariate statistical analyses (PCA, HCPC, NMDS), IndVal (indicator value analysis) and graph-network analysis. The coastal station was found to be more variable than the offshore one, being directly affected by the Western Adriatic Current and therefore by riverine inputs. The two stations appeared to be more different in winter and autumn, and more similar in summer when riverine waters spread offshore in stratified conditions. Due to its more oligotrophic condition, the offshore phytoplankton community showed a higher biodiversity than the coastal one, where phytoplankton blooms occurred frequently.

Graph-network analysis turned out to be a useful tool to study the phytoplankton community through the number of interactions occurring among phytoplankton taxa, that was higher at the offshore station.

This study highlighted that any evaluation of the Good Environmental Status (as required by the Marine Strategy Framework Directive) should consider the oceanographic differences between different areas, combining several statistical approaches.

1.2.2 Introduction

The Northern Adriatic Sea (NAS), the northernmost basin of the Mediterranean Sea, represents one of the most productive areas of the Mediterranean Sea and is characterized by a shallow depth, a high riverine input (mainly from the Po River), and by a dominant cyclonic circulation (Artegiani et al., 1997a; Campanelli et al., 2011; Degobbis et al., 2000; Grilli et al., 2020).

In the NAS, the trophic state and the seasonal rhythm of phytoplankton communities are directly influenced by the vertical structure of the water column (stratification vs mixing) (Neri et al., 2022) and the circulation regime: the Western Adriatic Current (WAC) conveys southwards the nutrient-rich waters from the northern subbasin (Artegiani et al., 1997b; Campanelli et al., 2011; Marini et al., 2008) and the Eastern Adriatic Current flows northwards along the eastern coast, bringing Ionian saltier, warmer and more oligotrophic waters (Poulain and Cushman-Roisin, 2001). In the recent decade, other forcings, such as an increasing anthropogenic pressure and significant meteoclimatic alterations superimposed, determining new tendencies in the seasonal trend of trophic status and of planktonic communities (Cibic et al., 2018; Grilli et al., 2020; Ninčević Gladan et al., 2010; Totti et al., 2019).

Data from Long-Term Ecological Research (LTER) are crucial to study potential tendencies and changes in the phytoplankton community (Cerino et al., 2019; Marić et al., 2012; Mozetič et al., 2010; Neri et al., 2022; Totti et al., 2019) and to disentangling its variability, basic structure, phenology and regularity (Longobardi et al., 2022; Vascotto et al., 2021; Winder and Cloern, 2010). Four LTER marine areas are present in the NAS (Gulf of Venice, Gulf of Trieste, Po River delta, and Senigallia-Susak Transect), where the interannual variability of physical parameters, trophic condition and phytoplankton variability have been intensively studied. Among these, the Senigallia-Susak Transect (SST) is located in the lower part of the NAS, where the WAC becomes more distinct (Russo and Artegiani, 1996). Since 1988, data of phytoplankton (abundance and biomass) and abiotic parameters have been collected in the SST, with a ca. monthly frequency. Previous studies on the SST have already highlighted that the annual cycle of phytoplankton differed between the coastal and offshore stations: in the coastal station the phytoplankton annual maximum occurs in winter months (Totti et al., 2019), while offshore in June–July (Neri et al., 2022).

Phytoplankton is a well-known ecosystem service provider, as it produces more than 50% of the world's oxygen, contributes to ocean carbon cycling, climate regulation and to higher trophic level/food production (Blanchard et al., 2012; Falkowski et al., 2004; Hays et al., 2005; Khatiwala et

al., 2009; Martin et al., 2011; Richardson et al., 2000; Tweddle et al., 2018; Vallina and Simó, 2007, 2008/56/EC). The fast turnover and the high sensitiveness to environmental conditions make the phytoplankton an optimal proxy reflecting the main changes in the marine ecosystems. Therefore, phytoplankton has been included in the Marine Strategy Framework Directive for the assessment of the Good Environmental Status (GES) of pelagic habitats (2008/56/EC). Although it is particularly accounted for diversity and food web descriptors, many authors suggested that phytoplankton should be even more considered in the pressure-related descriptors and the marine management processes (European Commission, 2010, 2017; McQuatters-Gollop et al., 2015, 2019, 2022; Murillas-Maza et al., 2020; Tweddle et al., 2018). To describe the phytoplankton community structure, it is recommended to use a combination of aspects and metrics, e.g., abundances, biomass, intensity of blooms, composition, diversity indices (Cozzoli et al., 2017; Francé et al., 2021; Hering et al., 2010; Varkitzi et al., 2018). Functional diversity should also be considered as it takes into account the "role" of the organisms in the ecosystem, what they do and how they interact, influencing ecosystem processes and functioning (Díaz and Cabido, 2001; Lyashevska and Farnsworth, 2012; Petchey and Gaston, 2006). The use of graphs (a mathematical formalism useful for describing and representing a relationship on a finite and discrete set of elements, Harary, 1969), or networks, based on interactions, regardless the type, can give insights into the properties and dynamics of communities, as this method simplifies an ecological system representing the interactions among organisms in terms of nodes (taxa) and edges (relationships) (Costa et al., 2019; D'Alelio et al., 2016; Delmas et al., 2018). Graph-network analysis applied on phytoplankton data could provide information on interspecific interactions and functioning of this trophic level which is the basis of most food webs. Another useful tool providing information on the "importance" of the taxa in the community is given by indicator value analysis (IndVal) which reveals key taxa of a certain grouping factor (e.g., season, environmental conditions), based on relative abundances and frequencies (Dufrêne and Legendre, 1997).

Most of the studies about testing and application of phytoplankton indicators in the Mediterranean Sea cover coastal areas, while the literature related to open water stations is much scarcer (Francé et al., 2021; Markogianni et al., 2017; Ninčević -Gladan et al., 2015; Varkitzi et al., 2018).

In this study, several statistical descriptors (diversity indices, multivariate analyses, IndVal and graph-network analyses) were used (i) to compare the phytoplankton community structure between two stations located in the SST, one coastal and one offshore, and thus differently affected by oceanographic conditions and (ii) to test the suitability of these descriptors in highlighting the main features of the two stations in terms of community composition (e.g. opportunistic/seasonal taxa), main forcings affecting the phytoplankton dynamics, and functioning in terms of species interactions.

1.2.3 Materials and methods

Study area and sampling

The sampling stations are located along the Senigallia-Susak Transect which is included in the LTER Italian stations. Two stations were considered for the study: SG01 (bottom depth: 12 m) and SG05 (bottom depth: 55 m), located at 1.2 and 15 nM from the western NA coast, respectively (Fig. 1).

For both stations, data were collected from 1988 to 2019 on board of several oceanographic vessels (S. Lo Bianco, Tecnopesca 2, G. Dallaporta, Tethis, Copernaut Franca, Urania, Alliance, Minerva, Bannock, D'Ancona, Actea). Sampling was carried out with approximately a monthly frequency, although sometimes quarterly and with some periods of interruptions, particularly for the offshore station (the longest of which was between 2003 and 2012 for phytoplankton sampling), due to greater difficulties in sampling. Conductivity-Temperature-Depth (CTD) data were acquired by a Neil Brown Instrument System (NBIS) (from 1988 to 1991), and later by a SeaBird Electronic SBE 911plus (after 1992).

Niskin bottles or Rosette system were used to collect water samples for determination of dissolved inorganic nutrients (nitrite-NO_2, nitrate- NO_3, ammonia-NH_4, orthophosphate-PO_4 and orthosilicate-$Si(OH)_4$) and for phytoplankton analysis at the following depths: surface (1 m) and bottom (12 m)

for SG01 and surface (1 m), base of mixed layer, maximum fluorescence depth (when present) and bottom for SG05.

Samples for nutrient analysis were filtered (GF/F Whatman, 0.7 μm), and preserved at –22 °C in polyethylene Falcon until analysis. Phytoplankton samples were collected in 250 ml dark glass bottles and stored at 4 °C until analysis after adding 0.8% prefiltered and neutralized formaldehyde (Throndsen, 1978).

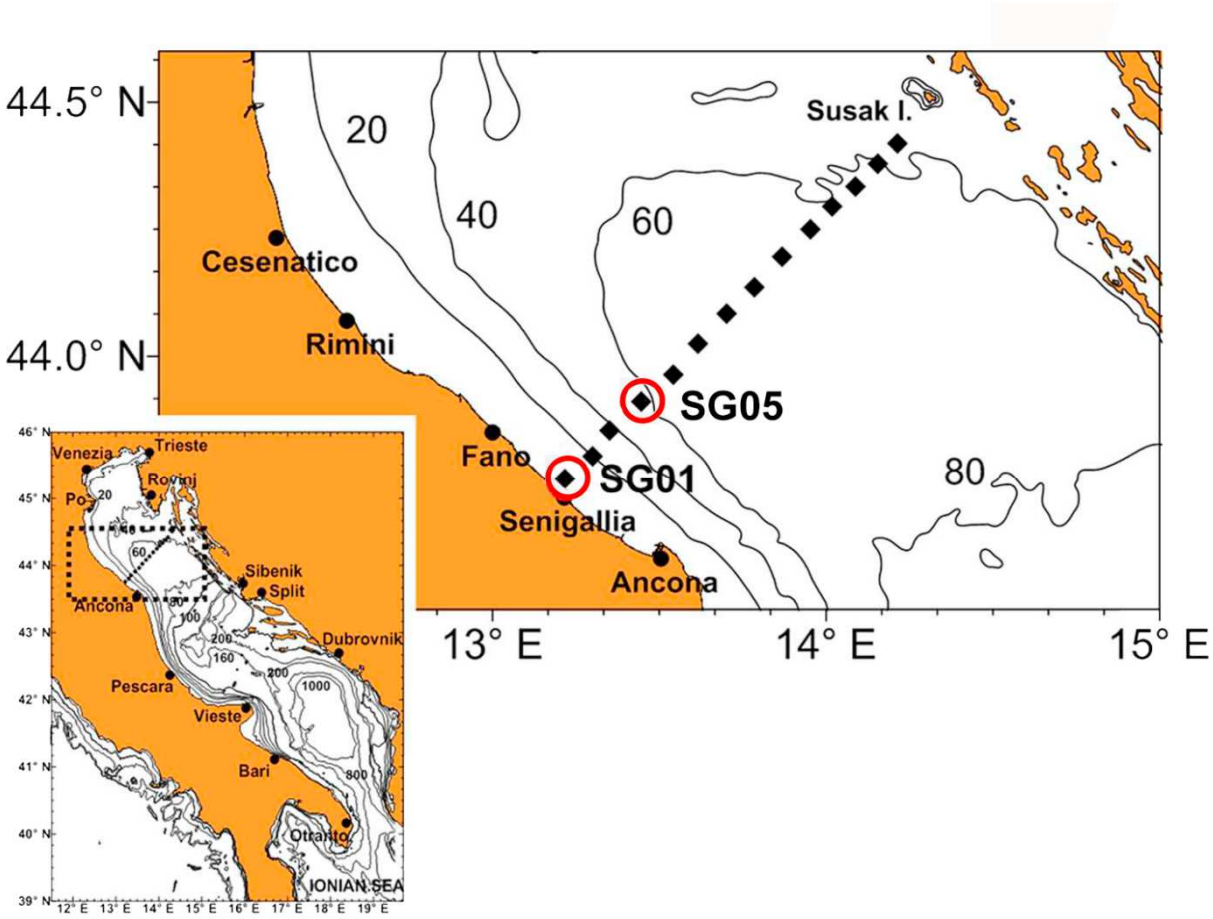

Fig. 1. Map of the study area. The Senigallia-Susak Transect (dotted line) and the sampling stations are shown. Coastal (SG01) and offshore (SG05) stations are highlighted by the red circles.

Nutrient analysis

PerkinElmer spectrophotometer 550A model (1988–1998), autoanalyzer TRAACS 800 BRAN + LUEBBE (1999–2005) and QUAATRO Technicon (after 2005) were used for nutrient analyses

(Strickland and Parsons, 1972). Dissolved Inorganic Nitrogen (DIN) concentration is intended as the sum of NO_2, NO_3 and NH_4 concentrations.

Phytoplankton analysis

An inverted microscope (ZEISS Axiovert 135) equipped with phase contrast was used for the identification and counting of phytoplankton, following the Utermöhl method (Edler and Elbrachter, 2010). Counting was carried out at 400x magnification, along transects or in random visual fields, depending on cell abundance, to count a minimum of 200 cells. Moreover, a half of the Utermöhl chamber was analyzed at 200x magnification for a more precise estimation of less abundant microphytoplanktonic taxa.

Phytoplankton taxa were grouped into major groups (diatoms, dinoflagellates, coccolithophores, phytoflagellates and others), and abundances were expressed as cells l^{-1}. Dinoflagellates were considered as a taxonomical group and both autotrophic and heterotrophic species were included in counting. Phytoflagellates are an informal group that includes haptophytes (except coccolithophores), cryptophytes, chrysophytes, dictyochophytes, raphidophytes, chlorophytes and euglenophytes.

Others include cyanophytes and incertae sedis, although this group was not considered for the study.

Data analysis

Only the surface (0.5 m) depth was considered for the data analysis, leading to a dataset of 7482 samples of Temperature, Salinity, DIN, PO_4, $Si(OH)_4$ DIN:PO_4, $Si(OH)_4$:DIN and phytoplankton abundances. All the analyses were performed using the R software (R Core Team, 2021), version 4.1.1. Principal Component Analysis (PCA) and Hierarchical Clustering on Principal Components (HCPC) were performed on Temperature, Salinity, DIN, PO_4, $Si(OH)_4$, DIN/PO_4 and $Si(OH)_4$/DIN ratios. In order to allow comparability, data were scaled prior to analysis. PCA and HCPC functions from the FactoMineR package (Lê et al., 2008) were used. In the same way, PCA and HCPC were performed also using the main phytoplankton group abundances.

Phytoplankton groups were analyzed through Non-Metric Multidimensional Scaling (NMDS), using the metaMDS function from the vegan package (Oksanen et al., 2022) and setting the autotransform as true. In order to have an insight on the seasonality, NMDS was performed on the different seasons, which were divided as follows: winter (January–March), spring (April–June), summer (July–September), autumn (October–December), as already done in other studies (Bernardi Aubry et al., 2006; Grilli et al., 2005, 2020). Permutational multivariate analysis of variance (PERMANOVA) was used to test for significant differences among the groups that were highlighted by the NMDS, using the adonis function in the vegan package (Oksanen et al., 2022). An analysis of multivariate homogeneity (PERMDISP) (Anderson, 2006) was performed using the betadisper function from the vegan package (Oksanen et al., 2022) as PERMANOVA is sensitive to data dispersion (Anderson, 2001).

For each season, Shannon diversity index (H′) (Shannon, 1948) and Pielou's evenness (J′) (Pielou, 1975) were used to study diversity and equitability, calculated using the diversity function available in the vegan package (Oksanen et al., 2022). To avoid the influence of the sample sizes to the diversity, rarefied richness was also measured using the rarefy function (vegan package). Margalef and Menhinick indices were calculated using the corresponding functions in the abdiv package (Bittinger, 2020). Two-sample Wilcoxon tests (also known as "Mann-Whitney" test) was used to check for significant differences between the two stations, using the Wilcox.test function in the stats package (R Core Team, 2021). Pearson's correlations among indices were calculated using rcorr function from the Hmisc package (Harrell, 2022) to study the relationships among them and uniqueness of the information given by each index.

The interactions among the phytoplankton community in the different seasons of each station were investigated by graph-network analysis, where a graph is a mathematical formalism useful for describing and representing a relationship on a finite and discrete set of elements (Harary, 1969). The graph-network analysis was performed using the igraph package in R (Csardi and Nepusz, 2006). Species abundances were log transformed prior to the analysis and undetermined taxa were excluded

for this analysis. Pearson's correlations between species were calculated using the stats package (R Core Team, 2021). Only the correlations with the statistical significance coefficient ($p \leq 0.05$) were selected for the construction of the graph. Positive and negative interactions were considered separately. In our study, we relied on the construction of undirected weighted graphs for station description, formally defined on a triple of sets as G = (V, E, W), in which V and E are respectively the set of vertices and edges, W is the set of weights associated to edges given by correlation values. The study makes use of both local and global measures to identify meaningful features of networks. In particular, we considered the closeness centrality measure (Freeman, 1979) and the degree (Harary, 1969) to study the capability of each taxon to interact with others in the system. The closeness parameter measures how "close" a node (species) is to all the others in the network and how quickly it communicates with the others (Mason and Verwoerd, 2007): the node with the highest closeness value would more likely influence the overall network (Costa et al., 2019; Estrada and Bodin, 2008). Instead, the degree is the number of connections and so the number of nodes another one is connected to, giving an idea of the involvement of a species in the network, without taking into account the weight, and so the strength, of the connection itself (Opsahl et al., 2010), therefore providing a different information on the community dynamics.

For small and disconnected networks (i.e., where a maximum of 5 vertices for each connected subgraph was present) only the degree was considered. Furthermore, we calculated the network betweenness, the diameter and the clustering coefficient (even if not discussed). The detailed methods and the equations used for the graph-network analysis are presented in Supplementary Materials.

The Indicator Value (IndVal), which combines the relative abundance and relative frequency of occurrence of a species in a given period (Dufrêne and Legendre, 1997), was calculated for each station to identify the phytoplankton key species for each season in the networks that resulted from the graph-network analysis. The INDSPANA software (version 1.1) was used.

1.2.4 Results

Physical and chemical parameters

The PCA biplot of physical and chemical parameters for the two stations is shown in Fig. 2A. The first two axes explained 59% of the total variability. Discrimination between the sampling stations was primarily driven by differences in DIN, which gave the major contribution to the ordination, followed by salinity, $Si(OH)_4$ and DIN/PO_4. SG01, located in the coastal area, appeared more variable and influenced by changes in the concentrations of the chemical parameters than SG05, the offshore station, which showed more stable conditions and higher salinity values (Fig. 2A).

The HCPC analyses performed on the physico-chemical parameters clustered the sampling points in three main groups (Fig. 2B). Two groups included several SG01 samples, one characterized by higher values of phosphorous and silicates, and the other with lower values. Almost all SG05 sampling points (and few SG01 ones) were grouped into a third cluster which was characterized by high salinity and low nutrient concentrations. A similar pattern was also observed for the HCPC performed on the main phytoplankton group abundances as the sampling points clustered in three groups (Fig. S1B). One group was characterized by high values of coccolithophores and included only SG01 samples (with just one exception), while another group was characterized by high abundances of diatoms and phytoflagellates (almost all SG01 samples). Almost all the SG05 sampling points were included in a third group together with several SG01 sampling points.

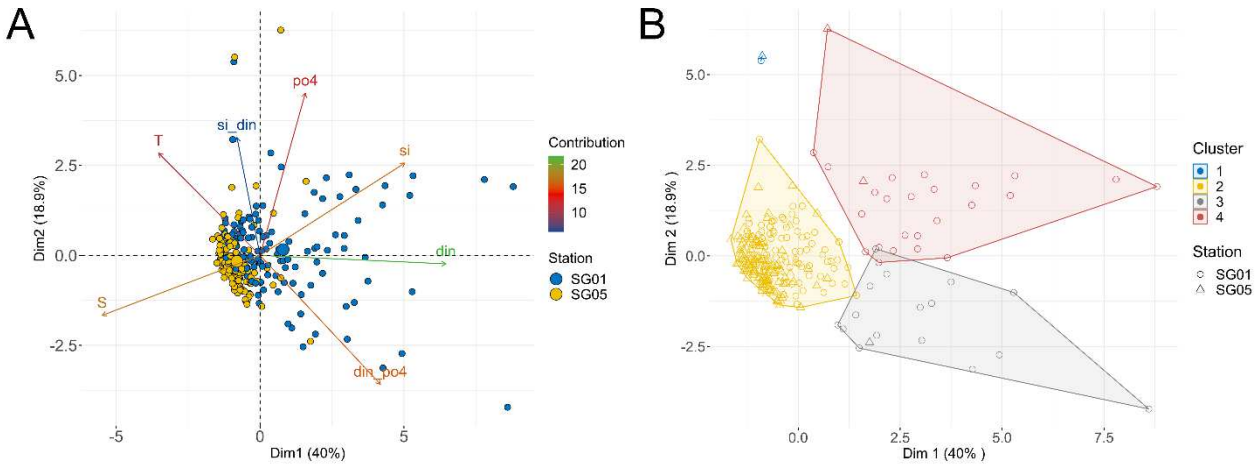

Fig. 2. Principal Component Analysis (PCA) (A) and Hierarchical Clustering on Principal Components (HCPC) (B) performed on physical-chemical parameters (Temperature (T), Salinity (S), DIN (din), PO_4 (po4), $Si(OH)_4$ (si), DIN/PO_4 (din_po4) and $Si(OH)_4$/DIN (si_din)) in SG01 and SG05. In the PCA biplot the variables (vectors) are presented by their contributions to the principal components (gradient colours of vectors). In the HCPC plot the clusters are represented by a different colour.

Phytoplankton groups

The mean seasonal values of abundances of each phytoplankton group are shown in Table 1. In winter, significant higher values of diatoms ($p < 0.001$), dinoflagellates ($p < 0.05$) and phytoflagellates ($p < 0.001$) were found in SG01 compared to SG05. On the contrary, coccolithophores showed significant higher values in SG05 than in SG01 ($p < 0.001$).

In spring, summer and autumn, significant higher values of diatoms ($p < 0.01$, $p < 0.01$, $p < 0.05$, respectively), dinoflagellates ($p < 0.001$, $p < 0.05$, $p < 0.01$, respectively) and phytoflagellates ($p < 0.001$) were found in SG01 than in SG05, while no significant difference between the two stations was observed for the coccolithophores ($p \geq 0.05$).

Table 1. Seasonal mean abundances (mean ± standard error, cells l^{-1}) of diatoms, dinoflagellates, coccolithophores and phytoflagellates for each station (SG01 and SG05) and season. Differences between the two stations are expressed as ns, not significant; *$p < 0.05$; **$p < 0.01$; ***$p < 0.001$.

		Mean ± std. error (cells l^{-1})			
Station	**Season**	**Diatoms**	**Dinoflagellates**	**Coccolithophores**	**Phytoflagellates**
SG01	Winter	6,466,862 ± 1,422,876	56,299 ± 7,682	19,194 ± 4,693	3,503,962 ± 545,124
SG05		110,792 ± 33,054	19,183 ± 2,890	26,497 ± 5,585	501,589 ± 43,029
p-Level		***	*	***	***
SG01	Spring	2,453,544 ± 637,242	155,958 ± 18,666	43,417 ± 9,709	2,631,848 ± 225,760
SG05		334,466 ± 94,910	55,529 ± 5,877	31,857 ± 11,370	922,234 ± 124,585
p-Level		**	***	ns	***
SG01	Summer	543,100 ± 94,769	84,709 ± 12,731	16,186 ± 3,456	2,016,555 ± 164,520
SG05		231,219 ± 77,968	43,780 ± 7,371	8,831 ± 2,364	484,784 ± 53,842
p-Level		**	*	ns	***
SG01	Autumn	1,269,870 ± 325,545	77,508 ± 9,986	120,190 ± 97,733	2,587,784 ± 281,576
SG05		203,113 ± 39,037	23,086 ± 2,549	16,242 ± 2,089	381,088 ± 31,244
p-Level		*	**	ns	***

The results of the Non-Metric Multidimensional Scaling (NMDS), performed for each season on the abundances of each phytoplankton group, are represented in Fig. 3. A marked divergence between samples belonging to the two stations was observed in winter (Fig. 3A), whilst no clear distinction was found in spring (Fig. 3B) and summer (Fig. 3C), and only a slight difference was observed in autumn (Fig. 3D). Comparing the two stations in each season, the PERMANOVA analysis highlighted significant differences between SG01 and SG05 ($p < 0.001$), supporting the ordination results. Significant values of dispersions were observed in winter and autumn ($p < 0.001$ and $p < 0.001$, respectively), while in spring and summer any significant dispersion was found ($p > 0.05$).

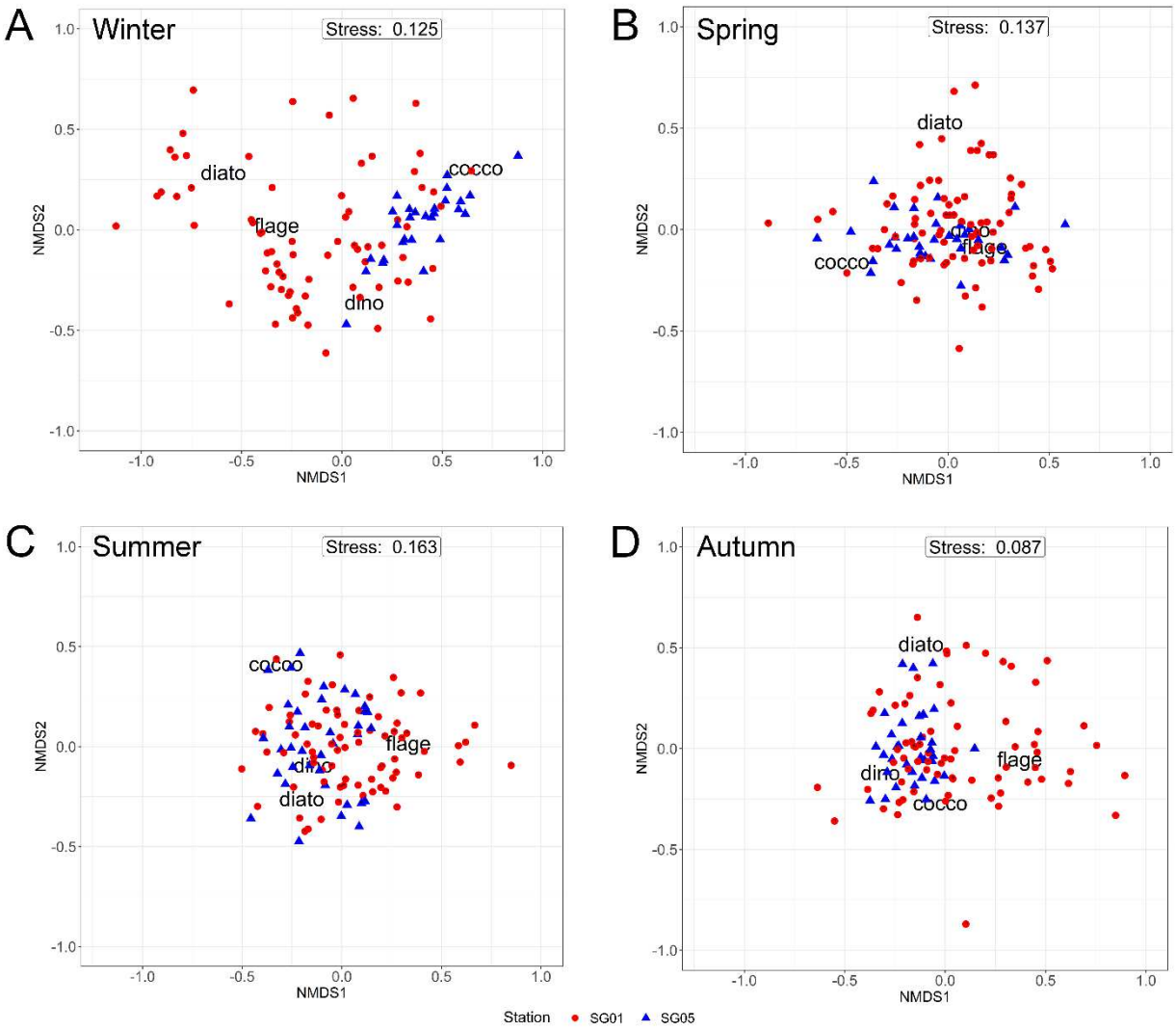

Fig. 3. NMDS performed on winter (A), spring (B), summer (C), autumn (D) on the abundances of each phytoplankton group in SG01 and SG05: diatoms (diato), dinoflagellates (dino), coccolithophores (cocco), phytoflagellates (flage).

Diversity

The total list of taxa (Table S1) included 174 Bacillariophyceae (diatoms), 136 Dinophyceae (dinoflagellates), 32 Prymnesiophyceae (of which 30 coccolithophores), 5 Cryptophyceae, 8 Chrysophyceae, 3 Raphidophyceae, 9 Dictyochophyceae, 6 Chlorophyceae, 4 Euglenophyceae, 1 cyanobacteria.

The diversity indices, performed for each season, are shown in Fig. 4. All indices (Shannon diversity index (H), Pielou's evenness (J), Rarefied richness, Menhinick and Margalef indices) highlighted higher values in SG05 than in SG01 in winter (Wilcoxon test, $p < 0.001$) and in autumn (Wilcoxon test, $p < 0.01$ for rarefied richness and Shannon and Menhinick indices; $p < 0.05$ for evenness and Margalef index). In spring, Shannon diversity index (Wilcoxon test, $p < 0.05$), Pielou's evenness (Wilcoxon test, $p < 0.01$) and Menhinick index (Wilcoxon test, $p < 0.05$) were found to be higher in SG05, while no differences were observed in terms of rarefied richness and Margalef index (Wilcoxon test, $p > 0.05$). No significant differences between the two stations were found in summer (Wilcoxon test, $p > 0.05$).

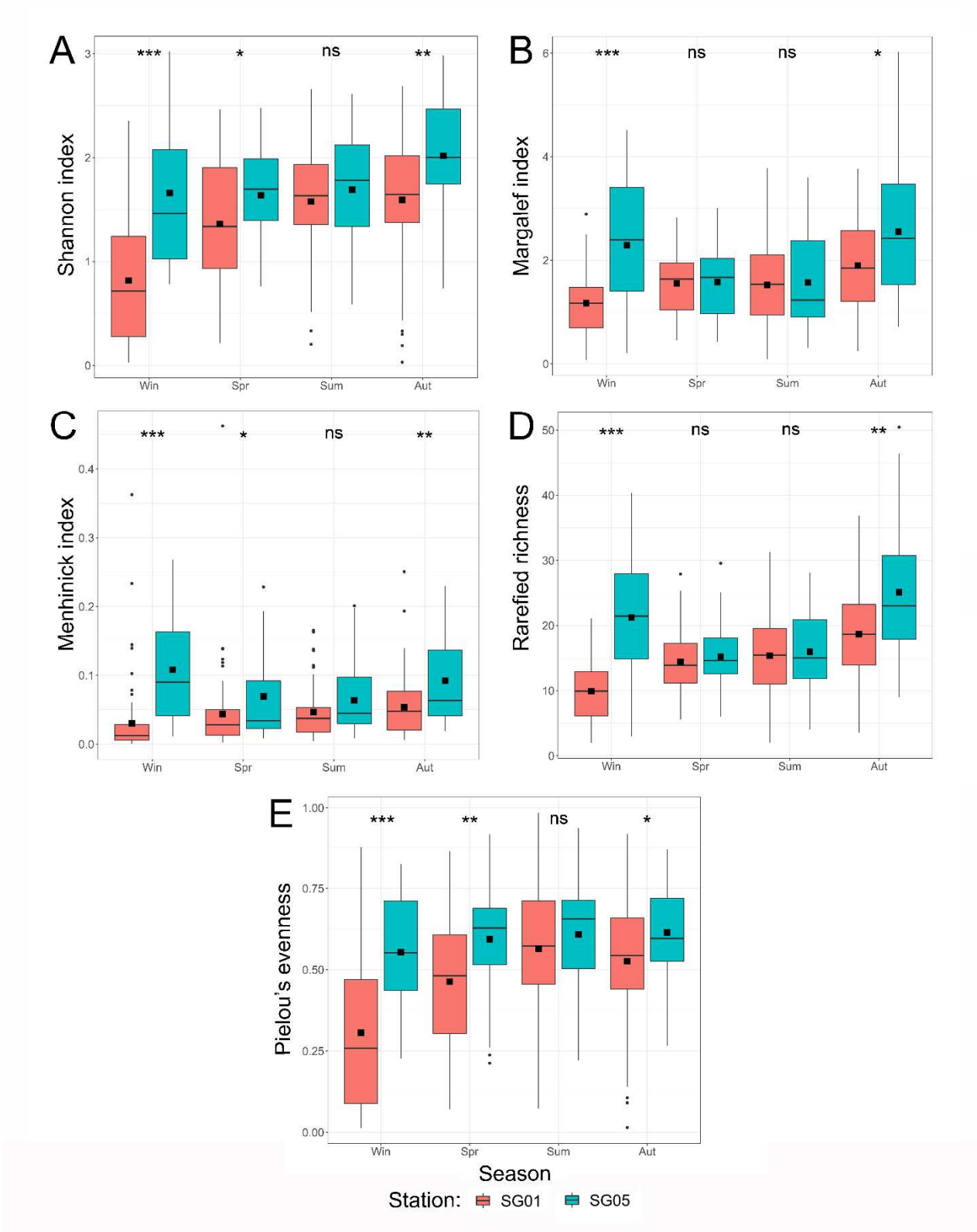

Fig. 4. Shannon index (A), Margalef index (B), Menhinick index (C), Rarefied richness (D) and Pielou's evenness (E), calculated for each season, are shown for both stations. Box plots report the data distribution with the mean (□), the median (line), the interquartile range (box), the non-outlier range (vertical bars), the outliers (○). *** ($p \prec 0.001$), ** ($p \prec 0.01$), * ($p \prec 0.05$), ns (not significant).

In both stations and in all the seasons, significant correlations were observed between most of the indices (Table 2), but with the following exceptions.

In winter, in SG01 station, no correlation was found for Pielou's evenness vs Margalef index, while in SG05, for Pielou's evenness vs Menhinick and vs Margalef indices and for Pielou's evenness and Rarefied richness.

In spring, in SG01 station no correlation was found for Pielou's evenness vs Margalef and vs Menhinick and for Menhinick vs Shannon index, while in SG05 for Pielou's evenness vs Rarefied richness and vs Menhinick index and for Shannon index vs Margalef and vs Menhinick indices.

In summer, in both stations, no correlation was found for Pielou's evenness vs Rarefied richness and vs Menhinick and for Shannon vs Menhinick. In SG05 Shannon index showed no correlation also vs Margalef index. In autumn, both in SG01 and SG05, Pielou's evenness was not correlated with Rarefied richness, Menhinick and Margalef indices.

Table 2. Correlations between the different indices (Rarefied richness, Pielou's evenness, Shannon, Margalef, Menhinick indices) in SG01 (A,C,E,G) and SG05 (B,D,F,H) in winter (A,B), spring (C,D), summer (E,F) and autumn (G,H). Values indicated in italic are significant at $p < 0.05$, those in bold italic are significant at $p < 0.01$, those in bold italic and underlined are significant at $p < 0.001$.

A

	R.richness	Shannon	Evenness	Margalef	Menhinick
R.richness	1				
Shannon	***0.76***	1			
Evenness	***0.62***	***0.95***	1		
Margalef	***0.72***	***0.39***	0.2	1	
Menhinick	***0.75***	***0.77***	***0.68***	***0.61***	1

B

	R.richness	Shannon	Evenness	Margalef	Menhinick
R.richness	1				
Shannon	***0.68***	1			
Evenness	0.03	***0.6***	1		
Margalef	***0.98***	***0.58***	-0.11	1	
Menhinick	***0.83***	***0.65***	0.12	***0.82***	1

C

	R.richness	Shannon	Evenness	Margalef	Menhinick
R.richness	1				
Shannon	***0.66***	1			
Evenness	***0.43***	***0.93***	1		
Margalef	***0.72***	*0.23*	-0.07	1	
Menhinick	***0.41***	0.2	0.12	***0.42***	1

D

	R.richness	Shannon	Evenness	Margalef	Menhinick
R.richness	1				
Shannon	***0.54***	1			
Evenness	-0.05	***0.71***	1		
Margalef	***0.79***	0.23	*-0.37*	1	
Menhinick	***0.62***	0.28	-0.04	***0.69***	1

E

	R.richness	Shannon	Evenness	Margalef	Menhinick
R.richness	1				
Shannon	***0.57***	1			
Evenness	-0.06	***0.7***	1		
Margalef	***0.89***	***0.32***	***-0.31***	1	
Menhinick	***0.48***	0.15	-0.09	***0.53***	1

F

	R.richness	Shannon	Evenness	Margalef	Menhinick
R.richness	1				
Shannon	***0.44***	1			
evenness	-0.18	***0.76***	1		
Margalef	***0.95***	0.25	*-0.37*	1	
Menhinick	***0.68***	0.19	-0.26	***0.79***	1

G

	R.richness	Shannon	evenness	Margalef	Menhinick
R.richness	1				
Shannon	***0.6***	1			
Evenness	0.03	***0.74***	1		
Margalef	***0.91***	***0.4***	-0.19	1	
Menhinick	***0.32***	***0.34***	0.19	***0.33***	1

H

	R.richness	Shannon	Evenness	Margalef	Menhinick
R.richness	1				
Shannon	***0.65***	1			
Evenness	0.02	***0.74***	1		
Margalef	***0.94***	***0.54***	-0.11	1	
Menhinick	***0.76***	***0.56***	0.14	***0.81***	1

Phytoplankton community composition: indicator value analysis

The IndVal was calculated seasonally for each station (Table S2), highlighting the representative taxa for each station on a seasonal basis.

In the SG01 station, in winter the representative taxa were *Skeletonema marinoi*, *Chaetoceros curvisetus*, *Thalassiosira rotula*, *Dictyocha fibula*, *Chaetoceros danicus*. In spring, the taxa with significant values were *Dactyliosolen fragilissimus*, *Prorocentrum micans*, *Nitzschia longissima*, *Cyclotella* spp., *Tripos fusus*, *Pseudo-nitzschia* cfr. *delicatissima*, *Prorocentrum cordatum*, *Alexandrium* spp. In summer, the most representative taxa were *Proboscia alata*, *Guinardia flaccida*, *Nitzschia gobbii*, *Calycomonas* sp., *Prorocentrum compressum*. In autumn, significant taxa were *Lioloma pacificum*, *Asterionellopsis glacialis*, *Chaetoceros affinis*.

In the SG05 station, in winter the most representative taxa were *Skeletonema marinoi*, *Emiliania huxleyi*, *Pseudosolenia calcar avis*, *Chaetoceros affinis* and *Diploneis* spp. In spring, significant taxa were *Dactyliosolen fragilissimus*, *Cyclotella* spp., *Prorocentrum micans*, *Euglena* spp. In summer, *Proboscia alata*, *Cerataulina pelagica*, *Pseudoscourfielda marina* and *Calycomonas* sp. were found to have significant values. In autumn, most significant taxa were *Guinardia striata*, *Lioloma pacificum*, *Cylindrotheca closterium*, *Asterionellopsis glacialis*, *Pseudo-nitzschia* cfr. *delicatissima*, *Pleurosigma* spp.

Graph-network analysis

The results of the graph-network analysis, performed on each season, showed that the networks based on positive interactions (Fig. 5) were characterized by a higher number of vertices (taxa) and edges (interactions) than the ones based on negative interactions (Fig. S2), which often showed many disconnected subgraphs. Network betweenness, diameter, clustering coefficient (not discussed in this study) are shown in Table 3.

The winter networks based on positive interactions were characterized by 47 taxa and 200 interactions in the coastal station SG01 (Fig. 5A) and 54 taxa (of which 2 disconnected, i.e., *Chaetoceros*

compressus and *Pseudosolenia calcar avis*), and 178 interactions in the offshore station SG05 (Fig. 5B). The two stations showed similarities in terms of closeness ranges (0.007–0.020 and 0.009–0.020 in SG01 and SG05, respectively). The species with the highest value of closeness was *Leptocylindrus danicus* in SG01 (closeness = 0.020), and *Chaetoceros lorenzianus* in SG05 (closeness = 0.020). *Chaetoceros curvisetus* was the one with the highest number of total interactions in both stations (degree = 22 and 19, in SG01 and SG05, respectively). As regards the networks based on negative interactions (Fig. S2 A,B), in both stations, *Emiliania huxleyi* was the species with the highest values of closeness and degree. Considering both types of winter networks, stronger interactions were found in SG05 than in SG01: SG05 showed the 85% and 68% of the positive and negative correlations with $r \geq 0.4$, while in SG01 station most of the correlations (94% and 81% for positive and negative interactions, respectively) were weak ($r < 0.4$). The spring networks built on positive interactions were characterized by 50 taxa and 171 interactions in the SG01 station (Figs. 5C) and 49 taxa (of which 2 disconnected, i.e., *Chaetoceros compressus*, *Leptocylindrus minimus*), and 110 interactions in the SG05 station (Fig. 5D). The two stations showed similarities in terms of closeness ranges (0.007–0.018 in SG01 and 0.007–0.019 in SG05). In SG01 *Thalassionema nitzschioides* was the species with the highest value of closeness (0.018), although *Cerataulina pelagica* had the highest degree value (18). Offshore, *Chaetoceros tortissimus* showed both the maximum of closeness (0.019) and degree (11). Instead, in the negative networks, in the coastal station (Fig. S2C) *Pseudokephyrion* spp. was the species with the maximum of closeness (0.04), while *Pseudoscourfieldia marina* showed the highest value of degree (6). The offshore network (Fig. S2D) was characterized by several disconnected subgraphs. *Calycomonas* sp., *Emiliania huxleyi* and *Dactyliosolen fragilissimus* were the species showing the higher number of negative interactions. In the SG05 station, the networks showed a 68% and 11% of strong positive and negative correlations ($r \geq 0.4$), respectively. No interaction with $r < 0.3$ was found in both graphs. On the contrary, in the SG01 station, most of the correlations were very weak as the 51% and the 83% of positive and negative interactions, respectively, showed $r < 0.3$.

Summer networks based on positive correlations were characterized by 48 nodes (taxa) and 154 edges (interactions) in SG01 (Fig. 5E) and 54 taxa (of which two disconnected, i.e. *Chaetoceros costatus*, *Dactyliosolen fragilissimus*), and 129 interactions in SG05 (Fig. 5F). The coastal station showed higher closeness ranges (0.007–0.017) than the offshore one (0.005–0.015). In the first case, *Chaetoceros lorenzianus* was the species with the highest value of closeness, although *Chaetoceros curvisetus* showed the maximum of degree (14). In the second case, *Syracosphaera pulchra* showed the highest value of closeness (0.015) and of degree (14). As regards the networks based on negative interactions (Figs. S2E and F), in both stations *Pseudoscourfieldia marina* was the species with the maximum of closeness (0.05 and 0.10 in SG01 and SG05, respectively) and degree (13 and 9 in SG01 and SG05, respectively). The networks of the SG01 station were characterized by weak interactions among taxa, as only the 16% and 5% of positive and negative correlations, respectively, showed $r \geq 0.4$. In the SG05 networks, about half of the correlations were found with $r \geq 0.4$ (50% and 44% for positive and negative correlations, respectively).

Autumn networks based on positive interactions were characterized by 51 vertices (taxa) and 278 edges (interactions) at the SG01 station (Fig. 5G), while 56 vertices and 225 edges were found at SG05 (Fig. 5H). The two stations showed similar closeness ranges (0.007–0.020 and 0.006–0.019 in SG01 and SG05, respectively). In SG01, the maximum of closeness was observed for *Cerataulina pelagica* (0.020), which was also the species with the highest number of interactions, together with *Dactyliosolen fragilissimus* (degree = 25). In SG05, *Chaetoceros curvisetus* was the species with the maximum closeness (0.019) and degree (22). The negative networks were both strongly disconnected. In SG01, *Tripos muelleri*, *Calciosolenia murrayi* and *Pseudo-nitzschia* cfr. *pseudodelicatissima* were the species showing the higher number of negative interactions (Fig. S2G), while in SG05 *Calycomonas* sp., and *Emiliania huxleyi* showed the highest degree value (Fig. S2H). Stronger interactions were found for SG05 than for SG01. The latter was characterized by weak positive (73% with $r \leq 0.4$, of which 42% with $r < 0.3$) and negative (100% with $r < 0.4$, of which 92% with $r < 0.3$)

interactions. Instead, in SG05 67% and 42% were the percentages of positive and negative correlations with $r \geq 0.4$.

Table 3

Network parameters calculated on the seasonal network of both stations.

		Attributes		
		Network betweenness	**Diameter**	**Clustering coefficient**
SG01	**Winter**	0.15	4.09	0.49
SG01	**Spring**	0.13	4.77	0.35
SG01	**Summer**	0.11	4.19	0.38
SG01	**Autumn**	0.10	4.00	0.59
SG05	**Winter**	0.14	3.75	0.49
SG05	**Spring**	0.14	3.54	0.34
SG05	**Summer**	0.16	5.8	0.31
SG05	**Autumn**	0.09	4.57	0.48

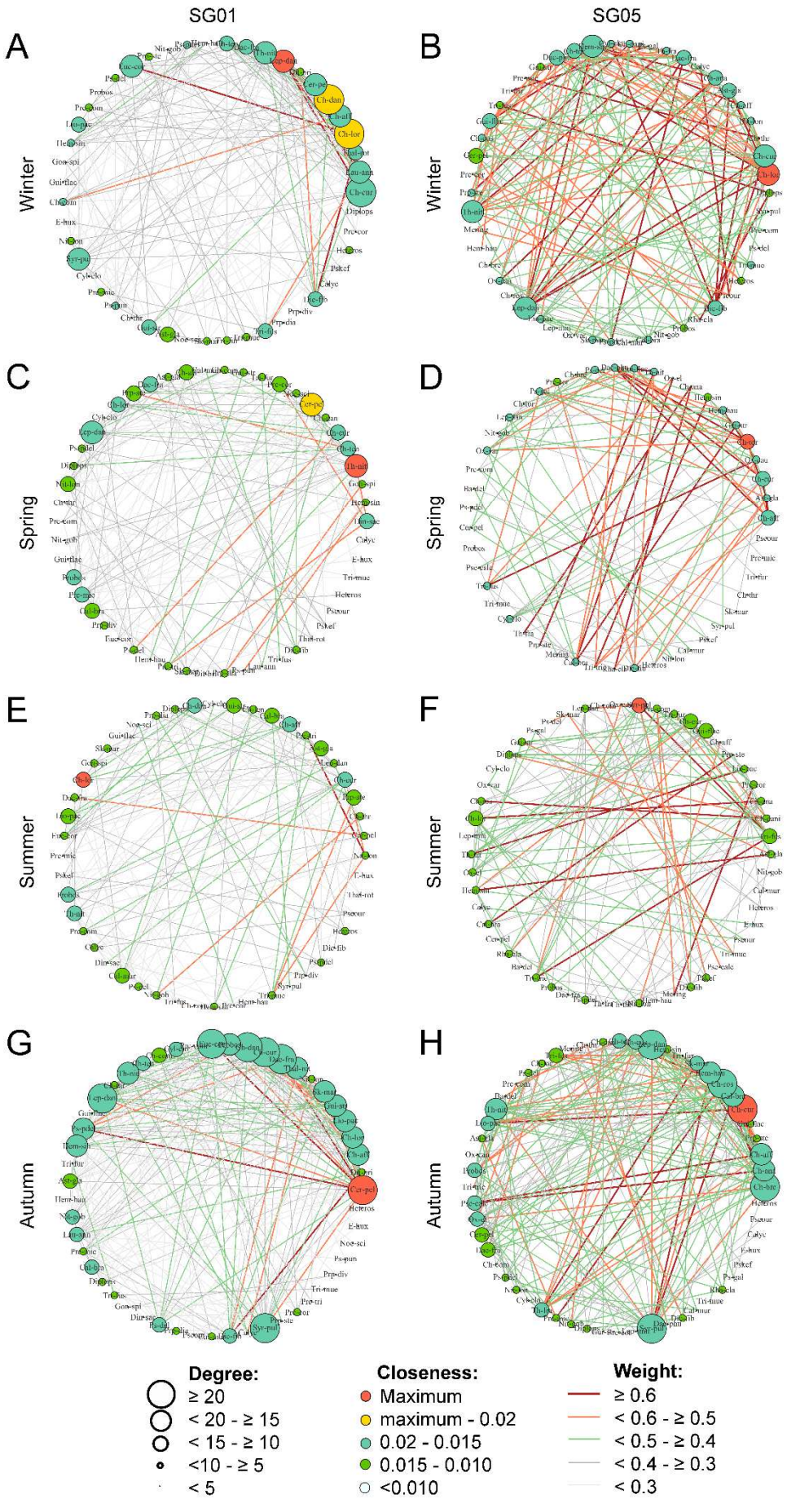

Fig. 5. Networks based on winter (A,B), spring (C,D), summer (E,F), autumn (G,H) positive correlations in SG01 (A,C,E,G) and SG05 (B,D,F,H). The dimension of the circle is proportional to the degree and the different colours are related to closeness. Line colours and thickness depend on the strength of the interaction. The names of the taxa are abbreviated as shown in Supplementary Table 3.

1.2.5 Discussion

In this study we highlighted the key role of the oceanographic conditions in discriminating the two stations along the Senigallia-Susak Transect and the ability of the used indices and descriptors in underlying the differences in the phytoplankton communities. In both stations a clear seasonal rhythm in the annual cycle of phytoplankton was highlighted, but this rhythm markedly differed between the two stations, reflecting the different oceanographic regimes. Indeed, offshore (55 m depth) the main seasonal driver is the vertical structure of the water column (i.e., mixing vs stratification) which influences the conditions for the phytoplankton at the surface and in the whole mixed layer, in terms of light and nutrient availability. On the contrary, in the shallower coastal station (10 m depth), where the water column is mixed almost throughout the year, the main constrain is the outflow of riverine waters (itself related to the rain regime) carried by the WAC.

The statistical comparison of the offshore and coastal stations in terms of physico-chemical parameters highlighted that the offshore station, located beyond the WAC, is more stable than the coastal one, as the latter is more affected by changes in the meteorological conditions. Indeed, the western Adriatic coast is directly influenced by the continental waters (Totti and Artegiani, 2001), among which the Po River stands out, characterized by a much higher concentration of nitrogen, compared to phosphorous (Grilli et al., 2020). These waters conveyed by the WAC reduce salinity and increase nitrate and silicate concentrations (Artegiani et al., 1997b; Campanelli et al., 2011; Marini et al., 2008), which are those factors mostly discriminating the coastal sampling points by the PCA. The offshore station is not directly affected by freshwater inputs, except when the riverine waters expand eastward during stratification (Neri et al., 2022). Consequently, the environmental conditions of the offshore station result more stable throughout the year.

The effects of the different environmental conditions and oceanographic circulation along the SST are also evident considering the diversity of the phytoplankton community and the seasonal variability of each phytoplankton group, as well as the structure of the communities in terms of interspecific interactions. In this regard, the two stations differed mainly in winter and autumn as suggested by the

diversity indices and NMDS analysis. Indeed, Campanelli et al. (2011) observed that the riverine input in the NAS affected nutrient concentrations and phytoplankton growth particularly in those seasons. On the contrary, the two stations appeared to be more similar in summer, as shown by the more grouped samples and by comparable diversity indices, due to the spreading south-eastward of the floods of the Po River in stratified conditions (Neri et al., 2022). This variability among seasons was also highlighted both by the HCPC and NMDS performed on the phytoplankton abundances and by the significant dispersion of the samples.

As the effect of the riverine input is more evident along the coast, higher phytoplankton abundances were found always in the coastal station. Only in winter coccolithophores were found to have higher mean abundances offshore, in correspondence of high salinity values (Neri et al., 2022; Totti et al., 2019), as commonly reported worldwide (Baumann et al., 2005; Menschel et al., 2016).

Diversity indices have been suggested and used to analyse the phytoplankton diversity for the GES assessment in the Mediterranean Sea, as they were found to be able to distinguish different environments and different anthropogenic impacted areas (mainly coastal) (Francé et al., 2021; Rombouts et al., 2019; Varkitzi et al., 2018). In this study, all the tested diversity indices agreed in highlighting a higher similarity in summer between the two stations and a higher diversity in the offshore station. This higher diversity in the offshore station can be related to the oligotrophic conditions of waters beyond the WAC, and it was observed even in other Adriatic and Mediterranean oligotrophic areas (Bužančić et al., 2016; Francé et al., 2021; Varkitzi et al., 2020), but it could be partly influenced by the methodological approach of the Utermöhl method. In fact, the sample volume settled in the cylinder/chamber for analysis is normally higher in offshore stations (40–100 ml) than in coastal ones (5–25) due to different cell concentrations, increasing the probability to find rarer species. Comparing the diversity indices, as expected, significant relationships were found among them for most combinations. However, the correlations and the significances changed among the seasons and between the stations, suggesting that a combination of indices is more appropriate to describe the phytoplankton diversity, and to better estimate its variation in time and space. In both

stations and in all the seasons, Pielou's evenness showed no significant correlations with other indices, as already found by Rombouts et al. (2019), suggesting that this index could give not redundant information when combined with others. In some cases, also the Shannon index showed no significant correlations, suggesting a usefulness of this indicator.

The IndVal analyses highlighted taxa that are key elements of a certain season based on their abundance and frequency of occurrence (Dufrêne and Legendre, 1997), showing some differences and similarities between the two stations, as reported in previous studies in the same area (Neri et al., 2022; Totti et al., 2019). Regardless to any environmental variability, some phytoplankton species expressed a marked seasonal behaviour (see also Longobardi et al., 2022), as for example *Skeletonema marinoi* that is a significant indicator of the winter community. In other cases, the timing of species could be directly affected by changes in the trophic state, mainly linked to the riverine inputs, which could lead to increase/decrease in abundances, also favouring opportunistic taxa to the detriment of others. Indicator species are related to the specific environmental conditions of a certain period (stratification/mixing regime, photoperiod etc.), while non-indicator taxa are not apparently linked with certain environmental factors and are more homogeneously distributed throughout the year. As a consequence, the latter show more interactions with the overall phytoplankton community, as noticeable from the graph-network analysis, through which we represented the interactions among organisms in a "simplified" way (in terms of nodes, i.e. taxa, and edges, i.e. relationships). In our study, the highest values of closeness (which takes into account the number of interactions and their strength) were found for species identified as non-indicator and therefore for ones not considered as key species of a certain season (e.g., *Leptocylindrus danicus*, *Thalassionema nitzschioides*, *Chaetoceros lorenzianus*, *Cerataulina pelagica* in the coastal station and *Chaetoceros lorenzianus*, *C. tortissimus*, *C. curvisetus*, *Leptocylindrus danicus* and *Syracosphaera pulchra* offshore). Few exceptions were found in the coastal station, for some widespread taxa (i.e., *Chaetoceros danicus* and *Proboscia alata*) that showed high values of closeness even in those seasons for which they are indicators. Considering the degree (which does not consider the weight, and so the strength, of the

connection itself), some differences were observed between the two stations. Offshore, key species (following the IndVal analysis) were found to have a low number of total interactions (e.g., *Skeletonema marinoi* and *Pseudosolenia calcar avis* in winter, *Prorocentrum micans* in spring, *Pseudoscourfieldia marina* and *Cerataulina pelagica* in summer and *Cylindrotheca closterium* in autumn). On the contrary, the coastal station did not show a clear pattern, underlying the role of the marked seasonality related to direct riverine inputs. Indeed, here some indicator taxa were found to have low degree values (e.g., *Skeletonema marinoi* in winter, *Tripos fusus* in spring and *Guinardia flaccida* in summer), while others showed high degree values (e.g., *Chaetoceros danicus* and *C. curvisetus* in winter, *Prorocentrum micans* in spring, *Proboscia alata* in summer).

As expected, the networks based on negative correlations were made of a lower number of vertices and edges than the ones with positive correlations and were often disconnected (and thus difficult to be interpreted). Without a prey-predator context, the negative interactions among phytoplankton taxa can underly competition for the same resources (nutrients, light, etc.) but also temporal changes of single taxa, that produce a negative correlation, as the case of *Emiliania huxleyi* (the species with the highest values of closeness and degree in the negative networks, in both stations), whose decrease has been reported by previous studies (Neri et al., 2022; Totti et al., 2019).

The offshore station was found to have stronger relationships both in the network based on positive and negative correlations, due to its higher stability and to the different seasonal behaviour of the oceanographic conditions respect to the coastal station, allowing the establishment of stronger connections. In the offshore station, the weaker relationships were found in summer, the season where a major similarity between the two stations was also highlighted by the NMDS analysis, underlying again the role of water stratification in affecting phytoplankton community (Neri et al., 2022).

Metrics based on network approaches (such as the Ecological Network Analysis indices) have been proposed as food web indicators, as they cross multiple trophic levels and can give a holistic view on the trophic web (Fath et al., 2019; McQuatters-Gollop et al., 2022; Safi et al., 2019; Tomczak et al., 2013). In our study, graph-network analysis based on positive and negative interactions was able to

detect differences in phytoplankton community/functionality of the two stations and changes in the phytoplankton abundances.

1.2.6 Conclusions

Ecosystem comparison of long-term data series allows a better understanding of the uniqueness of the environments, the key aspects controlling biodiversity and productivity, as well as the processes adopted to respond to natural and human-induced pressures (Acri et al., 2020; Kröncke et al., 2019; Megrey et al., 2009; Murawski et al., 2010), which is fundamental for an effective marine ecosystem management. In our study we combined different approaches to compare coastal and offshore areas located along the Senigallia-Susak Transect in the NAS, both in terms of physico-chemical parameters and phytoplankton community, and to gain insights in the functioning of the phytoplankton community and the main forcings affecting it.

The multivariate statistical analyses showed that the coastal station is more variable and directly affected by riverine inputs than the offshore one, which is located beyond the WAC, leading to differences in both phytoplankton abundances and community structure. These differences should be taken in consideration when any evaluation of Good Environmental Status is carried on. The two stations were more different in winter and autumn when the water masses are clearly separated, and more similar in summer, when coastal waters spread offshore during the stratification regime.

Higher abundances of all groups except coccolithophores were found in the coastal station, while the offshore station was characterized by higher diversity than the coastal one. All the used diversity indices were able to discriminate between stations and highlighted the effect of the different environmental/oceanographic conditions on the phytoplankton diversity. Pielou's evenness could give non-redundant information as low, and in some case not significant, correlations were found with other indices.

The graph-network analysis, which can be used to study the interactions inside a community, revealed a phytoplankton community structure that is highly influenced by oceanographic conditions and

confirmed that non-indicator species have more interactions because are more present throughout the year. The networks were able to detect the differences between the two stations in the terms of phytoplankton communities and dynamics, referable to different environmental and oceanographic conditions, and long-term variations in the abundances. Therefore, graph-network analysis could be a useful tool, not only for the food web descriptors, but also to highlight structure and differences in the phytoplankton communities, which are the basis of most food webs and provide many ecosystem services. Instead, the IndVal analysis is useful to find out the key taxa of a certain season. In this way, the combination of the two analyses can give different information, in some way complementary and non-redundant, on the phytoplankton community structure and composition.

In conclusion, the combination of different methods, such as statistical analysis, biodiversity indices, Indicator Value analysis and graph network analysis, allows insights in the "functioning" of different areas and the forcings affecting phytoplankton communities, necessary information to assess the environmental status of different areas.

1.2.7 References

2008/56/EC. Directive of the European Parliament and of the Council of 17 June 2008 establishing a framework for community action in the field of marine environmental policy (Marine Strategy Framework Directive) (Text with EEA relevance).

Acri, F., Bastianini, M., Bernardi Aubry, F., Camatti, E., Boldrin, A., Bergami, C., Cassin, D., De Lazzari, A., Finotto, S., Minelli, A., Oggioni, A., Pansera, M., Sarretta, A., Socal, G., Pugnetti, A., 2020. A long-term (1965–2015) ecological marine database from the LTER-Italy Northern Adriatic Sea site: Plankton and oceanographic observations. Earth Syst. Sci. Data 12, 215–230. https://doi.org/10.5194/essd-12-215-2020

Anderson, M.J., 2001. A new method for non-parametric multivariate analysis of variance. Austral Ecol. 26, 32–46. https://doi.org/https://doi.org/10.1111/j.1442-9993.2001.01070.pp.x

Anderson, M.J., 2006. Distance-based tests for homogeneity of multivariate dispersions. Biometrics 62, 245–253. https://doi.org/https://doi.org/10.1111/j.1541-0420.2005.00440.x

Artegiani, A., Bregant, D., Paschini, E., Pinardi, N., Raicich, F., Russo, A., 1997a. The Adriatic Sea general circulation. Part I: air-sea interactions and water mass structure. J. Phys. Oceanogr. 27, 1492–1514. https://doi.org/10.1175/1520-0485(1997)027<1492:TASGCP>2.0.CO;2

Artegiani, A., Bregant, D., Paschini, E., Pinardi, N., Raicich, F., Russo, A., 1997b. The Adriatic Sea general circulation. Part II: baroclinic circulation structure. J. Phys. Oceanogr. 27, 1515–1532. https://doi.org/10.1175/1520-0485(1997)027<1515:TASGCP>2.0.CO;2

Baumann, K., Andruleit, H., Böckel, B., Geisen, M., Kinkel, H., 2005. The significance of extant coccolithophores as indicators of ocean water masses, surface water temperature, and palaeoproductivity: a review. Paläontologische Zeitschrift 79, 93–112.

Bernardi Aubry, F., Acri, F., Bastianini, M., Bianchi, F., Cassin, D., Pugnetti, A., Socal, G., 2006. Seasonal and interannual variations of phytoplankton in the Gulf of Venice (Northern Adriatic Sea). Chem. Ecol. 22, 71–91. https://doi.org/10.1080/02757540600687962

Blanchard, J.L., Jennings, S., Holmes, R., Harle, J., Merino, G., Allen, J.I., Holt, J., Dulvy, N.K., Barange, M., 2012. Potential consequences of climate change for primary production and fish production in large marine ecosystems. Philos. Trans. R. Soc. B Biol. Sci. 367, 2979–2989. https://doi.org/10.1098/rstb.2012.0231

Bittinger, K., 2020. abdiv: Alpha and Beta Diversity Measures. R package version 0.2.0.

Bužančić, M., Ninčević Gladan, Ž., Marasović, I., Kušpilić, G., Grbec, B., 2016. Eutrophication influence on phytoplankton community composition in three bays on the eastern Adriatic coast. Oceanologia 58, 302–316. https://doi.org/10.1016/j.oceano.2016.05.003

Campanelli, A., Grilli, F., Paschini, E., Marini, M., 2011. The influence of an exceptional Po River flood on the physical and chemical oceanographic properties of the Adriatic Sea. Dyn. Atmos. Ocean. 52, 284–297. https://doi.org/10.1016/j.dynatmoce.2011.05.004

Cerino, F., Fornasaro, D., Kralj, M., Giani, M., Cabrini, M., 2019. Phytoplankton temporal dynamics in the coastal waters of the north-eastern Adriatic Sea (Mediterranean Sea) from 2010 to 2017. Nat. Conserv. 34, 343–372. https://doi.org/10.3897/natureconservation.34.30720

Cibic, T., Cerino, F., Karuza, A., Fornasaro, D., Comici, C., Cabrini, M., 2018. Structural and functional response of phytoplankton to reduced river inputs and anomalous physical-chemical conditions in the Gulf of Trieste (northern Adriatic Sea). Sci. Total Environ. 636, 838–853. https://doi.org/10.1016/j.scitotenv.2018.04.205

Costa, A., Martín González, A.M., Guizien, K., Doglioli, A.M., Gómez, J.M., Petrenko, A.A., Allesina, S., 2019. Ecological networks: Pursuing the shortest path, however narrow and crooked. Sci. Rep. 9. https://doi.org/10.1038/s41598-019-54206-x

Cozzoli, F., Stanca, E., Selmeczy, G.B., Francé, J., Varkitzi, I., Basset, A., 2017. Sensitivity of phytoplankton metrics to sample-size: A case study on a large transitional water dataset (WISER). Ecol. Indic. 82, 558–573. https://doi.org/10.1016/j.ecolind.2017.07.022

Csardi, G., Nepusz, T., 2006. The igraph software package for complex network research. InterJournal, Complex Syst. 1965. https://igraph.org

D'Alelio, D., Libralato, S., Wyatt, T., Ribera D'Alcalà, M., 2016. Ecological-network models link diversity, structure and function in the plankton food-web. Sci. Rep. 6, 21806. https://doi.org/10.1038/srep21806

Degobbis, D., Precali, R., Ivancic, I., Smodlaka, N., Fuks, D., Kveder, S., 2000. Long-term changes in the northern Adriatic ecosystem related to anthropogenic eutrophication, Int. J. Environ. Pollut. 13, 495–533. https://doi.org/10.1504/IJEP.2000.002332

Delmas, E., Besson, M., Brice, M.H., Burkle, L.A., Dalla Riva, G.V., Fortin, M.J., Gravel, D., Guimarães, P.R., Hembry, D.H., Newman, E.A., Olesen, J.M., Pires, M.M., Yeakel, J.D., Poisot, T., 2018. Analysing ecological networks of species interactions. Biol. Rev. 94, 16–36. https://doi.org/10.1111/brv.12433

Díaz, S., Cabido, M., 2001. Vive la différence: Plant functional diversity matters to ecosystem processes. Trends Ecol. Evol. 16, 646–655. https://doi.org/10.1016/S0169-5347(01)02283-2

Dufrêne, M., Legendre, P., 1997. Species assemblages and indicator species: the need for a flexible asymmetrical approach. Ecol. Monogr. 67, 345–366. https://doi.org/10.2307/2963459

Edler, L., Elbrachter, M., 2010. The Utermöhl method for quantitative phytoplankton analysis, in: Karlson, B., Cusack, C., Bresnan, E. (Eds.), *Microscopic and molecular methods for quantitative phytoplankton analysis.* IOC UNESCO, Manuals and Guides, 55: 13–20.

Estrada, E., Bodin, Ö., 2008. Using network centrality measures to manage landscape connectivity. Ecol. Appl. 18, 1810–1825.

European Commission, 2010. Commission Decision of 1 September 2010 on criteria and methodological standards on good environmental status of marine waters 2010/ 477/EU.

European Commission, 2017. Commission Decision (EU) 2017/848 of 17 May 2017, laying down criteria and methodological standards on good environmental status of marine waters and specifications and standardised methods for monitoring and assessment, and repealing Decision 2010/447/EU. Official J. Eur. Union L 125 (18.5.2017), 43–74.

Falkowski, P.G., Katz, M.E., Knoll, A.H., Quigg, A., Raven, J.A., Schofield, O., Taylor, F.J.R., 2004. The evolution of modern eukaryotic phytoplankton. Science 305, 354 – 360. https://doi.org/10.1126/science.1095964

Fath, B.D., Asmus, H., Asmus, R., Baird, D., Borrett, S.R., de Jonge, V.N., Ludovisi, A., Niquil, N., Scharler, U.M., Schückel, U., Wolff, M., 2019. Ecological network analysis metrics: The need for an entire ecosystem approach in management and policy. Ocean Coast. Manag. 174, 1–14. https://doi.org/10.1016/j.ocecoaman.2019.03.007

Francé, J., Varkitzi, I., Stanca, E., Cozzoli, F., Skejić, S., Ungaro, N., Vascotto, I., Mozetič, P., Ninčević Gladan, Ž., Assimakopoulou, G., Pavlidou, A., Zervoudaki, S., Pagou, K., Basset, A., 2021. Large-scale testing of phytoplankton diversity indices for environmental assessment in Mediterranean sub-regions (Adriatic, Ionian and Aegean Seas). Ecol. Indic. 126, 107630. https://doi.org/10.1016/j.ecolind.2021.107630

Freeman, L.C., 1979. Centrality in social networks conceptual clarification. Soc. Networks 1, 215–239. https://doi.org/10.1016/0378-8733(78)90021-7

Grilli, F., Paschini, E., Precali, R., Russo, A., Supić, N., 2005. Circulation and horizontal fluxes in the northern Adriatic Sea in the period June 1999–July 2002. Part I: Geostrophic circulation and current measurement. Sci. Total Environ. 353, 57–67. https://doi.org/10.1016/j.scitotenv.2005.09.008

Grilli, F., Accoroni, S., Acri, F., Bernardi Aubry, F., Bergami, C., Cabrini, M., Campanelli, A., Giani, M., Guicciardi, S., Marini, M., Neri, F., Penna, A., Penna, P., Pugnetti, A., Ravaioli, M., Riminucci, F., Ricci, F., Totti, C., Viaroli, P., Cozzi, S., 2020. Seasonal and interannual trends of oceanographic parameters over 40 years in the Northern Adriatic Sea in relation to nutrient loadings using the EMODnet chemistry data portal. Water 12, 2280. https://doi.org/10.3390/w12082280

Harary, F., 1969. Graph Theory. CRC Press. https://doi.org/10.1201/9780429493768

Harrell, F.E.J., 2022. Hmisc: Harrell Miscellaneous. R package version 4.7-0.

Hays, G.C., Richardson, A.J., Robinson, C., 2005. Climate change and marine plankton. Trends Ecol. Evol. 20, 337–344. https://doi.org/10.1016/j.tree.2005.03.004

Hering, D., Birk, S., Solheim, A.L., Moe, J., Carvalho, L., Borja, A., Hendriksen, P., Krause-Jensen, D., Lauridsen, T., Sondergaard, M., Pont, D., Johnson, R., Kolada, A., Porst, G., Marba, N., Noges, P., Ott, I., Marques, J.C., Irvine, K., Basset, A., 2010. Wiser Deliverable 2.2-2: Guidelines for indicator development 1–22.

Khatiwala, S., Primeau, F., Hall, T., 2009. Reconstruction of the history of anthropogenic CO_2 concentrations in the ocean. Nature 462, 346–349. https://doi.org/10.1038/nature08526

Kröncke, I., Neumann, H., Dippner, J.W., Holbrook, S., Lamy, T., Miller, R., Padedda, B.M., Pulina, S., Reed, D.C., Reinikainen, M., Satta, C.T., Sechi, N., Soltwedel, T., Suikkanen, S., Lugliè, A., 2019. Comparison of biological and ecological long-term trends related to northern hemisphere climate in different marine ecosystems. Nat. Conserv. 34, 311–341. https://doi.org/10.3897/natureconservation.34.30209

Lê, S., Josse, J., Husson, F., 2008. FactoMineR: An R package for multivariate analysis. J. Stat. Softw. 25, 1–18. https://doi.org/10.18637/jss.v025.i01

Longobardi, L., Dubroca, L., Margiotta, F., Sarno, D., Zingone, A., 2022. Photoperiod-driven rhythms reveal multi-decadal stability of phytoplankton communities in a highly fluctuating coastal environment. Sci. Rep. 12, 3908. https://doi.org/10.1038/s41598-022-07009-6

Lyashevska, O., Farnsworth, K.D., 2012. How many dimensions of biodiversity do we need? Ecol. Indic. 18, 485–492. https://doi.org/10.1016/j.ecolind.2011.12.016

Marić, D., Kraus, R., Godrijan, J., Supić, N., Djakovac, T., Precali, R., 2012. Phytoplankton response to climatic and anthropogenic influences in the north-eastern Adriatic during the last four decades. Estuar. Coast. Shelf Sci. 115, 98–112. https://doi.org/10.1016/j.ecss.2012.02.003

Marini, M., Jones, B.H., Campanelli, A., Grilli, F., Lee, C.M., 2008. Seasonal variability and Po River plume influence on biochemical properties along western Adriatic coast. J. Geophys. Res. Ocean. 113, C05S90. https://doi.org/10.1029/2007JC004370

Markogianni, V., Varkitzi, I., Pagou, K., Pavlidou, A., Dimitriou, E., 2017. Nutrient flows and related impacts between a Mediterranean river and the associated coastal area. Cont. Shelf Res. 134, 1–14. https://doi.org/10.1016/j.csr.2016.12.014

Martin, P., Lampitt, R.S., Jane Perry, M., Sanders, R., Lee, C., D'Asaro, E., 2011. Export and mesopelagic particle flux during a North Atlantic spring diatom bloom. Deep Sea Res. Part I Oceanogr. Res. Pap. 58, 338–349. https://doi.org/10.1016/j.dsr.2011.01.006

Mason, O., Verwoerd, M., 2007. Graph theory and networks in biology. IET Syst. Biol. https://doi.org/10.1049/iet-syb:20060038

McQuatters-Gollop, A., Edwards, M., Helaouët, P., Johns, D.G., Owens, N.J.P., Raitsos, D.E., Schroeder, D., Skinner, J., Stern, R.F., 2015. The Continuous Plankton Recorder survey: How can long-term phytoplankton datasets contribute to the assessment of Good Environmental Status? Estuar. Coast. Shelf Sci. 162, 88–97. https://doi.org/10.1016/j.ecss.2015.05.010

McQuatters-Gollop, A., Atkinson, A., Aubert, A., Bedford, J., Best, M., Bresnan, E., Cook, K., Devlin, M., Gowen, R., Johns, D.G., Machairopoulou, M., McKinney, A., Mellor, A., Ostle, C., Scherer, C., Tett, P., 2019. Plankton lifeforms as a biodiversity indicator for regional-scale assessment of pelagic habitats for policy. Ecol. Indic. 101, 913–925. https://doi.org/10.1016/j.ecolind.2019.02.010

McQuatters-Gollop, A., Guérin, L., Arroyo, N.L., Aubert, A., Artigas, L.F., Bedford, J., Corcoran, E., Dierschke, V., Elliott, S.A.M., Geelhoed, S.C.V., Gilles, A., González-Irusta, J.M., Haelters, J., Johansen, M., Le Loc'h, F., Lynam, C.P., Niquil, N., Meakins, B., Mitchell, I., Padegimas, B., Pesch, R., Preciado, I., Rombouts, I., Safi, G., Schmitt, P., Schückel, U., Serrano, A., Stebbing, P., De la Torriente, A., Vina-Herbon, C., 2022. Assessing the state of marine biodiversity in the Northeast Atlantic. Ecol. Indic. 141. https://doi.org/10.1016/j.ecolind.2022.109148

McQuatters-Gollop, A., Guérin, L., Arroyo, N.L., Aubert, A., Artigas, L.F., Bedford, J., Corcoran, E., Dierschke, V., Elliott, S.A.M., Geelhoed, S.C.V., Gilles, A., González-Irusta, J.M., Haelters, J.,

Johansen, M., Le Loc'h, F., Lynam, C.P., Niquil, N., Meakins, B., Mitchell, I., Padegimas, B., Pesch, R., Preciado, I., Rombouts, I., Safi, G., Schmitt, P., Schückel, U., Serrano, A., Stebbing, P., De la Torriente, A., Vina-Herbon, C., 2022. Assessing the state of marine biodiversity in the Northeast Atlantic. Ecol. Indic. 141, 109148. https://doi.org/10.1016/j.ecolind.2022.109148

Murillas-Maza, A., Uyarra, M.C., Papadopoulou, K.N., Smith, C.J., Gorjanc, S., Klancnik, K., Paramana, T., Chalkiadaki, O., Dassenakis, M., Pavicic, M., 2020. Programmes of measures of the marine strategy framework directive: Are they contributing to achieving good environmental status in the Mediterranean? Mar. Pollut. Bull. 161, 111715. https://doi.org/10.1016/j.marpolbul.2020.111715

Megrey, B.A., Link, J.S., Hunt, G.L., Moksness, E., 2009. Comparative marine ecosystem analysis: Applications, opportunities, and lessons learned. Prog. Oceanogr. 81, 2–9. https://doi.org/10.1016/j.pocean.2009.04.002

Menschel, E., González, H.E., Giesecke, R., 2016. Coastal-oceanic distribution gradient of coccolithophores and their role in the carbonate flux of the upwelling system off Concepción, Chile (36°S). J. Plankton Res. 38, 798–817. https://doi.org/10.1093/plankt/fbw037

Mozetič, P., Solidoro, C., Cossarini, G., Socal, G., Precali, R., Francé, J., Bianchi, F., De Vittor, C., Smodlaka, N., Fonda Umani, S., 2010. Recent trends towards oligotrophication of the Northern Adriatic: evidence from chlorophyll a time series. Estuar. Coast. 33, 362–375. https://doi.org/10.1007/s12237-009-9191-7

Murawski, S.A., Steele, J.H., Taylor, P., Fogarty, M.J., Sissenwine, M.P., Ford, M., Suchman, C., 2010. Why compare marine ecosystems? ICES J. Mar. Sci. 67, 1–9. https://doi.org/10.1093/icesjms/fsp221

Neri, F., Romagnoli, T., Accoroni, S., Campanelli, A., Marini, M., Grilli, F., Totti, C., 2022. Phytoplankton and environmental drivers at a long-term offshore station in the northern Adriatic Sea (1988–2018). Cont. Shelf Res. 242, 104746. https://doi.org/10.1016/j.csr.2022.104746

Ninčević Gladan, Ž., Marasović, I., Grbec, B., Skejić, S., Bužančić, M., Kušpilić, G., Matijević, S., Matić, F., 2010. Inter-decadal variability in phytoplankton community in the middle Adriatic (Kaštela Bay) in relation to the North Atlantic Oscillation. Estuar. Coast. 33, 376–383. https://doi.org/10.1007/s12237-009-9223-3

Ninčević-Gladan, Ž., Bužančić, M., Kušpilić, G., Grbec, B., Matijević, S., Skejić, S., Marasović, I., Morović, M., 2015. The response of phytoplankton community to anthropogenic pressure gradient in the coastal waters of the eastern Adriatic Sea. Ecol. Indic. 56, 106–115. https://doi.org/10.1016/j.ecolind.2015.03.018

Oksanen, J., Simpson, G.L., Blanchet, F.G., Kindt, R., Legendre, P., Minchin, P.R., O'Hara, R.B., Solymos, P., Stevens, M.H.H., Szoecs, E., Wagner, H., Barbour, M., Bedward, M., Bolker, B., Borcard, D., Carvalho, G., Chirico, M., De Caceres, M., Durand, S., Evangelista, H.B.A., FitzJohn, R., Friendly, M., Furneaux, B., Hannigan, G., Hill, M.O., Lahti, L., McGlinn, D., Ouellette, M.-H., Ribeiro Cunha, E., Smith, T., Stier, A., Ter Braak, C.J.F., Weedon, J., 2022. vegan: Community Ecology Package. R package version 2.6-2.

Opsahl, T., Agneessens, F., Skvoretz, J., 2010. Node centrality in weighted networks: Generalizing degree and shortest paths. Soc. Networks 32, 245–251. https://doi.org/10.1016/j.socnet.2010.03.006

Petchey, O.L., Gaston, K.J., 2006. Functional diversity: back to basics and looking forward. Ecol. Lett. 9, 741–758. https://doi.org/https://doi.org/10.1111/j.1461-0248.2006.00924.x

Pielou, E.C., 1975. Ecological diversity. John Wiley & Sons, New York.

Poulain, P.-M., Cushman-Roisin, B., 2001. Circulation. In: Cushman-Roisin, B., Gačić, M., Poulain, P.-M., Artegiani, A. (Eds), *Physical oceanography of the Adriatic Sea: Past, present and future.* Kluwer Academic Publishers, Dordrecht, The Netherlands, pp. 67–109.

R Core Team, 2021. R: A language and environment for statistical computing.

Richardson, K., Visser, A.W., Pedersen, F.B., 2000. Subsurface phytoplankton blooms fuel pelagic production in the North Sea. J. Plankton Res. 22, 1663–1671. https://doi.org/10.1093/plankt/22.9.1663

Rombouts, I., Simon, N., Aubert, A., Cariou, T., Feunteun, E., Guérin, L., Hoebeke, M., McQuatters-Gollop, A., Rigaut-Jalabert, F., Artigas, L.F., 2019. Changes in marine phytoplankton diversity: Assessment under the Marine Strategy Framework Directive. Ecol. Indic. 102, 265–277. https://doi.org/10.1016/j.ecolind.2019.02.009

Russo, A., Artegiani, A., 1996. Adriatic Sea hydrography. Sci. Mar. 60, 33–43.

Safi, G., Giebels, D., Arroyo, N.L., Heymans, J.J., Preciado, I., Raoux, A., Schückel, U., Tecchio, S., de Jonge, V.N., Niquil, N., 2019. Vitamine ENA: A framework for the development of ecosystem-based indicators for decision makers. Ocean Coast. Manag. 174, 116–130. https://doi.org/10.1016/j.ocecoaman.2019.03.005

Shannon, C.E., 1948. A mathematical theory of communication. Bell Syst. Tech. J. 27, 379–423. https://doi.org/10.1002/j.1538-7305.1948.tb01338.x

Strickland, J.D.H., Parsons, T.R., 1972. A practical handbook of seawater analysis, Bullettin 167, 2nd ed. Printing and Publishing Supply and Services Canada, Ottawa, ON, Canada.

Throndsen, J., 1978. Preservation and storage. In: Sournia, A. (Eds.), *Phytoplankton Manual. Monographs on Oceanographic Methodology*. UNESCO, Paris, pp. 69–74.

Tomczak, M.T., Heymans, J.J., Yletyinen, J., Niiranen, S., Otto, S.A., Blenckner, T., 2013. Ecological Network Indicators of Ecosystem Status and Change in the Baltic Sea. PLoS One 8, e75439. https://doi.org/10.1371/journal.pone.0075439

Totti, C., Artegiani, A., 2001. Phytoplankton time series in the northern Adriatic Sea: the Senigallia transect (1988–1994). Arch. Ocean. Limnol 22, 107–112.

Totti, C., Romagnoli, T., Accoroni, S., Coluccelli, A., Pellegrini, M., Campanelli, A., Grilli, F., Marini, M., 2019. Phytoplankton communities in the northwestern Adriatic Sea: Interdecadal variability over a 30-years period (1988–2016) and relationships with meteoclimatic drivers. J. Mar. Syst. 193, 137–153. https://doi.org/10.1016/j.jmarsys.2019.01.007

Tweddle, J.F., Gubbins, M., Scott, B.E., 2018. Should phytoplankton be a key consideration for marine management? Mar. Policy 97, 1–9. https://doi.org/10.1016/j.marpol.2018.08.026

Vallina, S.M., Simó, R., 2007. Strong Relationship Between DMS and the Solar Radiation Dose over the Global Surface Ocean. Science 315, 506–508. https://doi.org/10.1126/science.1133680

Varkitzi, I., Francé, J., Basset, A., Cozzoli, F., Stanca, E., Zervoudaki, S., Giannakourou, A., Assimakopoulou, G., Venetsanopoulou, A., Mozetič, P., Tinta, T., Skejic, S., Vidjak, O., Cadiou, J.F., Pagou, K., 2018. Pelagic habitats in the Mediterranean Sea: A review of Good Environmental Status (GES) determination for plankton components and identification of gaps and priority needs to improve coherence for the MSFD implementation. Ecol. Indic. 95, 203–218. https://doi.org/10.1016/j.ecolind.2018.07.036

Varkitzi, I., Psarra, S., Assimakopoulou, G., Pavlidou, A., Krasakopoulou, E., Velaoras, D., Papathanassiou, E., Pagou, K., 2020. Phytoplankton dynamics and bloom formation in the

oligotrophic Eastern Mediterranean: Field studies in the Aegean, Levantine and Ionian seas. Deep. Res. Part II Top. Stud. Oceanogr. 171, 104662. https://doi.org/10.1016/j.dsr2.2019.104662

Vascotto, I., Mozetič, P., Francé, J., 2021. Phytoplankton Time-Series in a LTER site of the Adriatic Sea: methodological approach to decipher community structure and indicative taxa. Water 13, 2045. https://doi.org/10.3390/w13152045

Winder, M., Cloern, J.E., 2010. The annual cycles of phytoplankton biomass. Philos. Trans. R. Soc. B 365, 3215–3226. https://doi.org/10.1098/rstb.2010.0125

1.2.8 Supplementary materials

Supplementary methods

In our study we relied on the construction of undirected weighted graphs for stations description, formally defined on a triple of sets as G = (V, E, W), in which V and E are respectively the set of vertices and edges, W is the set of weights associated to edges given by correlation values. The study makes use of both local and global measures to identify meaningful features of networks, the latter usually extending to the whole graph the properties of single vertices and edges.

The capability of each species to interact and communicate with other subjects in the system is evaluated by using the closeness centrality measure (Freeman, 1979), formally stated for each vertex *v* as $C(v) = 1/\sum_{u \neq v \in V} l_{uv}$, where l_{uv} is the length of the geodesic connecting *u* to *v*. Basically the formula computes the inverse of the geodesic lengths from all vertices to *v* and measures how fast information can propagate through the network reaching *v*. The larger is the distance separating *v* from other vertices, the smaller will be the centrality and relevance of *v* in the network structure. In our study, lengths are computed by considering edge weights *w* temporarily transformed into 1 – *w*, so that large values of correlations correspond to close vertices.

A similar analysis can be performed by relying on betweenness centrality (Freeman, 1979), where the importance of a vertex *v* is assessed by counting the number of geodesics passing through *v*:

$$B(v) = \sum_{s \neq v \neq t \in V} \sigma_{st}(v)/\sigma_{st}.$$

Here σ_{st} is the number of geodesics connecting two vertices *s* and *t*, whereas $\sigma_{st}(v)$ gives the number of geodesics going from *s* to *t* and passing through *v*. Hence, $B(v)$ is the fraction of geodesics touching *v*. A high value of betweenness indicates a crucial and influential member of the network, whose interactions are meaningful to the graph cohesion. A similar indicator can be constructed for each edge *e* as $B_e(e) = \sum_{s \neq t \in V} \sigma_{st}(e)/\sigma_{st}$,

giving information about the importance of single connections between species to the network structure. A global measure of centralization for the whole graph can be obtained by computing the subsequent expression based on the closeness (or betweenness) values of vertices:

$$C(G) = \sum_{v \in V} [\max_{u} C(u) - C(v)].$$

The tendency of a species to aggregate and build clusters with other species can be studied by introducing the notion of clustering coefficient (Wasserman and Faust, 1994). In simple unweighted graphs, the clustering coefficient of vertex *v* is given by the ratio among the number of triangles (complete subgraphs of three vertices) *v* participates and the number of triples (subgraph of three vertices and at least two edges) it joins. The extension to the weighted case brings to the formula (Barrat et al., 2004): $K(v) = \frac{1}{\sum_{(v,u)\in E} w_{vu}(d_v - 1)} \sum_{u,z \in V} \frac{w_{vu}+w_{vz}}{2} a_{vu} a_{vz} a_{uz}$ in which d_v is the degree of vertex *v* and a_{vu} is the entry of the adjacency matrix, being 1 if $(v, u) \in$ E and 0 otherwise. The clustering coefficient value is rewarded for vertices that have strong ties with vertices directly connected between them, thus creating strict triadic bounds. This condition can be interpretated as a condition of tough connection and interaction among members. The definition of clustering coefficient can then be extended to the whole network by summing up $K(v)$ for all the vertices.

References

Barrat, A., Barthélemy, M., Pastor-Satorras, R., Vespignani, A., 2004. The architecture of complex weighted networks. PNAS 101 (11) 3747–3752. https://doi.org/https://doi.org/10.1073/pnas.0400087101

Freeman, L.C., 1979. Centrality in social networks conceptual clarification. Soc. Networks 1, 215–239. https://doi.org/https://doi.org/10.1016/0378-8733(78)90021-7

Wasserman, S., Faust, K., 1994. Social network analysis: Methods and applications. Cambridge university press.

Table S1. List of taxa

Bacillariophyceae

Achnantes spp.
Amphora peragalloi Cleve
Amphora spp.
Asterionella formosa Hassal
Asterionellopsis glacialis (Castracane) Round
Asteromphalus cfr. *hookeri* Ehrenberg
Asteromphalus cfr. *hyalinus* Karsten
Asteromphalus cfr. *sarcophagus* Wallich
Asteromphalus robustus Castracane
Asteromphalus spp.
Azpeitia nodulifera (A.Schmidt) G.Fryxell & P.A.Sims
Bacillaria paxillifera (O.F. Müller) Hendey
Bacteriastrum cfr. *delicatulum* Cleve
Bacteriastrum cfr. *elongatum* Cleve
Bacteriastrum cfr. *hyalinum* Lauder
Bacteriastrum cfr. *mediterraneum* J. Pavillard
Bacteriastrum elegans J. Pavillard
Bacteriastrum spp.
Bacteriosira fragilis Gran
Campylodiscus spp.
Cerataulina pelagica (Cleve) Hendey
Chaetoceros affinis Lauder
Chaetoceros anastomosans Grunow in van Heurck
Chaetoceros atlanticus Cleve
Chaetoceros atlanticus var. *neapolitana* (Schröder) Hustedt
Chaetoceros brevis Schütt
Chaetoceros cfr. *atlanticus* Cleve
Chaetoceros cfr. *constrictus* Gran
Chaetoceros cfr. *fragilis* Meunier
Chaetoceros cfr. *muelleri* Lemmermann
Chaetoceros cfr. *neogracilis* VanLandingham
Chaetoceros cfr. *pseudocrinitus* Ostenfeld
Chaetoceros cfr. *simplex* Ostenfeld
Chaetoceros cfr. *socialis* Lauder
Chaetoceros cfr. *vixvisibilis* Schiller
Chaetoceros compressus Lauder
Chaetoceros convolutus Castracane
Chaetoceros costatus Pavillard
Chaetoceros curvisetus Cleve
Chaetoceros dadayi Pavillard
Chaetoceros danicus Cleve
Chaetoceros decipiens Cleve
Chaetoceros densus Cleve
Chaetoceros dichaeta Ehrenberg
Chaetoceros didymus Ehremberg
Chaetoceros diversus Cleve
Chaetoceros eibenii Grunow in Van Heurck
Chaetoceros laciniosus Schütt
Chaetoceros lauderi Ralfs in Lauder
Chaetoceros lorenzianus Grunow
Chaetoceros messanensis Castracane
Chaetoceros muelleri Lemmermann
Chaetoceros peruvianus Brightwell
Chaetoceros pseudocrinitus Ostenfeld
Chaetoceros radicans Schütt
Chaetoceros rostratus Lauder
Chaetoceros similis Cleve
Chaetoceros simplex Ostenfeld
Chaetoceros socialis Lauder
Chaetoceros spp.
Chaetoceros subtilis Cleve
Chaetoceros tenuissimus Meunier
Chaetoceros teres Cleve
Chaetoceros tetrastichon Cleve
Chaetoceros throndsenii Marino, Montresor & Zingone
Chaetoceros tortissimus Gran
Chaetoceros wighamii Brightwell
Cocconeis scutellum Ehrenberg
Cocconeis spp.
Coscinodiscus centralis Ehrenberg
Coscinodiscus cfr. *asteromphalus* Ehrenberg
Coscinodiscus cfr. *oculus iridis* Ehrenberg
Coscinodiscus marginatus Ehrenberg
Coscinodiscus radiatus Ehremberg
Coscinodiscus spp.
Cyclophora spp.
Cyclotella caspia Grunow
Cyclotella glomerata H.Bachmann
Cyclotella spp.
Cylindrotheca cfr. *fusiformis* Reimann & J.C.Lewin
Cylindrotheca closterium (Ehrenberg) Lewin & Reimann
Cymatosira spp.
Dactyliosolen blavyanus (H. Peragallo) Hasle
Dactyliosolen fragilissimus (Bergon) Hasle
Dactyliosolen mediterraneus (H.Peragallo) H.Peragallo
Dactyliosolen phuketensis (Sundström) Hasle
Detonula pumila (Castracane) Gran
Diatoma cfr. *elongata* (Lyngbye) C.Agardh
Diploneis crabro Ehrenberg
Diploneis spp.
Ditylum brightwellii (West) Grunow in Van Heurck
Entomoneis cfr. *ornata* (J.W.Bailey) Reimer

Entomoneis spp.
Eucampia cornuta (Cleve) Grunow
Eucampia zodiacus f. *cylindricornis* Syvertsen
Fragilaria crotonensis Kitton
Fragilaria spp.
Fragilariopsis spp.
Gomphonema spp.
Grammatophora spp.
Guinardia flaccida (Castracane) H. Peragallo
Guinardia striata (Stolterfoth) Hasle
Halamphora coffeiformis (C.Agardh) Mereschkowsky
Hantzschia spp.
Haslea wawrickae (Hustedt) Simonsen
Hemiaulus hauckii Grunow in van Heurck
Hemiaulus sinensis Greville
Lauderia annulata Cleve
Leptocylindrus cfr. *danicus* Cleve
Leptocylindrus convexus Nanjappa and Zingone
Leptocylindrus danicus Cleve
Leptocylindrus minimus Gran
Leptocylindrus spp.
Licmophora cfr. *abbreviata* Agardh
Licmophora spp.
Lioloma pacificum (Cupp) Hasle
Melosira cfr. *dubia* Kützing
Melosira cfr. *nummuloides* C.Agardh
Melosira spp.
Navicula cfr. *ammophila* Grunow
Navicula distans (W. Smith) A. Schmidt
Navicula spp.
Nitzschia cfr. *bilobata* W. Smith
Nitzschia cfr. *incurva* Grunow
Nitzschia cfr. *lanceolata* W. Smith
Nitzschia cfr. *sigma* (Kützing) W.Smith
Nitzschia longissima (Brébisson in Kützing) Ralfs in Pritchard
Nitzschia sigma W. Smith
Nitzschia spp.
Nitzschia gobbii Accoroni, Romagnoli, Giulietti & Totti
Paralia sulcata (Ehremberg) Cleve
Phaeodactylum tricornutum Bohlin
Plagiotropis lepidoptera (Gregory) Kuntze
Plagiotropis spp.
Pleurosigma affine Grunow
Pleurosigma cfr. *angulatum* (Quekett) W.Smith
Pleurosigma cfr. *elongatum* W.Smith
Pleurosigma rigidum W.Smith
Pleurosigma spp.
Proboscia alata (Brightwell) Sundström
Psammodictyon spp.
Pseudo-nitzschia cfr. *delicatissima* (Cleve) Heiden in Heiden & Kolbe
Pseudo-nitzschia cfr. *fraudulenta* (Cleve) Hasle
Pseudo-nitzschia cfr. *galaxiae* N.Lundholm & Moestrup
Pseudo-nitzschia cfr. *granii* var. *granii* (Hasle) Hasle
Pseudo-nitzschia cfr. *lineola* (Cleve) Hasle
Pseudo-nitzschia cfr. *pseudodelicatissima* (Hasle) Hasle
Pseudo-nitzschia multistriata (Takano) Takano
Pseudo-nitzschia pungens (Grunow ex Cleve) Hasle
Pseudo-nitzschia spp.
Pseudosolenia calcar avis (Schultze) B.G.Sundström
Rhizosolenia castracanei var. *castracanei* H. Peragallo
Rhizosolenia cfr. *shrubsolei* Cleve
Rhizosolenia cfr. *styliformis* T.Brightwell
Rhizosolenia hebetata Bailey
Rhizosolenia imbricata Brightwell
Rhizosolenia robusta Norman in Pritchard
Rhizosolenia setigera Brightwell
Rhizosolenia spp.
Skeletonema marinoi Sarno & Zingone
Surirella ovata Kutzing
Surirella spp.
Synedra spp.
Tenuicylindrus belgicus (Meunier) D.Nanjappa & A.Zingone
Thalassionema bacillare (Heiden) Kolbe
Thalassionema frauenfeldii (Grunow) Hallegraeff
Thalassionema nitzschioides (Grunow) Mereschkowsky
Thalassionema spp.
Thalassiosira angustelineata (A.W.F.Schmidt) G.Fryxell & Hasle
Thalassiosira cfr. *rotula* Meunier
Thalassiosira rotula Meunier
Thalassiosira spp.
Thalassiosira subtilis (Ostenfeld) Gran
Tropidoneis spp.
Und. centric diatoms <20 µm
Und. centric diatoms >20 µm
Und. pennate diatoms <20 µm
Und. pennate diatoms >20 µm
Und. diatoms

Dinophyceae
Akashiwo sanguinea (K.Hirasaka) Gert Hansen & Moestrup
Alexandrium cfr. *tamarense* (Lebour) Balech
Alexandrium minutum Halim
Alexandrium spp.
Amphidinium spp.

Amylax triacantha (Jorgensen) Sournia
Azadinium caudatum (Halldal) Nézan & Chomérat
Ceratocorys kofoidii Paulsen
Cysts of Dinophyceae
Cochlodinium spp.
Coolia cfr. *monotis* Meunier
Corythodinium constrictum (F.Stein) F.J.R.Taylor
Desmocapsa gelatinosa Pascher
Dinophysis acuminata Claparède & Lachmann
Dinophysis caudata Saville-Kent
Dinophysis fortii Pavillard
Dinophysis sacculus Stein
Dinophysis sphaerica F.Stein
Dinophysis spp.
Dinophysis tripos Gourret
Diplopsalis group Bergh
Goniodoma polyedricum (Pouchet) Jorgensen
*Gonyaulax fragil*is (Schutt) Kofoid
Gonyaulax polygramma Stein
Gonyaulax spinifera (Claparède & Lachmann) Diesing
Gonyaulax spp.
Gymnodinium cfr. *caput* J.Schiller
Gymnodinium elongatum Hope
Gymnodinium spp.
Gyrodinium lachrima (Meunier) Kofoid & Swezy
Gyrodinium spp.
Karenia papilionacea A.J.Haywood & K.A.Steidinger
Karenia spp.
Kofoidinium velleloides Pavillard
Lingulodinium polyedra (Stein) Dodge
Mesoporos perforatus (Gran) Lillick
Mesoporos spp.
Noctiluca scintillans (Macartney) Kofoid & Swezy
Ornithocercus magnificus Stein
Oxyphysis oxytoxoides Kofoid
Oxytoxum caudatum Schiller
Oxytoxum cfr. *elongatum* Wood
Oxytoxum cfr. *milneri* Murray et Whitting
Oxytoxum crassum Schiller
Oxytoxum gracile Schiller
Oxytoxum laticeps Schiller
Oxytoxum parvum Schiller
Oxytoxum sceptrum (Stein) Schroder
Oxytoxum scolopax Stein
Oxytoxum spp.
Oxytoxum variabile Schiller
Phalacroma rotundatum (Claparéde & Lachmann) Kofoid & Michener
Phalacroma cfr. *mitra* Schütt
Phalacroma cfr. *ovum* Schütt
Phalacroma cfr. *porosum* Kofoid
Phalacroma rotundatum (Claparéde & Lachmann) Kofoid & Michener
Phalacroma spp.
Podolampas palmipes Stein
Podolampas spinifer Okamura
Pronoctiluca acuta (Lohmann) Schiller
Pronoctiluca pelagica Fabre - Domergue
Pronoctiluca spp.
Pronoctiluca spinifera (Lohmann) Schiller
Prorocentrum aporum (Schiller) Dodge
Prorocentrum balticum (Lohmann) Loeblich
Prorocentrum cfr. *cordatum* (Pavillard) J.Schiller
Prorocentrum cfr. *dactylus* (Stein) Dodge
Prorocentrum cfr. *lima* (Ehremberg) Dodge
Prorocentrum cfr. *nanum* Schiller
Prorocentrum cfr. *rotundatum* Schiller
Prorocentrum cfr. *vaginulum* (Stein) Dodge
Prorocentrum compressum (J.W.Bailey) Abé ex Dodge
Prorocentrum cordatum (Pavillard) J.Schiller
Prorocentrum dactylus (Stein) Dodge
Prorocentrum dentatum Stein
Prorocentrum gracile Schutt
Prorocentrum lima (Ehremberg) Dodge
Prorocentrum micans Ehremberg
Prorocentrum rotundatum Schiller
Prorocentrum spp.
Prorocentrum triestinum Schiller
Prorocentrum vaginulum (Stein) Dodge
Protoceratium reticulatum (Claparède & Lachmann) Bütschli
Protoperidinium bipes (Paulsen) Balech
Protoperidinium bispinum (Schiller) Balech
Protoperidinium brevipes (Paulsen) Balech
Protoperidinium brochi (Kofoid & Swezy) Balech
Protoperidinium cfr. *bispinum* (Schiller) Balech
Protoperidinium cfr. *brochi* (Kofoid & Swezy) Balech
Protoperidinium cfr. *globulus* (F.Stein) Balech
Protoperidinium cfr. *granii* (Ostenfeld) Balech
Protoperidinium cfr. *oceanicum* (Vanhöffen) Balech
Protoperidinium cfr. *oviforme* (P.J.L.Dangeard) Balech
Protoperidinium cfr. *ovum* (Schiller) Balech
Protoperidinium cfr. *pentagonum* (Murray & Black.) Loeb. & Tappan
Protoperidinium cfr. *steinii* (Jorgensen) Balech
Protoperidinium claudicans (Paulsen) Balech
Protoperidinium conicum (Gran) Balech
Protoperidinium depressum (Bailey) Balech

Protoperidinium diabolus (Cleve) Balech
Protoperidinium divergens (Ehrenberg) Balech
Protoperidinium grande (Kofoid) Balech
Protoperidinium leonis (Pavillard) Balech
Protoperidinium minusculum Pavillard
Protoperidinium oceanicum (VanHoffen) Balech
Protoperidinium parcum (Balech) Balech
Protoperidinium pellucidum Bergh
Protoperidinium spp.
Pseliodinium vaubanii Sournia
Pyrocystis cfr. *obtusa* Pavillard
Pyrocystis lunula (Schutt) Schutt
Pyrocystis spp.
Pyrophacus horologicum Stein
Scrippsiella spp.
Scrippsiella trochoidea (Stein) Loeblich
Spatulodinium pseudonoctiluca (Pouchet) Cachon & Cachon ex Loeblich & Loeblich
Tripos candelabrum (Ehrenberg) F.Gómez
Tripos carriensis (Gourret) F.Gómez
Tripos cfr. *strictus* (Okamura & Nishikawa) F.Gómez
Tripos extensus (Gourret) F.Gómez
Tripos furca (Ehrenberg) F.Gómez
Tripos fusus (Ehrenberg) F.Gómez
Tripos hexacanthus (Gourret) F.Gómez
Tripos horridus (Cleve) F.Gómez
Tripos kofoidii (Jörgenen) F.Gómez
Tripos lineatus (Ehrenberg) F.Gómez
Tripos longirostrus Gourret(Gourret) F.Gómez
Tripos macroceros (Ehrenberg) F.Gómez
Tripos massiliensis (Gourret) F.Gómez
Tripos muelleri Bory
Tripos pentagonus (Gourret) F.Gómez
Tripos pulchellus (Schröder) F.Gómez
Tripos setaceus (Jørgesen) F.Gómez
Tripos spp.
Tripos teres (Kofoid) F.Gómez
Tripos trichoceros (Ehrenberg) Gómez
Tripos vultur (Cleve) Hallegraeff & Huisman
Und. dinoflagellates
Und. naked dinoflagellates <20 µm
Und. naked dinoflagellates >20 µm
Und. thecate dinoflagellates <20 µm
Und. thecate dinoflagellates >20 µm

Prymnesiophyceae
Chrysochromulina spp.
Corymbellus aureus J.C.Green
Und. prymnesiophytes

Prymnesiophyceae (Coccolithophores)
Acanthoica quattrospina Ehrenberg
Calcidiscus leptoporus (Murray & Blackman) Loeblich & Tappan
Calciopappus caudatus Gaarder & Ramsfjell
Calciosolenia brasiliensis (Lohmann) J.R.Young
Calciosolenia murrayi Gran
Calyptrosphaera oblonga Lohmann
Calyptrosphaera sphaeroidea Schiller
Calyptrosphaera spp.
Chrysotila spp.
Coccolithus pelagicus f. *hyalinus* (K.R.Gaarder & J.Markali) A.Kleijne
Coccolithus pelagicus subsp. *braarudii* (K.R.Gaardner) M.Geisen, C.Billard, A.T.C.Broerse, L.Cros, I.Probert & J.C.Young
Coronosphaera mediterranea (Lohmann) Gaarder in Gaarder & Heimdal
Daktylethra pirus (Kamptner) Norris
Emiliania huxleyi (Lohmann) W.W.Hay & H.P.Mohler
Halopappus adriaticus Schiller
Helicosphaera carteri (Wallich) Kamptner
Helicosphaera pavimentum Okada et McIntyre
Helladosphaera cornifera (Schiller) Kamptner
Michaelsarsia elegans Gran
Ophiaster hydroideus (Lohmann) Lohmann
Rhabdolithes claviger Murray & Blackman
Syracosphaera cfr. *histrica* Kamptner
Syracosphaera cfr. *pulchra* Lohmann
Syracosphaera hystrica Kamptner
Syracosphaera pulchra Lohmann
Syracosphaera rotula Okada & McIntyre
Syracosphaera spp.
Tergestiella adriatica Kamptner
Umbellosphaera tenuis (Kamptner) Paasche
Und. coccolithophores
Zygosphaera spp.

Cryptophyceae
Cryptomonas spp.
Hillea fusiformis (J.Schiller) J.Schiller
Hillea marina Butcher
Leucocryptos cfr. *marina* (Braarud) Butcher
Plagioselmis sp.
Und. cryptophytes

Chrysophyceae
Calycomonas spp.
Dinobryon cfr. *balticum* (Schütt) Lemmermann

Dinobryon faculiferum Willén
Dinobryon porrectum Schiller
Dinobryon spp.
Meringosphaera mediterranea Lohmann
Meringosphaera tenerrima Schiller
Pseudokephyrion spp.
Und. chrysophytes

Raphidophyceae
Fibrocapsa japonica S.Toriumi & H.Takano
Heterosigma spp.
Olisthodiscus luteus N.Carter

Dictyochophyceae
Dictyocha crux Ehrenberg
Dictyocha fibula Ehrenberg
Distephanopsis staurodon (Ehrenberg) Desikachary & Prema
Octactis octonaria (Ehrenberg) Hovasse
Octactis speculum (Ehrenberg) F.H.Chang, J.M.Grieve & J.E.Sutherland
Parapedinella cfr. *reticulata* S.M.Pedersen & H.A.Thomsen
Octactis spp.
Parapedinella spp.
Vicicitus globosus (Y.Hara & Chihara) F.H.Chang

Chlorophyceae
Halosphaera spp.
Nephroselmis spp.
Pachysphaera spp.
Pseudoscourfieldia marina (J.Throndsen) Manton
Pterosperma nationalis Lohmann
Pyramimonas spp.
Und. chlorophytes

Euglenophyceae
Euglena cfr. *acusformis* J.Schiller
Euglena spp.
Eutreptia lanowii Steuer
Eutreptiella hirudoidea Butcher
Und. euglenophytes

Cyanophyceae
Spirulina spp.
Und. cyanophyceae
Und. Oscillatoriales

Other flagellates
Und. phytoflagellates <10 µm
Und. phytoflagellates >10 µm

Table S2. List of phytoplankton taxa characterized by the highest IndVal for each season calculated for the surface layer in the coastal (A) and offshore (B) station. Values indicated in italic are significant at $p < 0.05$, those in bold italic are significant at $p < 0.01$, those in bold italic and underlined are significant at $p < 0.001$. The shades of colour are proportional to the IndVal values, from dark green to white, in decreasing order.

A	Winter	Spring	Summer	Autumn
Skeletonema marinoi	***77.291***	2.652	0.001	2.316
Thalassiosira spp.	27.857	8.255	1.226	6.01
Chaetoceros curvisetus	*26.878*	6.001	1.334	7.076
Thalassiosira rotula	***24.48***	0.036	0	14.745
Dictyocha fibula	*18.744*	0.085	0.02	16.732
Chaetoceros danicus	***11.698***	0.212	0.192	25.973
Dactyliosolen fragilissimus	2.482	***40.166***	8.736	16.568
Chaetoceros spp.	11.129	39.17	3.683	12.991
Prorocentrum micans	1.121	*38.116*	6.726	18.436
Nitzschia longissima	0.718	***38.11***	0.392	0.275
Cyclotella spp.	2.113	***35.393***	7.866	7.553
Tripos fusus	6.404	*32.963*	1.204	6.607
Pseudo-nitzschia cfr. *delicatissima*	8.793	*32.632*	4.45	3.825
Thalassionema nitzschioides	1.078	27.302	16.87	8.468
Chaetoceros tenuissimus	2.486	24.697	0.719	1.383
Cylindrotheca closterium	4.779	24.098	12.169	21.351
Prorocentrum cordatum	0.877	*23.982*	5.876	3.093
Euglena spp.	6.776	23.96	1.205	13.852
Alexandrium spp.	1.767	***20.942***	4.237	3.457
Tripos furca	0.596	20.058	10.852	9.92
Diplopsalis group	9.015	17.723	0.831	8.363
Proboscia alata	0.5	2.35	***50.508***	9.219
Guinardia flaccida	1.48	0.295	***31.147***	4.327
Cerataulina pelagica	4.482	17.992	29.248	17.331
Nitzschia gobbii	0.297	0.289	***28.101***	4.164
Pseudo-nitzschia cfr. *pseudodelicatissima*	1.778	13.337	23.975	14.281
Calycomonas sp.	0.105	11.434	***21.004***	1.423
Chaetoceros lorenzianus	1.791	2.176	20.643	14.838
Guinardia striata	0.022	0.004	19.995	6.599
Prorocentrum compressum	0.178	9.945	***18.131***	0.532
Calciosolenia brasiliensis	0.01	9.657	14.519	11.466
Rhizosolenia spp.	2.719	1.008	12.34	7.132
Protoperidinium spp.	9.908	7.303	6.066	1.897
Lioloma pacificum	0.018	0	2.741	***50.25***
Emiliania huxleyi	4.622	9.292	0.718	38.346
Leptocylindrus danicus	3.549	4.334	24.915	26.821
Asterionellopsis glacialis	5.887	1.013	0.022	***24.92***
Chaetoceros affinis	0.578	0.284	5.732	***24.884***
Pleurosigma spp.	2.703	2.398	14.764	20.961
Syracosphaera pulchra	3.752	14.887	5.198	16.644

B	Winter	Spring	Summer	Autumn
Skeletonema marinoi	***49.463***	1.16	0	1.586
Emiliania huxleyi	***40.561***	18.877	0.64	18.278
Pseudosolenia calcar avis	***34.602***	0.018	6.042	0.218
Chaetoceros affinis	*26.098*	0.147	2.122	8.493
Diploneis spp.	***25.876***	1.554	0.017	9.795
Hemiaulus sinensis	25.608	0.559	0.058	4.022
Dactyliosolen fragilissimus	2.109	*42.007*	18.728	6.287
Cyclotella spp.	0.25	***36.182***	5.448	0.781
Prorocentrum micans	0.489	*30.307*	11.676	2.008
Euglena spp.	1.603	*25.986*	1	8.323
Chaetoceros spp.	5.635	25.672	10.774	17.853
Tripos furca	1.564	18.365	2.053	1.738
Thalassionema nitzschioides	3	16.5	2.721	7.159
Pseudokephyrion spp.	0.607	15.538	1.962	7.521
Nitzschia longissima	0.639	6.923	1.023	1.959
Proboscia alata	0.907	3.7	***61.656***	6.948
Cerataulina pelagica	3.113	6.225	***55.636***	6.372
Pseudoscourfieldia marina	0.012	7.662	***41.003***	0.678
Calycomonas sp.	0.31	5.445	***40.722***	3.868
Guinardia flaccida	12.767	0.309	26.603	12.168
Hemiaulus hauckii	5.492	4.575	23.235	11.93
Pseudo-nitzschia cfr. *pseudodelicatissima*	1.507	17.996	21.663	18.022
Nitzschia gobbii	0.799	3.621	21.607	3.635
Rhizosolenia spp.	14.651	0.078	19.996	3.875
Rhabdolithes claviger	0.13	5.75	18.45	8.128
Protoperidinium spp.	1.719	3.623	16.228	3.515
Tripos fusus	1.632	9.542	14.349	6.411
Bacteriastrum spp.	0.755	0.684	12.67	11.768
Guinardia striata	2.58	0.014	6.607	***47.805***
Lioloma pacificum	0.104	0	1.742	***47.496***
Cylindrotheca closterium	3.822	4.245	18.916	***41.982***
Asterionellopsis glacialis	5.967	0.05	0.085	***32.948***
Pseudo-nitzschia cfr. *delicatissima*	0.838	6.583	0.273	*29.752*
Leptocylindrus danicus	3.068	6.358	22.669	27.491
Pleurosigma spp.	7.202	0	5.807	***26.712***
Chaetoceros lorenzianus	8.458	3.734	4.671	25.231
Chaetoceros curvisetus	11.533	3.295	0.202	21.477
Thalassionema frauenfeldii	9.295	0.628	0.55	18.908
Calciosolenia brasiliensis	8.771	1.813	8.785	17.309
Dictyocha fibula	7.801	0.066	2.801	16.845
Syracosphaera pulchra	10.339	8.147	8.85	16.725
Oxytoxum caudatum	0.257	9.579	2.57	10.822

Table S3. List of taxa names and abbreviations used in the graph-network analysis.

Taxa	Abbreviation		
Asterionellopsis glacialis	Ast-gla	*Leptocylindrus minimus*	Lep-min
Bacteriastrum cfr. *delicatulum*	Ba-del	*Lioloma pacificum*	Lio-pac
Calciosolenia brasiliensis	Cal-bra	*Meringosphaera mediterranea*	Mering
Calciosolenia murrayi	Cal-mur	*Nitzschia longissima*	Nit-lon
Calycomonas sp.	Calyc	*Nitzschiella*	Nit-gob
Cerataulina pelagica	Cer-pel	*Noctiluca scintillans*	Noc-sci
Chaetoceros affinis	Ch-aff	*Oxytoxum caudatum*	Ox-cau
Chaetoceros anastomosans	Ch-ana	*Oxytoxum* cfr. *elongatum*	Ox-el
Chaetoceros brevis	Ch-bre	*Oxytoxum variabile*	Ox-var
Chaetoceros compressus	Ch-com	*Proboscia alata*	Probos
Chaetoceros costatus	Ch-cos	*Prorocentrum compressum*	Prc-com
Chaetoceros curvisetus	Ch-cur	*Prorocentrum cordatum*	Prc-cor
Chaetoceros danicus	Ch-dani	*Prorocentrum micans*	Prc-mic
Chaetoceros lorenzianus	Ch-lor	*Prorocentrum triestinum*	Prc-tri
Chaetoceros rostratus	Ch-ros	*Protoperidinium* cfr. *steinii*	Prp-ste
Chaetoceros tenuissimus	Ch-ten	*Protoperidinium diabolus*	Prp-dia
Chaetoceros throndsenii	Ch-thr	*Protoperidinium divergens*	Prp-div
Chaetoceros tortissimus	Ch-tor	*Pseudokephyrion* spp.	Pskef
Cylindrotheca closterium	Cyl-clo	*Pseudo-nitzschia* cfr. *delicatissima*	Ps-del
Dactyliosolen fragilissimus	Dac-fra	*Pseudo-nitzschia* cfr. *galaxiae*	Ps-gal
Dactyliosolen phuketensis	Dac-phu	*Pseudo-nitzschia* cfr. *pseudodelicatissima*	Ps-pdel
Dictyocha fibula	Dic-fib	*Pseudo-nitzschia pungens*	Ps-pun
Dinophysis sacculus	Din-sac	*Pseudoscourfieldia marina*	Pscour
Diplopsalis group	Diplops	*Pseudosolenia calcar avis*	Pse-calc
Ditylum brightwellii	Dit-bri	*Rhabdolithes claviger*	Rha-cla
Emiliania huxleyi	E-hux	*Skeletonema marinoi*	Sk-mar
Eucampia cornuta	Euc-cor	*Syracosphaera pulchra*	Syr-pul
Gonyaulax spinifera	Gon-spi	*Thalassionema frauenfeldii*	Th-fra
Guinardia flaccida	Gui-flac	*Thalassionema nitzschioides*	Th-nit
Guinardia striata	Gui-str	*Thalassiosira rotula*	Thal-rot
Hemiaulus hauckii	Hem-hau	*Tripos furca*	Tri-fur
Hemiaulus sinensis	Hem-sin	*Tripos fusus*	Tri-fus
Heterosigma spp.	Heteros	*Tripos muelleri*	Tri-mue
Lauderia annulata	Lau-ann	*Tripos trichoceros*	Tri-tric
Leptocylindrus danicus	Lep-dan		

Table S4. Summary table comparing the taxa with the 3 highest values of closeness and degree for each season and station. The * indicates that the taxa showed significant IndVal values for that season and station.

		Closeness		Degree	
Station	***Season***	***Taxon***	***Value***	***Taxon***	***Value***
Coastal station (SG01)	**Winter**	*Leptocylindrus danicus*	0.0204	*Chaetoceros curvisetus**	22
		Chaetoceros lorenzianus	0.0201	*Chaetoceros danicus**	21
		*Chaetoceros danicus**	0.0201	*Chaetoceros lorenzianus*	20
	Spring	*Thalassionema nitzschioides*	0.0178	*Cerataulina pelagica*	18
		Cerataulina pelagica	0.0176	*Thalassionema nitzschioides* *Leptocylindrus danicus*	16
		Leptocylindrus danicus	0.0173	*Prorocentrum micans**	14
	Summer	*Chaetoceros lorenzianus*	0.0167	*Chaetoceros curvisetus*	14
		Chaetoceros curvisetus	0.0164	*Calciosolenia brasiliensis* *Chaetoceros affinis* *Chaeroceros lorenzianus* *Lioloma pacificum*	12
		*Proboscia alata**	0.0163	*Calciosolenia murreyi* *Proboscia alata**	11
	Autumn	*Cerataulina pelagica*	0.0204	*Cerataulina pelagica* *Dactyliosolen fragilissimus*	25
		Leptocylindrus danicus	0.0197	*Chaetoceros curvisetus* *Leptocylindrus danicus*	24
		Dactyliosolen fragilissimus	0.0190	*Chaetoceros danicus* *Eucampia cornuta* *Syracosphaera pulchra*	22
Offshore station (SG05)	**Winter**	*Chaetoceros lorenzianus*	0.0196	*Chaetoceros curvisetus*	19
		Leptocylindrus danicus	0.0196	*Chaetoceros lorenzianus* *Leptocylindrus danicus*	18
		Chaetoceros curvisetus	0.0191	*Hemiaulus sinensis* *Thalassionema nitzschioides*	16
	Spring	*Chaetoceros tortissimus*	0.0191	*Chaetoceros tortissimus*	11
		Asterionellopsis glacialis	0.0191	*Chaetoceros curvisetus* *Chaetoceros affinis*	10
		Pseudo-nitzschia galaxiae	0.0191	*Dactyliosolen phuketensis* *Guinardia flaccida*	9
	Summer	*Syracosphaera pulchra*	0.0150	*Syracosphaera pulchra*	14
		Tripos fusus	0.0144	*Chaetoceros curvisetus* *Tripos fusus*	11
		Oxytoxum cfr. *elongatum*	0.0141	*Chaetoceros lorenzianus* *Guinardia flaccida*	10
	Autumn	*Chaetoceros curvisetus*	0.0191	*Chaetoceros curvisetus*	22
		Chaetoceros rostratus	0.0187	*Chaetoceros rostratus*	21
		Chaetoceros brevis	0.0183	*Chaetoceros brevis* *Leptocylindrus danicus* *Syracosphaera pulchra*	20

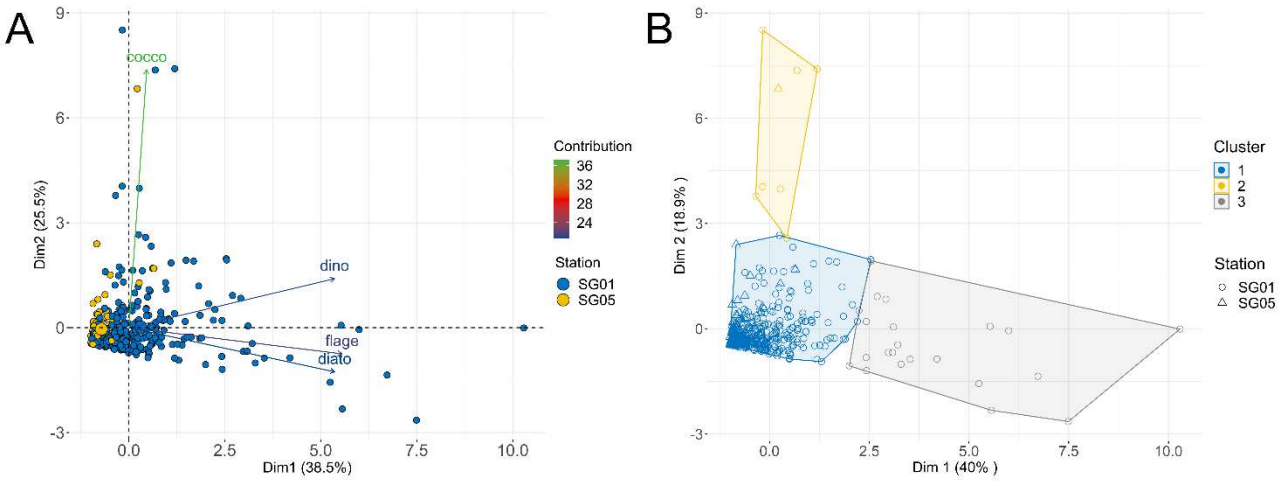

Fig. S1. Principal Component Analysis (PCA, A) and Hierarchical Clustering on Principal Components (HCPC, B) performed on diatom (diato), dinoflagellate (dino), coccolithophore (cocco) and phytoflagellate (flage) abundances in SG01 (blue colour in A and circle in B) and SG05 (yellow colour in A and triangle in B). In the PCA biplot the variables (vectors) are presented by their contributions to the principal components (gradient colours of vectors). In the HCPC plot the clusters are represented by a different colour.

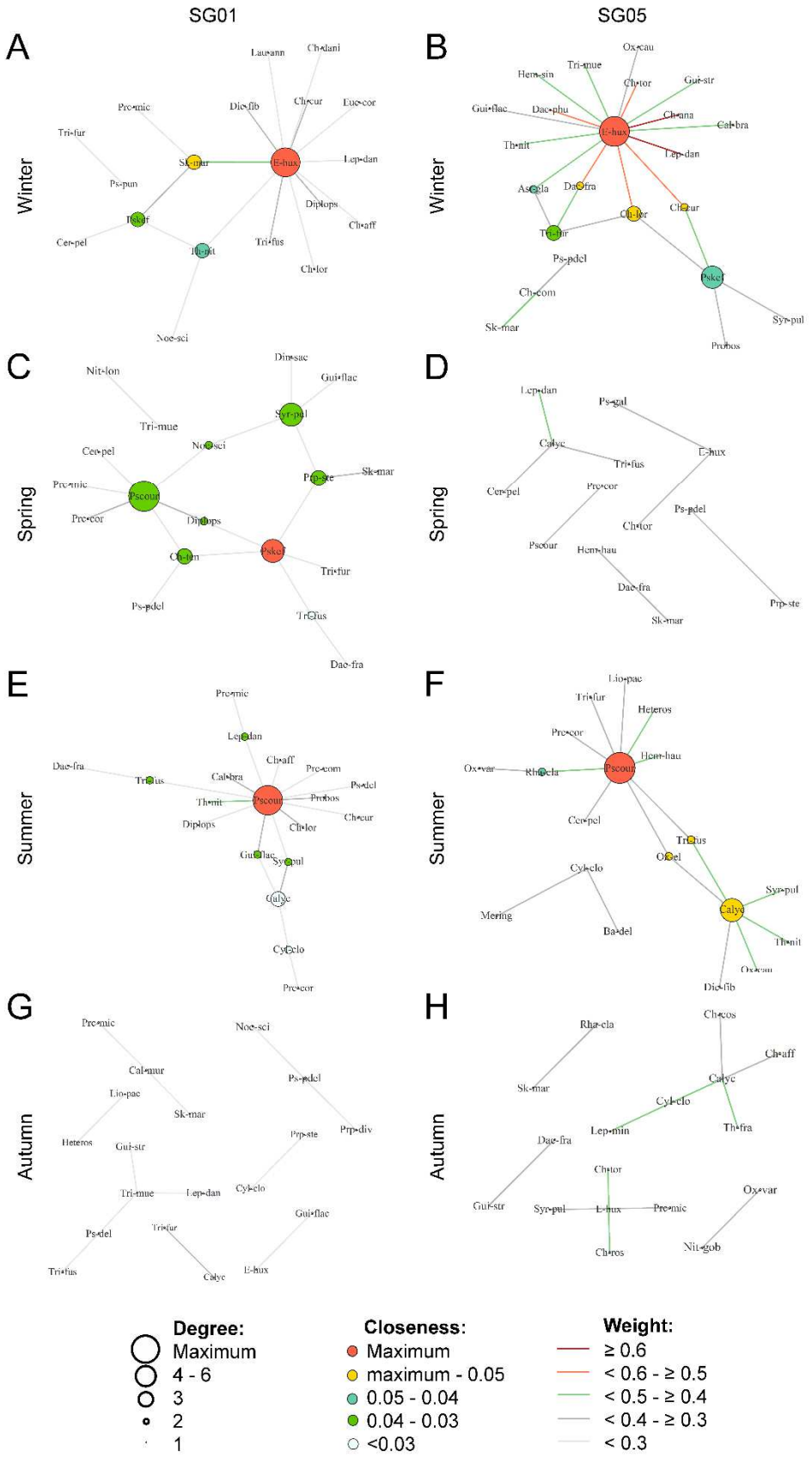

Fig. S2. Networks based on winter (A,B), spring (C,D), summer (E,F), autumn (G,H) negative correlations in SG01 (left) and SG05 (right). The dimension of the circle is proportional to the degree and the different colours are related to closeness. Line colours and thickness depend on the strength of the interaction. The names of the taxa are abbreviated as shown in Supplementary Table 3.

Chapter 2

Effects of ocean warming and marine heatwaves on the phytoplankton biomass in the Northern Adriatic Sea

Submitted to *Progress in Oceanography*

Effects of ocean warming and marine heatwaves on the phytoplankton biomass in the Northern Adriatic Sea

Francesca Neri[1]*, Angela Garzia[1,2], Marika Ubaldi[1,3,4], Stefano Accoroni[1,5], Alessandro Coluccelli[7], Francesco Memmola[1,5], Pierpaolo Falco[1,5+], Cecilia Totti[1,6+]

[1]Dipartimento di Scienze della Vita e dell'Ambiente, Università Politecnica delle Marche, via Brecce Bianche, 60131 Ancona, Italy

[2]Dipartimento di Ingegneria Civile, Edile e Ambientale, Via Eudossiana,18, 00184, Roma, Italy

[3]Dipartimento di Scienze della Terra e del Mare, Via Archirafi 22, 90123 Palermo, Italy

[4]National Biodiversity Future Center, Piazza Marina 61, 90133 Palermo, Italy

[5]Fano Marine Center, The Inter-Institute Center for Research on Marine Biodiversity, Resources and Biotechnologies (FMC), viale Adriatico 1/N, 61032 Fano, Italy

[6]Consorzio Interuniversitario per le Scienze del Mare, CoNISMa, ULR Ancona, Ancona, Italy

[7]Istituto di Scienze dell'Atmosfera e del Clima, ISAC-CNR, Via Gobetti 101, 40129 Bologna, Italy

[+] These authors equally contributed to the ms

*Corresponding Author: f.neri@pm.univpm.it

Keywords

Marine heatwaves, phytoplankton, northern Adriatic Sea, chlorophyll-a

2.1 Abstract

In the present study, we investigated the potential effects of increasing of Sea Surface Temperature (SST) and marine heatwaves (MHWs) on the phytoplankton biomass, in terms of chlorophyll-a (chl-a), in the Northern Adriatic Sea (NAS). We considered different sub-areas, taking into account the different trophic and oceanographic conditions. Increasing trends of SST and MHWs were found in every sub-area, coupled with a general decrease of chl-a. These trends varied on a seasonal basis, and differently in each subarea. Negative correlations between SST and chl-a trends were found in the entire NAS. In the eastern coast and in the area with depth lower than 40 m negative correlations between MHWs and chl-a were observed, while positive correlations were found in the offshore sub-area. These results indicate that MHWs and SST increases, together with stratification/mixing, are strongly affecting the phytoplankton communities of the NAS.

2.2 Introduction

Marine heatwaves (MHWs) are generally defined as anomalously warm water events, with temperature higher than typical values, and persisting for a long period of time. These events can be triggered by different atmospheric and/or oceanographic processes, from local and regional to large-climate scales and teleconnections (Behrens et al., 2019; Bian et al., 2023; Dalsin et al., 2023; Heidemann and Ribbe, 2019; Holbrook et al., 2019; Ibrahim et al., 2021; Sen Gupta et al., 2020; Vogt et al., 2022).

The increase of sea water temperature and the marine heatwaves are having several huge impacts on the marine communities, like coral reefs (Le Nohaïc et al., 2017; Wyatt et al., 2023), birds (Jones et al., 2018; Piatt et al., 2020), zooplankton (Evans et al., 2020), fish biodiversity (Free et al., 2023), top predators (Welch et al., 2023), seagrasses and habitat-forming species (e.g. Michaud et al., 2022; Serrano et al., 2021; Smale et al., 2019; Smale and Wernberg, 2013; Stipcich et al., 2022), with effects varying from individual to ecosystem level, ranging from physiological adjustments and processes to mortality (Smith et al., 2023).

Despite their importance in the marine ecosystems (Blanchard et al., 2012; Khatiwala et al., 2009; Naselli-Flores and Padisák, 2023; Tweddle et al., 2018; Vallina and Simó, 2007), the effects of heatwaves on phytoplanktonic communities are still less documented. Several studies have shown that the response of chlorophyll-a (chl-a) to MHWs occurrence changes depending on both latitude and trophic conditions, with an increase of chl-a at high latitudes and nutrient-rich waters, and a decrease at mid- low-latitudes and in more oligotrophic waters (Hayashida et al., 2020; Le Grix et al., 2021; Montie et al., 2020; Noh et al., 2022; Sen Gupta et al., 2020).

The Mediterranean Sea is highly sensitive to climate change, and marine heatwaves are projected to increase in the early future (Darmaraki et al., 2019; Diffenbaugh et al., 2007; Giorgi, 2006; Lionello and Scarascia, 2018; Pisano et al., 2020). Several studies have been observing an increase in MHWs frequency, duration and intensity in the entire Mediterranean Sea (Hamdeno and Alvera-Azcaráte, 2023; Ibrahim et al., 2021; Juza et al., 2022; Kuglitsch et al., 2010; Simon et al., 2022), and a negative relationship between Sea Surface Temperature Anomaly (associated with MHWs) and chl-a has been reported (Hamdeno and Alvera-Azcaráte, 2023), particularly with intense and long MHWs, and more in the Western than the Eastern Mediterranean. Moreover, Soulié et al. (2023) observed, through mesocosm studies in the Thau lagoon, that MHWs led to changes in phytoplankton physiological processes and in the phytoplankton community structure.

Most of the studies focusing on the effects of MHWs on phytoplankton are related to global or large scales. However, phytoplankton abundances, mean annual cycle and species composition show a strong variability on seasonal, interannual and spatial scales. An example is given by the Northern Adriatic Sea (NAS), where marked differences in terms of phytoplankton abundance, biomass and composition are found between coastal and offshore waters (Neri et al., 2023, 2022) and among different areas of the basin, like eastern and western coasts (Cabrini et al., 2012; Cerino et al., 2019; Marić et al., 2012; Totti et al., 2019; Vascotto et al., 2021), gulfs and lagoons (Bernardi Aubry et al., 2022, 2021). The NAS is a shallow-depth basin, with high riverine inputs (mainly from the Po River in the western area of the NAS) and a dominant surface cyclonic circulation with the Western Adriatic

Current (WAC), flowing southward along the western areas and bringing fresher and nutrient-rich waters from the northern areas, and the northward Eastern Adriatic Current, which brings saltier and more oligotrophic waters from the Ionian Sea along the eastern coast into the Adriatic Sea (Artegiani et al., 1997b; Poulain and Cushman-Roisin, 2001). The combined effects of riverine inputs, circulation dynamics, shallow depths, and wind patterns contribute to the hydrological and physico-chemical variability of the NAS, rendering it highly susceptible to climate change and ocean warming, as previously observed for the entire Adriatic Sea, with potential consequences on the phytoplankton communities (Grbec et al., 2019).

The aim of the study is to (i) highlight the trends of temperature and their relationship with those of chl-a (considered as a proxy of phytoplankton biomass) on a seasonal basis in the NAS, taking into account the peculiarities of the different areas of the basin and to (ii) analyse the effect of marine heatwaves on the chl-a.

2.3 Materials and methods

Study area and datasets

The study area is the entire NAS sub basin, considering as its southern boundary limit the latitude corresponding to 100 m isobath (Artegiani et al., 1997a). For MHWs and satellite chl-a analyses, we divided the NAS in sub-areas, based on depth and/or trophic conditions: (i) the Western Coast (WC) strongly affected by the Po river outflow and by the Western Adriatic Current, (ii) the Venice Lagoon (VL), (iii) the Gulf of Trieste (GoT), (iv) the Eastern Coast (EC) affected by the Eastern Adriatic Current (therefore, more oligotrophic than the WC area), (v) the remaining sub-area with depth <40 m (L40) and (vi) that > 40 m (H40) (Fig. 1).

Sea Surface Temperature values (SST, °C) from 1st January 1982 to 31st December 2022 were taken from the Copernicus Marine Service (CMEMS, https://marine.copernicus.eu/). The CMEMS Reprocessed (REP) Mediterranean (MED) dataset (DOI:10.48670/moi-00173; Merchant et al., 2019;

Pisano et al., 2016; Saha et al., 2018) consists of daily and optimally interpolated satellite-based estimates of SST at 0.05° resolution grid.

Daily chlorophyll-a concentration (chl-a, mg m^{-3}) from 1st January 1992 to 31st December 2022 were obtained from CMEMS. The dataset (DOI:10.48670/moi-00299) have a resolution of 1 x 1 km and was evaluated through region-specific algorithms (Berthon and Zibordi, 2004; Volpe et al., 2019). For both SST and chl-a, the Northern Adriatic data were extracted from the Mediterranean datasets.

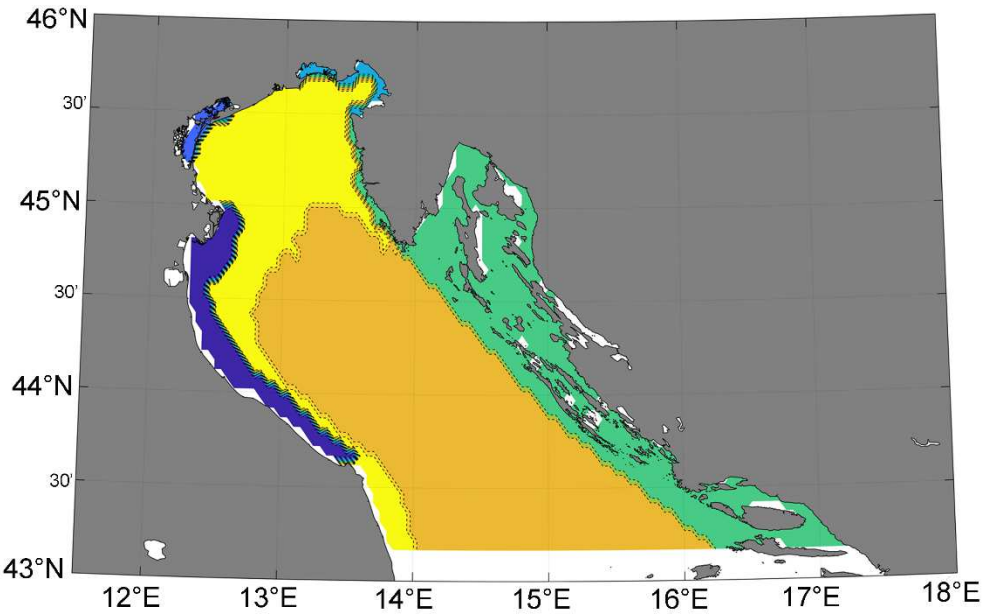

Fig. 1 Northern Adriatic Sea sub-areas considered in the present study: Western Coast (WC, dark blue), Venice Lagoon (VL, blue), Gulf of Trieste (GoT, light blue), Eastern Coast (EC, green), sub-area with depth <40 m (L40, yellow) and sub-area with depth >40 m (H40, orange).

Marine Heatwaves

MHWs were defined, following the definition of Hobday et al. (2016) as an event lasting at least five consecutive days where SST exceeds the variable 90th percentile threshold based on a 30-year climatological mean (1982-2012). Two consecutive MHW events within two days were considered as a unique event (Hobday et al., 2016). MHWs events were considered on a seasonal basis and seasons were defined as follow: winter from January to March, spring from April to June, summer from July to September, autumn from October to December. For each season, MHWs were described

by frequency (number of events in each year), duration (duration of the event in days), days (sum of MHW days in each year) and mean (°C), maximum (°C) and cumulative intensity (°C.days), i.e. the integrated sea surface temperature anomaly during the event, as defined by Hobday et al. (2016, 2018).

The MATLAB M_MHW toolbox v. 1.0 was used for MHW metric calculation (Zhao and Marin, 2019).

Statistical analyses

All the statistical analyses were performed using R software v. 4.1.1 (R Core Team, 2021).

A X-11 decomposition method was used (Dagum and Bianconcini, 2016) to decompose SST and chl-a time series (Xt) in its trend (Tt), seasonal (St) and irregular (It) components:

$$Xt = Tt + St + It$$

The interannual trend component was extracted:

$$Tt = Xt - St - It$$

The X-11 decomposition was performed using the seas function from the R seasonal package (Sax and Eddelbuettel, 2018).

Then, the Mann-Kendall test (Kendall, 1975; Mann, 1945) and the Sen's method (Sen, 1968) were applied on the trend component of the decomposed SST and chl-a time series, to check for an upward/downward trend (and to estimate the slope (°C/year for the SST and mg m^{-3}/year for the chl-a), respectively. MannKendall and sens.slope functions from the Kendall (McLeod, 2022) and trend (Pohlert, 2023) packages were used, respectively. Similarly, Mann-Kendall test (Kendall, 1975; Mann, 1945) and the Sen's method (Sen, 1968) were applied on the seasonal mean values of SST and chl-a to estimate the trends of the winter, spring, summer and autumn seasons. As regards the chl-a time series of the VL sub-area, the years 2012-2016 and 2022 were not considered for the time series decomposition to obtain a regular frequency (i.e. 12 months per year), as required from the test. Mann-

Kendall test was also used to check for potential upward/downward trend of MHW metrics (frequency, duration, intensities and days).

To check for correlations between X-11 decomposed trends of SST and chl-a, Spearman correlations were performed using the rcorr function from the Hmisc package (Harrell, 2022). Similarly, correlations were performed between chl-a and MHW frequency, duration, day, mean, max and cumulative intensities.

Kruskal-Wallis rank sum test was performed to test for significant differences between sub-areas in each season and among seasons in each sub-area, and pairwise wilcoxon rank sum tests were conducted when significant differences were observed. The kruskal.test and the pairwise.wilcox.test functions from the stats package was used.

2.4 Results

SST and chl-a trends

The decomposed SST in each sub-area is shown in Figure 2. Significantly increasing trends of SST were observed in the entire NAS ($p < 0.001$), with the highest increase in the H40 (0.048 ± 0.004 °C/y, Fig. 2B) and EC sub-areas (0.046 ± 0.004 °C/y, Fig. 2C). An increase of 0.044 ± 0.004, 0.042 ± 0.004, 0.041 ± 0.004 and 0.038 ± 0.004 °C/y were detected, in the L40 (Fig. 2E), GoT (Fig. 2D), VL (Fig. 2F) and WC (Fig. 2A) respectively.

Considering the trends in each season (Table 1), the increase of temperature was found in all the sub-areas in spring and summer, ($p < 0.001$). In winter, it was observed in the EC, H40 ($p < 0.001$, for both), GoT, VL, L40 ($p < 0.05$, for all three). In autumn, the increase was found in the EC ($p < 0.001$), H40 ($p < 0.001$) and L40 ($p < 0.05$) sub-areas.

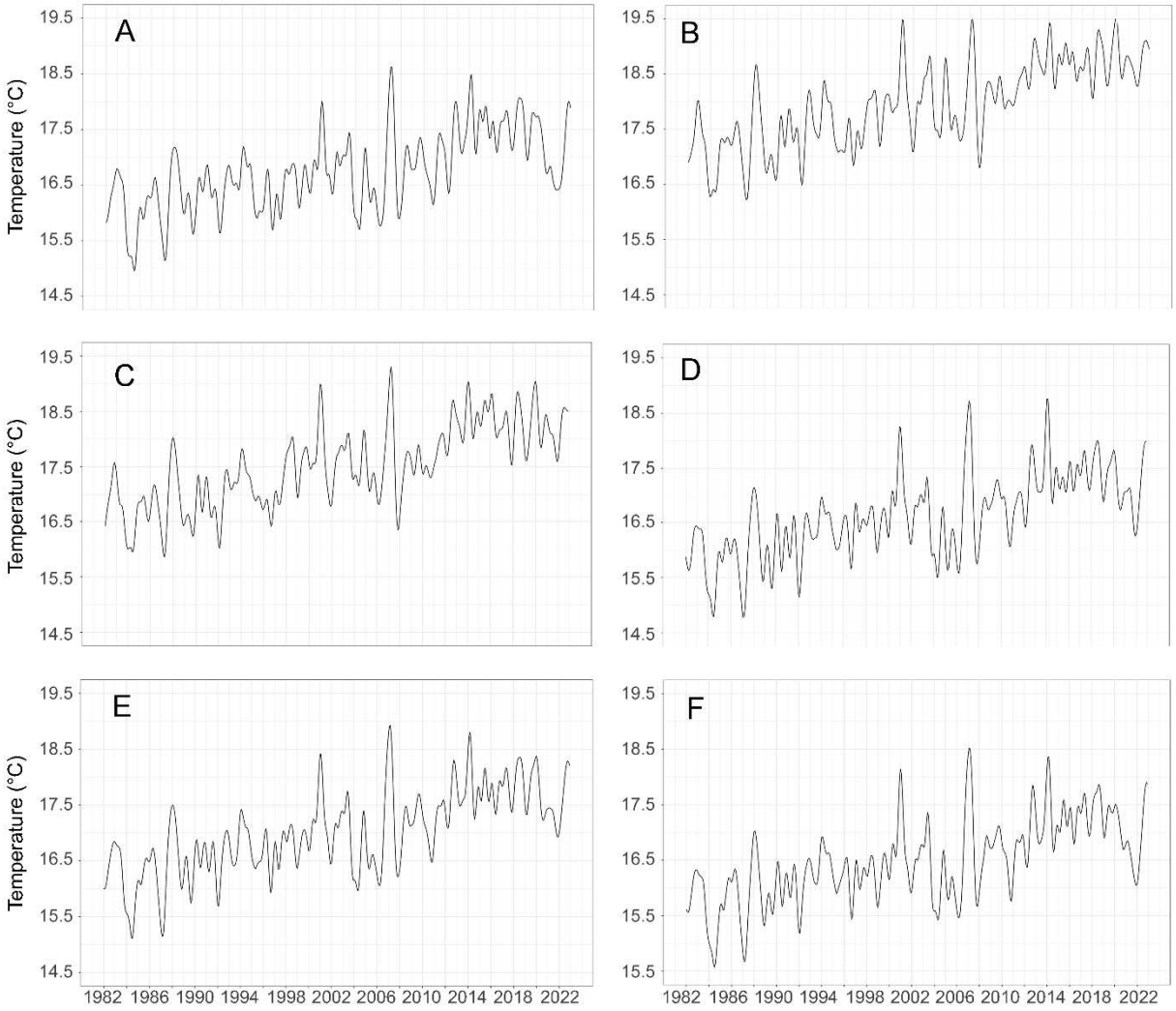

Fig. 2 X-11 decomposed trend of Sea Surface Temperature time series (°C, 1982-2022) in the Western Coast (WC, A), sub-area with depth >40 m (H40, B), Eastern Coast (EC, C), Gulf of Trieste (GoT, D), area with depth <40 m (L40, E) and Venice Lagoon (VL, F).

Table 1. Mann-Kendall τ and Sen's slope (°C/y) calculated for the Sea Surface Temperature in winter (Win), spring (Spr), summer (Sum) and autumn (Aut) in each sub-area: Western Coast (WC), Venice Lagoon (VL), Gulf of Trieste (GoT), Eastern Coast (EC), remaining sub-area with depth greater and lower than 40m (H40 and L40, respectively). ns, not significant; *$p < 0.05$; **$p < 0.01$; ***$p < 0.001$.

Sub-area	Season	τ	p-value	Slope °C/y
WC	Win	0.1	ns	0.04 ± 0.08
	Spr	0.54	***	0.29 ± 0.08
	Sum	0.57	***	0.21 ± 0.08
	Aut	0.12	ns	0.05 ± 0.08
VL	Win	0.21	*	0.07 ± 0.08
	Spr	0.64	***	0.33 ± 0.08
	Sum	0.58	***	0.21 ± 0.08
	Aut	0	ns	0.001 ± 0.08
GoT	Win	0.28	*	0.11 ± 0.08
	Spr	0.57	***	0.29 ± 0.08
	Sum	0.54	***	0.18 ± 0.08
	Aut	0.15	ns	0.05 ± 0.08
EC	Win	0.51	***	0.14 ± 0.04
	Spr	0.56	***	0.23 ± 0.08
	Sum	0.56	***	0.19 ± 0.04
	Aut	0.38	***	0.12 ± 0.08
H40	Win	0.47	***	0.15 ± 0.12
	Spr	0.55	***	0.24 ± 0.24
	Sum	0.55	***	0.2 ± 0.24
	Aut	0.38	***	0.13 ± 0.12
L40	Win	0.28	*	0.1 ± 0.08
	Spr	0.55	***	0.3 ± 0.08
	Sum	0.56	***	0.2 ± 0.08
	Aut	0.21	*	0.07 ± 0.08

Significantly decreasing trends of chl-a were observed in all the sub-areas ($p < 0.001$), except for the VL ($p > 0.05$, Fig. 3F). The highest decrease was observed in WC (-0.072 ± 0.012 mg m^{-3} y^{-1}, Fig. 3A). In GoT (Fig. 3D) and L40 (Fig. 3E), a decrease of -0.017 ± 0.005 mg m^{-3} y^{-1} was found. In the H40 (Fig. 3B) and EC (Fig. 3C) sub-areas a decrease of -0.003 ± 0.001 mg m^{-3} y^{-1} and -0.001 ± 0.0004 mg m^{-3}/y was observed, respectively.

Considering each season separately, decreasing trends were found (Table 2) in autumn in each sub-area ($p < 0.05$, $p < 0.01$, $p < 0.001$). In winter, significant decreases of chl-a were found in the WC and GoT sub-areas (-0.44 ± 0.4 and -0.08 ± 0.08 mg $m^{-3}y^{-1}$, respectively, $p < 0.05$). In spring, decrease

of chl-a were observed in WC (-0.38 ± 0.4 mg m^{-3} y^{-1}), and in summer in EC (-0.003 ± 0.004 mg m^{-3} y^{-1}, $p < 0.05$).

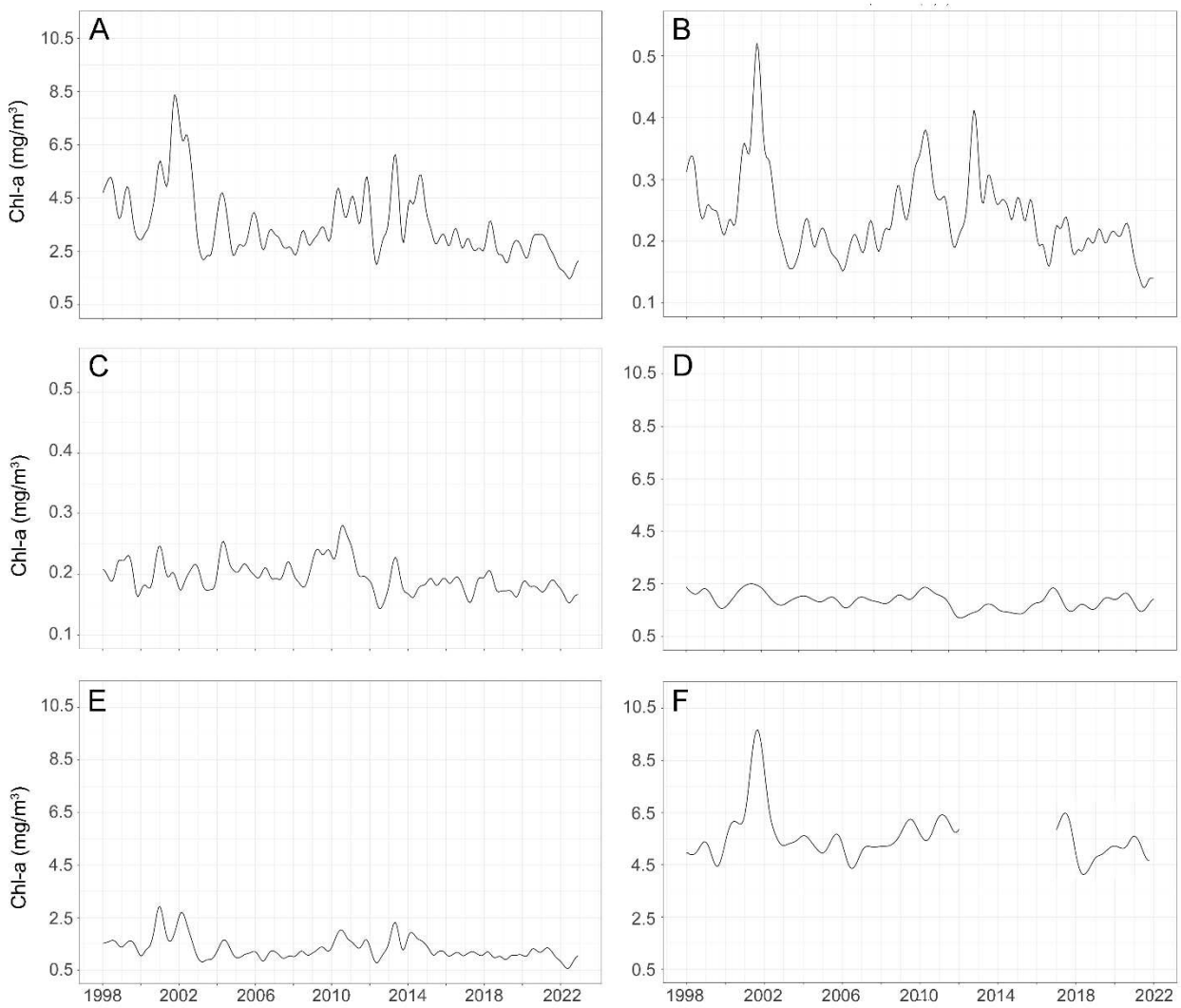

Fig. 3 X-11 decomposed trend of chlorophyll-a time series (mg m^{-3}, 1998-2022) in the Western Coast (WC, A), sub-area with depth >40 m (H40, B), Eastern Coast (EC, C), Gulf of Trieste (GoT, D), area with depth <40 m (L40, E) and Venice Lagoon (VL, F). Note the different y-scales.

Table 2. Mann-Kendall τ and Sen's slope (mg m^{-3} y^{-1}) calculated for the chl-a in winter (Win), spring (Spr), summer (Sum) and autumn (Aut) in each sub-area: Western Coast (WC), Venice Lagoon (VL), Gulf of Trieste (GoT), Eastern Coast (EC), remaining sub-area with depth greater and lower than 40m (H40 and L40, respectively). ns, not significant; *$p < 0.05$; **$p < 0.01$; ***$p < 0.001$.

Sub-area	Season	τ	p-value	Slope mg m^{-3} y^{-1}
WC	Win	-0.34	*	-0.44 ± 0.4
	Spr	-0.29	*	-0.38 ± 0.4
	Sum	-0.19	ns	-0.08 ± 0.14
	Aut	-0.35	*	-0.24 ± 0.22
VL	Win	-0.13	ns	-0.06 ± 0.09
	Spr	0.12	ns	0.09 ± 0.32
	Sum	-0.15	ns	-0.28 ± 0.28
	Aut	-0.37	*	-0.27 ± 0.18
GoT	Win	-0.36	*	-0.08 ± 0.08
	Spr	-0.01	ns	-0.01 ± 0.16
	Sum	-0.15	ns	-0.06 ± 0.12
	Aut	-0.45	**	-0.12 ± 0.04
EC	Win	-0.03	ns	-0.001 ± 0.01
	Spr	-0.2	ns	-0.004 ± 0.01
	Sum	-0.31	*	-0.003 ± 0.004
	Aut	-0.47	**	-0.02 ± 0.01
H40	Win	-0.13	ns	-0.01 ± 0.018
	Spr	-0.14	ns	-0.01 ± 0.04
	Sum	-0.27	ns	-0.006 ± 0.008
	Aut	-0.46	**	-0.03 ± 0.04
L40	Win	-0.27	ns	-0.09 ± 0.14
	Spr	-0.16	ns	-0.06 ± 0.14
	Sum	-0.21	ns	-0.04 ± 0.06
	Aut	-0.49	***	-0.1 ± 0.12

Negative correlations were found between the X-11 decomposed trend of SST and chl-a (Table S1).

Marine heatwaves

Maps of seasonal MHW metrics in the NAS are shown in Fig. S1–S6. The highest values of MHW frequency (Fig. S1), mean (Fig. S3), max (Fig. S4), cumulative (Fig. S5) intensities and days (Fig. S6) were found in spring and summer. In some sub-areas (GoT, EC, L40, H40) the highest values of duration and days (Fig. S2, S6, respectively) were found in winter.

The trends of MHWs metrics are shown in Table 3. In the WC sub-area, several metrics of MHWs were observed as increasing: frequency and days in spring, summer and autumn ($p < 0.001$, 0.001 and 0.05, respectively); duration in winter and spring ($p < 0.05$ and 0.001, respectively); mean and max intensities in summer ($p < 0.05$).

In the VL and GoT sub-areas, increasing trends of MHWs frequency, duration and days were found in winter, spring and summer ($p < 0.01$, 0.001 and 0.001, respectively), and an increase of max intensity was observed in summer ($p < 0.05$). Furthermore, in the VL increasing trends of max intensity were also found in spring ($p < 0.05$), while in the GoT, an increase of MHWs days was also observed in autumn ($p < 0.05$).

In the EC and H40 sub-areas, increasing trends of MHWs frequency, duration and days were found in winter, spring, summer and autumn ($p < 0.001$, 0.001, 0.01, 0.01, respectively for both sub-areas). Mean, max and cumulative intensities showed an increase in summer ($p < 0.05$). Furthermore, cumulative intensities showed increasing trends ($p < 0.05$) in autumn in both stations and in winter in EC.

In the L40 sub-area, an increasing trend of frequency, duration and days was found in winter, summer and autumn ($p < 0.01$, 0.001 and 0.05, respectively). Duration and days also showed an increase in spring ($p < 0.001$). Mean and max intensities showed an increase in summer ($p < 0.01$) and cumulative intensity in spring ($p < 0.05$).

Table 3. Results of the Mann-Kendall test (Kendall's tau statistic) of the Mann-Kendall marine heatwaves frequency (number of events in each year), duration (duration of the event in days), days (sum of MHW days in each year) and mean (MeanInt, °C), maximum (MaxInt, °C) and cumulative intensity (CumInt, °C.days) (mean, maximum and integrated sea surface anomaly during/over the event) in each sub-areas: Western Coast (WC), Venice Lagoon (VL), Gulf of Trieste (GoT), Eastern Coast (EC), remaining sub-area with depth greater and lower than 40 m (H40 and L40, respectively). Values in bold, bold and italic, bold italic and underlined represent $p < 0.05$, 0.01 and 0.001, respectively.

Sub-area	Season	frequency	duration	MeanInt	MaxInt	CumInt	days
WC	win	0.2	**0.28**	0.08	0.09	0.09	0.22
	spr	***0.51***	***0.44***	-0.06	0.05	0.05	***0.5***
	sum	***0.5***	***0.39***	**0.32**	**0.35**	0.25	***0.46***
	aut	**0.26**	0.15	0.18	0.21	0.22	**0.25**
VL	win	***0.32***	***0.33***	0.25	0.26	0.07	***0.34***
	spr	***0.57***	***0.49***	0.16	**0.3**	0.28	***0.58***
	sum	***0.58***	***0.47***	0.29	**0.3**	0.17	***0.53***
	aut	0.15	0.15	0	-0.02	0.12	0.17
GoT	win	***0.38***	***0.38***	0.09	0.08	-0.01	***0.39***
	spr	***0.53***	***0.52***	0.07	0.15	0.25	***0.54***
	sum	***0.56***	***0.45***	0.27	**0.34**	0.19	***0.52***
	aut	0.23	0.17	-0.16	-0.07	-0.08	**0.23**
EC	win	***0.42***	***0.45***	0.19	0.19	**0.33**	***0.44***
	spr	***0.52***	***0.51***	0.04	0.14	0.21	***0.53***
	sum	***0.58***	***0.47***	***0.43***	***0.46***	***0.37***	***0.53***
	aut	***0.35***	***0.31***	-0.02	0.07	***0.34***	***0.34***
H40	win	***0.45***	***0.4***	-0.09	0.04	0.24	***0.45***
	spr	***0.48***	***0.49***	-0.04	0.07	0.14	***0.49***
	sum	***0.48***	***0.36***	**0.34**	***0.4***	**0.27**	***0.45***
	aut	***0.29***	***0.31***	-0.11	0.02	**0.25**	***0.33***
L40	win	***0.31***	***0.32***	0.13	0.11	0.17	***0.32***
	spr	0.52	***0.52***	0.14	0.21	**0.28**	***0.54***
	sum	***0.5***	***0.41***	***0.36***	***0.37***	0.24	***0.48***
	aut	**0.26**	**0.23**	0.09	0.11	0.15	**0.25**

Correlations between marine heatwaves and chl-a

The significant correlations between MHWs parameters and chl-a are shown in Table 6. In the EC, negative correlations were observed in summer with MHWs frequency ($p < 0.01$) and days ($p < 0.05$), and in autumn with each MHWs metrics ($p < 0.001$ and $p < 0.05$).

In the L40 sub-area, negative correlations ($p < 0.05$) were found in summer between MHWs frequency, mean and max intensities and days, and chl-a.

In the H40 sub-area, positive correlations ($p < 0.05$) were found in winter between MHWs mean, max, cumulative intensities, and chl-a.

In the other sub-areas, no correlation was found between MHWs parameters and chl-a.

Table 6. Significant correlations between marine heatwaves parameters (frequency, duration, days, mean (MeanInt), maximum (MaxInt), cumulative intensity (CumInt)) and chlorophyll-a in each subarea (EC, L40, H40 represent Eastern Coast, area with depth lower and greater 40m, respectively). Correlations resulting not significant ($p > 0.05$) are not shown. ns, not significant; *$p < 0.05$; **$p < 0.01$; ***$p < 0.001$.

Area	Season	Parameters		Rho	p-value
EC	summer	Frequency	chl	-0.56	**
EC	summer	Days	chl	-0.45	*
EC	autumn	Frequency	chl	-0.73	***
EC	autumn	Duration	chl	-0.68	***
EC	autumn	MeanInt	chl	-0.49	*
EC	autumn	MaxInt	chl	-0.61	**
EC	autumn	CumInt	chl	-0.68	***
EC	autumn	Days	chl	-0.74	***
L40	summer	Frequency	chl	-0.47	*
L40	summer	MeanInt	chl	-0.42	*
L40	summer	MaxInt	chl	-0.40	*
L40	summer	Days	chl	-0.45	*
H40	winter	MeanInt	chl	0.46	*
H40	winter	MaxInt	chl	0.47	*
H40	winter	CumInt	chl	0.41	*

2.5 Discussion

In this study we highlighted that marine heatwaves and ocean warming are exerting a huge impact on phytoplankton biomass in the Northern Adriatic Sea, with differences depending on the background conditions.

The observed increase of Sea Surface Temperature (SST) in each sub-area of the NAS is in agreement with that already documented in the Adriatic and in the rest of the Mediterranean Sea (Hamdeno and

Alvera-Azcaráte, 2023; Ibrahim et al., 2021; Mohamed et al., 2019; Pastor et al., 2020, 2018; Pisano et al., 2020). However, such increases were not homogeneous in the study area, but exhibited a spatial variability, with values ranging from 0.048 ± 0.004 and 0.046 ± 0.004 °C/y in the Eastern and deeper sub-areas of the NAS, respectively, to 0.038 ± 0.004 °C/y in the Western Coast sub-area. A seasonal variability was also observed, as in each sub-area, the spring season (April-June) showed the highest increase, followed by summer (July-September), while the lowest increase was found in autumn or winter. This variability was also reported by other studies in the Mediterranean Sea, which related the seasonal and spatial variabilities of SST increase to circulation, mean air-sea heat fluxes, ocean processes (e.g., advection and vertical mixing of heat) and changes in atmospheric phenomena like in the North Atlantic Oscillation (López García and Camarasa Belmonte, 2011; Pisano et al., 2020; Skliris et al., 2012). In our study area, the different contribution of riverine inputs and the different depth of water column could also play an important role in influencing the seasonal SST trends in the different sub-areas.

Recent studies have highlighted that the increasing trend of temperature itself could influence the observed trend of occurrence and metrics (i.e. frequency, intensities and duration) of marine heatwaves (Amaya et al., 2023; Martínez et al., 2023; Xu et al., 2022). This could explain the high values and increasing trend of MHW metrics that we observed in spring and summer (where increasing trends of temperature were observed). However, in this study increasing trends of MHW metrics were also observed in seasons in which the increasing trend of temperature was not observed, suggesting that other phenomena (e.g. atmospheric pressure, winds) could affect the MHW assessment. Furthermore, recently, Martinez et al. (2023) claimed that, when the effects of marine heatwaves on the ecosystems are addressed, the combined marine heatwave and temperature trend (i.e. total heat exposure/stress) should be considered. Indeed, independently on the definition and calculation of the marine heatwave trends, previous studies highlighted, at a global scale, negative relationships between MHWs and chl-a, particularly at low and mid-latitudes (Noh et al., 2022; Sen

Gupta et al., 2020), and that these relationships are influenced by the background nutrient conditions (Hayashida et al., 2020).

In our study, negative correlations between MHWs and chlorophyll-a were observed in summer and autumn in the eastern coast and in the L40 sub-areas, as the long period of stratification (which is typical during MHW events) coupled with the high temperatures in shallow areas, can prevent the mixing of the water column and the consequent replenishment of nutrients in the photic zone.

On the contrary, the temporary stabilization of a nutrient-rich mixed water column in the deeper open waters in winter, explains the increase in chlorophyll-a coupled with that of MHWs (Fischer et al., 2014).

As regards the general trend of chl-a concentration, significantly decreasing trends were observed in the entire Northern Adriatic Sea in the period 1998 to 2022, in agreement with the future projections recently reported by Mentaschi et al. (2024). These results suggest that the trend towards oligotrophication, typical of the years 2000-2007 (Colella et al., 2016; Giani et al., 2012; Marić et al., 2012; Mozetič et al., 2010) and reversed in the 2010s (Cozzi et al., 2020; Kotta and Kitsiou, 2019; Salgado-Hernanz et al., 2019), has been re-established. The decrease in phytoplankton biomass observed in our study (with the only exception in Venice Lagoon) varied between sub-areas and among seasons. In autumn it was observed in each sub-area, in agreement with Grilli et al. (2020) although they considered a different period (1971–2015), while in winter it was recorded in the Gulf of Trieste and in the Western Coast and in summer only in the Eastern Coast. These decreases of chl-a could be related to the increasing of sea water temperatures and marine heatwave metrics, that are coupled with changes in the oceanographic conditions (e.g. longer period of stratification preventing the mixing of the water column), with effects on physicochemical characteristic of seawater, as found for other climatic process (Leterme et al., 2005; Ninčević Gladan et al., 2010). The chl-a decrease observed in winter has been already reported in other studies and related to the increase of temperature and consequent phenomena, like changes in nutrient concentrations, and high North Atlantic Oscillation index (Borkman and Smayda, 2009; Cabrini et al., 2012; Cerino et al., 2019). These trends

reflect the decreasing of the winter bloom, sustained in the NAS by small colonial diatoms (mainly *Skeletonema marinoi*) and representing one of the most regular phenomena in the phytoplankton annual cycle of the NAS leading to the most significant biomass increase during the year (Bernardi Aubry et al., 2004; Totti et al., 2005).

In addition, in our study we observed negative correlations between the trends of SST and chl-a, as previously reported by Hamdeno and Alvera-Azcaráte (2023), suggesting the SST warming as one of the factors that negatively affect phytoplankton communities. Indeed, previous studies have highlighted that higher temperatures could imbalance the ratio between photosynthesis and respiration, favouring respiration and a potential biomass decrease (Boscolo-Galazzo et al., 2018; O'Connor et al., 2009). Considering each season separately, as expected, decreasing trends of chl-a were not always found, even if increasing trends of temperature were observed. This is explained considering that temperature is not the only parameter that affect phytoplankton growth, and other phenomena, like the reduction in the Po River inputs, are surely negatively affecting the phytoplankton biomass (Cibic et al., 2018). However, the effect of SST warming on phytoplankton is enhanced when it is coupled with other phenomena, like stratification and shallow depth, and changes in the wind intensities and air-sea heat fluxes, the combination of which is also involved in the establishment of marine heatwaves (Holbrook et al., 2019; Sen Gupta et al., 2020; Vogt et al., 2022).

2.6 Conclusions

Sea Surface Temperature (SST) and marine heatwaves (MHWs) are increasing worldwide due to climate change. Their effect on the phytoplankton communities have often been studied at global scales. In the present study, the trends of SST, MHWs, chl-a and their relationships were analysed in different areas of the Northern Adriatic Sea, characterized by differences in trophic and/or oceanographic conditions.

Increasing trends of SST were observed in the entire Northern Adriatic Sea, although with a marked spatial and seasonal variability, with the highest increase in spring and summer. MHW metrics were found as increasing in each sub-area, with differences in the different seasons.

Contrarily, decreasing trends of chl-a were found in the entire Northern Adriatic Sea, suggesting a tendency towards oligotrophication.

The decrease of the annual winter bloom, which have represented the most regular event in the phytoplankton cycle was confirmed.

Negative correlations between trends of chl-a and SST suggested that the ocean warming is negatively affecting phytoplankton biomass. The negative and positive correlations between chl-a and MHW metrics in the different seasons and sub-areas of the NAS suggest that marine heatwaves are affecting phytoplankton biomass in different ways depending on the background conditions and the involved processes (e.g. preventing the water column mixing in areas characterized by upwelling or stabilizing the water column in open waters).

Overall, the present study highlighted that the increase of SST and MHWs, that are coupled with changes in the oceanographic and physicochemical characteristics of seawater, are affecting the phytoplankton biomass of the NAS, with potential consequences on the trophic webs and economic activities like fisheries.

2.7 References

Amaya, D., Jacox, M.G., Fewings, M.R., Saba, V.S., Stuecker, M.F., Rykaczewski, R.R., Ross, A.C., Stock, C.A., Capotondi, A., Petrik, C.M., Bograd, S.J., Alexander, M.A., Cheng, W., Hermann, A.J., Kearney, K.A., Powell, B.S., 2023. Marine heatwaves need clear definitions so coastal communities can adapt. Nature 616, 29–32. https://doi.org/10.1038/d41586-023-00924-2

Artegiani, A., Bregant, D., Paschini, E., Pinardi, N., Raicich, F., Russo, A., 1997a. The Adriatic Sea general circulation. Part I: air-sea interactions and water mass structure. J. Phys. Oceanogr. 27, 1492–1514. https://doi.org/10.1175/1520-0485(1997)027<1492:TASGCP>2.0.CO;2

Artegiani, A., Bregant, D., Paschini, E., Pinardi, N., Raicich, F., Russo, A., 1997b. The Adriatic Sea general circulation. Part II: baroclinic circulation structure. J. Phys. Oceanogr. 27, 1515–1532. https://doi.org/10.1175/1520-0485(1997)027<1515:TASGCP>2.0.CO;2

Behrens, E., Fernandez, D., Sutton, P., 2019. Meridional oceanic heat transport influences marine heatwaves in the Tasman Sea on interannual to decadal timescales. Front. Mar. Sci. 6, 228. https://doi.org/10.3389/fmars.2019.00228

Bernardi Aubry, F., Berton, A., Bastianini, M., Socal, G., Acri, F., 2004. Phytoplankton succession in a coastal area of the NW Adriatic, over a 10-year sampling period (1990-1999). Cont. Shelf Res. 24, 97–115. https://doi.org/10.1016/j.csr.2003.09.007

Bernardi Aubry, F., Acri, F., Finotto, S., Pugnetti, A., 2021. Phytoplankton dynamics and water quality in the Venice Lagoon. Water 13, 2780; https://doi.org/10.3390/w13192780

Bernardi Aubry, F., Acri, F., Bastianini, M., Finotto, S., Pugnetti, A., 2022. Differences and similarities in the phytoplankton communities of two coupled transitional and marine ecosystems (the Lagoon of Venice and the Gulf of Venice - Northern Adriatic Sea). Front. Mar. Sci. 9, 974967. https://doi.org/10.3389/fmars.2022.974967

Berthon, J.F., Zibordi, G., 2004. Bio-optical relationships for the northern Adriatic Sea. Int. J. Remote Sens. 25, 1527–1532. https://doi.org/10.1080/01431160310001592544

Bian, C., Jing, Z., Wang, H., Wu, L., Chen, Z., Gan, B., Yang, H., 2023. Oceanic mesoscale eddies as crucial drivers of global marine heatwaves. Nat. Commun. 14, 2970. https://doi.org/10.1038/s41467-023-38811-z

Blanchard, J.L., Jennings, S., Holmes, R., Harle, J., Merino, G., Allen, J.I., Holt, J., Dulvy, N.K., Barange, M., 2012. Potential consequences of climate change for primary production and fish production in large marine ecosystems. Philos. Trans. R. Soc. B Biol. Sci. 367, 2979–2989. https://doi.org/10.1098/rstb.2012.0231

Borkman, D.G., Smayda, T., 2009. Multidecadal (1959–1997) changes in Skeletonema abundance and seasonal bloom patterns in Narragansett Bay, Rhode Island, USA. J. Sea Res. 61, 84–94. https://doi.org/https://doi.org/10.1016/j.seares.2008.10.004

Boscolo-Galazzo, F., Crichton, K.A., Barker, S., Pearson, P.N., 2018. Temperature dependency of metabolic rates in the upper ocean: a positive feedback to global climate change? Glob. Planet. Change 170, 201–212. https://doi.org/https://doi.org/10.1016/j.gloplacha.2018.08.017

Cabrini, M., Fornasaro, D., Cossarini, G., Lipizer, M., Virgilio, D., 2012. Phytoplankton temporal changes in a coastal northern Adriatic site during the last 25 years. Estuar. Coast. Shelf Sci. 115, 113–124. https://doi.org/10.1016/j.ecss.2012.07.007

Cerino, F., Fornasaro, D., Kralj, M., Giani, M., Cabrini, M., 2019. Phytoplankton temporal dynamics in the coastal waters of the north-eastern Adriatic Sea (Mediterranean Sea) from 2010 to 2017. Nat. Conserv. 34, 343–372. https://doi.org/10.3897/natureconservation.34.30720

Cibic, T., Cerino, F., Karuza, A., Fornasaro, D., Comici, C., Cabrini, M., 2018. Structural and functional response of phytoplankton to reduced river inputs and anomalous physical-chemical conditions in the Gulf of Trieste (northern Adriatic Sea). Sci. Total Environ. 636, 838–853. https://doi.org/10.1016/j.scitotenv.2018.04.205

Colella, S., Falcini, F., Rinaldi, E., Sammartino, M., Santoleri, R., 2016. Mediterranean ocean colour chlorophyll trends. PLoS One 11(6), e0155756.. https://doi.org/10.1371/journal.pone.0155756

Cozzi, S., Cabrini, M., Kralj, M., De Vittor, C., Celio, M., Giani, M., 2020. Climatic and anthropogenic impacts on environmental conditions and phytoplankton community in the Gulf of Trieste (Northern Adriatic Sea). Water 12, 2652. https://doi.org/10.3390/w12092652

Dagum, E.B., Bianconcini, S., 2016. Time Series Components. In: Dagum, E.B. and Bianconcini, S. (Eds), *Seasonal Adjustment Methods and Real Time Trend-Cycle Estimation*. Springer, Cham., pp. 29–57. https://doi.org/10.1007/978-3-319-31822-6_2

Dalsin, M., Walter, R.K., Mazzini, P.L.F., 2023. Effects of basin-scale climate modes and upwelling on nearshore marine heatwaves and cold spells in the California Current. Sci. Rep. 13, 12389. https://doi.org/10.1038/s41598-023-39193-4

Darmaraki, S., Somot, S., Sevault, F., Nabat, P., 2019. Past variability of Mediterranean Sea marine heatwaves. Geophys. Res. Lett. 46, 9813–9823. https://doi.org/10.1029/2019GL082933

Diffenbaugh, N.S., Pal, J.S., Giorgi, F., Gao, X., 2007. Heat stress intensification in the Mediterranean climate change hotspot. Geophys. Res. Lett. 34, L11706. https://doi.org/10.1029/2007GL03000

Evans, R., Lea, M.A., Hindell, M.A., Swadling, K.M., 2020. Significant shifts in coastal zooplankton populations through the 2015/16 Tasman Sea marine heatwave. Estuar. Coast. Shelf Sci. 235, 106538. https://doi.org/10.1016/j.ecss.2019.106538

Fischer, A.D., Moberg, E.A., Alexander, H., Brownlee, E.F., Hunter-Cevera, K.R., Pitz, K.J., Rosengard, S.Z., Sosik, H.M., 2014. Sixty years of Sverdrup: a retrospective of progress in the study of phytoplankton blooms. Oceanography 27, 222–235. https://doi.org/10.5670/oceanog.2014.26

Free, C.M., Anderson, S.C., Hellmers, E.A., Muhling, B.A., Navarro, M.O., Richerson, K., Rogers, L.A., Satterthwaite, W.H., Thompson, A.R., Burt, J.M., Gaines, S.D., Marshall, K.N., White, J.W., Bellquist, L.F., 2023. Impact of the 2014–2016 marine heatwave on US and Canada West Coast fisheries: surprises and lessons from key case studies. Fish Fish. 24, 652–674. https://doi.org/https://doi.org/10.1111/faf.12753

Giani, M., Djakovac, T., Degobbis, D., Cozzi, S., Solidoro, C., Fonda Umani, S., 2012. Recent changes in the marine ecosystems of the northern Adriatic Sea. Estuar. Coast. Shelf Sci. 115, 1–13. https://doi.org/10.1016/j.ecss.2012.08.023

Giorgi, F., 2006. Climate change hot-spots. Geophys. Res. Lett. 33. https://doi.org/https://doi.org/10.1029/2006GL025734

Grbec, B., Matić, F., Paklar, G.B., Morović, M., Popović, R., Vilibić, I., 2019. Long-term trends, variability and extremes of in situ sea surface temperature measured along the eastern Adriatic coast and its relationship to hemispheric processes. In: Vilibić, I., Horvath, K., Palau, J.L. (Eds), *Meteorology and Climatology of the Mediterranean and Black Seas.* Springer International Publishing, Cham, pp. 311–326. https://doi.org/10.1007/978-3-030-11958-4_19

Grilli, F., Accoroni, S., Acri, F., Bernardi Aubry, F., Bergami, C., Cabrini, M., Campanelli, A., Giani, M., Guicciardi, S., Marini, M., Neri, F., Penna, A., Penna, P., Pugnetti, A., Ravaioli, M., Riminucci, F., Ricci, F., Totti, C., Viaroli, P., Cozzi, S., 2020. Seasonal and interannual trends of oceanographic parameters over 40 years in the Northern Adriatic Sea in relation to nutrient loadings using the EMODnet chemistry data portal. Water 12, 2280. https://doi.org/10.3390/w12082280

Hamdeno, M., Alvera-Azcaráte, A., 2023. Marine heatwaves characteristics in the Mediterranean Sea: case study the 2019 heatwave events. Front. Mar. Sci. 10, 1093760. https://doi.org/10.3389/fmars.2023.1093760

Harrell, F.E.J., 2022. Hmisc: Harrell Miscellaneous. R package version 4.7-0.

Hayashida, H., Matear, R.J., Strutton, P.G., 2020. Background nutrient concentration determines phytoplankton bloom response to marine heatwaves. Glob. Chang. Biol. 26, 4800–4811. https://doi.org/10.1111/gcb.15255

Heidemann, H., Ribbe, J., 2019. Marine heat waves and the influence of El Niño off southeast Queensland, Australia. Front. Mar. Sci. 6, 56. https://doi.org/10.3389/fmars.2019.00056

Hobday, A.J., Alexander, L. V., Perkins, S.E., Smale, D.A., Straub, S.C., Oliver, E.C.J., Benthuysen, J.A., Burrows, M.T., Donat, M.G., Feng, M., Holbrook, N.J., Moore, P.J., Scannell, H.A., Sen Gupta, A., Wernberg, T., 2016. A hierarchical approach to defining marine heatwaves. Prog. Oceanogr. 141, 227–238. https://doi.org/10.1016/j.pocean.2015.12.014

Hobday, A.J., Oliver, E.C.J., Gupta, A. Sen, Benthuysen, J.A., Burrows, M.T., Donat, M.G., Holbrook, N.J., Moore, P.J., Thomsen, M.S., Wernberg, T., Smale, D.A., 2018. Categorizing and naming marine heatwaves. Oceanography 31, 162–173. https://doi.org/https://doi.org/10.5670/oceanog.2018.205

Holbrook, N.J., Scannell, H.A., Sen Gupta, A., Benthuysen, J.A., Feng, M., Oliver, E.C.J., Alexander, L. V., Burrows, M.T., Donat, M.G., Hobday, A.J., Moore, P.J., Perkins-Kirkpatrick, S.E., Smale, D.A., Straub, S.C., Wernberg, T., 2019. A global assessment of marine heatwaves and their drivers. Nat. Commun. 10, 2624. https://doi.org/10.1038/s41467-019-10206-z

Ibrahim, O., Mohamed, B., Nagy, H., 2021. Spatial variability and trends of marine heat waves in the Eastern Mediterranean Sea over 39 years. J. Mar. Sci. Eng. 9(6), 643. https://doi.org/10.3390/jmse9060643

Jones, T., Parrish, J.K., Peterson, W.T., Bjorkstedt, E.P., Bond, N.A., Ballance, L.T., Bowes, V., Hipfner, J.M., Burgess, H.K., Dolliver, J.E., Lindquist, K., Lindsey, J., Nevins, H.M., Robertson, R.R., Roletto, J., Wilson, L., Joyce, T., Harvey, J., 2018. Massive mortality of a planktivorous seabird in response to a marine heatwave. Geophys. Res. Lett. 45, 3193–3202. https://doi.org/10.1002/2017GL076164

Juza, M., Fernández-Mora, A., Tintoré, J., 2022. Sub-regional marine heat waves in the Mediterranean Sea from observations: long-term surface changes, sub-surface and coastal responses. Front. Mar. Sci. 9, 785771. https://doi.org/10.3389/fmars.2022.785771

Kendall, M., 1975. Multivariate Analysis. Charles Griffin & Company Ltd., London, UK.

Khatiwala, S., Primeau, F., Hall, T., 2009. Reconstruction of the history of anthropogenic CO2 concentrations in the ocean. Nature 462, 346–349. https://doi.org/10.1038/nature08526

Kotta, D., Kitsiou, D., 2019. Chlorophyll in the eastern Mediterranean Sea: correlations with environmental factors and trends. Environments 6, 98. https://doi.org/10.3390/environments6080098

Kuglitsch, F.G., Toreti, A., Xoplaki, E., Della-Marta, P.M., Zerefos, C.S., Trke, M., Luterbacher, J., 2010. Heat wave changes in the eastern Mediterranean since 1960. Geophys. Res. Lett. 37, L04802. https://doi.org/10.1029/2009GL041841

Le Grix, N., Zscheischler, J., Laufkötter, C., Rousseaux, C.S., Frölicher, T.L., 2021. Compound high-temperature and low-chlorophyll extremes in the ocean over the satellite period. Biogeosciences 18, 2119–2137. https://doi.org/10.5194/bg-18-2119-2021

Le Nohaïc, M., Ross, C.L., Cornwall, C.E., Comeau, S., Lowe, R., McCulloch, M.T., Schoepf, V., 2017. Marine heatwave causes unprecedented regional mass bleaching of thermally resistant corals in northwestern Australia. Sci. Rep. 7, 14999. https://doi.org/10.1038/s41598-017-14794-y

Leterme, S.C., Edwards, M., Seuront, L., Attrill, M.J., Reid, P.C., John, A.W.G., 2005. Decadal basin-scale changes in diatoms, dinoflagellates, and phytoplankton color across the North Atlantic. Limnol. Oceanogr. 50, 1244–1253. https://doi.org/10.4319/lo.2005.50.4.1244

Lionello, P., Scarascia, L., 2018. The relation between climate change in the Mediterranean region and global warming. Reg. Environ. Chang. 18, 1481–1493. https://doi.org/10.1007/s10113-018-1290-1

López García, M.J., Camarasa Belmonte, A.M., 2011. Recent trends of SST in the Western Mediterranean basins from AVHRR Pathfinder data (1985-2007). Glob. Planet. Change 78, 127–136. https://doi.org/10.1016/j.gloplacha.2011.06.001

Mann, H.B., 1945. Nonparametric tests against trend. Econometrica 13, 245–259. https://doi.org/10.2307/1907187

Marić, D., Kraus, R., Godrijan, J., Supić, N., Djakovac, T., Precali, R., 2012. Phytoplankton response to climatic and anthropogenic influences in the north-eastern Adriatic during the last four decades. Estuar. Coast. Shelf Sci. 115, 98–112. https://doi.org/10.1016/j.ecss.2012.02.003

Martínez, J., Leonelli, F.E., García-Ladona, E., Garrabou, J., Kersting, D.K., Bensoussan, N., Pisano, A., 2023. Evolution of marine heatwaves in warming seas: the Mediterranean Sea case study. Front. Mar. Sci. 10, 1193164. https://doi.org/10.3389/fmars.2023.1193164

McLeod, A.I., 2022. Kendall: Kendall rank correlation and Mann-Kendall trend test. R package version 2.2.1. https://CRAN.R-project.org/package=Kendall

Mentaschi, L., Lovato, T., Butenschön, M., Alessandri, J., Aragão, L., Verri, G., Guerra, R., Coppini, G., Pinardi, N., 2024. Projected climate oligotrophication of the Adriatic marine ecosystems. Front. Clim. 6, 1338374. https://doi.org/10.3389/fclim.2024.1338374

Merchant, C.J., Embury, O., Bulgin, C.E., Block, T., Corlett, G.K., Fiedler, E., Good, S.A., Mittaz, J., Rayner, N.A., Berry, D., Eastwood, S., Taylor, M., Tsushima, Y., Waterfall, A., Wilson, R., Donlon, C., 2019. Satellite-based time-series of sea-surface temperature since 1981 for climate applications. Sci. Data 6, 223. https://doi.org/10.1038/s41597-019-0236-x

Michaud, K.M., Reed, D.C., Miller, R.J., 2022. The Blob marine heatwave transforms California kelp forest ecosystems. Commun. Biol. 5, 1143. https://doi.org/10.1038/s42003-022-04107-z

Mohamed, B., Abdallah, A.M., Alam El-Din, K., Nagy, H., Shaltout, M., 2019. Inter-annual variability and trends of sea level and sea surface temperature in the Mediterranean Sea over the last 25 years. Pure Appl. Geophys. 176, 3787–3810. https://doi.org/10.1007/s00024-019-02156-w

Montie, S., Thomsen, M.S., Rack, W., Broady, P.A., 2020. Extreme summer marine heatwaves increase chlorophyll a in the Southern Ocean. Antarct. Sci. 32, 508–509. https://doi.org/DOI: 10.1017/S0954102020000401

Mozetič, P., Solidoro, C., Cossarini, G., Socal, G., Precali, R., Francé, J., Bianchi, F., De Vittor, C., Smodlaka, N., Fonda Umani, S., 2010. Recent trends towards oligotrophication of the Northern Adriatic: evidence from chlorophyll a time series. Estuaries Coasts 33, 362–375. https://doi.org/10.1007/s12237-009-9191-7

Naselli-Flores, L., Padisák, J., 2023. Ecosystem services provided by marine and freshwater phytoplankton. Hydrobiologia 850, 2691–2706. https://doi.org/10.1007/s10750-022-04795-y

Neri, F., Romagnoli, T., Accoroni, S., Campanelli, A., Marini, M., Grilli, F., Totti, C., 2022. Phytoplankton and environmental drivers at a long-term offshore station in the northern Adriatic Sea (1988–2018). Cont. Shelf Res. 242, 104746. https://doi.org/10.1016/j.csr.2022.104746

Neri, F., Romagnoli, T., Accoroni, S., Ubaldi, M., Garzia, A., Pizzuti, A., Campanelli, A., Grilli, F., Marini, M., Totti, C., 2023. Phytoplankton communities in a coastal and offshore stations of the northern Adriatic Sea approached by network analysis and different statistical descriptors. Estuar. Coast. Shelf Sci. 282, 108224. https://doi.org/10.1016/j.ecss.2023.108224

Ninčević Gladan, Ž., Marasović, I., Grbec, B., Skejić, S., Bužančić, M., Kušpilić, G., Matijević, S., Matić, F., 2010. Inter-decadal variability in phytoplankton community in the middle Adriatic

(Kaštela Bay) in relation to the North Atlantic Oscillation. Estuaries Coasts 33, 376–383. https://doi.org/10.1007/s12237-009-9223-3

Noh, K.M., Lim, H.G., Kug, J.S., 2022. Global chlorophyll responses to marine heatwaves in satellite ocean color. Environ. Res. Lett. 17, 064034. https://doi.org/10.1088/1748-9326/ac70ec

O'Connor, M.I., Piehler, M.F., Leech, D.M., Anton, A., Bruno, J.F., 2009. Warming and resource availability shift food web structure and metabolism. PLOS Biol. 7, e1000178. https://doi.org/10.1371/journal.pbio.1000178

Pastor, F., Valiente, J.A., Khodayar, S., 2020. A warming Mediterranean: 38 years of increasing sea surface temperature. Remote Sens. 12(17), 2687. https://doi.org/10.3390/RS12172687

Pastor, F., Valiente, J.A., Palau, J.L., 2018. Sea Surface Temperature in the Mediterranean: trends and spatial patterns (1982–2016). Pure Appl. Geophys. 175, 4017–4029. https://doi.org/10.1007/s00024-017-1739-z

Piatt, J.F., Parrish, J.K., Renner, H.M., Schoen, S.K., Jones, T.T., Arimitsu, M.L., Kuletz, K.J., Bodenstein, B., García-Reyes, M., Duerr, R.S., Corcoran, R.M., Kaler, R.S.A., McChesney, G.J., Golightly, R.T., Coletti, H.A., Suryan, R.M., Burgess, H.K., Lindsey, J., Lindquist, K., Warzybok, P.M., Jahncke, J., Roletto, J., Sydeman, W.J., 2020. Extreme mortality and reproductive failure of common murres resulting from the northeast Pacific marine heatwave of 2014-2016. PLoS One 15, e0226087.

Pisano, A., Buongiorno Nardelli, B., Tronconi, C., Santoleri, R., 2016. The new Mediterranean optimally interpolated pathfinder AVHRR SST Dataset (1982–2012). Remote Sens. Environ. 176, 107–116. https://doi.org/https://doi.org/10.1016/j.rse.2016.01.019

Pisano, A., Marullo, S., Artale, V., Falcini, F., Yang, C., Leonelli, F.E., Santoleri, R., Nardelli, B.B., 2020. New evidence of Mediterranean climate change and variability from Sea Surface Temperature observations. Remote Sens. 12, 132. https://doi.org/10.3390/RS12010132

Pohlert, T., 2023. trend: Non-parametric trend tests and change-point detection. R package version 1.1.5. https://CRAN.R-project.org/package=trend

Poulain, P.-M., Cushman-Roisin, B., 2001. Circulation. In: Cushman-Roisin, B., Gačić, M., Poulain, P.-M., Artegiani, A. (Eds), *Physical oceanography of the Adriatic Sea: Past, present and future.* Kluwer Academic Publishers, Dordrecht, The Netherlands, pp. 67–109.

R Core Team, 2021. R: A language and environment for statistical computing.

Saha, K., Zhao, X., Zhang, H., Casey, K.S.., Zhang, D., Baker-Yeboah, S., Kilpatrick, K.A.., Evans, R.H.., Ryan, T., Relph, J.M., 2018. AVHRR Pathfinder version 5.3 level 3 collated (L3C) global 4km sea surface temperature for 1981-present. Dataset; Subset: 1982-2022. NOAA National Centers for Environmental Information: Asheville, NC, USA, 2018.

Salgado-Hernanz, P.M., Racault, M.-F., Font-Muñoz, J.S., Basterretxea, G., 2019. Trends in phytoplankton phenology in the Mediterranean Sea based on ocean-colour remote sensing. Remote Sens. Environ. 221, 50–64. https://doi.org/https://doi.org/10.1016/j.rse.2018.10.036

Sax, C., Eddelbuettel, D., 2018. Seasonal Adjustment by X-13ARIMA-SEATS in R. J. Stat. Softw. 87(11), 1–17. https://doi.org/10.18637/jss.v087.i11

Sen Gupta, A., Thomsen, M., Benthuysen, J.A., Hobday, A.J., Oliver, E., Alexander, L. V., Burrows, M.T., Donat, M.G., Feng, M., Holbrook, N.J., Perkins-Kirkpatrick, S., Moore, P.J., Rodrigues, R.R., Scannell, H.A., Taschetto, A.S., Ummenhofer, C.C., Wernberg, T., Smale, D.A., 2020. Drivers and impacts of the most extreme marine heatwaves events. Sci. Rep. 10, 19359. https://doi.org/10.1038/s41598-020-75445-3

Sen, P.K., 1968. Estimates of the Regression Coefficient Based on Kendall's Tau. J. Am. Stat. Assoc. 63, 1379–1389. https://doi.org/10.1080/01621459.1968.10480934

Serrano, O., Arias-Ortiz, A., Duarte, C.M., Kendrick, G.A., Lavery, P.S. (2021). Impact of marine heatwaves on seagrass ecosystems. In: Canadell, J.G., Jackson, R.B. (Eds), *Ecosystem collapse and climate change*. Ecological Studies, Vol 241, pp. 345–364. Springer, Cham. https://doi.org/10.1007/978-3-030-71330-0_13

Simon, A., Plecha, S.M., Russo, A., Teles-Machado, A., Donat, M.G., Auger, P.A., Trigo, R.M., 2022. Hot and cold marine extreme events in the Mediterranean over the period 1982-2021. Front. Mar. Sci. 9, 892201. https://doi.org/10.3389/fmars.2022.892201

Skliris, N., Sofianos, S., Gkanasos, A., Mantziafou, A., Vervatis, V., Axaopoulos, P., Lascaratos, A., 2012. Decadal scale variability of sea surface temperature in the Mediterranean Sea in relation to atmospheric variability. Ocean Dyn. 62, 13–30. https://doi.org/10.1007/s10236-011-0493-5

Smale, D.A., Wernberg, T., 2013. Extreme climatic event drives range contraction of a habitat-forming species. Proc. R. Soc. B Biol. Sci. 280, 20122829. https://doi.org/10.1098/rspb.2012.2829

Smale, D.A., Wernberg, T., Oliver, E.C.J., Thomsen, M., Harvey, B.P., Straub, S.C., Burrows, M.T., Alexander, L. V., Benthuysen, J.A., Donat, M.G., Feng, M., Hobday, A.J., Holbrook, N.J., Perkins-Kirkpatrick, S.E., Scannell, H.A., Sen Gupta, A., Payne, B.L., Moore, P.J., 2019. Marine heatwaves threaten global biodiversity and the provision of ecosystem services. Nat. Clim. Chang. 9, 306–312. https://doi.org/10.1038/s41558-019-0412-1

Smith, K.E., Burrows, M.T., Hobday, A.J., King, N.G., Moore, P.J., Sen Gupta, A., Thomsen, M.S., Wernberg, T., Smale, D.A., 2023. Biological impacts of marine heatwaves. Ann. Rev. Mar. Sci. 15, 119–145. https://doi.org/10.1146/annurev-marine-032122-121437

Soulié, T., Vidussi, F., Mas, S., Mostajir, B., 2023. Functional and structural responses of plankton communities toward consecutive experimental heatwaves in Mediterranean coastal waters. Sci. Rep. 13, 8050. https://doi.org/10.1038/s41598-023-35311-4

Stipcich, P., Marín-Guirao, L., Pansini, A., Pinna, F., Procaccini, G., Pusceddu, A., Soru, S., Ceccherelli, G., 2022. Effects of current and future summer marine heat waves on *Posidonia oceanica*: plant origin matters? Front. Clim. 4, 844831. https://doi.org/10.3389/fclim.2022.844831

Totti, C., Cangini, M., Ferrari, C., Kraus, R., Pompei, M., Pugnetti, A., Romagnoli, T., Vanucci, S., Socal, G., 2005. Phytoplankton size-distribution and community structure in relation to mucilage occurrence in the northern Adriatic Sea. Sci. Total Environ. 353, 204–217. https://doi.org/10.1016/J.SCITOTENV.2005.09.028

Totti, C., Romagnoli, T., Accoroni, S., Coluccelli, A., Pellegrini, M., Campanelli, A., Grilli, F., Marini, M., 2019. Phytoplankton communities in the northwestern Adriatic Sea: Interdecadal variability over a 30-years period (1988–2016) and relationships with meteoclimatic drivers. J. Mar. Syst. 193, 137–153. https://doi.org/10.1016/j.jmarsys.2019.01.007

Tweddle, J.F., Gubbins, M., Scott, B.E., 2018. Should phytoplankton be a key consideration for marine management? Mar. Policy 97, 1–9. https://doi.org/10.1016/j.marpol.2018.08.026

Vallina, S.M., Simó, R., 2007. Strong relationship between DMS and the solar radiation dose over the global surface ocean. Science 315, 506–508. https://doi.org/10.1126/science.1133680

Vascotto, I., Mozetič, P., Francé, J., 2021. Phytoplankton Time-Series in a LTER site of the Adriatic Sea: methodological approach to decipher community structure and indicative taxa. Water 13, 2045. https://doi.org/10.3390/w13152045

Vogt, L., Burger, F.A., Griffies, S.M., Frölicher, T.L., 2022. Local drivers of marine heatwaves: a global analysis with an Earth system model. Front. Clim. 4, 847995. https://doi.org/10.3389/fclim.2022.847995

Volpe, G., Colella, S., Brando, V.E., Forneris, V., La Padula, F., Di Cicco, A., Sammartino, M., Bracaglia, M., Artuso, F., Santoleri, R., 2019. Mediterranean ocean colour Level 3 operational multi-sensor processing. Ocean Sci. 15, 127–146. https://doi.org/10.5194/os-15-127-2019

Welch, H., Savoca, M.S., Brodie, S., Jacox, M.G., Muhling, B.A., Clay, T.A., Cimino, M.A., Benson, S.R., Block, B.A., Conners, M.G., Costa, D.P., Jordan, F.D., Leising, A.W., Mikles, C.S., Palacios, D.M., Shaffer, S.A., Thorne, L.H., Watson, J.T., Holser, R.R., Dewitt, L., Bograd, S.J., Hazen, E.L., 2023. Impacts of marine heatwaves on top predator distributions are variable but predictable. Nat. Commun. 14, 5188. https://doi.org/10.1038/s41467-023-40849-y

Wyatt, A.S.J., Leichter, J.J., Washburn, L., Kui, L., Edmunds, P.J., Burgess, S.C., 2023. Hidden heatwaves and severe coral bleaching linked to mesoscale eddies and thermocline dynamics. Nat. Commun. 14, 25. https://doi.org/10.1038/s41467-022-35550-5

Xu, T., Newman, M., Capotondi, A., Stevenson, S., Di Lorenzo, E., Alexander, M.A., 2022. An increase in marine heatwaves without significant changes in surface ocean temperature variability. Nat. Commun. 13, 7396. https://doi.org/10.1038/s41467-022-34934-x

Zhao, Z., Marin, M., 2019. A MATLAB toolbox to detect and analyze marine heatwaves. J. Open Source Softw. 4, 1124. https://doi.org/10.21105/joss.01124

2.8 Supplementary materials

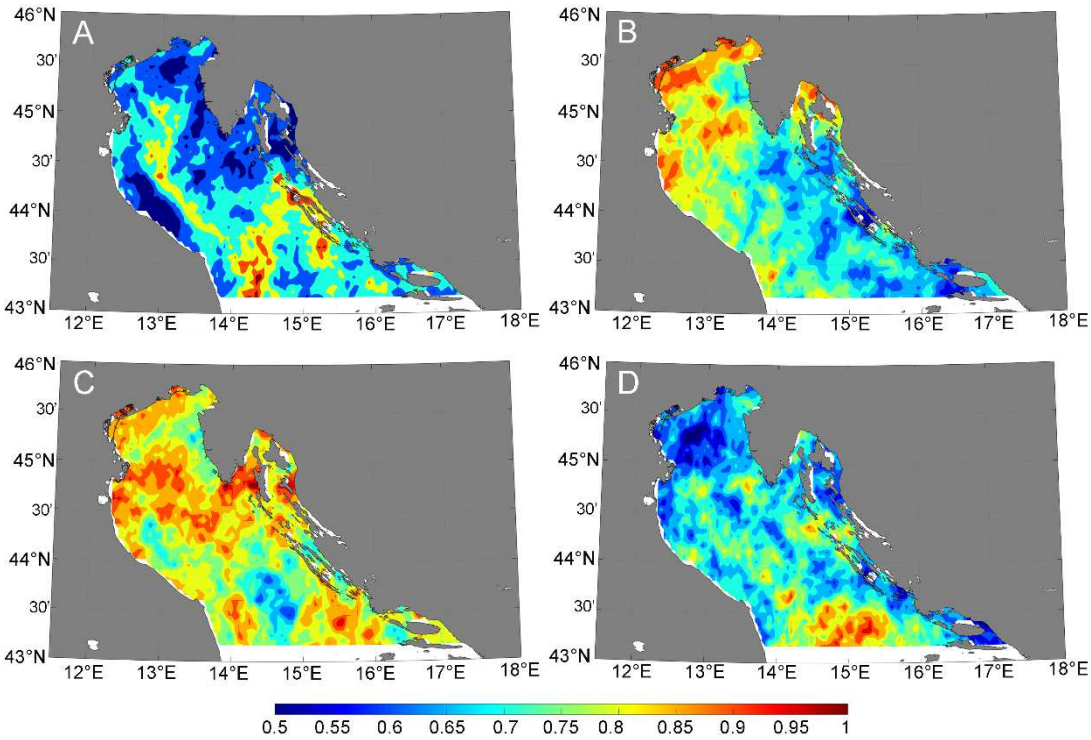

Fig. S1. Map of mean marine heatwave frequency (number of events in each year) in the Northern Adriatic Sea (1982-2022) in winter (A), spring (B), summer (C) and autumn (D).

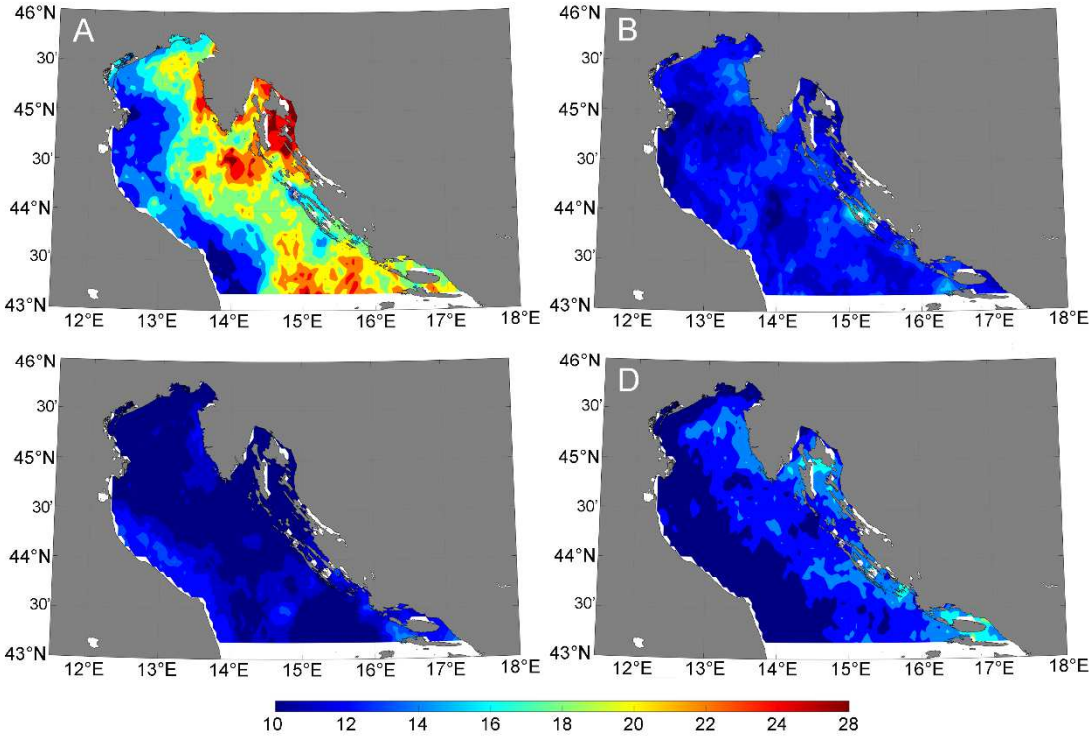

Fig. S2. Map of mean marine heatwave duration (duration of the event in days) in the Northern Adriatic Sea (1982-2022) in winter (A), spring (B), summer (C) and autumn (D).

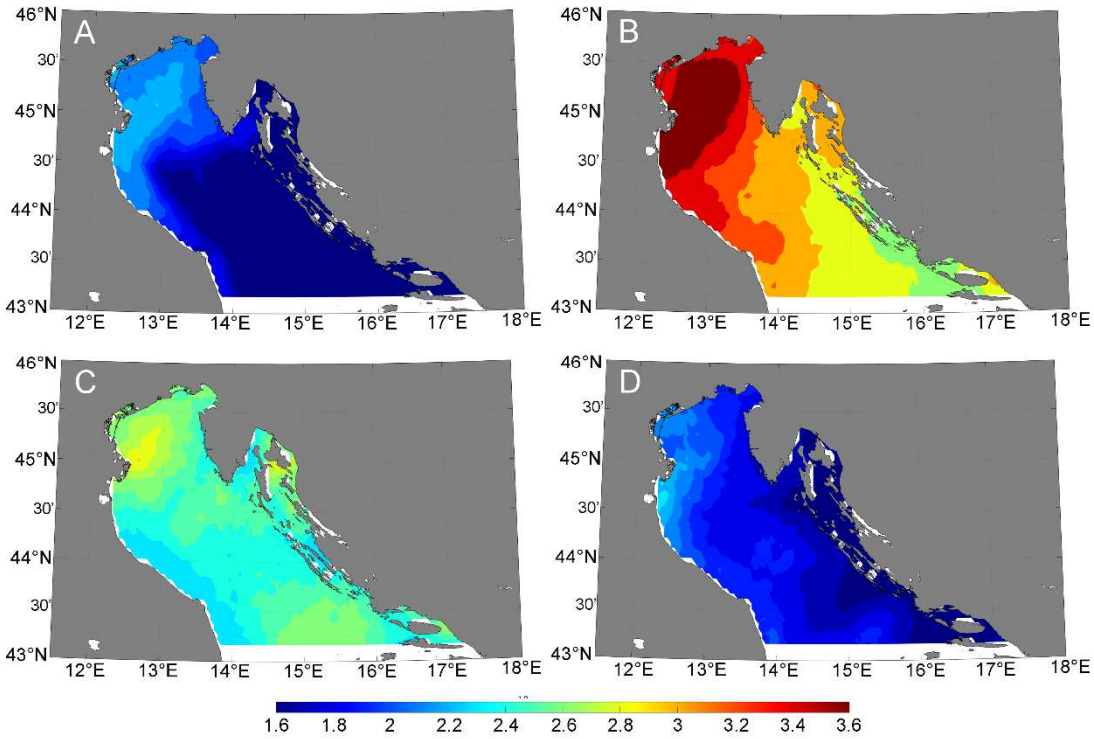

Fig. S3. Map of mean marine heatwave mean intensity (°C) in the Northern Adriatic Sea (1982-2022) in winter (A), spring (B), summer (C) and autumn (D).

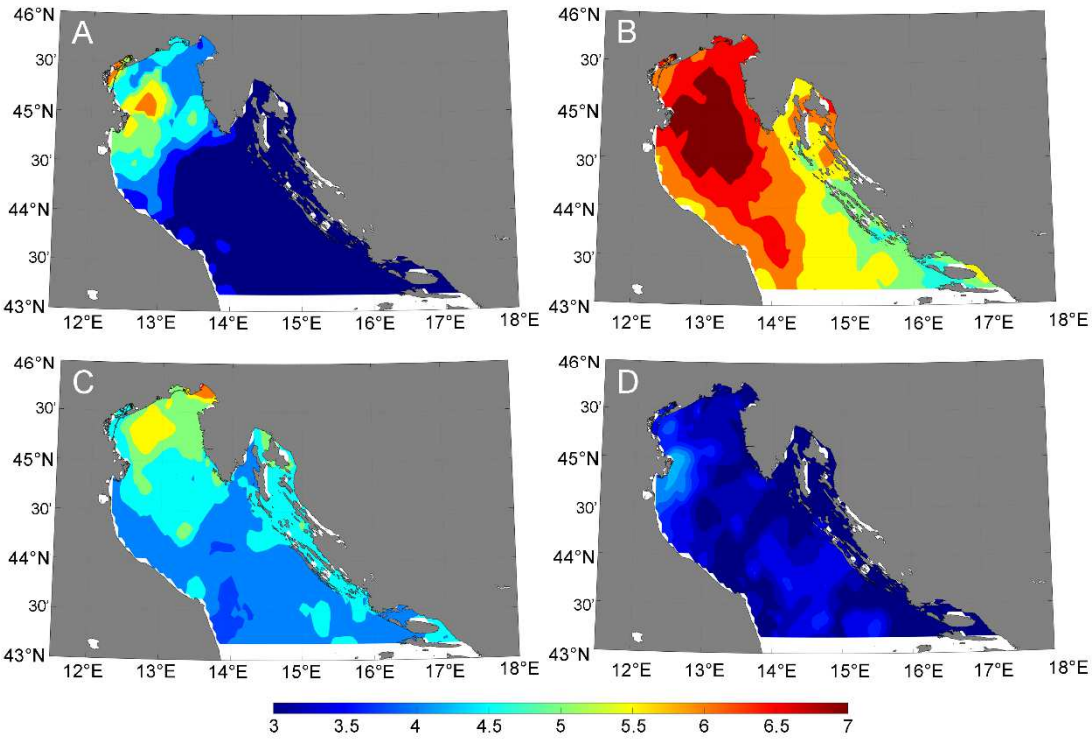

Fig. S4. Map of mean marine heatwave max intensity (°C) in the Northern Adriatic Sea (1982-2022) in winter (A), spring (B), summer (C) and autumn (D).

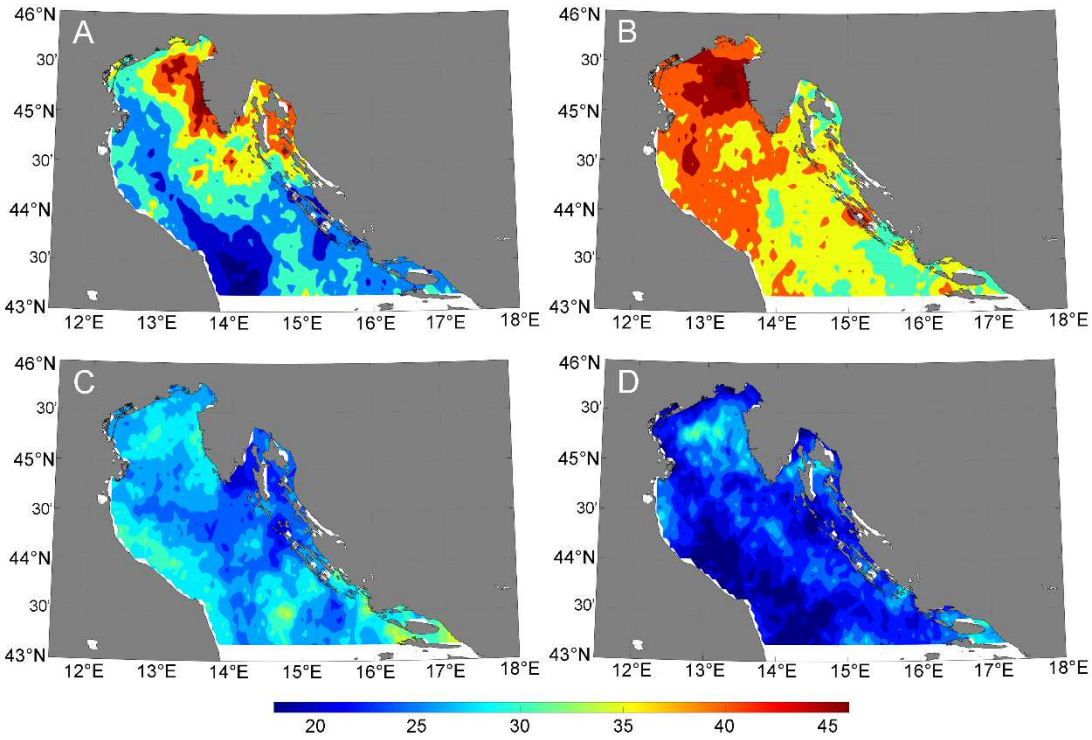

Fig. S5. Map of mean marine heatwave cumulative intensity (°C.days) in the Northern Adriatic Sea (1982-2022) in winter (A), spring (B), summer (C) and autumn (D).

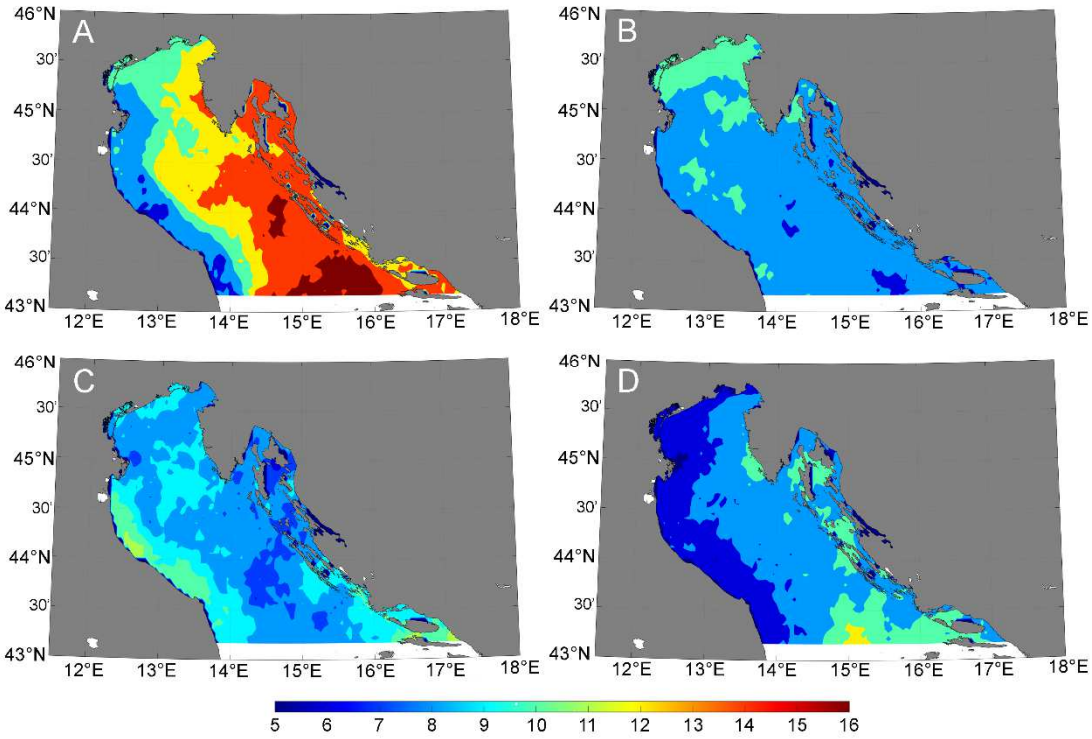

Fig. S6. Map of mean marine heatwave days (sum of marine heatwave days in each year) in the Northern Adriatic Sea (1982-2022) in winter (A), spring (B), summer (C) and autumn (D).

Table S1. Spearman correlations (rho) between the X-11 decomposed trend of SST and chl-a in each sub-area: Western Coast (WC), Venice Lagoon (VL), Gulf of Trieste (GoT), Eastern Coast (EC), remaining sub-area with depth greater and lower than 40m (H40 and L40, respectively).

Sub-area	Correlation (rho)	p-value
WC	-0.12	***p* < 0.05**
VL	0.15	***p* < 0.05**
GoT	-0.33	***p < 0.001***
EC	-0.46	***p < 0.001***
H40	-0.13	***p* < 0.05**
L40	-0.14	***p* < 0.05**

Chapter 3

Comparative analysis of phytoplankton diversity using microscopy and metabarcoding: insights from an eLTER station in the Northern Adriatic Sea

Submitted to *Marine Environmental Research*

Comparative analysis of phytoplankton diversity using microscopy and metabarcoding: insights from an eLTER station in the Northern Adriatic Sea

Francesca Neri[1], Marika Ubaldi[1,2,3], Stefano Accoroni[1,4,5], Sara Ricci[6], Elisa Banchi[3,7], Tiziana Romagnoli[1], Cecilia Totti[1,5]

[1] Dipartimento di Scienze della Vita e dell'Ambiente, Università Politecnica delle Marche, Via Brecce Bianche, 60131 Ancona, Italy

[2] Dipartimento di Scienze della Terra e del Mare, Via Archirafi 22, 90123 Palermo, Italy

[3] National Biodiversity Future Center, Piazza Marina 61, 90133 Palermo, Italy

[4] Fano Marine Center, The Inter- Institute Center for Research on Marine Biodiversity, Resources and Biotechnologies (FMC), Viale Adriatico 1/N, 61032 Fano, Italy

[5] Consorzio Interuniversitario per le Scienze del Mare, CoNISMa, ULR Ancona, Ancona, Italy

[6] Center for Animal Nutrition and Welfare, Clinical Department for Farm Animals and Safety of Food Systems, University of Veterinary Medicine Vienna, 1210 Vienna, Austria

[7] National Institute of Oceanography and Applied Geophysics - OGS, via Piccard 54, 34151 Trieste, Italy

*Corresponding Author: f.neri@univpm.it

Keywords:

Microalgae, diversity, environmental DNA, Long Term Ecological Research, amplicon sequencing

3.1 Abstract

The monitoring of phytoplankton is crucial to highlight changes in the marine ecosystems related to climate change or anthropogenic pressures and has been traditionally performed using microscopy. In the present study, the phytoplankton community structure of an eLTER station in the Northern Adriatic Sea was analyzed combining two approaches for the first time in the study area, i.e. microscopy and eDNA metabarcoding (targeting V4 and V9 regions of the 18S rRNA gene, and using PR2 and SILVA as reference databases), to highlight the strengths and weaknesses of these two methods.

Metabarcoding revealed a so far unknown phytoplankton diversity of the eLTER station (99 genera and 151 species), particularly for those taxa whose identification is difficult or impossible using microscopy. However, microscopy detected 14 genera and 44 species not revealed by metabarcoding analysis. Among the different applied approaches, the use of V4 as target 18S region and PR2 as reference database led to the identification of the highest number of genera and species. Only a small percentage of genera and species were shared by the two methods (microscopy and metabarcoding), 18S regions (V4 and V9) and reference databases (PR2 and SILVA).

In general, metabarcoding showed a community characterized by a higher number of phytoflagellate and dinoflagellate genera and species, in comparison with microscopy where diatom and dinoflagellate taxa were the most represented. Moreover, metabarcoding failed to reveal almost all the coccolithophores.

The results confirmed metabarcoding as a powerful tool detecting taxa that are not identifiable under microscopy, particularly when different regions and databases are used. However, it should still be combined with microscopy to have a more detailed information on the community and to counteract the drawbacks of metabarcoding, such as gaps in the reference databases.

3.2 Introduction

Phytoplankton communities play essential roles in the marine ecosystems, not only for their oxygen production and contribution to higher trophic level/food production, but also for their involvement in biogeochemical cycles, drawdown of CO_2 from the air, and climate regulation (Araujo et al., 2022; Blanchard et al., 2012; Falkowski, 2012; Hays et al., 2005; Naselli-Flores and Padisák, 2023; Vallina and Simó, 2007). Phytoplankton communities are characterized by high turnover, and they can reveal changes in the marine ecosystems due to their rapid response to environmental and oceanographic conditions.

In the Northern Adriatic Sea (NAS), one of the most productive areas of the Mediterranean Sea (D'Ortenzio and Ribera d'Alcalà, 2009), the long-term phytoplankton response to environmental and climatic changes, such as riverine runoff, temperature increases and nutrient availability, has been well documented in several European Long Term Ecological Research (eLTER) sites (https://elter-ri.eu/) reporting changes in abundance, biomass and/or shifts in the seasonal rhythm of the major blooms (Bernardi Aubry et al., 2012; Cerino et al., 2019; Cozzi et al., 2020; Marić et al., 2012; Mozetič et al., 2010; Neri et al., 2022, 2023; Totti et al., 2019; Vascotto et al., 2021).

A reliable identification of phytoplankton up to the lower taxonomic level (i.e., species) is essential for several reasons, e.g., to detect toxic species for human and marine ecosystems (Pinto et al., 2023), to document allochthonous species that can alter the ecosystem equilibrium (Zenetos et al., 2010), and to assess biodiversity. The estimation of biodiversity in pelagic habitats has been included in the assessment of the Good Environmental Status (2008/56/EC), and many indicators related to phytoplankton (e.g. shifts in productivity, life forms, composition in terms of non-indigenous or toxic species, changes in the spatial and temporal diversity) have been proposed to be considered in the management policies (Francé et al., 2021; McQuatters-Gollop et al., 2019; Rombouts et al., 2019; Tweddle et al., 2018; Varkitzi et al., 2018; Wasmund et al., 2017).

Traditionally, the monitoring of phytoplankton communities has been conducted by expert taxonomists through inverted light microscopy, which provides detailed information on composition,

abundances and biomass based on morphological criteria. However, this approach is time consuming, and the less abundant/smaller species may be overlooked or misidentified. Moreover, the accurate identification can be further prevented by (i) several ultrastructural taxonomic details only visible by electron microscopy, (ii) presence of taxa difficult to distinguish morphologically, as they lack diagnostic morphology (cryptic species; Struck et al., 2017)) and (iii) morphological diagnostic characters which vary under different environmental conditions.

For these reasons, increasing number of studies have been using DNA metabarcoding to investigate phytoplankton communities (Almandoz et al., 2024; Caracciolo et al., 2022; Gaonkar et al., 2020; Gaonkar and Campbell, 2023; Grižančić et al., 2023; Penna et al., 2017; Piredda et al., 2018; Specchia et al., 2023). This method, in addition to its capability to assess the whole biodiversity, including taxa (e.g. rare and cryptic ones) that are difficult to identify by light microscopy, allows higher comparability between studies compared to only relying on light microscopy which is heavily user dependent (Turk Dermastia et al., 2023). On the other hand, metabarcoding provides only relative abundance values, and taxonomic assignment depends on reference databases, the incompleteness and errors of which can affect the biodiversity assessment (Tzafesta et al., 2022; Weigand et al., 2019). In order to take advantage of the potential of both traditional and molecular approaches and to achieve the most reliable phytoplankton identification, an increasing number of studies have therefore coupled microscopy and metabarcoding, highlighting important differences, e.g. in the community composition and/or relative abundances (Abad et al., 2016; Andersson et al., 2023; Bilbao et al., 2023; Esenkulova et al., 2020; Pierce et al., 2023; Piredda et al., 2017; Santi et al., 2021; Turk Dermastia et al., 2023), and emphasizing the importance of combining these methods for the monitoring of this planktonic fraction.

The aim of this study was to compare and integrate the biodiversity and taxonomic composition of phytoplankton determined by microscopy and DNA metabarcoding at the eLTER Senigallia coastal station, in the northern Adriatic Sea. DNA metabarcoding analysis was performed with different markers (18S rRNA V4 and V9) and using different reference databases (PR2 (Guillou et al., 2013)

and SILVA (Quast et al., 2013)), which allowed the evaluation of the different combinations in the assessment of phytoplankton communities. The analysis of the potential strengths and weaknesses of the microscopic and molecular methods, as well as of the main biases introduced by each approach allowed to highlight the best practice in the analysis and to achieve the most accurate and reliable representation of these important organisms in coastal environments.

3.3 Methods

Sampling

The sampling station is represented by the SG01 station (43.755° N, 13,2105° E, Fig. 1), the coastal station of the eLTER Senigallia-Susak transect (DEIMS.iD: https://deims.org/be8971c2-c708-4d6e-a4c7-f49fcf1623c1). For both microscopy and metabarcoding, samples were collected monthly at the surface (0.5 m) using Niskin bottles from February to October 2019 on board of the Actea oceanographic vessel.

Phytoplankton samples for microscopy analyses were collected in 250 ml dark glass bottles and preserved by adding 0.8% prefiltered and neutralized formaldehyde (Throndsen, 1978). For metabarcoding, 2 L of seawater were filtered in cellulose nitrate filters (47 mm diameter, 1.2 μm pore-size, Sartorius), and preserved at -20 °C.

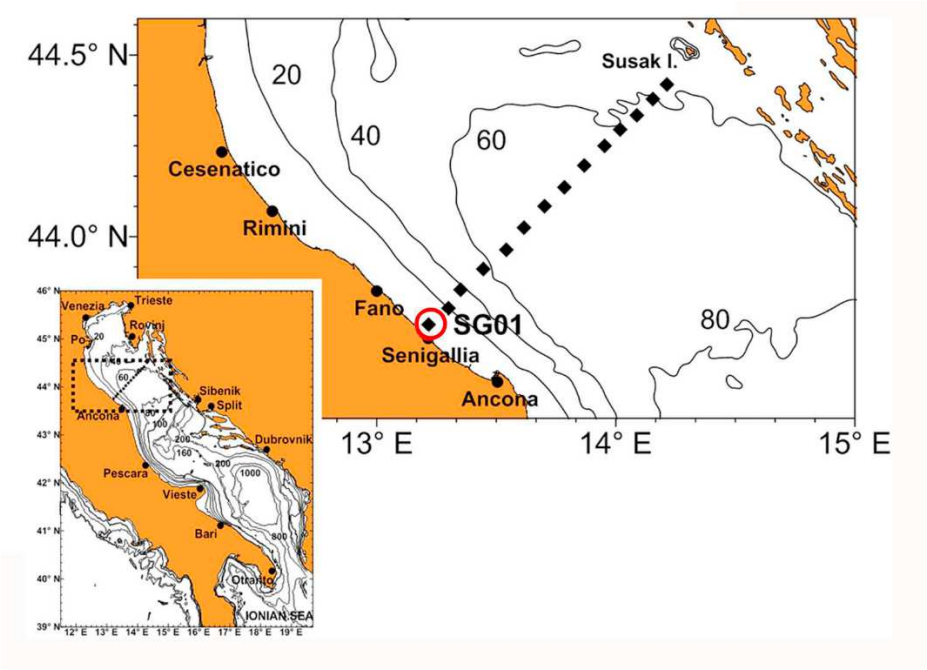

Fig. 1. Map of the study area. The dashed line represents the eLTER Senigallia-Susak transect, with the study station (SG01) highlighted by a red circle.

DNA extraction, sequencing and metabarcoding analysis

DNA was extracted using the DNeasy PowerWater Kit (QIAGEN, Germany) following the manufacturer's instructions. The filters were cut in half, each half was extracted separately and then pooled after elution. Quantity of the extracted DNA was assessed with Qubit Fluorimeter (Thermo Fisher Scientific). The V4 and V9 regions of the 18S rRNA gene were amplified following the Illumina Sequencing Library Preparation protocol (with 30 PCR cycles in the amplicon PCR) with the primers V4 18S Next.For and V4 18S Next.Rev primers for V4 (Piredda et al. 2017), giving amplicons of ~470 bp, and the primers V9 18S Next.For and V9 18S Next.Rev primers for V9 (Piredda et al. 2017), giving amplicons of ~270 bp. The sample of May failed to amplify for the V4 region, thus was not sequenced. Library preparation (including IDT for Illumina UD index set D (Illumina, San Diego, CA, USA), primers with sequence complementary to overhang adapter and sample specific barcodes), 2 × 250 bp paired end sequencing of equimolar ratios of the purified amplicon libraries on an Illumina MiSeq platform (Illumina, San Diego, CA, USA) and

demultiplexing were performed at the Department of Bioscience, Biotechnology and Biopharmaceutics at Università degli Studi di Bari.

For each raw read, quality and presence of adapters were inspected using FASTQC (v. 0.10.1) (Andrews and Braham Bioinformatics, 2010) and primers were trimmed using cutadapt (v. 4.5) (Martin, 2011). Sequences were then processed and analysed using QIIME2 (v. 2023.2) (Bolyen et al., 2019).

Quality filtering, denoising and pairing of the reads were performed with DADA2 (Callahan et al., 2016).

Taxonomy was assigned to amplicon sequence variants (ASVs) with a Naive Bayes classifier (Bokulich et al., 2018) trained for the specific 18S rRNA gene target region (V4, V9) against the PR2 v. 5.0.1 (Guillou et al., 2013) and SILVA 138 99% (Quast et al., 2013) reference databases.

Microscopy analysis

An inverted microscope (ZEISS Axiovert 135) equipped with phase contrast was used for the identification and counting of phytoplankton, following the Utermöhl method (Edler and Elbrachter, 2010). Counting was carried out at 400x magnification, along transects or in random visual fields, depending on cell abundance, to count a minimum of 200 cells. Moreover, a half of the Utermöhl chamber was analyzed at 200x magnification to provide a more accurate estimation of the larger and rarer species, that strongly influence the biomass value. Phytoplankton taxa were identified at the lowest possible taxonomical rank, and finally grouped in major groups, i.e. diatoms, dinoflagellates, coccolithophores, and phytoflagellates. Dinoflagellates were considered as a taxonomical group, with both autotrophic and heterotrophic species. Phytoflagellates include all groups that are not identifiable by light microscopy, often not at the class level, e.g., haptophytes (except coccolithophores), cryptophytes, chrysophytes, dictyochophytes, raphidophytes, chlorophytes and euglenophytes.

Data analyses

Data analyses were performed using R software (R Core Team, 2021) on presence/absence data obtained from the two applied methods, microscopy and metabarcoding. Within the metabarcoding method, analyses were further categorized based on different markers (V4 and V9) and databases (SILVA and PR2), for a total of five approaches: (i) microscopy, (ii) V4-SILVA, (iii) V9-SILVA, (iv) V4-PR2, and (v) V9-PR2.

To allow the comparison between microscopy and metabarcoding, phyla or classes not belonging to phytoplankton (e.g., ciliates, choanoflagellates, tintinnids, metazoans), were removed from metabarcoding datasets using R package phyloseq (McMurdie and Holmes, 2013. In the same way, organelle sequences (mitochondrial, nucleomorphic) were not considered. As in microscopy phytoflagellates are considered a unique artificial group (e.g., Neri et al., 2023), for the comparison between methods, we maintained the same group also in the metabarcoding analysis.

Species and genus names were checked on Algaebase (Guiry and Guiry, 2024) and updated to the current accepted nomenclature. In cases of uncertain taxonomy, the ASVs (Amplicon Sequence Variant) were checked on NCBI, and mistakes were corrected or removed.

Statistical analyses were performed separately at both genus and species levels. Therefore, the ASVs whose taxonomy ended at higher levels, e.g. classes or higher (for genera analysis) and genus or higher (for species analysis) were removed. Venn diagrams were used to represent the number of genera and species found by the five different approaches and were built using the VennDiagram (Chen and Boutros, 2011) and eulerr (Larsson, 2022) R packages.

When the Venn diagrams highlighted taxa detected only by microscopy, Primer-BLAST (Ye et al., 2012) was used to exclude primer unsuitability as the reason for undetectability by verifying their specificity with available sequences deposited in GenBank for those taxa.

A Non-Metric Multidimensional Scaling (NMDS) was performed on the richness (i.e., number of genera and species in the different phytoplankton groups and on the presence-absence of taxa obtained from the five distinct approaches. The metaMDS function from the vegan package (Oksanen et al.,

2022) was used, setting the distance as bray and jaccard, when considering richness and presence-absence data, respectively. Permutational multivariate analysis of variance (PERMANOVA) was used to test for significant differences among the groups that were highlighted by the NMDS, using the adonis function in the vegan package (Oksanen et al., 2022).

3.4 Results

Phytoplankton groups

The proportions of genera and species in the different phytoplankton groups (diatoms, dinoflagellates, coccolithophores and phytoflagellates) found by the five distinct approaches based on microscopy and metabarcoding (V4-SILVA, V9-SILVA, V4-PR2 and V9-PR2) are shown in Fig. 2A and 2B, for genera and species, respectively.

Considering the identification at genus level throughout the study period, using microscopy, dinoflagellate and diatom genera represented the highest percentage (39.58 and 37.50% respectively), followed by coccolithophores (12.50%) and phytoflagellates (10.42%).

As regards metabarcoding, the phytoflagellates represented the highest percentage (41.07, 48.65, 43.30 and 43.24% for V4-PR2, V9-PR2, V4-SILVA and V9-SILVA, respectively), followed by dinoflagellates (38.39, 33.78, 34.02 and 39.19% for V4-PR2, V9-PR2, V4-SILVA and V9-SILVA, respectively) and diatoms (18.75, 17.57, 21.65 and 17.57% for V4-PR2, V9-PR2, V4-SILVA and V9-SILVA. Coccolithophore genera comprised 1.79% and 1.02% with V4-PR2 and V4-SILVA, respectively, while no coccolithophores were observed when using the V9 marker with either the SILVA or PR2 databases.

As regards the percentage of identified species, using microscopy, the highest percentages of species were represented by diatoms and dinoflagellates (42.42 and 40.91%, respectively), followed by coccolithophores (12.12%) and phytoflagellates (4.55%). When employing V4-PR2, 39.09% of species were dinoflagellates, 33.64% were phytoflagellates, 25.45% were diatoms and 1.82% were coccolithophores. With V4-SILVA, 38.46% of species belonged to phytoflagellates, 32.31 % to

diatoms, 27.69% to dinoflagellates and 1.54% to coccolithophores. Using V9-PR2, the majority of species were phytoflagellates (56.63%), followed by dinoflagellates (30.12%) and diatoms (13.25%), while with V9-SILVA, 40.98% of species were dinoflagellates, 39.34% were phytoflagellates and 19.67% were diatoms. The V9 marker did not detect any coccolithophores in either database.

The percentages of genera and species in the different phytoplankton groups in each month are shown in Fig. S1A and B, respectively. It can be observed that the percent values show a high variability in each month and for each considered approach.

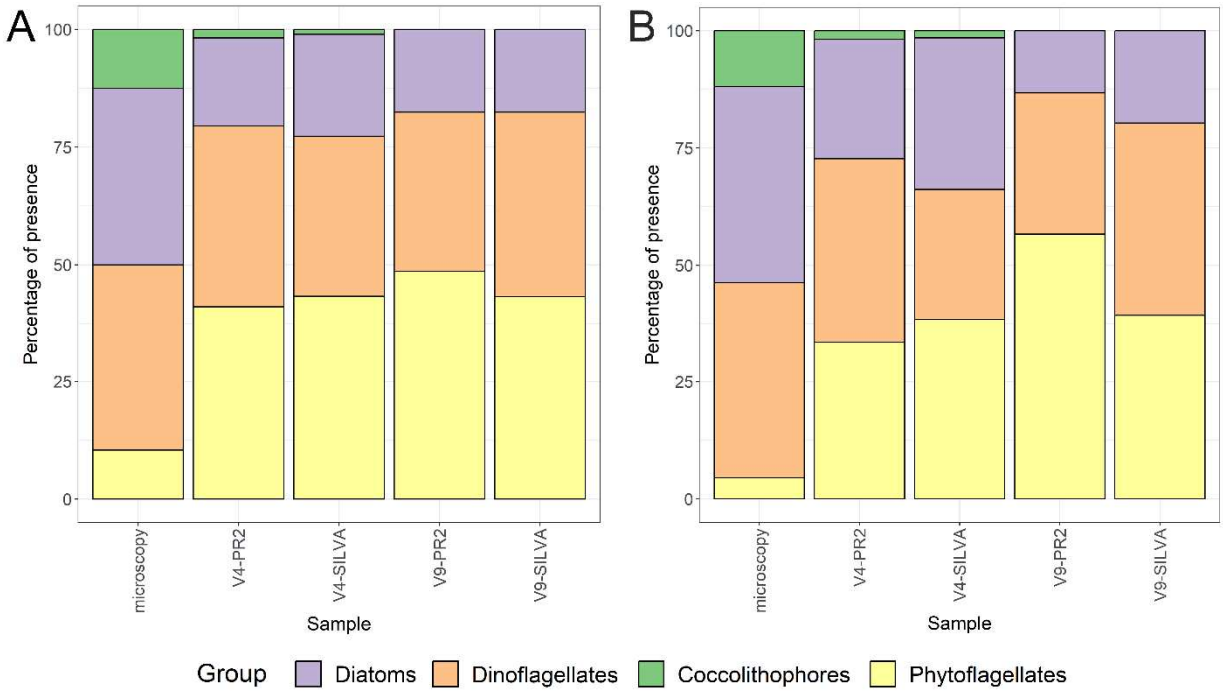

Fig. 2. Bar plots representing the percentages of presence of genera (A) and species (B) belonging to diatoms (violet), dinoflagellates (orange), coccolithophores (green) and phytoflagellates (yellow) obtained using the five applied approaches: microscopy, V4-PR2, V4-SILVA, V9-PR2 and V9-SILVA.

Genus identification

By combining microscopy and metabarcoding results, a total of 171 genera (Table S1) were recorded. Microscopy identified 48 genera, while metabarcoding identified 112 genera with V4-PR2, 97 with V4-SILVA, 75 with V9-PR2 and 75 with V9-SILVA.

The combination of microscopy, V4-PR2 and V4-SILVA resulted in a total of 151 genera. Among these, the following 24 genera (representing 16% of the total) were detected by all approaches (Fig. 3A): 13 diatoms (*Amphora*, *Asteromphalus*, *Cerataulina*, *Chaetoceros*, *Cyclotella*, *Leptocylindrus*, *Nitzschia*, *Pleurosigma*, *Proboscia*, *Pseudo-nitzschia*, *Skeletonema*, *Thalassionema*, *Thalassiosira*), 10 dinoflagellates (*Alexandrium*, *Akashiwo*, *Gonyaulax*, *Gymnodinium*, *Noctiluca*, *Phalacroma*, *Protoceratium*, *Protoperidinium*, *Scrippsiella*, *Tripos*), and 1 dictyochophycean (*Dictyocha*). Coccolithophores were not identified by all three approaches together. The number of genera identified by both microscopy and V4 metabarcoding was 6 (4%) and 2 (1%) with PR2 and SILVA, respectively, while V4-PR2 and V4-SILVA shared 50 genera (33%). Considering genera observed uniquely by one approach, 32 (21%) were detected only by V4-PR2, 21 (14%) by V4-SILVA, and 16 (11%) by microscopy.

Regarding microscopy, V9-PR2 and V9-SILVA, their combination led to a total of 125 genera. Among these, the following 17 genera (representing 14% of the total) were common among all approaches (Fig. 3B): 7 diatoms (*Chaetoceros*, *Cyclotella*, *Leptocylindrus*, *Pleurosigma*, *Pseudo-nitzschia*, *Skeletonema*, *Thalassiosira*), 9 dinoflagellates (*Alexandrium*, *Gonyaulax*, *Gymnodinium*, *Karenia*, *Noctiluca*, *Prorocentrum*, *Protoceratium*, *Protoperidinium*, *Tripos*), and 1 dictyochophycean (*Dictyocha*). No coccolithophore was identified by the three approaches together. No genera were identified by both microscopy and V9-PR2, while microscopy and V9-SILVA shared 4 genera (3%). V9-PR2 and V9-SILVA shared 35 genera (28%). Considering the genera that were observed uniquely by each approach, 27 genera (22%) was detected only by microscopy, 23 (18%) by V9-PR2 and 19 (15%) by V9-SILVA.

Metabarcoding based approaches (V4-PR2, V4-SILVA, V9-PR2, V9-SILVA) detected a high number of genera never revealed by microscopy analysis (Table S2), including naked dinoflagellates (e.g. *Grammatodinium*, *Gyrodiniellum*, *Karlodinium*, *Lebouridinium*, *Lepidodinium*, *Levanderina*, *Margalefidinium*, *Paragymnodinium*, *Proterythropsis*, *Polykrikos*, *Syltodinium*, *Torodinium*) and thecate dinoflagellates (e.g. *Archaeperidinium*, *Fragilidium*, *Heterodinium*, *Triadinium*). Moreover,

metabarcoding provided the best resolution for the phytoflagellate group, in particular 7 chrysophyceans (10.00% of total phytoflagellate diversity, mostly revealed by V4-SILVA), 7 dictyochophyceans (10.00%, mostly revealed by V4-PR2 and V4-SILVA), 7 mamiellophyceans (10.00%, mostly in V9-PR2), 6 chlorophyceans (8.57%, mostly in V4-PR2) and 6 cryptophyceans (8.57%, mostly found by V9-SILVA and V4-SILVA).

For those genera revealed microscopy but not by metabarcoding, primers for V4 and V9 regions of the 18S rRNA gene were checked and found to be suitable for them (i.e. no mismatches were observed or more rarely just single mismatches in the middle of the primers were detected).

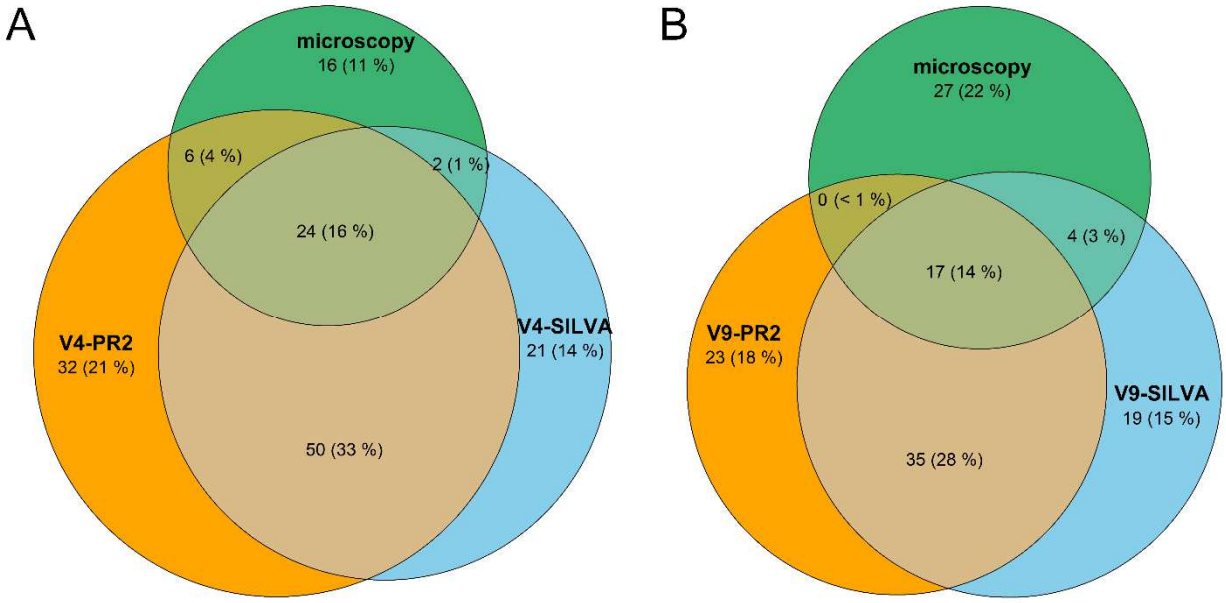

Fig. 3 Venn diagrams representing the number (and percentage) of shared and unique genera considering microscopy (green) and metabarcoding, using V4 (A) and V9 (B) 18S rRNA regions and PR2 (orange) and SILVA (blue) as reference databases for the taxonomic assignment.

Species identification

A total of 238 species (Table S2) were recorded combining microscopy and metabarcoding results. Microscopy identified 66 species, while metabarcoding identified 110 species with V4-PR2, 65 with V4-SILVA, 85 with V9-PR2 and 62 with V9-SILVA.

The combination of microscopy, V4-PR2 and V4-SILVA resulted in a total of 186 species, as depicted in the associated Venn diagram (Fig. 4A). The three approaches shared 7 species (4%): 3 diatoms (*Cerataulina pelagica*, *Chaetoceros affinis*, *Pseudo-nitzschia pseudodelicatissima*) and 4 dinoflagellates (*Akashiwo sanguinea*, *Noctiluca scintillans*, *Protoceratium reticulatum*, *Protoperidinium bipes*). Neither coccolithophores nor phytoflagellates were identified by all three approaches together. The number of species identified by both microscopy and V4 metabarcoding was 8 (4%) and 3 (2%) with PR2 and SILVA, respectively, while V4-PR2 and V4-SILVA shared 31 species (17%). Considering the species revealed uniquely by each approach, 48 (26%) were observed only using microscopy, 64 (35%) with V4-PR2 and 24 (13%) using V4-SILVA.

A total of 172 species were found combining microscopy, V9-PR2 and V9-SILVA. These three approaches shared 4 species (2%) (Fig. 4B), 1 diatom (*Chaetoceros affinis*) and 3 dinoflagellates (*Gonyaulax spinifera*, *Noctiluca scintillans* and *Protoceratium reticulatum*). Neither coccolithophores nor phytoflagellates were identified by all three approaches. The number of species shared by both microscopy and V9 metabarcoding was 2 (1%) and 5 (3%) with PR2 and SILVA, respectively, while V9-PR2 and V9-SILVA shared 26 (15%) species. Regarding the uniqueness of each approach, 55 species (32%) were revealed only by microscopy, 53 (31%) by V9-PR2 and 27 (16%) by V9-SILVA.

Metabarcoding based approaches (V4-PR2, V4-SILVA, V9-PR2, V9-SILVA) detected a high number of taxa not revealed by microscopy analysis (Table S2), including naked dinoflagellates (e.g. *Gymnodinium catenatum*, *Gymnodinium dorsalisulcum*, *Gymnodinium impudicum*, *Gymnodinium smaydae*, *Gyrodiniellum shiwhaense*, *Gyrodinium dominans*, *Gyrodinium fusiforme*, *Gyrodinium jinhaense*, *Karenia mikimotoi*, *Paragymnodinium shiwhaense*, *Polykrikos geminatus*, *Polykrikos hartmannii*, *Polykrikos kofoidii*, *Polykrikos schwartzii*), thecate dinoflagellates (e.g. *Alexandrium andersonii*, *Alexandrium catenella*, *Alexandrium hiranoi*, *Alexandrium insuetum*, *Alexandrium margalefii*, *Gonyaulax polygramma*, *Gonyaulax whaseongensis*) and phytoflagellates species, in particular 11 non-calcified coccolithophyceans (13.92%, particularly by V9-PR2), 10

mamiellophyceans (12.66%, V4-PR2 and V9-PR2), 9 pyramimonadophyceans (11.39%, particularly by V9-PR2), 7 dictyochophyceaens (8.86%, V9-PR2) and 7 cryptophyceaens (8.86%, mostly found by V4-SILVA).

For those species not revealed by metabarcoding but by microscopy, primers for V4 and V9 regions of the 18S rRNA gene were checked and found to be suitable for them (i.e. no mismatches were observed or more rarely just single mismatches in the middle of the primers were detected).

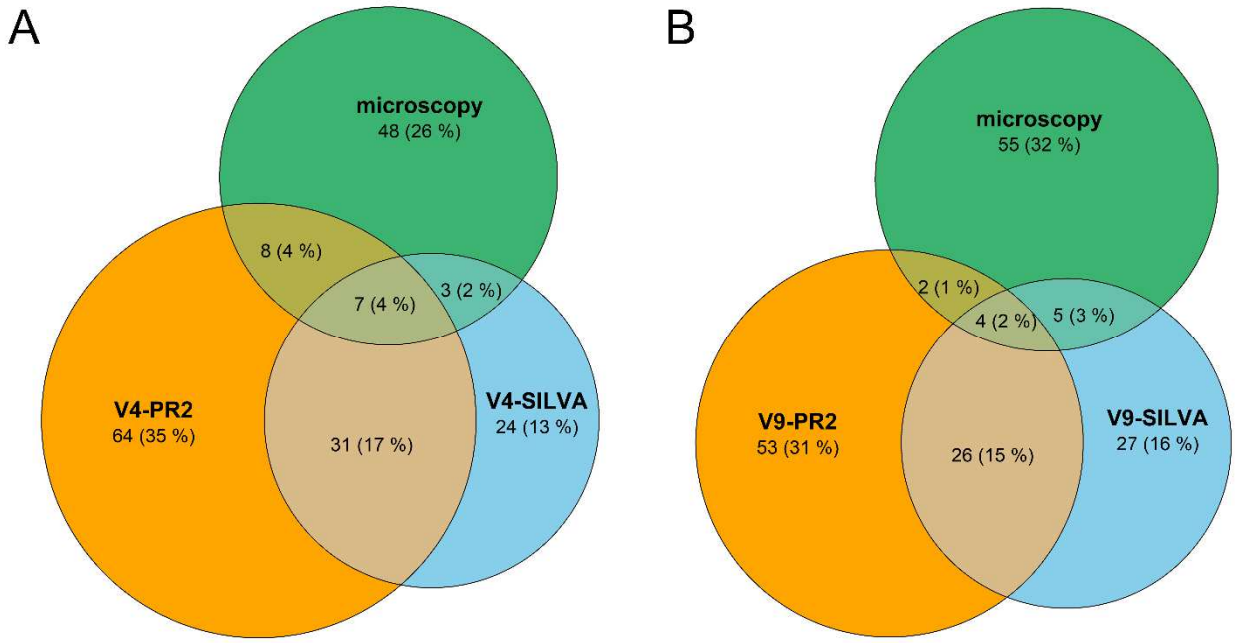

Fig. 4. Venn diagrams representing the number (and percentage) of shared and unique species considering microscopy (green) and metabarcoding, using V4 (A) and V9 (B) 18S rRNA regions and PR2 (orange) and SILVA (blue) as reference databases for the taxonomic assignment.

Phytoplankton communities

The results of the Non-Metric Multidimensional Scaling (NMDS), performed on the richness of genera and species in the different phytoplankton groups are shown in Fig. 5A and B, respectively.

In both cases, a clear divergence between microscopy and metabarcoding can be observed, while no clear difference was observed among approaches based on metabarcoding (V4-SILVA, V4-PR2, V9-SILVA and V9-PR2).

Considering the presence-absence of genera and species (Fig. S2A, B), a clear difference between microscopy and metabarcoding (V4-SILVA, V4-PR2, V9-SILVA and V9-PR2) is evident at both genus and species levels. At species level, a distinct difference is noticeable even within the metabarcoding approach between the two different markers, V4 (V4-SILVA and V4-PR2), and V9 (V9-SILVA and V9-PR2).

Comparing the five approaches, the PERMANOVA analysis highlighted significant differences among approaches, both considering the richness in the phytoplankton group and the presence-absence of genera ($p < 0.01$, $p < 0.001$, respectively) and species ($p < 0.001$).

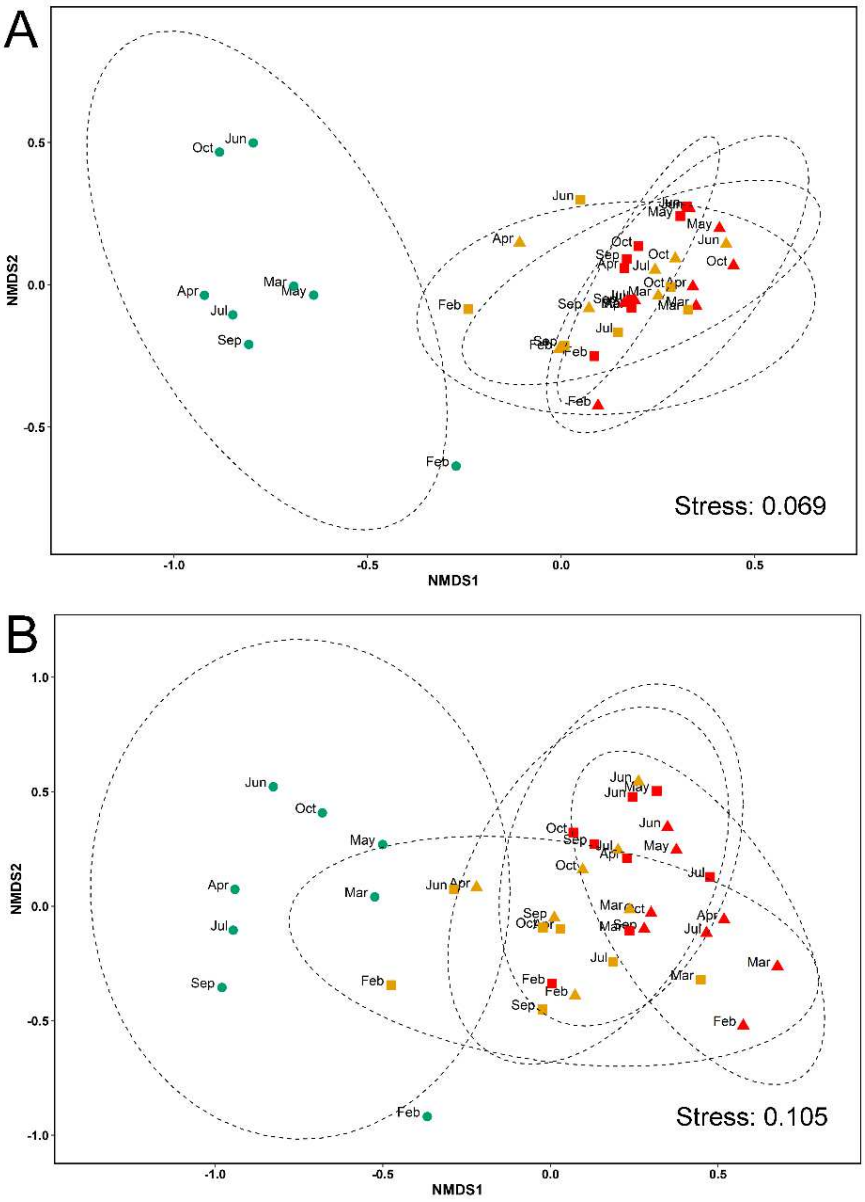

Fig. 5. NMDS performed on the richness of genera (A) and species (B) in the different phytoplankton groups of the five applied approaches: microscopy (green, ●), V4-SILVA (yellow, ■), V4-PR2 (yellow, ▲), V9-SILVA (red, ■) and V9-PR2 (red, ▲).

3.5 Discussion

In this study, we combined microscopy and metabarcoding results for the first time in our study area, revealing important differences between the methods. The phytoplankton community of the eLTER SG01 station has been investigated through microscopy since 1988, highlighting a high biodiversity, with 479 species overall identified (Neri et al., 2023; Totti et al., 2002, 2005, 2019). However,

metabarcoding, combining the two markers (V4 and V9 of 18S rRNA gene) and reference databases (PR2 and SILVA), revealed a previously unknown diversity, as 99 genera (8 diatoms, 32 dinoflagellates (mainly gymnodinioid forms), 1 coccolithophore, 58 phytoflagellates), and 151 species (23 diatoms, 50 dinoflagellates, 1 coccolithophore and 77 phytoflagellates) were recorded for the first time. The higher richness highlighted by the molecular method may be related to different reasons, as previously reported in other studies (Bilbao et al., 2023; Mordret et al., 2023; Pierce et al., 2023; Piredda et al., 2017; Santi et al., 2021). For some taxa, such as for the naked dinoflagellates or the raphidophytes that lack a cell wall, the formaldehyde fixation does alter the shape of the cell preventing the identification (Fiocca et al., 2014; Menden-Deuer and Lessard, 2001; Throndsen, 1978). Furthermore, some ultrastructural diagnostic characters can be distinguished only under the electron microscopy (scanning or transmission) analysis, which is not suitable in routine monitoring. This explains the new diversity found in the phytoflagellate group, as already observed in other areas (Almandoz et al., 2024), although with differences among the metabarcoding approaches.

In addition, it should be considered that the volume of subsamples processed in metabarcoding is much higher than in microscopy, which increases the probability of finding rare taxa (Bilbao et al., 2023; Gran-Stadniczeñko et al., 2019; Piredda et al., 2017). Indeed, in the microscopy analysis, the volume of the subsample settled for the observation (5 to 100 ml), and the portion of settling chamber analysed for counting (1–2 transect, 20–60 random fields) leads to analyse volumes actually much lower (0.05 to 2 ml) compared to metabarcoding that process a larger volume of seawater (2 L in the present study). Furthermore, as also reported by Mordret et al. (2023), some of the taxa that were recorded for the first time by metabarcoding were parasites and symbionts and thus not targeted in the microscopy analysis (e.g. *Pelagodinium bei*, *Blastodinium* spp., *Zooxanthella* spp.). Nevertheless, it has to be considered that, while microscopy could introduce errors related to the operator, the higher diversity inferred from metabarcoding could be inflated by errors arising from PCR and/or sequencing or the subsequent bioinformatic pipeline (e.g. false positives/negatives, artefactual variant diversity

estimates) (Behnke et al., 2011; Ershova et al., 2023; Marinchel et al., 2023; Preston et al., 2022; Santoferrara, 2019).

Despite the higher richness obtained by the combination of different markers (V4 and V9) and databases (PR2, SILVA), several genera (3 diatoms, 3 dinoflagellates, 4 coccolithophores and 4 phytoflagellates) and species (17 diatoms, 20 dinoflagellates, 6 coccolithophores and 3 phytoflagellates) were detected only using microscopy. Some of these taxa (e.g., most of the coccolithophores and all the *Oxytoxum* species) were found to be absent in the databases, underlying the need to implement the reference databases with new sequences, obtained from monoclonal cultures (Mordret et al., 2023; Piredda et al., 2017; Santi et al., 2021; Turk Dermastia et al., 2023; Tzafesta et al., 2022). Considering the taxa already present in the databases, but not detected by neither databases and markers, the reason could rely also on the fact that metabarcoding is based on universal primers, which could preferentially amplify other taxa (Kelly et al., 2019; Pawlowski et al., 2011; Stoeck et al., 2010), and on metabarcoding markers which could be similar in different taxa (Gran-Stadniczeñko et al., 2019; Mordret et al., 2018; Piganeau et al., 2011). In the present study, unsuitability of the primers should not be a reason for undetectability of taxa, as no multiple mismatches nor mismatches in critical positions, which could abolish amplification (Stadhouders et al., 2010), were found.

The higher richness obtained from metabarcoding is not observed for each 18S region and reference database in the same way, particularly at the species level. Indeed, the use of V4 and V9 led to identify a higher number of species than microscopy when combined with PR2 as database, but to a lower number of species when SILVA was used. Overall, the combination of V4, as 18S region, and PR2, as reference database, led to a higher diversity, both in terms of genera and species. Only a small component of the total richness was found to be in common to all the different methods and databases (15 genera and 3 species), while an important percentage of genera and species was detected uniquely in V4-PR2, V4-SILVA, V9-PR2, V9-SILVA or microscopy, highlighting that the combination of

different methods, markers and databases is necessary to have a more detailed information on the phytoplankton community composition.

The different "resolution" among the approaches (i.e. in general metabarcoding harvest more taxa than microscopy, but some groups are strongly overlooked by the former) strongly affects the phytoplankton group percent composition in terms of richness: using metabarcoding, the most diversified groups were phytoflagellates (considering genera) and phytoflagellates and dinoflagellates (considering species), while using microscopy, diatoms and dinoflagellates were more diversified. Moreover, metabarcoding failed to identify the majority of genera and species of coccolithophores, highlighting that relying solely on metabarcoding could overlook an important component of the phytoplankton community.

This suggests that the different methods, markers and databases do not always give the same information in terms of seasonal composition of the phytoplankton communities and thus that the two methods (microscopy and metabarcoding) should be combined to obtain a more detailed information on the community.

3.6 Conclusions

In conclusion, this study highlights the importance of combining microscopy and metabarcoding for a more comprehensive understanding of phytoplankton communities. Indeed, while microscopy analysis is still essential in the phytoplankton monitoring providing abundance and biomass values, metabarcoding represents a valid approach to implement the evaluation of phytoplankton diversity. In particular, metabarcoding certainly lead to recognise cryptic/pseudocryptic species and/or low-abundant (often potentially toxic) species. However, different regions and databases should still be combined with microscopy to have a more detailed information on the community and to counteract the drawbacks of metabarcoding.

Undoubtedly, the resolution provided by metabarcoding is constantly increasing thanks to the rapidity with which the molecular approach is improving. However, the metabarcoding approach still exhibits

significant gaps in the reference databases, especially for underrepresented groups such as coccolithophores. These gaps could be addressed by incorporating sequences of missing species, ideally obtained from the same type locality as in the original species description.

3.7 Acknowledgements

This study was supported by LifeWatch Italy through the project "LifeWatch 2019 LW_061121".

Authors acknowledge the staff of the Department of Bioscience, Biotechnology and Biopharmaceutics at Università degli Studi di Bari for sequencing. We are grateful to Federica Cerino (National Institute of Oceanography and Applied Geophysics, OGS) for her coordination and collaboration in providing fundings. We acknowledge the crews of the Actea oceanographic vessel involved in the sampling activities.

3.8 References

2008/56/EC. Directive 2008/56/EC of the European Parliament and of the Council of 17 June 2008 establishing a framework for community action in the field of marine environmental policy (Marine Strategy Framework Directive) (Text with EEA relevance).

Abad, D., Albaina, A., Aguirre, M., Laza-Martínez, A., Uriarte, I., Iriarte, A., Villate, F., Estonba, A., 2016. Is metabarcoding suitable for estuarine plankton monitoring? A comparative study with microscopy. Mar. Biol. 163, 1–13. https://doi.org/10.1007/s00227-016-2920-0

Almandoz, G.O., Fabro, E., Sprong, P., Mascioni, M., Antoni, J., Ferrario, M., Metfies, K., Barrera, F.M., 2024. Metabarcoding and microscopy characterization of phytoplankton from frontal areas of the Argentine Sea. Front. Mar. Sci. 10. https://doi.org/10.3389/fmars.2023.1306336

Andersson, A., Zhao, L., Brugel, S., Figueroa, D., Huseby, S., 2023. Metabarcoding vs Microscopy: comparison of methods to monitor phytoplankton communities. Water 3, 2671–2680. https://doi.org/10.1021/acsestwater.3c00176

Andrews, S., Braham Bioinformatics, 2010. FastQC: a quality control tool for high throughput sequence data. Available online at: https://www.bioinformatics.babraham.ac.uk/projects/fastqc/.

Araujo, G.S., Pacheco, D., Cotas, J., da Silva, J.W.A., Saboya, J., Moreira, R.T., Pereira, L., 2022. Plankton: environmental and economic importance for a sustainable future. In: Pereira, L., Gonçalves, A.M. (Eds.), *Plankton Communities*. IntechOpen, Rijeka, pp. 1–21. https://doi.org/10.5772/intechopen.100433

Behnke, A., Engel, M., Christen, R., Nebel, M., Klein, R.R., Stoeck, T., 2011. Depicting more accurate pictures of protistan community complexity using pyrosequencing of hypervariable SSU rRNA gene regions. Environ. Microbiol. 13, 340–349. https://doi.org/10.1111/j.1462-2920.2010.02332.x

Bernardi Aubry, F., Cossarini, G., Acri, F., Bastianini, M., Bianchi, F., Camatti, E., De Lazzari, A., Pugnetti, A., Solidoro, C., Socal, G., 2012. Plankton communities in the northern Adriatic Sea: patterns and changes over the last 30 years. Estuar. Coast. Shelf Sci. 115, 125–137. https://doi.org/https://doi.org/10.1016/j.ecss.2012.03.011

Bilbao, J., Pavloudi, C., Blanco-Rayón, E., Franco, J., Madariaga, I., Seoane, S., 2023. Phytoplankton community composition in relation to environmental variability in the Urdaibai estuary (SE Bay of Biscay): microscopy and eDNA metabarcoding. Mar. Environ. Res. 191, 106175. https://doi.org/10.1016/j.marenvres.2023.106175

Blanchard, J.L., Jennings, S., Holmes, R., Harle, J., Merino, G., Allen, J.I., Holt, J., Dulvy, N.K., Barange, M., 2012. Potential consequences of climate change for primary production and fish production in large marine ecosystems. Philos. Trans. R. Soc. B 367, 2979–2989. https://doi.org/10.1098/rstb.2012.0231

Bokulich, N.A., Kaehler, B.D., Rideout, J.R., Dillon, M., Bolyen, E., Knight, R., Huttley, G.A., Gregory Caporaso, J., 2018. Optimizing taxonomic classification of marker-gene amplicon sequences with QIIME 2's q2-feature-classifier plugin. Microbiome 6, 90. https://doi.org/10.1186/s40168-018-0470-z

Bolyen, E., Rideout, J.R., Dillon, M.R., Bokulich, N.A., Abnet, C.C., Al-Ghalith, G.A., Alexander, H., Alm, E.J., Arumugam, M., Asnicar, F., Bai, Y., Bisanz, J.E., Bittinger, K., Brejnrod, A., Brislawn, C.J., Brown, C.T., Callahan, B.J., Caraballo-Rodríguez, A.M., Chase, J., Cope, E.K., Da Silva, R., Diener, C., Dorrestein, P.C., Douglas, G.M., Durall, D.M., Duvallet, C., Edwardson, C.F., Ernst, M., Estaki, M., Fouquier, J., Gauglitz, J.M., Gibbons, S.M., Gibson, D.L., Gonzalez, A., Gorlick, K., Guo, J., Hillmann, B., Holmes, S., Holste, H., Huttenhower, C., Huttley, G.A., Janssen, S., Jarmusch, A.K., Jiang, L., Kaehler, B.D., Kang, K. Bin, Keefe, C.R., Keim, P., Kelley, S.T., Knights, D., Koester, I., Kosciolek, T., Kreps, J., Langille, M.G.I., Lee, J., Ley, R., Liu, Y.X., Loftfield, E., Lozupone, C., Maher, M., Marotz, C., Martin, B.D., McDonald, D., McIver, L.J., Melnik, A. V., Metcalf, J.L., Morgan, S.C., Morton, J.T., Naimey, A.T., Navas-Molina, J.A., Nothias, L.F., Orchanian, S.B., Pearson, T., Peoples, S.L., Petras, D., Preuss, M.L., Pruesse, E., Rasmussen, L.B., Rivers, A., Robeson, M.S., Rosenthal, P., Segata, N., Shaffer, M., Shiffer, A., Sinha, R., Song, S.J., Spear, J.R., Swafford, A.D., Thompson, L.R., Torres, P.J., Trinh, P., Tripathi, A., Turnbaugh, P.J., Ul-Hasan, S., van der Hooft, J.J.J., Vargas, F., Vázquez-Baeza, Y., Vogtmann, E., von Hippel, M., Walters, W., Wan, Y., Wang, M., Warren, J., Weber, K.C., Williamson, C.H.D., Willis, A.D., Xu, Z.Z., Zaneveld, J.R., Zhang, Y., Zhu, Q., Knight, R., Caporaso, J.G., 2019. Reproducible, interactive, scalable and extensible microbiome data science using QIIME 2. Nat. Biotechnol. 37, 852–857. https://doi.org/10.1038/s41587-019-0209-9

Callahan, B.J., McMurdie, P.J., Rosen, M.J., Han, A.W., Johnson, A.J.A., Holmes, S.P., 2016. DADA2: high-resolution sample inference from Illumina amplicon data. Nat. Methods 13, 581–583. https://doi.org/10.1038/nmeth.3869

Caracciolo, M., Rigaut-Jalabert, F., Romac, S., Mahé, F., Forsans, S., Gac, J.P., Arsenieff, L., Manno, M., Chaffron, S., Cariou, T., Hoebeke, M., Bozec, Y., Goberville, E., Le Gall, F., Guilloux, L., Baudoux, A.C., de Vargas, C., Not, F., Thiébaut, E., Henry, N., Simon, N., 2022. Seasonal dynamics of marine protist communities in tidally mixed coastal waters. Mol. Ecol. 31, 3761–3783. https://doi.org/10.1111/mec.16539

Cerino, F., Fornasaro, D., Kralj, M., Giani, M., Cabrini, M., 2019. Phytoplankton temporal dynamics in the coastal waters of the north-eastern Adriatic Sea (Mediterranean Sea) from 2010 to 2017. Nat. Conserv. 34, 343–372. https://doi.org/10.3897/natureconservation.34.30720

Chen, H., Boutros, P.C., 2011. VennDiagram: a package for the generation of highly-customizable Venn and Euler diagrams in R. BMC Bioinformatics 12, 35. https://doi.org/10.1186/1471-2105-12-35

Cozzi, S., Cabrini, M., Kralj, M., De Vittor, C., Celio, M., Giani, M., 2020. Climatic and anthropogenic impacts on environmental conditions and phytoplankton community in the Gulf of Trieste (Northern Adriatic Sea). Water 12(9) 2652. https://doi.org/10.3390/w12092652

D'Ortenzio, F., Ribera d'Alcalà, M., 2009. On the trophic regimes of the Mediterranean Sea: a satellite analysis. Biogeosciences 5, 139–148. https://doi.org/10.5194/bgd-5-2959-2008.

Edler, L., Elbrachter, M., 2010. The Utermöhl method for quantitative phytoplankton analysis. In: Karlson, B., Cusack, C., Bresnan, E. (Eds.), *Microscopic and molecular methods for quantitative phytoplankton analysis*. IOC UNESCO, Manuals and Guides 55, pp. 13–20.

Ershova, E.A., Wangensteen, O.S., Falkenhaug, T., 2023. Mock samples resolve biases in diversity estimates and quantitative interpretation of zooplankton metabarcoding data. Mar. Biodivers. 53, 66. https://doi.org/10.1007/s12526-023-01372-x

Esenkulova, S., Sutherland, B.J.G., Tabata, A., Haigh, N., Pearce, C.M., Miller, K.M., 2020. Operational taxonomic unit comparing metabarcoding and morphological approaches to identify phytoplankton taxa associated with harmful algal blooms. Facets 5, 784–811. https://doi.org/10.1139/FACETS-2020-0025

Falkowski, P., 2012. Ocean Science: The power of plankton. Nature 483, S17–S20. https://doi.org/10.1038/483S17a

Fiocca, A., Vadrucci, M.R., Mazziotti, C., 2014. Influence of chemical fixative on the cell size of phytoplankton guilds. Transit. Waters Bull. 8(1), 1–9. https://doi.org/10.1285/i1825229Xv8n1p1

Francé, J., Varkitzi, I., Stanca, E., Cozzoli, F., Skejić, S., Ungaro, N., Vascotto, I., Mozetič, P., Ninčević Gladan, Ž., Assimakopoulou, G., Pavlidou, A., Zervoudaki, S., Pagou, K., Basset, A., 2021. Large-scale testing of phytoplankton diversity indices for environmental assessment in Mediterranean sub-regions (Adriatic, Ionian and Aegean Seas). Ecol. Indic. 126. https://doi.org/10.1016/j.ecolind.2021.107630

Gaonkar, C.C., Campbell, L., 2023. Metabarcoding reveals high genetic diversity of harmful algae in the coastal waters of Texas, Gulf of Mexico. Harmful Algae 121. https://doi.org/10.1016/j.hal.2022.102368

Gaonkar, C.C., Piredda, R., Sarno, D., Zingone, A., Montresor, M., Kooistra, W.H.C.F., 2020. Species detection and delineation in the marine planktonic diatoms *Chaetoceros* and *Bacteriastrum* through metabarcoding: making biological sense of haplotype diversity. Environ. Microbiol. 22, 1917–1929. https://doi.org/10.1111/1462-2920.14984

Gran-Stadniczeñko, S., Egge, E., Hostyeva, V., Logares, R., Eikrem, W., Edvardsen, B., 2019. Protist diversity and seasonal dynamics in Skagerrak plankton communities as revealed by metabarcoding and microscopy. J. Eukaryot. Microbiol. 66, 494–513. https://doi.org/10.1111/jeu.12700

Grižančić, L., Baričević, A., Tanković, M.S., Vlašiček, I., Knjaz, M., Podolšak, I., Kogovšek, T., Pfannkuchen, M.A., Pfannkuchen, D.M., 2023. A metabarcode based (species) inventory of the northern Adriatic phytoplankton. Biodivers. Data J. 11, e106947. https://doi.org/10.3897/BDJ.11.E106947

Guillou, L., Bachar, D., Audic, S., Bass, D., Berney, C., Bittner, L., Boutte, C., Burgaud, G., de Vargas, C., Decelle, J., del Campo, J., Dolan, J.R., Dunthorn, M., Edvardsen, B., Holzmann, M., Kooistra, W.H.C.F., Lara, E., Le Bescot, N., Logares, R., Mahé, F., Massana, R., Montresor, M., Morard,

R., Not, F., Pawlowski, J., Probert, I., Sauvadet, A.-L., Siano, R., Stoeck, T., Vaulot, D., Zimmermann, P., Christen, R., 2013. The Protist Ribosomal Reference database (PR2): a catalog of unicellular eukaryote Small Sub-Unit rRNA sequences with curated taxonomy. Nucleic Acids Res. 41, D597–D604. https://doi.org/10.1093/nar/gks1160

Guiry, M.D., Guiry, G.M., 2024. AlgaeBase. World-wide electronic publication, National University of Ireland, Galway. https://www.algaebase.org.

Hays, G.C., Richardson, A.J., Robinson, C., 2005. Climate change and marine plankton. Trends Ecol. Evol. 20, 337–344. https://doi.org/10.1016/j.tree.2005.03.004

Kelly, R.P., Shelton, A.O., Gallego, R., 2019. Understanding PCR processes to draw meaningful conclusions from environmental DNA studies. Sci. Rep. 9, 12133. https://doi.org/10.1038/s41598-019-48546-x

Larsson, J., 2022. eulerr: area-proportional Euler and Venn Diagrams with ellipses. R package version 7.0.0.

Marić, D., Kraus, R., Godrijan, J., Supić, N., Djakovac, T., Precali, R., 2012. Phytoplankton response to climatic and anthropogenic influences in the north-eastern Adriatic during the last four decades. Estuar. Coast. Shelf Sci. 115, 98–112. https://doi.org/10.1016/j.ecss.2012.02.003

Marinchel, N., Marchesini, A., Nardi, D., Girardi, M., Casabianca, S., Vernesi, C., Penna, A., 2023. Mock community experiments can inform on the reliability of eDNA metabarcoding data: a case study on marine phytoplankton. Sci. Rep. 13, 20164. https://doi.org/10.1038/s41598-023-47462-5

Martin, M., 2011. Cutadapt removes adapter sequences from high-throughput sequencing reads. EMBnet.Journal 17, 10–12.

McMurdie, P.J., Holmes, S., 2013. Phyloseq: An R package for reproducible interactive analysis and graphics of microbiome census data. PLoS One 8(4), e61217. https://doi.org/10.1371/journal.pone.0061217

McQuatters-Gollop, A., Atkinson, A., Aubert, A., Bedford, J., Best, M., Bresnan, E., Cook, K., Devlin, M., Gowen, R., Johns, D.G., Machairopoulou, M., McKinney, A., Mellor, A., Ostle, C., Scherer, C., Tett, P., 2019. Plankton lifeforms as a biodiversity indicator for regional-scale assessment of pelagic habitats for policy. Ecol. Indic. 101, 913–925. https://doi.org/10.1016/j.ecolind.2019.02.010

Menden-Deuer, S., Lessard, E.J., 2001. Effect of preservation on dinoflagellate and diatom cell volume and consequences for carbon biomass predictions. Mar. Ecol. Prog. Ser. 222, 41–50.

Mordret, S., Piredda, R., Vaulot, D., Montresor, M., Kooistra, W.H.C.F., Sarno, D., 2018. dinoref: A curated dinoflagellate (Dinophyceae) reference database for the 18S rRNA gene. Mol. Ecol. Resour. 18, 974–987. https://doi.org/https://doi.org/10.1111/1755-0998.12781

Mordret, S., Piredda, R., Zampicinini, G., Kooistra, W.H.C.F., Zingone, A., Montresor, M., Sarno, D., 2023. Metabarcoding reveals marked seasonality and a distinctive winter assemblage of dinoflagellates at a coastal LTER site in the Gulf of Naples. Mar. Ecol. 44(3), e12758. https://doi.org/10.1111/maec.12758

Mozetič, P., Solidoro, C., Cossarini, G., Socal, G., Precali, R., Francé, J., Bianchi, F., De Vittor, C., Smodlaka, N., Fonda Umani, S., 2010. Recent trends towards oligotrophication of the northern Adriatic: evidence from chlorophyll a time series. Estuaries Coasts 33, 362–375. https://doi.org/10.1007/s12237-009-9191-7

Naselli-Flores, L., Padisák, J., 2023. Ecosystem services provided by marine and freshwater phytoplankton. Hydrobiologia 850, 2691–2706. https://doi.org/10.1007/s10750-022-04795-y

Neri, F., Romagnoli, T., Accoroni, S., Campanelli, A., Marini, M., Grilli, F., Totti, C., 2022. Phytoplankton and environmental drivers at a long-term offshore station in the northern Adriatic Sea (1988–2018). Cont. Shelf Res. 242, 104746. https://doi.org/10.1016/j.csr.2022.104746

Neri, F., Romagnoli, T., Accoroni, S., Ubaldi, M., Garzia, A., Pizzuti, A., Campanelli, A., Grilli, F., Marini, M., Totti, C., 2023. Phytoplankton communities in a coastal and offshore stations of the northern Adriatic Sea approached by network analysis and different statistical descriptors. Estuar. Coast. Shelf Sci. 282, 108224. https://doi.org/10.1016/j.ecss.2023.108224

Oksanen, J., Simpson, G.L., Blanchet, F.G., Kindt, R., Legendre, P., Minchin, P.R., O'Hara, R.B., Solymos, P., Stevens, M.H.H., Szoecs, E., Wagner, H., Barbour, M., Bedward, M., Bolker, B., Borcard, D., Carvalho, G., Chirico, M., De Caceres, M., Durand, S., Evangelista, H.B.A., FitzJohn, R., Friendly, M., Furneaux, B., Hannigan, G., Hill, M.O., Lahti, L., McGlinn, D., Ouellette, M.-H., Ribeiro Cunha, E., Smith, T., Stier, A., Ter Braak, C.J.F., Weedon, J., 2022. vegan: Community Ecology Package. R package version 2.6-2. https://CRAN.R-project.org/package=vegan

Pawlowski, J., Christen, R., Lecroq, B., Bachar, D., Shahbazkia, H.R., Amaral-Zettler, L., Guillou, L., 2011. Eukaryotic richness in the abyss: insights from pyrotag sequencing. PLoS One 6(4), e18169. https://doi.org/10.1371/journal.pone.0018169

Penna, A., Casabianca, S., Guerra, A.F., Vernesi, C., Scardi, M., 2017. Analysis of phytoplankton assemblage structure in the Mediterranean Sea based on high-throughput sequencing of partial 18S rRNA sequences. Mar. Genomics 36, 49–55. https://doi.org/10.1016/j.margen.2017.06.001

Pierce, E., Torano, O., Lin, Y.Y., Schnetzer, A., Marchetti, A., 2023. Comparison of advanced methodologies for diatom identification within dynamic coastal communities. Limnol. Oceanogr. Methods 21, 687–702. https://doi.org/10.1002/lom3.10575

Piganeau, G., Eyre-Walker, A., Grimsley, N., Moreau, H., 2011. How and why DNA barcodes underestimate the diversity of microbial eukaryotes. PLoS One 6(2), e16342. https://doi.org/10.1371/journal.pone.0016342

Pinto, A., Botelho, M.J., Churro, C., Asselman, J., Pereira, P., Pereira, J.L., 2023. A review on aquatic toxins - Do we really know it all regarding the environmental risk posed by phytoplankton neurotoxins? J. Environ. Manag. 345, 118769. https://doi.org/https://doi.org/10.1016/j.jenvman.2023.118769

Piredda, R., Claverie, J.M., Decelle, J., de Vargas, C., Dunthorn, M., Edvardsen, B., Eikrem, W., Forster, D., Kooistra, W.H.C.F., Logares, R., Massana, R., Montresor, M., Not, F., Ogata, H., Pawlowski, J., Romac, S., Sarno, D., Stoeck, T., Zingone, A., 2018. Diatom diversity through HTS-metabarcoding in coastal European seas. Sci. Rep. 8, 18059. https://doi.org/10.1038/s41598-018-36345-9

Piredda, R., Tomasino, M.P., D'Erchia, A.M., Manzari, C., Pesole, G., Montresor, M., Kooistra, W.H.C.F., Sarno, D., Zingone, A., 2017. Diversity and temporal patterns of planktonic protist assemblages at a Mediterranean Long Term Ecological Research site. FEMS Microbiol. Ecol. 93(1), fiw200. https://doi.org/10.1093/femsec/fiw200

Preston, M., Fritzsche, M., Woodcock, P., 2022. JNCC Report understanding and mitigating errors and biases in metabarcoding: an introduction for non-specialists. JNCC Report 699.

Quast, C., Pruesse, E., Yilmaz, P., Gerken, J., Schweer, T., Yarza, P., Peplies, J., Glöckner, F.O., 2013. The SILVA ribosomal RNA gene database project: improved data processing and web-based tools. Nucleic Acids Res. 41(D1), D590–D596. https://doi.org/10.1093/nar/gks1219

R Core Team, 2021. R: A language and environment for statistical computing.

Rombouts, I., Simon, N., Aubert, A., Cariou, T., Feunteun, E., Guérin, L., Hoebeke, M., McQuatters-Gollop, A., Rigaut-Jalabert, F., Artigas, L.F., 2019. Changes in marine phytoplankton diversity: assessment under the Marine Strategy Framework Directive. Ecol. Indic. 102, 265–277. https://doi.org/10.1016/j.ecolind.2019.02.009

Santi, I., Kasapidis, P., Karakassis, I., Pitta, P., 2021. A comparison of DNA metabarcoding and microscopy methodologies for the study of aquatic microbial eukaryotes. Diversity 13(5), 180. https://doi.org/10.3390/d13050180

Santoferrara, L.F., 2019. Current practice in plankton metabarcoding: optimization and error management. J. Plankton Res. 41, 571–582. https://doi.org/10.1093/plankt/fbz041

Specchia, V., Zangaro, F., Tzafesta, E., Saccomanno, B., Vadrucci, M.R., Pinna, M., 2023. Environmental DNA detects biodiversity and ecological features of phytoplankton communities in Mediterranean transitional waters. Sci. Rep. 13, 15192. https://doi.org/10.1038/s41598-023-42389-3

Stadhouders, R., Pas, S.D., Anber, J., Voermans, J., Mes, T.H.M., Schutten, M., 2010. The effect of primer-template mismatches on the detection and quantification of nucleic acids using the 5′ Nuclease Assay. J. Mol. Diagn. 12(1), 109–117, https://doi.org/10.2353/jmoldx.2010.090035

Stoeck, T., Bass, D., Nebel, M., Christen, R., Jones, M.D.M., Breiner, H.W., Richards, T.A., 2010. Multiple marker parallel tag environmental DNA sequencing reveals a highly complex eukaryotic community in marine anoxic water. Mol. Ecol. 19, 21–31. https://doi.org/10.1111/j.1365-294X.2009.04480.x

Struck, T.H., Feder, J.L., Bendiksby, M., Birkeland, S., Cerca, J., Gusarov, V.I., Kistenich, S., Larsson, K.H., Liow, L.H., Nowak, M.D., Stedje, B., Bachmann, L., Dimitrov, D., 2017. Finding evolutionary processes hidden in cryptic species. Trends Ecol. Evol. 33, 153–163. https://doi.org/10.1016/j.tree.2017.11.007

Throndsen, J., 1978. Preservation and storage. In: Sournia, A. (Ed.), *Phytoplankton manual. Monographs on oceanographic methodology*. UNESCO, Paris, pp. 69–74.

Totti, C., Cucchiari, E.M., Romagnoli, T., 2002. Intra and interannual variability of phytoplankton in coastal area of Senigallia (northern Adriatic Sea) from 1988 to 2000. Biol. Mar. Mediterr. 9, 391–399.

Totti, C., Cangini, M., Ferrari, C., Kraus, R., Pompei, M., Pugnetti, A., Romagnoli, T., Vanucci, S., Socal, G., 2005. Phytoplankton size-distribution and community structure in relation to mucilage occurrence in the northern Adriatic Sea. Sci. Total Environ. 353, 204–217. https://doi.org/10.1016/J.SCITOTENV.2005.09.028

Totti, C., Romagnoli, T., Accoroni, S., Coluccelli, A., Pellegrini, M., Campanelli, A., Grilli, F., Marini, M., 2019. Phytoplankton communities in the northwestern Adriatic Sea: Interdecadal variability over a 30-years period (1988–2016) and relationships with meteoclimatic drivers. J. Mar. Syst. 193, 137–153. https://doi.org/10.1016/j.jmarsys.2019.01.007

Turk Dermastia, T., Vascotto, I., Francé, J., Stanković, D., Mozetič, P., 2023. Evaluation of the rbcL marker for metabarcoding of marine diatoms and inference of population structure of selected genera. Front. Microbiol. 14, 1071379.https://doi.org/10.3389/fmicb.2023.1071379

Tweddle, J.F., Gubbins, M., Scott, B.E., 2018. Should phytoplankton be a key consideration for marine management? Mar. Policy 97, 1–9. https://doi.org/10.1016/j.marpol.2018.08.026

Tzafesta, E., Saccomanno, B., Zangaro, F., Vadrucci, M.R., Specchia, V., Pinna, M., 2022. DNA barcode gap analysis for multiple marker genes for phytoplankton species biodiversity in Mediterranean aquatic ecosystems. Biology 11, 1277. https://doi.org/10.3390/biology11091277

Vallina, S.M., Simó, R., 2007. Strong relationship between DMS and the solar radiation dose over the global surface ocean. Science 315, 506–508. https://doi.org/10.1126/science.1133680

Varkitzi, I., Francé, J., Basset, A., Cozzoli, F., Stanca, E., Zervoudaki, S., Giannakourou, A., Assimakopoulou, G., Venetsanopoulou, A., Mozetič, P., Tinta, T., Skejic, S., Vidjak, O., Cadiou, J.F., Pagou, K., 2018. Pelagic habitats in the Mediterranean Sea: a review of Good Environmental Status (GES) determination for plankton components and identification of gaps and priority needs to improve coherence for the MSFD implementation. Ecol. Indic. 95, 203–218. https://doi.org/10.1016/j.ecolind.2018.07.036

Vascotto, I., Mozetič, P., Francé, J., 2021. Phytoplankton Time-Series in a LTER site of the Adriatic Sea: methodological approach to decipher community structure and indicative taxa. Water 13, 2045. https://doi.org/10.3390/w13152045

Wasmund, N., Kownacka, J., Göbel, J., Jaanus, A., Johansen, M., Jurgensone, I., Lehtinen, S., Powilleit, M., 2017. The diatom/dinoflagellate index as an indicator of ecosystem changes in the Baltic Sea 1. principle and handling instruction. Front. Mar. Sci. 4, 22. https://doi.org/10.3389/FMARS.2017.00022

Weigand, H., Beermann, A.J., Čiampor, F., Costa, F.O., Csabai, Z., Duarte, S., Geiger, M.F., Grabowski, M., Rimet, F., Rulik, B., Strand, M., Szucsich, N., Weigand, A.M., Willassen, E., Wyler, S.A., Bouchez, A., Borja, A., Čiamporová-Zaťovičová, Z., Ferreira, S., Dijkstra, K.-D.B., Eisendle, U., Freyhof, J., Gadawski, P., Graf, W., Haegerbaeumer, A., van der Hoorn, B.B., Japoshvili, B., Keresztes, L., Keskin, E., Leese, F., Macher, J.N., Mamos, T., Paz, G., Pešić, V., Pfannkuchen, D.M., Pfannkuchen, M.A., Price, B.W., Rinkevich, B., Teixeira, M.A.L., Várbíró, G., Ekrem, T., 2019. DNA barcode reference libraries for the monitoring of aquatic biota in Europe: gap-analysis and recommendations for future work. Sci. Total Environ. 678, 499–524. https://doi.org/https://doi.org/10.1016/j.scitotenv.2019.04.247

Ye, J., Coulouris, G., Zaretskaya, I., Cutcutache, I., Rozen, S., Madden, T.L., 2012. Primer-BLAST: a tool to design target-specific primers for polymerase chain reaction. BMC bioinformatics, 13, 134. https://doi.org/10.1186/1471-2105-13-134

Zenetos, A., Gofas, S., Verlaque, M., Cinar, M.E., Garcia Raso, J.E., Bianchi, C.N., Morri, C., Azzurro, E., Bilecenoglu, M., Froglia, C., Siokou, I., Violanti, D., Sfriso, A., San Martin, G., Giangrande, A., Katagan, T., Ballesteros, E., Ramos-Espla, A.A., Mastrototaro, F., Ocana, O., Zingone, A., Gambi, M.C., Streftaris, N., 2010. Alien species in the Mediterranean Sea by 2010. A contribution to the application of European Union's Marine Strategy Framework Directive (MSFD). Part I. Spatial distribution. Mediterr. Mar. Sci. 11(2), 381. https://doi.org/10.12681/mms.87

3.8 Supplementary materials

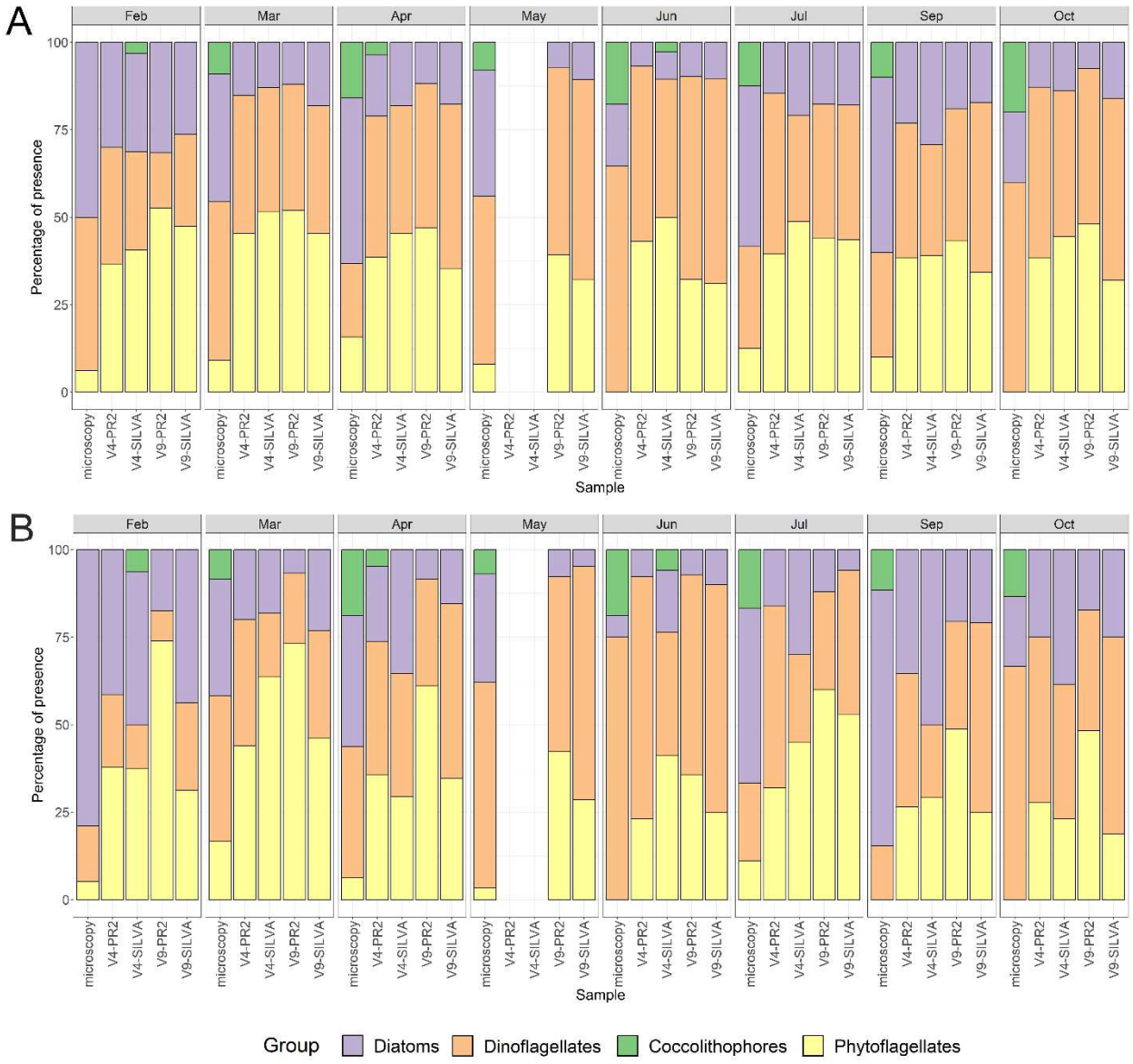

Fig. S1. Bar plots representing the percentages of presence of genera (A) and species (B) belonging to diatoms (violet), dinoflagellates (orange), coccolithophores (green) and phytoflagellates (yellow) obtained using the five applied approaches (microscopy, V4-PR2, V4-SILVA, V9-PR2 and V9-SILVA) in the different sampling months (Feb = February, Mar = March, Apr = April, May, Jun = June, Jul = July, Sep = September, Oct = October).

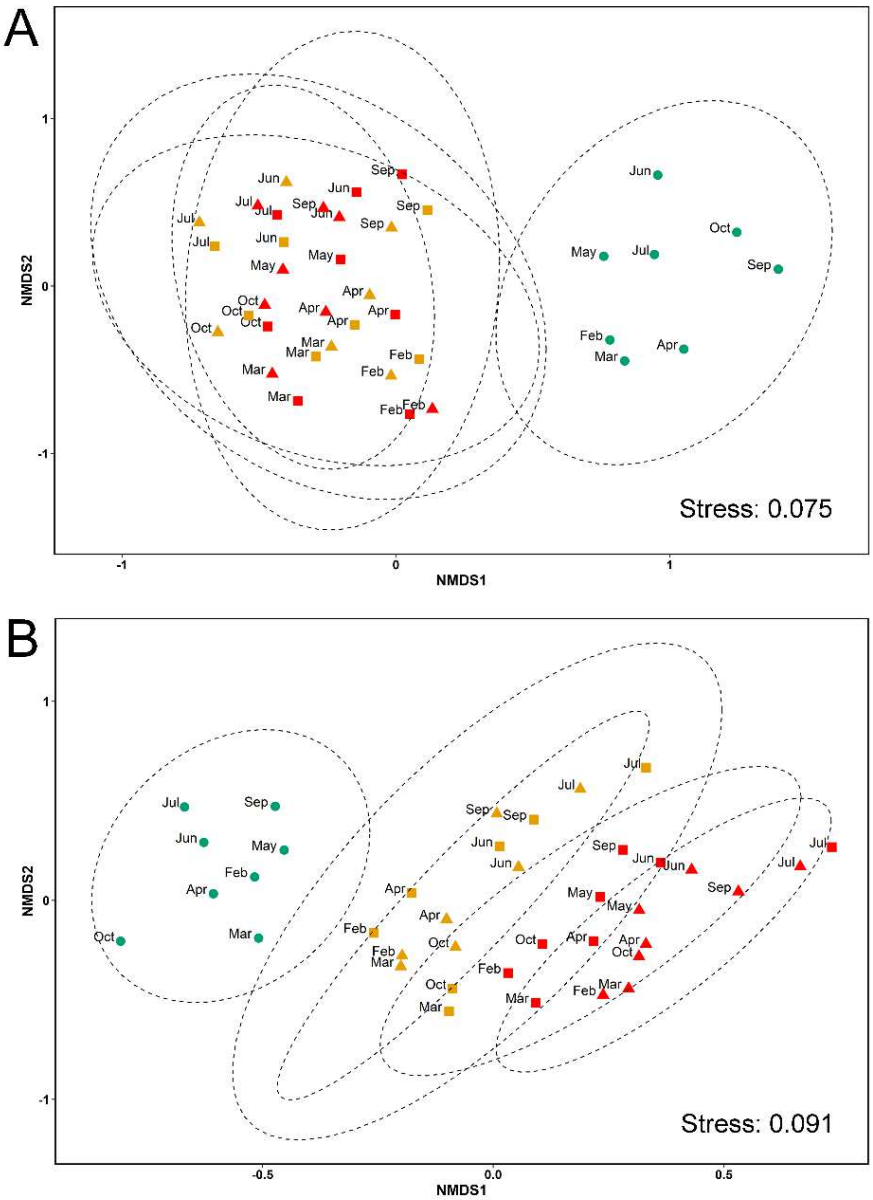

Fig. S2. NMDS performed on the presence-absence genera (A) and species (B) on the five applied approaches: microscopy (green, ●), V4-SILVA (yellow, ■), V4-PR2 (yellow, ▲), V9-SILVA (red, ■) and V9-PR2 (red, ▲).

Table S1. List of genera detected combining microscopy and metabarcoding using V4 and V9 as 18S regions, and PR2 and SILVA as reference databases (V4-PR2, V9-PR2, V4-SILVA, V9-SILVA).

Group	Genus	Method of detection
Dinoflagellates	*Akashiwo*	V4-PR2, V4-SILVA, microscopy
Dinoflagellates	*Alexandrium*	V4-PR2, V4-SILVA, microscopy, V9-PR2, V9-SILVA
Coccolithophores	*Algirosphaera*	V4-PR2
Dinoflagellates	*Amphidinium*	V4-SILVA
Diatoms	*Amphora*	V4-PR2, V4-SILVA, microscopy
Dinoflagellates	*Ansanella*	V4-PR2, V9-PR2
Dinoflagellates	*Archaeperidinium*	V4-PR2, V4-SILVA, V9-PR2, V9-SILVA
Diatoms	*Arcocellulus*	V4-SILVA
Diatoms	*Asteromphalus*	V4-PR2, V4-SILVA, microscopy
Phytoflagellates	*Aureococcus*	V4-PR2, V4-SILVA, V9-SILVA
Dinoflagellates	*Azadinium*	V4-SILVA
Diatoms	*Bacteriastrum*	microscopy
Phytoflagellates	*Bathycoccus*	V4-PR2, V4-SILVA
Phytoflagellates	*Bicosoeca*	V9-PR2
Dinoflagellates	*Biecheleria*	V4-PR2, V4-SILVA, V9-PR2, V9-SILVA
Dinoflagellates	*Biecheleriopsis*	V4-PR2, V9-PR2
Phytoflagellates	*Bigelowiella*	V9-SILVA
Dinoflagellates	*Blastodinium*	V4-PR2, V9-PR2
Dinoflagellates	*Blixaea*	V4-PR2, V4-SILVA
Phytoflagellates	*Bolidomonas*	V4-SILVA, V9-SILVA
Coccolithophores	*Calciosolenia*	microscopy
Coccolithophores	*Calyptrosphaera*	microscopy
Diatoms	*Ceratanaulus*	V9-PR2
Diatoms	*Cerataulina*	V4-PR2, V4-SILVA, microscopy
Diatoms	*Chaetoceros*	V4-PR2, V4-SILVA, microscopy, V9-PR2, V9-SILVA
Phytoflagellates	*Chattonella*	V4-PR2, V4-SILVA, V9-SILVA
Phytoflagellates	*Chlamydomonas*	V4-PR2, V4-SILVA
Phytoflagellates	*Chlorarachnion*	V4-PR2, V9-PR2, V9-SILVA
Phytoflagellates	*Chlorochytrium*	V9-SILVA
Phytoflagellates	*Chlorococcum*	V4-PR2
Phytoflagellates	*Chloroidium*	V4-PR2, V9-PR2, V9-SILVA
Phytoflagellates	*Chrysochromulina*	V4-PR2, V4-SILVA, V9-PR2
Phytoflagellates	*Chrysoculter*	V4-SILVA
Phytoflagellates	*Chrysolepidomonas*	V4-PR2, V4-SILVA
Phytoflagellates	*Chrysoxys*	V4-SILVA
Dinoflagellates	*Cochlodinium*	microscopy, V9-SILVA
Diatoms	*Cyclotella*	V4-PR2, V4-SILVA, microscopy, V9-PR2, V9-SILVA
Diatoms	*Cylindrotheca*	V4-SILVA, microscopy
Phytoflagellates	*Cymbomonas*	V4-PR2, V9-PR2, V9-SILVA
Diatoms	*Dactyliosolen*	microscopy
Phytoflagellates	*Desmodesmus*	V4-PR2, V9-PR2, V9-SILVA
Phytoflagellates	*Dictyocha*	V4-PR2, V4-SILVA, microscopy, V9-PR2, V9-SILVA
Phytoflagellates	*Dinobryon*	microscopy
Dinoflagellates	*Dinophysis*	V4-PR2, microscopy
Dinoflagellates	*Diplopsalis*	microscopy

Phytoflagellates	*Dolichomastix*	V4-PR2, V4-SILVA, V9-PR2, V9-SILVA
Coccolithophores	*Emiliania*	V4-SILVA, microscopy
Phytoflagellates	*Epipyxis*	V4-SILVA
Dinoflagellates	*Erythropsidinium*	V4-SILVA
Phytoflagellates	*Euglena*	microscopy
Diatoms	*Eupyxidicula*	V4-SILVA, V9-SILVA
Phytoflagellates	*Fibrocapsa*	V4-PR2, V4-SILVA, V9-PR2, V9-SILVA
Diatoms	*Fistulifera*	V4-PR2, V4-SILVA, V9-SILVA
Phytoflagellates	*Florenciella*	V4-PR2, V4-SILVA
Diatoms	*Fragilariopsis*	V9-PR2
Dinoflagellates	*Fragilidium*	V4-PR2, V4-SILVA, V9-PR2, V9-SILVA
Phytoflagellates	*Geminigera*	V4-SILVA, V9-SILVA
Phytoflagellates	*Goniomonas*	V4-PR2, V4-SILVA
Dinoflagellates	*Gonyaulax*	V4-PR2, V4-SILVA, microscopy, V9-PR2, V9-SILVA
Dinoflagellates	*Grammatodinium*	V4-PR2, V4-SILVA
Diatoms	*Guinardia*	V4-PR2, microscopy
Dinoflagellates	*Gymnodinium*	V4-PR2, V4-SILVA, microscopy, V9-PR2, V9-SILVA
Dinoflagellates	*Gyrodiniellum*	V9-PR2
Dinoflagellates	*Gyrodinium*	V4-PR2, V4-SILVA, V9-PR2
Phytoflagellates	*Halosphaera*	microscopy
Phytoflagellates	*Haptolina*	V4-PR2, V4-SILVA, V9-PR2
Phytoflagellates	*Hemiselmis*	V4-PR2, V4-SILVA, V9-PR2, V9-SILVA
Dinoflagellates	*Heterocapsa*	V4-PR2, V4-SILVA, V9-PR2, V9-SILVA
Dinoflagellates	*Heterodinium*	V4-SILVA
Diatoms	*Hyalosira*	V4-SILVA
Dinoflagellates	*Islandinium*	V4-PR2, V4-SILVA
Dinoflagellates	*Karenia*	V4-PR2, microscopy, V9-PR2, V9-SILVA
Dinoflagellates	*Karlodinium*	V4-PR2
Dinoflagellates	*Kofoidinium*	V4-PR2, microscopy
Dinoflagellates	*Lebouridinium*	V4-PR2
Dinoflagellates	*Leiocephalium*	V9-SILVA
Dinoflagellates	*Lepidodinium*	V4-PR2, V9-SILVA
Diatoms	*Leptocylindrus*	V4-PR2, V4-SILVA, microscopy, V9-PR2, V9-SILVA
Dinoflagellates	*Lessardia*	V4-PR2, V4-SILVA
Dinoflagellates	*Levanderina*	V4-PR2, V4-SILVA, V9-PR2, V9-SILVA
Dinoflagellates	*Lingulodinium*	microscopy, V9-SILVA
Phytoflagellates	*Lotharella*	V9-SILVA
Phytoflagellates	*Mamiella*	V4-PR2, V4-SILVA, V9-PR2, V9-SILVA
Phytoflagellates	*Mantoniella*	V9-PR2
Dinoflagellates	*Margalefidinium*	V4-PR2, V4-SILVA
Phytoflagellates	*Marsupiomonas*	V4-SILVA
Diatoms	*Mediolabrus*	V4-PR2
Diatoms	*Melosira*	V9-PR2, V9-SILVA
Coccolithophores	*Michaelsarsia*	microscopy
Phytoflagellates	*Microchloropsis*	V4-SILVA, V9-SILVA
Phytoflagellates	*Micromonas*	V4-PR2, V4-SILVA, V9-PR2, V9-SILVA
Phytoflagellates	*Microrhizoidea*	V9-PR2
Phytoflagellates	*Minorisa*	V4-PR2, V9-PR2, V9-SILVA
Diatoms	*Minutocellus*	V4-PR2, V9-PR2, V9-SILVA

Phytoflagellates	*Monoraphidium*	V4-PR2
Phytoflagellates	*Mychonastes*	V4-PR2, V4-SILVA, V9-PR2, V9-SILVA
Diatoms	*Navicula*	V4-PR2, V9-SILVA
Diatoms	*Neomoelleria*	V9-PR2, V9-SILVA
Diatoms	*Nitzschia*	V4-PR2, V4-SILVA, microscopy
Dinoflagellates	*Noctiluca*	V4-PR2, V4-SILVA, microscopy, V9-PR2, V9-SILVA
Phytoflagellates	*Ochromonas*	V4-SILVA
Phytoflagellates	*Ollicola*	microscopy
Phytoflagellates	*Ostreococcus*	V4-PR2, V4-SILVA, V9-PR2, V9-SILVA
Dinoflagellates	*Oxyphysis*	microscopy
Dinoflagellates	*Oxytoxum*	microscopy
Diatoms	*Papiliocellulus*	V4-PR2
Dinoflagellates	*Paragymnodinium*	V4-SILVA, V9-PR2, V9-SILVA
Phytoflagellates	*Paraphysomonas*	V4-PR2, V4-SILVA, V9-PR2, V9-SILVA
Phytoflagellates	*Partenskyella*	V9-PR2
Phytoflagellates	*Paulinella*	V4-PR2, V9-PR2
Phytoflagellates	*Pedinella*	V4-PR2, V4-SILVA, V9-PR2
Dinoflagellates	*Pelagodinium*	V4-PR2, V4-SILVA, V9-PR2, V9-SILVA
Phytoflagellates	*Pelagomonas*	V4-PR2
Phytoflagellates	*Phaeocystis*	V4-PR2, V4-SILVA, V9-PR2
Phytoflagellates	*Phaeomonas*	V4-PR2, V4-SILVA, V9-PR2
Dinoflagellates	*Phalacroma*	V4-PR2, V4-SILVA, microscopy, V9-SILVA
Phytoflagellates	*Picochlorum*	V4-PR2, V4-SILVA, V9-PR2, V9-SILVA
Phytoflagellates	*Picomonas*	V9-SILVA
Diatoms	*Pleurosigma*	V4-PR2, V4-SILVA, microscopy, V9-PR2, V9-SILVA
Dinoflagellates	*Polykrikos*	V4-PR2, V4-SILVA, V9-PR2, V9-SILVA
Phytoflagellates	*Poterioochromonas*	V4-PR2, V4-SILVA, V9-PR2, V9-SILVA
Phytoflagellates	*Poteriospumella*	V9-PR2
Diatoms	*Proboscia*	V4-PR2, V4-SILVA, microscopy
Dinoflagellates	*Prorocentrum*	V4-PR2, microscopy, V9-PR2, V9-SILVA
Phytoflagellates	*Proteomonas*	V4-PR2, V4-SILVA, V9-PR2, V9-SILVA
Dinoflagellates	*Proterythropsis*	V4-PR2, V4-SILVA
Dinoflagellates	*Protoceratium*	V4-PR2, V4-SILVA, microscopy, V9-PR2, V9-SILVA
Dinoflagellates	*Protodinium*	V4-PR2, V4-SILVA, V9-SILVA
Dinoflagellates	*Protoperidinium*	V4-PR2, V4-SILVA, microscopy, V9-PR2, V9-SILVA
Phytoflagellates	*Prototheca*	V9-PR2
Phytoflagellates	*Prymnesium*	V4-PR2, V4-SILVA
Dinoflagellates	*Pseliodinium*	V4-PR2
Phytoflagellates	*Pseudochattonella*	V4-PR2, V4-SILVA, V9-PR2, V9-SILVA
Diatoms	*Pseudogomphonema*	V9-PR2
Diatoms	*Pseudo-nitzschia*	V4-PR2, V4-SILVA, microscopy, V9-PR2, V9-SILVA
Phytoflagellates	*Pseudopedinella*	V4-PR2, V4-SILVA
Diatoms	*Pseudosolenia*	V4-PR2, V4-SILVA
Phytoflagellates	*Pterosperma*	V4-PR2
Phytoflagellates	*Pycnococcus*	V4-PR2, V4-SILVA, V9-PR2, V9-SILVA
Phytoflagellates	*Pyramimonas*	V4-PR2, V4-SILVA, V9-PR2, V9-SILVA
Dinoflagellates	*Pyrophacus*	V4-PR2, V4-SILVA
Coccolithophores	*Rhabdosphaera*	microscopy
Phytoflagellates	*Rhinomonas*	V4-SILVA

Phytoflagellates	*Rhizochromulina*	V4-SILVA, V9-PR2
Diatoms	*Rhizosolenia*	V4-PR2, V4-SILVA
Phytoflagellates	*Rhodomonas*	V4-PR2, V9-SILVA
Phytoflagellates	*Sarcinochrysis*	V4-PR2
Dinoflagellates	*Scrippsiella*	V4-PR2, V4-SILVA, microscopy, V9-SILVA
Dinoflagellates	*Sinophysis*	V4-SILVA, V9-SILVA
Diatoms	*Skeletonema*	V4-PR2, V4-SILVA, microscopy, V9-PR2, V9-SILVA
Dinoflagellates	*Spatulodinium*	V4-SILVA
Dinoflagellates	*Spiniferodinium*	V4-PR2
Dinoflagellates	*Stoeckeria*	V9-SILVA
Diatoms	*Sundstroemia*	V4-SILVA
Dinoflagellates	*Syltodinium*	V4-PR2
Diatoms	*Synedra*	microscopy
Coccolithophores	*Syracosphaera*	V4-PR2, microscopy
Phytoflagellates	*Teleaulax*	V4-PR2, V4-SILVA, V9-PR2, V9-SILVA
Phytoflagellates	*Telonema*	V4-PR2, V9-PR2
Phytoflagellates	*Tetraselmis*	V4-PR2, V4-SILVA, V9-PR2, V9-SILVA
Diatoms	*Thalassionema*	V4-PR2, V4-SILVA, microscopy
Diatoms	*Thalassiosira*	V4-PR2, V4-SILVA, microscopy, V9-PR2, V9-SILVA
Dinoflagellates	*Torodinium*	V4-PR2
Dinoflagellates	*Triadinium*	V9-PR2, V9-SILVA
Phytoflagellates	*Triparma*	V4-PR2, V4-SILVA, V9-PR2, V9-SILVA
Dinoflagellates	*Tripos*	V4-PR2, V4-SILVA, microscopy, V9-PR2, V9-SILVA
Phytoflagellates	*Vicicitus*	V4-PR2
Dinoflagellates	*Wangodinium*	V4-PR2
Dinoflagellates	*Warnowia*	V4-PR2, V9-PR2, V9-SILVA
Dinoflagellates	*Yihiella*	V4-PR2, V9-PR2
Dinoflagellates	*Zooxanthella*	V9-SILVA

Table S2. List of species detected combining microscopy and metabarcoding using V4 and V9 as 18S regions, and PR2 and SILVA as reference databases (V4-PR2, V9-PR2, V4-SILVA, V9-SILVA).

Group	Species	Method of detection
Dinoflagellates	*Akashiwo sanguinea*	V4-PR2, V4-SILVA, microscopy
Dinoflagellates	*Alexandrium andersonii*	V9-PR2, V9-SILVA
Dinoflagellates	*Alexandrium catenella*	V9-SILVA
Dinoflagellates	*Alexandrium hiranoi*	V9-PR2, V4-SILVA, V9-SILVA
Dinoflagellates	*Alexandrium insuetum*	V9-SILVA
Dinoflagellates	*Alexandrium margalefii*	V4-PR2, V9-PR2
Dinoflagellates	*Alexandrium minutum*	V4-PR2
Coccolithophores	*Algirosphaera robusta*	V4-PR2
Diatoms	*Amphora ovalis*	V4-PR2, V4-SILVA
Dinoflagellates	*Ansanella granifera*	V9-PR2
Dinoflagellates	*Archaeperidinium saanichi*	V4-SILVA, V9-SILVA
Diatoms	*Arcocellulus cornucervis*	V4-SILVA
Diatoms	*Asteromphalus hookeri*	microscopy
Phytoflagellates	*Aureococcus anophagefferens*	V4-PR2, V4-SILVA, V9-SILVA
Phytoflagellates	*Bathycoccus prasinos*	V4-PR2
Phytoflagellates	*Bicosoeca petiolata*	V9-PR2
Phytoflagellates	*Bicosoeca vacillans*	V9-PR2
Dinoflagellates	*Biecheleria brevisulcata*	V9-PR2
Dinoflagellates	*Biecheleria cincta*	V4-PR2
Dinoflagellates	*Biecheleriopsis adriatica*	V4-PR2, V9-PR2
Phytoflagellates	*Bigelowiella natans*	V9-SILVA
Dinoflagellates	*Blastodinium spinulosum*	V4-PR2
Dinoflagellates	*Blixaea quinquecornis*	V4-PR2, V4-SILVA
Coccolithophores	*Calciosolenia brasiliensis*	microscopy
Coccolithophores	*Calciosolenia murrayi*	microscopy
Coccolithophores	*Calyptrosphaera oblonga*	microscopy
Diatoms	*Ceratanaulus creticus*	V9-PR2
Diatoms	*Cerataulina pelagica*	V4-PR2, V4-SILVA, microscopy
Diatoms	*Chaetoceros affinis*	V4-PR2, V9-PR2, V4-SILVA, V9-SILVA, microscopy
Diatoms	*Chaetoceros anastomosans*	V4-PR2
Diatoms	*Chaetoceros brevis*	V4-PR2, V9-PR2
Diatoms	*Chaetoceros compressus*	microscopy
Diatoms	*Chaetoceros curvisetus*	V4-PR2, microscopy
Diatoms	*Chaetoceros danicus*	V4-PR2, microscopy
Diatoms	*Chaetoceros debilis*	V9-PR2
Diatoms	*Chaetoceros decipiens*	V4-PR2
Diatoms	*Chaetoceros didymus*	V4-SILVA, V9-SILVA, microscopy
Diatoms	*Chaetoceros diversus*	V4-PR2, microscopy
Diatoms	*Chaetoceros lauderi*	V4-PR2, V9-PR2
Diatoms	*Chaetoceros lorenzianus*	microscopy
Diatoms	*Chaetoceros minimus*	V4-PR2
Diatoms	*Chaetoceros muellerii*	V4-PR2, V9-PR2, V4-SILVA, V9-SILVA
Diatoms	*Chaetoceros protuberans*	V4-PR2, V9-PR2
Diatoms	*Chaetoceros socialis*	V4-PR2, V4-SILVA, V9-SILVA
Diatoms	*Chaetoceros tenuissimus*	microscopy

Diatoms	*Chaetoceros tetrastichon*	microscopy
Diatoms	*Chaetoceros throndsenii*	V4-PR2, V9-PR2, microscopy
Diatoms	*Chaetoceros tortissimus*	microscopy
Phytoflagellates	*Chattonella subsalsa*	V4-PR2, V4-SILVA, V9-SILVA
Phytoflagellates	*Chlamydomonas kuwadae*	V4-PR2
Phytoflagellates	*Chlorarachnion reptans*	V4-PR2, V9-PR2, V9-SILVA
Phytoflagellates	*Chlorochytrium lemnae*	V9-SILVA
Phytoflagellates	*Chloroidium saccharophilum*	V9-SILVA
Phytoflagellates	*Chrysochromulina acantha*	V9-PR2
Phytoflagellates	*Chrysochromulina campanulifera*	V9-PR2
Phytoflagellates	*Chrysochromulina cymbium*	V9-PR2
Phytoflagellates	*Chrysochromulina leadbeateri*	V4-PR2, V9-PR2, V4-SILVA
Phytoflagellates	*Chrysochromulina rotalis*	V4-PR2, V9-PR2
Phytoflagellates	*Chrysochromulina scutellum*	V9-PR2
Phytoflagellates	*Chrysochromulina simplex*	V9-PR2
Phytoflagellates	*Chrysochromulina spinifera*	V4-PR2, V9-PR2, V4-SILVA
Phytoflagellates	*Chrysochromulina tobinii*	V9-PR2
Phytoflagellates	*Chrysolepidomonas dendrolepidota*	V4-PR2, V4-SILVA
Diatoms	*Cyclotella choctawhatcheeana*	V4-SILVA
Diatoms	*Cyclotella litoralis*	V9-PR2
Diatoms	*Cylindrotheca closterium*	microscopy
Phytoflagellates	*Cymbomonas tetramitiformis*	V4-PR2, V9-PR2, V9-SILVA
Diatoms	*Dactyliosolen blavyanus*	microscopy
Diatoms	*Dactyliosolen fragilissimus*	microscopy
Phytoflagellates	*Desmodesmus abundans*	V9-PR2, V9-SILVA
Phytoflagellates	*Dictyocha fibula*	microscopy
Phytoflagellates	*Dictyocha octonaria*	V4-SILVA
Phytoflagellates	*Dictyocha speculum*	V4-PR2, V9-PR2, V9-SILVA
Phytoflagellates	*Dinobryon faculiferum*	microscopy
Phytoflagellates	*Dinobryon porrectum*	microscopy
Dinoflagellates	*Dinophysis sacculus*	microscopy
Phytoflagellates	*Dolichomastix tenuilepis*	V4-PR2, V9-PR2, V4-SILVA, V9-SILVA
Coccolithophores	*Emiliania huxleyi*	V4-SILVA, microscopy
Diatoms	*Eupyxidicula turris*	V4-SILVA, V9-SILVA
Phytoflagellates	*Fibrocapsa japonica*	V4-PR2, V9-PR2, V4-SILVA, V9-SILVA
Diatoms	*Fistulifera pelliculosa*	V9-SILVA
Diatoms	*Fistulifera saprophila*	V4-PR2, V4-SILVA
Dinoflagellates	*Fragilidium duplocampaniforme*	V4-PR2, V9-PR2
Dinoflagellates	*Fragilidium mexicanum*	V4-PR2, V9-PR2
Phytoflagellates	*Geminigera cryophila*	V9-SILVA
Phytoflagellates	*Goniomonas amphinema*	V4-PR2
Dinoflagellates	*Gonyaulax bohaiensis*	V4-PR2
Dinoflagellates	*Gonyaulax digitale*	V4-PR2, V9-PR2
Dinoflagellates	*Gonyaulax fragilis*	V4-PR2, V4-SILVA
Dinoflagellates	*Gonyaulax polygramma*	V4-PR2, V9-PR2
Dinoflagellates	*Gonyaulax spinifera*	V9-PR2, V9-SILVA, microscopy
Dinoflagellates	*Gonyaulax whaseongensis*	V4-PR2, V9-PR2
Dinoflagellates	*Grammatodinium tongyeonginum*	V4-PR2, V4-SILVA
Diatoms	*Guinardia delicatula*	V4-PR2

Diatoms	*Guinardia striata*	microscopy
Dinoflagellates	*Gymnodinium catenatum*	V4-PR2, V9-SILVA
Dinoflagellates	*Gymnodinium dorsalisulcum*	V4-PR2
Dinoflagellates	*Gymnodinium impudicum*	V4-PR2, V9-PR2, V4-SILVA, V9-SILVA
Dinoflagellates	*Gymnodinium smaydae*	V9-PR2, V9-SILVA
Dinoflagellates	*Gyrodiniellum shiwhaense*	V9-PR2
Dinoflagellates	*Gyrodinium dominans*	V4-PR2
Dinoflagellates	*Gyrodinium fusiforme*	V4-PR2
Dinoflagellates	*Gyrodinium jinhaense*	V4-PR2
Phytoflagellates	*Haptolina herdlensis*	V9-PR2
Phytoflagellates	*Hemiselmis aquamarina*	V4-PR2
Phytoflagellates	*Hemiselmis cryptochromatica*	V4-SILVA
Phytoflagellates	*Hemiselmis rufescens*	V4-SILVA, V9-SILVA
Dinoflagellates	*Islandinium tricingulatum*	V4-PR2
Dinoflagellates	*Karenia mikimotoi*	V9-SILVA
Dinoflagellates	*Karenia papilionacea*	microscopy
Dinoflagellates	*Kofoidinium pavillardii*	V4-PR2
Dinoflagellates	*Kofoidinium velleloides*	microscopy
Dinoflagellates	*Lebouridinium glaucum*	V4-PR2
Dinoflagellates	*Leiocephalium pseudosanguineum*	V9-SILVA
Dinoflagellates	*Lepidodinium viride*	V9-SILVA
Diatoms	*Leptocylindrus aporus*	V4-PR2, V9-PR2
Diatoms	*Leptocylindrus convexus*	microscopy
Diatoms	*Leptocylindrus danicus*	V4-SILVA, V9-SILVA, microscopy
Dinoflagellates	*Lessardia elongata*	V4-PR2, V4-SILVA
Dinoflagellates	*Levanderina fissa*	V4-PR2, V9-PR2, V4-SILVA, V9-SILVA
Dinoflagellates	*Lingulodinium polyedra*	V9-SILVA, microscopy
Phytoflagellates	*Lotharella oceanica*	V9-SILVA
Phytoflagellates	*Mamiella gilva*	V4-PR2, V9-PR2, V4-SILVA, V9-SILVA
Phytoflagellates	*Mantoniella squamata*	V9-PR2
Dinoflagellates	*Margalefidinium fulvescens*	V4-PR2, V4-SILVA
Diatoms	*Mediolabrus comicus*	V4-PR2
Diatoms	*Melosira varians*	V9-PR2, V9-SILVA
Coccolithophores	*Michaelsarsia adriatica*	microscopy
Coccolithophores	*Michaelsarsia elegans*	microscopy
Phytoflagellates	*Microchloropsis gaditana*	V4-SILVA
Phytoflagellates	*Microchloropsis salina*	V9-SILVA
Phytoflagellates	*Micromonas bravo*	V4-PR2, V9-PR2
Phytoflagellates	*Micromonas commoda*	V4-PR2, V9-PR2
Phytoflagellates	*Micromonas pusilla*	V4-SILVA
Phytoflagellates	*Microrhizoidea pickettheapsiorum*	V9-PR2
Phytoflagellates	*Minorisa minuta*	V4-PR2, V9-PR2
Diatoms	*Navicula phyllepta*	V4-PR2
Diatoms	*Neomoelleria antarctica*	V9-SILVA
Diatoms	*Nitzschia gobbii*	microscopy
Diatoms	*Nitzschia longissima*	microscopy
Diatoms	*Nitzschia microcephala*	V4-PR2, V4-SILVA
Diatoms	*Nitzschia sigma*	microscopy
Dinoflagellates	*Noctiluca scintillans*	V4-PR2, V9-PR2, V4-SILVA, V9-SILVA, microscopy

Phytoflagellates	*Ochromonas distigma*	V4-SILVA
Phytoflagellates	*Ostreococcus mediterraneus*	V4-PR2, V9-PR2
Phytoflagellates	*Ostreococcus tauri*	V4-PR2
Dinoflagellates	*Oxyphysis oxytoxoides*	V9-SILVA, microscopy
Dinoflagellates	*Oxytoxum caudatum*	microscopy
Dinoflagellates	*Oxytoxum elongatum*	microscopy
Dinoflagellates	*Oxytoxum laticeps*	microscopy
Dinoflagellates	*Oxytoxum scolopax*	microscopy
Diatoms	*Papiliocellulus elegans*	V4-PR2
Dinoflagellates	*Paragymnodinium shiwhaense*	V9-PR2, V4-SILVA, V9-SILVA
Phytoflagellates	*Paraphysomonas foraminifera*	V9-PR2
Phytoflagellates	*Paraphysomonas imperforata*	V4-SILVA, V9-SILVA
Phytoflagellates	*Partenskyella glossopodia*	V9-PR2
Phytoflagellates	*Paulinella chromatophora*	V9-PR2
Phytoflagellates	*Pedinella elastica*	V4-PR2, V9-PR2
Dinoflagellates	*Pelagodinium bei*	V4-PR2
Phytoflagellates	*Pelagomonas calceolata*	V4-PR2
Phytoflagellates	*Phaeocystis cordata*	V4-PR2, V9-PR2
Phytoflagellates	*Phaeomonas parva*	V4-PR2, V9-PR2, V4-SILVA
Dinoflagellates	*Phalacroma rotundatum*	microscopy
Dinoflagellates	*Picochlorum maculatum*	V9-PR2, V4-SILVA, V9-SILVA
Phytoflagellates	*Pleurosigma intermedium*	V9-PR2
Diatoms	*Pleurosigma planktonicum*	V4-SILVA
Diatoms	*Polykrikos geminatus*	V4-PR2, V9-PR2, V9-SILVA
Dinoflagellates	*Polykrikos hartmannii*	V9-PR2, V9-SILVA
Dinoflagellates	*Polykrikos kofoidii*	V4-PR2, V4-SILVA
Dinoflagellates	*Polykrikos schwartzii*	V4-PR2, V4-SILVA
Dinoflagellates	*Poterioochromonas malhamensis*	V4-PR2
Phytoflagellates	*Proboscia alata*	microscopy
Diatoms	*Prorocentrum compressum*	microscopy
Dinoflagellates	*Prorocentrum cordatum*	microscopy
Dinoflagellates	*Prorocentrum dentatum*	V9-SILVA
Dinoflagellates	*Prorocentrum micans*	microscopy
Dinoflagellates	*Prorocentrum triestinum*	microscopy
Dinoflagellates	*Protoceratium reticulatum*	V4-PR2, V9-PR2, V4-SILVA, V9-SILVA, microscopy
Dinoflagellates	*Protodinium simplex*	V4-PR2, V9-SILVA
Dinoflagellates	*Protoperidinium bipes*	V4-PR2, V4-SILVA, microscopy
Dinoflagellates	*Protoperidinium claudicans*	microscopy
Dinoflagellates	*Protoperidinium diabolus*	microscopy
Dinoflagellates	*Protoperidinium divergens*	microscopy
Dinoflagellates	*Protoperidinium ovum*	microscopy
Dinoflagellates	*Protoperidinium steinii*	microscopy
Dinoflagellates	*Prototheca wickerhamii*	V9-PR2
Phytoflagellates	*Pseliodinium fusus*	V4-PR2
Dinoflagellates	*Pseudochattonella farcimen*	V9-PR2
Phytoflagellates	*Pseudochattonella verruculosa*	V4-SILVA, V9-SILVA
Phytoflagellates	*Pseudo-nitzschia australis*	V9-SILVA
Diatoms	*Pseudo-nitzschia delicatissima*	microscopy
Diatoms	*Pseudo-nitzschia pseudodelicatissima*	V4-PR2, V4-SILVA, microscopy

Diatoms	*Pseudo-nitzschia pungens*	V4-PR2, V4-SILVA, V9-SILVA
Diatoms	*Pseudosolenia calcar-avis*	V4-PR2, V4-SILVA
Diatoms	*Pterosperma cristatum*	V4-PR2
Phytoflagellates	*Pycnococcus provasolii*	V4-PR2, V9-PR2, V4-SILVA, V9-SILVA
Phytoflagellates	*Pyramimonas aurea*	V9-PR2
Phytoflagellates	*Pyramimonas australis*	V4-SILVA
Phytoflagellates	*Pyramimonas disomata*	V9-PR2
Phytoflagellates	*Pyramimonas olivacea*	V9-PR2, V9-SILVA
Phytoflagellates	*Pyramimonas parkeae*	V9-PR2, V9-SILVA
Phytoflagellates	*Pyramimonas tetrarhynchus*	V9-PR2, V9-SILVA
Phytoflagellates	*Pyrophacus steinii*	V4-PR2, V4-SILVA
Dinoflagellates	*Rhabdosphaera clavigera*	microscopy
Coccolithophores	*Rhinomonas nottbecki*	V4-SILVA
Phytoflagellates	*Rhizochromulina marina*	V9-PR2
Phytoflagellates	*Rhizosolenia fallax*	V4-SILVA
Diatoms	*Rhizosolenia imbricata*	V4-PR2, V4-SILVA
Diatoms	*Scrippsiella acuminata*	V4-PR2
Dinoflagellates	*Scrippsiella trochoidea*	V9-SILVA
Dinoflagellates	*Skeletonema dohrnii*	V9-PR2, V9-SILVA
Diatoms	*Skeletonema marinoi*	V4-PR2, microscopy
Diatoms	*Spatulodinium pseudonoctiluca*	V4-SILVA
Dinoflagellates	*Sundstroemia setigera*	V4-SILVA
Diatoms	*Syltodinium listii*	V4-PR2
Dinoflagellates	*Syracosphaera pulchra*	V4-PR2, microscopy
Coccolithophores	*Teleaulax acuta*	V4-PR2, V9-PR2
Phytoflagellates	*Teleaulax amphioxeia*	V4-PR2, V9-PR2, V4-SILVA
Phytoflagellates	*Telonema antarcticum*	V4-PR2, V9-PR2
Phytoflagellates	*Telonema subtile*	V4-PR2
Phytoflagellates	*Tetraselmis convolutae*	V4-PR2
Phytoflagellates	*Tetraselmis marina*	V9-PR2, V4-SILVA
Phytoflagellates	*Thalassionema frauenfeldii*	V4-SILVA
Diatoms	*Thalassionema nitzschioides*	microscopy
Diatoms	*Thalassiosira profunda*	V4-PR2, V4-SILVA
Diatoms	*Thalassiosira rotula*	V9-SILVA, microscopy
Diatoms	*Triadinium polyedricum*	V9-PR2, V9-SILVA
Dinoflagellates	*Triparma laevis*	V4-PR2
Phytoflagellates	*Triparma mediterranea*	V4-PR2, V9-PR2
Phytoflagellates	*Triparma pacifica*	V4-PR2, V9-PR2, V4-SILVA, V9-SILVA
Phytoflagellates	*Triparma strigata*	V4-SILVA
Phytoflagellates	*Tripos extensus*	microscopy
Dinoflagellates	*Tripos furca*	V4-PR2, microscopy
Dinoflagellates	*Tripos fusus*	V4-PR2, V9-PR2, microscopy
Dinoflagellates	*Tripos tenuis*	V9-PR2, V9-SILVA
Dinoflagellates	*Vicicitus globosus*	V4-PR2
Phytoflagellates	*Wangodinium sinense*	V4-PR2
Dinoflagellates	*Yihiella yeosuensis*	V4-PR2, V9-PR2

General Conclusions

The monitoring of phytoplankton communities is essential to study the effects of changes in the environmental and oceanographic conditions, also related to climate change and/or to anthropogenic pressures. In this context, long-term data series allows a better understanding of the uniqueness of the environments, the key aspects controlling biodiversity and productivity, as well as potential tendencies and changes in the phytoplankton community, discriminating between a 'natural' long-term variability and shifts related to anthropogenic and climatic forcings.

The tendencies in the physico-chemical parameters and phytoplankton abundances observed in the present study in an eLTER site confirmed that the Northern Adriatic Sea (NAS) is facing significant changes, with potential consequences on the food webs and the marine ecosystems. This underscores the importance of long-term data collection and the need for continuous investigations of extended datasets to monitor the effects of these changes on marine ecosystems.

The investigation of the effects of extreme events (marine heatwaves) and ocean warming on phytoplankton biomass (chlorophyll-a) across the NAS, pointed out how these phenomena are contributing to the decline of the phytoplankton biomass, potentially affecting the structure of marine food webs, with effects on economic activities (eg., fishery and aquaculture). The variable responses observed in different areas of the NAS, related to the background trophic and oceanographic conditions, underlines the importance to study these phenomena in different LTER sites. The oligotrophication that the Adriatic Sea is facing, suggests the need to include the assessment of picophytoplankton in Long Term monitoring activities, which is normally not considered.

Phytoplankton biodiversity estimation is essential for many reasons, such as to detect toxic taxa and to assess the Good Environmental Status of pelagic habitats, and the debate over the best method for its assessment is still ongoing. In the present study, the comparison between the information on diversity obtained through microscopy and metabarcoding, revealed that the two methods should be combined to overcome their gaps and to gain a most comprehensive picture of phytoplankton community composition. In this scenario, the knowledge of phytoplankton communities from eLTER sites serves as a valuable tool for interpreting and combining these two methodologies.